NEUROBIOLOGICAL MECHANISMS INVOLVED IN THE LOSS OF CONTROL OVER FOOD INTAKE

Laura Domingo Rodriguez

DOCTORAL THESIS UPF / 2019

Thesis directors:

Dra. Elena Martín-García

Prof. Rafael Maldonado

Department of experimental and health sciences

Universitat Pompeu Fabra Barcelona

Step by step, bit by bit,
Stone by stone, brick by brick
Step by step, day by day,
Mile by mile, go your own way

(Whitney Houston)

És una previsió molt necessària
comprendre que no és possible preveure-ho tot

(Jean-Jaques Rousseau)

Abstract

The easy access to palatable foods is a major contributing factor for compulsive eating and development of food addiction, a disorder closely linked to obesity and binge eating disorder. The concept of food addiction is still controversial but a validated tool for diagnosis, the Yale food addiction scale (YFAS 2.0), is widely accepted. However, the complex multifactorial nature of this disorder and the unknown neurobiological mechanistic correlation explain the current lack of effective treatments. In this thesis, we used a food addiction mouse model to elucidate the crucial role of the glutamatergic cortico-striatal pathways modulated by the endocannabinoid and the dopamine systems as a critical mechanism for the loss of inhibitory control for palatable food seeking. This result was supported by electrophysiological recordings, genome-wide RNA and DNA methylome sequencing, chemogenetic interference and adenoviral gene delivery, giving an understanding of the food addiction construct at genetic, epigenetic, cellular, circuit and behavioral level. This thesis unravels a new neurobiological mechanism underlying resilience and vulnerability to develop food addiction, which is expected to pave ways for novel interventions to battle compulsive eating behavior and other related disorders.

Resum

El fàcil accés a aliments altament saborosos és un factor important que contribueix a la ingesta compulsiva i al desenvolupament de l'addicció al menjar. Aquest trastorn està molt vinculat a l'obesitat i al trastorn per afartament. El concepte d'addicció al menjar és controvertit, però l'aparició d'una eina diagnòstica valida, el *Yale food addiction scale (YFAS 2.0),* ha sigut àmpliament acceptada. Tot i això, la naturalesa complexa i multifactorial d'aquest trastorn i la desconeguda correlació neurobiològica expliquen la manca actual de tractaments efectius. En aquesta tesi, hem utilitzat un model d'addicció al menjar en ratolins per descobrir el paper crucial de les vies cortico-estriatals glutamatergiques modulades pels sistemes endocannabinoid i dopaminèrgic com a mecanisme clau per a la pèrdua del control inhibitori en la cerca d'aliments saborosos. Aquest resultat, amb el suport d'estudis electrofisiològics, seqüenciació d'ARN i d'ADN de tot el genoma i tècniques de "chemogenetics" ens donen una comprensió del trastorn a nivell genètic, epigenètic, cel·lular, de circuit i de comportament. Aquesta tesi revela un nou mecanisme neurobiològic subjacent a la resiliència i a la vulnerabilitat a desenvolupar addicció al menjar. S'espera que obri noves vies eficients d'intervenció per combatre el comportament d'ingesta compulsiva i altres trastorns relacionats.

Abbreviations

2-AG 2-arachidonoylglycerol

A_{2A}R Adenosine A_{2A} receptor

AAV Adeno-associated virus

AEA N-arachidonoylethanolamide

AgRP Agouti-related peptide

BDNF Brain-derived neurotrophic factor

BLA Basolateral amygdala

BMI Body mass index

Ca^{2+} Calcium

CAMKIIα Ca^{2+}/calmoduline-dependent kinase II alpha

cAMP Cyclic adenosine monophosphate

CART Cocaine- and amphetamine-regulated transcript

CB_1R Cannabinoid type-1 receptor

CB_2R Cannabinoid type-2 receptor

CNO Clozapine N-oxide

COMT Catechol-o-methyl-transferase

D_1R Dopamine type-1 receptor

D_2R Dopamine type-2 receptor

DA Dopamine

DARPP DA and cAMP-regulated phosphoprotein

DAT Dopamine transporter

dl Dorsolateral

dm Dorsomedial

DREADDs Designer receptors exclusively activated by designer drugs

DSE Depolarization-induced suppression of excitation

DSI Depolarization-induced suppression of inhibition

DSM Diagnostic and statistical manual of mental disorders

eCB-LTD Endocannabinoid-mediated long-term depression

eCB-STD Endocannabinoid-mediated short-term depression

fEPSP Field excitatory postsynaptic potentials

FR Fixed ratio

GAD65 Glutamic acid decarboxylase 65Kd isoform

GIRKs G protein-coupled inwardly rectifying potassium channels

GPCRs G protein-coupled receptors

Gpe Globus pallidus external part

Gpi Globus pallidus internal part

GPR G protein-coupled receptor

GWAS Genome-wide association study

hM3Dq Human muscarinic 3 DREADD receptor coupled to Gq

hM4Di Human muscarinic 4 DREADD receptor coupled to Gi

IL Infralimbic cortex

i.p Intraperitoneal

IP3 Inositol triphosphate

K^+ Potassium

L Layer

mAChRs Muscarinic acetylcholine receptors

MBD-seq Methyl-CpG-binding domain sequencing

mEPSC Miniature excitatory postsynaptic currents

mGluRs Metabotropic glutamate receptors

miRNAs microRNAs

miRISC miRNA-induced silencing complex

MSN Medium spiny neuron

mYFAS Modified yale food addiction scale

Na^+ Sodium

NAc Nucleus accumbens

NMDA N-methyl-D-aspartate

PFC Prefrontal cortex

PKA Protein kinase A

PL Prelimbic cortex

PLC Phospholipase C

POMC Pro-opiomelanocortin

PPF Paired pulse facilitation

PR Progressive ratio

rTMS Repetitive transcranial magnetic stimulation

s.c Subcutaneous

SNpr Substantia nigra pars reticulada

tDCS Transcranial direct current stimulation

vm Ventromedial

VTA Ventral tegmental área

WT Wild type

YFAS Yale food addiction scale

Δ9-THC Δ9-tetrahydrocannabinol

Index

Introduction

1. Eating disorders and obesity

1.1.Eating disorders

Eating disorders are defined as a persistent disturbance of eating or eating-related behavior that result in the altered consumption or absorption of food and that significantly impair physical health or psychosocial functioning (American Psychiatric Association, 2013). Eating disorders affect millions of individuals worldwide regardless of race, age, nationality, or sex but they most commonly occur among late adolescents and young women (Mishra *et al.*, 2017). Eating disorders are usually chronic, relapsing and are often associated with psychiatric comorbidity and medical sequels leading to considerable personal, familial, and social costs. Although the prevalence of eating disorders has remained stable (the cumulative lifetime risk by age 80 approximates 4.6%), the elevated mortality risk, the association with other psychiatric disorders, and an increased level of consciousness of eating disorders in general population, have increased the interest among the scientific community to investigate deeper the neurobiological mechanisms underpinning them (Smink *et al.*, 2012; Schaumberg *et al.*, 2017).

Our current understanding of eating disorders etiology is based on family, twin and adoption studies that have robustly shown that eating disorders reflect the pattern of complex trait inheritance being influenced by both genetic and environmental factors (Yilmaz *et al.*, 2015). At the same time, epigenetic mechanisms offer an added layer of gene regulation, which links external and internal environmental

stimuli as well as non-coding genetic variation with transcriptional consequences, altering downstream phenotypes (Hübel *et al.*, 2019).

1.1.1 Diagnosis of eating disorders

From a diagnostic perspective, the main psychiatry manual used to diagnose mental disorders by the American Psychiatric Association is the Diagnostic and Statistical Manual of Mental Disorders (DSM). In the fifth version of the manual (DSM-5), the eating disorders section is called "Feeding and Eating Disorders" and the diagnostic criteria are provided for three feeding disorders: pica, rumination and avoidant/restrictive food intake disorders; and three eating disorders: anorexia nervosa, bulimia nervosa and binge eating disorder.

1.1.1.1. Anorexia nervosa and bulimia nervosa

Anorexia nervosa and bulimia nervosa are the most common classical specific forms of eating disorders, they differ from binge eating disorder in terms of age at onset, gender and racial distribution, psychiatric comorbidity and association with obesity (Smink *et al.*, 2012). Briefly:

- **Anorexia nervosa:** This disease is defined by three essential features: (I) persistent energy intake restriction, (II) intense fear of gaining weight or becoming fat, or persistent behavior that interferes with weight gain, and (III) a disturbance in self-perceived weight or shape. The 12-month prevalence of anorexia nervosa is 0.4% among young females (American Psychiatric Association, 2013).

- **Bulimia nervosa:** This disorder is characterized by three essential features: (I) recurrent episodes of binge eating, (II) recurrent inappropriate compensatory behaviors to prevent weight gain (e.g, self-induced vomiting, diuretics, fasting or excessive exercise), and (III) self-evaluation that is unduly influenced by body shape and weight. The 12-month prevalence of bulimia nervosa is 1-1.5% among young females (American Psychiatric Association, 2013).

According to the DSM-5, some eating disorders symptoms resemble those types typically endorsed by individuals with substance use disorders, such as craving and compulsive use. These similarities may reflect the participation of similar neurobiological systems, including those involved in regulatory self-control and reward. Therefore, in the highly obesogenic environment in which our Western society is involved, much attention was given to eating disorders characterized by compulsive behavior and overeating as **binge eating disorder**, **obesity**, and importantly to the proposed construct of **food addiction**.

1.1.1.2. Binge eating disorder

Binge eating disorder is characterized by recurrent episodes of binge eating accompanied by a sense of lack of control, indicated by the inability to refrain from eating or stop eating once started. An “episode of binge eating” is defined as eating in a discrete period of time (within any 2 h period) an amount of food that is definitely larger than most individuals would eat in a similar period of time under similar

circumstances. Importantly, an occurrence of excessive food consumption must be accompanied by a sense of lack of control to be considered an episode of binge eating (American Psychiatric Association, 2013).

Individuals must experience at least three of the following impaired control behavioral indicators for the diagnosis of binge eating disorder: (I) eating rapidly, (II) eating until feeling uncomfortably full, (III) eating large amounts of food when not feeling physically hungry, (IV) eating alone because of feeling embarrassed, and (V) feeling disgusted with oneself, depressed, or very guilty afterward. The type of food consumed during binges varies both across individuals. Thus, binge eating disorder appears to be characterized more by an abnormality in the amount of food consumed than by craving for a specific nutrient (American Psychiatric Association, 2013).

Binge eating disorder has recurrent binge eating episodes in common with bulimia nervosa, but binge eating disorder differs from it because is not associated with the recurrent use of inappropriate compensatory behavior as in bulimia nervosa. In addition, binge eating disorder typically does not show marked or sustained dietary restrictions designed to influence body weight and shape (American Psychiatric Association, 2013).

Epidemiological studies indicate that binge eating disorder is the most prevalent eating disorder affecting between 2-5% of the adult population and more common in women than men (1.6% and 0.8% respectively) (Kessler *et al.*, 2013). It occurs in normal-weight,

overweight and obese individuals. Reports indicated a positive association between recurrent binge eating and weight gain. Indeed, there is a strong relationship between binge eating disorder and obesity in patients, as well as an association between the severity of binge eating and the degree of overweight (Wonderlich *et al.*, 2009). Although binge eating disorder is associated with overweight and obesity, it is important to highlight that not all individuals with binge eating disorder are obese. Conversely, the majority of obese humans do not have binge eating disorder, indicating that binge eating disorder is distinct from obesity. (Wonderlich *et al.*, 2009; Marcus and Wildes, 2012).

Psychiatric disorders, including anxiety and depression, are frequently comorbid with binge eating disorder and obesity. The lifetime prevalence for anxiety is estimated 29% and for major depressive disorder is 17% in the United States. This prevalence increased within the binge eating disorder subjects and obese population to 30-37% and 32.8% respectively (Grilo *et al.*, 2009; Kornstein *et al.*, 2016). Indeed, the symptomatology of distress regarding the lack of control in binge eating disorder subjects seems to elevate the psychiatric symptoms (Peterson *et al.*, 2012). Moreover, obese individuals with binge eating disorder have even greater rates of anxiety and depression than obese individuals without binge eating disorder. This could be explained by a possible binge eating to alleviate or escape symptoms of anxiety and depression in obese subjects with binge eating disorder.

1.2. Obesity

Obesity is a chronic disease, considered by many as a 21st century epidemic, defined as abnormal or excessive fat accumulation that may impair health (*WHO*, 2017). Obesity has profound medical consequences and is associated with an increased risk for cardiovascular disease, diabetes, cancer and other diseases (Bray, 2004). The body mass index (BMI) is the current tool used to classify overweight and obesity in adults. It is a ratio of weight to height that is calculated by a person's weight in kilograms divided by the square of his height in meters (kg/m^2). BMI is strongly associated with adiposity and obesity-related morbidity (González-Muniesa *et al.*, 2017). WHO classification using BMI define: BMI < 18.5 – underweight; BMI 18.5-24.9 – normal weight; BMI 25-29.9 – overweight; and BMI > 30 – obese.

Since the middle of the 20th century, overweight and obesity prevalence has increased dramatically affecting currently more than 1.9 billion adults representing 39% of the total population (39% of men and 40% of women). Of these, over 650 million adults were obese in 2016, about 13% of the world's adult population (11% of men and 15% of women) (*WHO*, 2017). Importantly, the prevalence of overweight and obesity among children and adolescents aged 5-19 has also risen radically from 4% in 1975 to over 18% in 2016. The rise has occurred similarly among both boys and girls: 18% of girls and 19% of boys were overweight in 2016. This high prevalence translates into a global health cost equivalent to 2.8% of the world's gross domestic product or approximately US$2 trillion (*WHO*, 2017).

The factors that induce obesity are still not understood. Obesity is induced by an imbalance between energy intake and energy expenditure resulting in the storage of non-essential lipids in adipose cells. According to this, obesity at a population level could be the result of low physical activity and the overconsumption of high energy foods above the need of the individual. However, the etiology of obesity is much more complex. The factors that induce obesity are heterogeneous and involve interactions among genetic, individual, environmental, and social factors (Sellayah *et al.*, 2014). Thus, obesity is a multifactorial disease resulting from different alterations of complex internal and environmental factors that interact to result in a diversity of **obese phenotypes**.

Particular obese phenotypes are characterized by an excessive motivational drive for food, compulsive consumption of food and the inability to restrain from eating despite the desire to do so. These symptoms are similar to those presented by individuals who are addicted to drugs and are described in the DSM for substance use disorders (Volkow and O'Brien, 2007). Preclinical and clinical studies have provided several evidences reporting neurobiological substrates similar and the equal dopamine (DA)-modulated circuits impairments between obese individuals and drug-addicted individuals (N. D. Volkow *et al.*, 2011; Tomasi and Volkow, 2013; Volkow and Baler, 2015). These similar neuroadaptations in the reward system (decrease in striatal dopamine type-2 receptors (D_2R)) leading to compulsive use have been reported in obese and drug-addicted individuals (N. D Volkow *et al.*,

2008). Indeed, dopaminergic signaling changes have been linked with decreased metabolic activity in prefrontal areas in obese humans, as previously reported in cocaine abusers (Nora D. Volkow *et al.*, 2008; Nora D Volkow *et al.*, 2011).

Despite the important progression of metabolic treatments and the treatment for medical complications of obesity, the prevalence rates of obesity continue to increase and not effective treatment is still available. There is a significant failure in behavioral treatments centered to sustain weight loss. Currently, it is very difficult to sustain decreased food consumption (dieting) and increased physical activity in patients. Therefore, obesity could not be considered only as a metabolic disorder, at least some forms of obesity must be considered as a mental disorder (Volkow and O'Brien, 2007; Lerma-Cabrera *et al.*, 2016). However, obesity is not currently included in the DSM-5, neither in the feeding and eating disorders nor in the substance use disorders sections despite several authors argued to include a component of obesity as a mental disorder due to its addictive dimensionality. In this framework, certain foods, mainly highly palatable foods, seem to have addictive properties promoting excessive consumption of highly palatable diets and increasing the risk of developing obesity and eating disorders.

Thus, studying the construct of **food addiction** as a determinant influencing factor in excessive food intake is attracting attention and may help the development of better therapeutic interventions to

diminish the pathologically intense drive for food seeking and consumption in specific obese phenotype.

2. Food addiction as a concept

The term **food addiction** was first introduced in the scientific literature by Theron Randolph in 1956, who described it as "a specific adaptation to one or more regularly consumed foods to which a person is highly sensitive, [which] produces a common pattern of symptoms descriptively similar to those of other addictive processes". He noted that it happens with the consumption of foods such as corn, wheat, coffee, milk, eggs and potatoes (Randolph, 1956). Nowadays, the view shifts to the potentially addictive properties of processed foods with high sugar and fat content. Thus, the current concept of food addiction includes the idea that some specific kinds of foods (highly processed, highly palatable, and highly caloric) have an addictive potential contributing to overeating and may explain the addictive behavior of some forms of obesity.

2.1. Food addiction: a construct of increasing interest

As a consequence of the worldwide obesity problem, the concept of food addiction has drastically increased its interest and the number of studies dealing with this topic substantially augmented in the last 10 years (Figure 1).

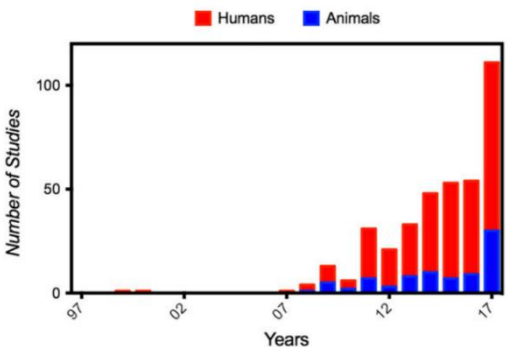

Figure 1. **Number of animal and human studies published on food addiction from 1997 to 2017** (Meule, 2015; Fernandez-Aranda *et al.*, 2018).

However, the association between food and addiction dates back to the 19th century (Figure 2), where the *Journal of Inebriety* in 1880 used the term addiction referred to chocolate (Weiner and White, 2007). Then, in the middle of the 20th century, the term food addiction was widely used among scientists and laypersons. Indeed, it was used by self-help groups like Overeaters Anonymous founded in 1960, a self-help organization based on the 12-step program first used in Alcoholics Anonymous with the goal of decreasing overeating (Russell-Mayhew *et al.*, 2010). In the 1980s, the food addiction research was focused on anorexia nervosa and bulimia nervosa trying to understand some parts of the pathology from an addiction perspective (Feldman and Eysenck, 1986; De Silva and Eysenck, 1987). The studies on addictive personality in bulimia nervosa were accompanied by the development of the "Foodaholics Group Treatment Program". After these first attempts to describe eating disorders as an addiction, a major change in the research emerged in the 1990s focused on chocolate. It was described that chocolate has a combination of high fat and sugar content, which makes it a "hedonically ideal substance". Several studies were performed comparing consumption patterns and the physiological response to chocolate exposure between "chocolate addicts" and controls (Hetherington and MacDiarmid, 1993; Bruinsma and Taren, 1999). However, the studies were limited by the fact that the term food addiction was poorly or not defined and the participants were recruited based on non-standardized self-identification reports. A few years later, in the early 2000s, the focus shift to the examination of neuronal mechanisms underpinning overeating and obesity that may parallel

findings from substance dependence (N. D Volkow *et al.*, 2008). Human studies using neuroimaging reported that a "reward deficiency syndrome" correlated with lower striatal D_2R availability in obese individuals as compared to controls similar to what has been found in individuals with substance dependence (Wang *et al.*, 2001). Other studies reported similar brain areas activation during the craving for food and drugs (Pelchat *et al.*, 2004). Importantly, the food addiction-like rodent models appeared showed in these models an overlapping neuronal circuit in the processing of food and drug-related cues and in the control of eating behavior and substance use (Pelchat *et al.*, 2004) (Figure 2).

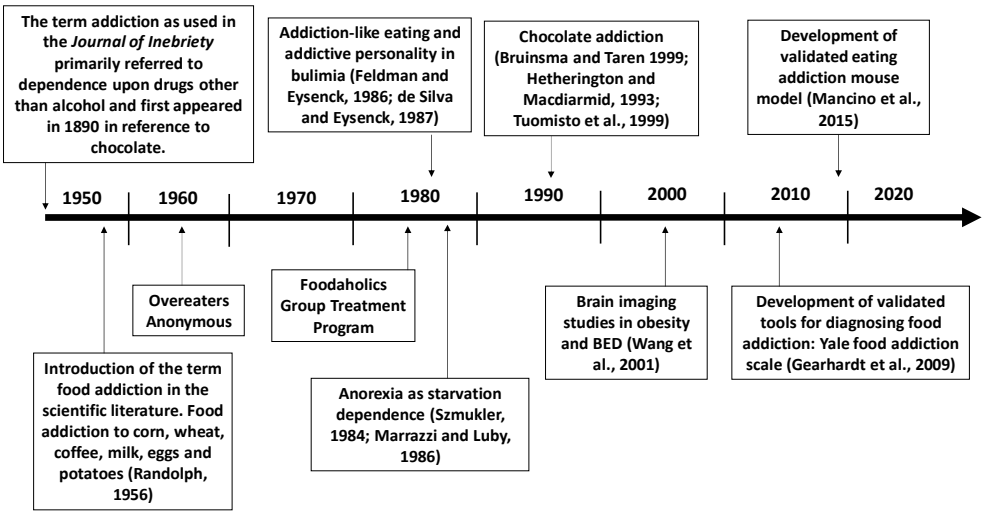

Figure 2. Some focus areas with selected references in the history of food addiction research (Adapted from Meule, 2015; Davis, 2016).

Finally, in the 2010s, the development of validated tools for diagnosing food addiction (Gearhardt *et al.*, 2009) and the increasing interest for this field has driven several animal and human studies investigating the

neurobiological mechanisms involved in this pathology and the development of potential therapeutic targets (Lindgren *et al.*, 2018). Nevertheless, although food addiction has been debated in the scientific community for decades, it is still a controversial topic making it an exciting field for developing research (Figure 2).

2.2. Food addiction diagnostic tool: Yale Food Addiction Scale

Food addiction is not currently recognized as a disorder in the DSM-5, as a result of a lack of consensus about the term food addiction. However, the urgency of a precise way to capture the symptomatology of food addiction led to the development of an operationally useful diagnostic tool, the **Yale Food Addiction Scale (YFAS)** by Gearhardt *et al*. in 2009 (Gearhardt *et al.*, 2009). This 25-item self-report instrument measures the presence of food addiction symptoms based primarily on the diagnostic criteria for substance dependence in the DSM-IV-TR adapted to the context of food, with additional items to assess the significance of distress or impairment caused by the symptoms. The YFAS has good internal consistency, convergent validity with related measures of eating behavior (e.g. emotional eating) and discriminant validity with measures of substance use (Gearhardt *et al.*, 2009). Thus, YFAS is currently the only validated and reliable tool to operationalize addictive-like eating behavior.

In 2014, it was developed the modified YFAS (**mYFAS**) that was an abbreviated version of the YFAS. Different to the YFAS, the mYFAS consisted of 9 self-report questions, which 7 of them assessed the 7

DSM-IV-TR substance use disorder criteria and 2 added questions that evaluated clinically significant impairment and distress. The mYFAS was useful in large epidemiologic cohorts and for samples with high participant burden or when a brief screener of food addiction symptomatology may be sufficient (Flint *et al.*, 2014).

In 2016, an update of the YFAS was published, the **YFAS 2.0**, to reflect the changes in substance use disorder diagnostic criteria in the latest version of the DSM (DSM-5) (Gearhardt *et al.*, 2016). The DSM-5 combines the categories of substance abuse and substance dependence, reflected in the DSM-IV, into a single unified category, and measures severity on a continue scale from mild (2–3 symptoms endorsed), moderate (4–5 symptoms endorsed) and severe (6 or more symptoms endorsed) out of 11 total symptoms (versus the previous 7 in the DSM-IV) (American Psychiatric Association, 2013). In the DSM-5, the term *addiction* is synonymous with the classification of severe substance use disorder (Volkow *et al.*, 2016).

To maintain consistency with the current diagnostic understanding of addiction, the 35-item YFAS 2.0 assesses the 11 substance use disorder symptoms included in the DSM-5. It is specified that when the ingredient is made of highly processed foods, the sufficient diagnostic criteria to be considered food addicted is reduced from three to two symptoms but an impairment or distress symptoms are also needed. Moreover, YFAS 2.0 uses mild, moderate or severe specifiers for the diagnostic threshold (Gearhardt *et al.*, 2016).

The YFAS 2.0 is similar to the original YFAS in terms of convergent, incremental and discriminant validity with eating-related construct, and seems to have better internal consistency (Gearhardt *et al.*, 2016). Using the YFAS 2.0, there are 6% more individuals that met the diagnostic criteria compared to the YFAS. This could be explained because the original YFAS only evaluates the dependence criteria and now the YFAS 2.0 assess dependence and abuse criteria (Gearhardt *et al.*, 2016). The new version of the YFAS is widely accepted and was translated/validated and used in different languages, including a Spanish version (Fernandez-Aranda *et al.*, 2018; Granero *et al.*, 2018).

Finally, it has been newly developed a modified YFAS 2.0 (**mYFAS 2.0**), an abbreviate version for use in large epidemiological cohorts and as a brief screening measure (Schulte and Gearhardt, 2017). The mYFAS 2.0 selects one question as a screener for each substance use disorder symptom compared with the multiple questions endorsing each individual symptom in the extended YFAS 2.0.

2.2.1. Food addiction prevalence based on the YFAS

Based on the YFAS scale, the prevalence of food addiction is 19.9% in the adult population (Pursey *et al.*, 2014). It affects 2-12% of healthy BMI individuals (Schulte and Gearhardt, 2018), but is double prevalent in obese subjects (ranging from 18-24%) and even higher in patients with eating disorders, particularly binge eating disorder and bulimia nervosa (ranging from 50 to 85% respectively) (Davis *et al.*, 2011; Hilker *et al.*, 2016; Burrows *et al.*, 2017). Regarding gender, food addiction seems to be more prevalent in females than males in both obese and

healthy BMI populations (24.9% and 11.1% respectively in females and 12.2% and 6.4% respectively in males) (Pursey *et al.*, 2014).

2.3. Food addiction and its comorbid diseases

Current research has demonstrated substantial comorbidity between food addiction and other eating disorders such as binge eating disorder. Clinical studies found that at least 50% of adults with binge eating disorder also met criteria for food addiction (Davis *et al.*, 2011), while a similar proportion of YFAS food addiction was revealed in obese patients with binge eating disorder (Gearhardt *et al.*, 2012). However, it is worthy to mention that not all the individuals who met the food addiction criteria (30%) are clinically significant binge eaters confirming that they are two independent disorders (Davis *et al.*, 2011).

The presence of food addiction in the absence of binge eating disorder could be explained by the hypothesis that food addiction could be developed after a large, severe and compulsive form of binge eating disorder. It is postulated that at the beginning there is an occasional overeating that displays no behavioral pathology nor psychiatric disturbances. Later, mild and intermittent "loss of control" eating appears, which manifests as episodic binges that tend to become more compulsive and more frequent in some individuals over time. When these behaviors become severe, binge eating disorder diagnosis may be warranted. At the end, binge eating disorder displays significant psychopathology and strong addictive tendencies towards food in certain vulnerable individuals. This suggests that chronic binge eating

disorder develops into a more severe syndrome and it seems more appropriate to describe their condition as food addiction (Figure 3) (Davis, 2013, 2016).

Figure 3. A downwardly escalating dimension of overeating and behaviors reflecting increased severity and compulsiveness (Modified from Davis, 2013).

Another point of view explaining the absence of binge eating disorder in food addiction is explained by the different patterns of consumption contributing to a feeling of loss of control, as has been reported in all substance use disorders. For example, alcohol-use disorder patients could consume alcohol in a binge-drinking episode or consume the same volume of alcohol over the course of the day. Equally, the addictive-like eating seen in food addiction could occur by bingeing or "grazing" (Davis, 2016). "Grazing" is an eating behavior characterized by repetitive eating (more than twice) of small/modest amounts of food in an unplanned manner. The term also implies the inability to resist such repetitive snacking despite intentions to stop and has been quantified by at least 2 self-report grazing questionnaires, which are useful for research and clinical purposes. Grazing it has been associated with less weight and eventually weight regain (Conceição *et al.*, 2014).

Overall, these outcomes suggest that although a considerable overlapping exists between binge eating disorder and food addiction, there are behavioral and theoretical features that differentiate both

pathologies. Thus, food addiction could be an identifiable clinical syndrome.

Furthermore, food addiction has also been associated with overweight and obesity. In humans, symptoms of food addiction are more prevalent among adults in the overweight and obese BMI categories (24.9%) compared to adults in the normal BMI category (11.1%) (Pursey *et al.*, 2014). It is reported that participants who met the YFAS criteria had higher lifetime BMI and this correlation was higher than participants only with binge eating disorder, bulimia nervosa or healthy controls (Gearhardt *et al.*, 2014). Moreover, numerous studies have described that individuals with obesity who meet criteria for food addiction have greater levels of eating disorder psychopathology, poorer general and health-related quality of life, greater depressive symptoms, and higher scores on impulsivity and self-control measures (Ivezaj *et al.*, 2016). A positive association between food addiction severity levels and impairments in decision-making and attentional capacity was found in individuals with obesity (Steward *et al.*, 2018). Together, these findings underscore the importance of studying the relationship between food addiction and obesity and compulsive eating as a potential transdiagnostic construct across eating-related disorders (Fernandez-Aranda *et al.*, 2018; Cassin *et al.*, 2019).

2.4. Food addiction: a controversial construct

The concept of food addiction has sparked much controversy among researchers and it is currently basically divided into three prevailing views:

1. There is enough scientific evidence to show that intake of certain foods, usually highly caloric and processed foods that contain a large amount of carbohydrates and/or fat, have an addictive potential producing similar behavioral alteration than drugs of abuse. Therefore, food addiction represents a substance use disorder (Ifland *et al.*, 2015; Schulte and Gearhardt, 2017).

2. Food addiction is not a valid concept because a specific addictive substance has not been identified in foods. Therefore, it may be the act of eating rather than the substance itself (food) which is addictive, suggesting that the term "eating addiction" which represents a behavioral addiction may be more appropriate (Hebebrand et al., 2014).

3. Neither food nor eating addiction represent valid concepts questioning the existence of underlying addictive processes when considering eating disorders and obesity (Finlayson, 2017; Rogers, 2017).

The statement that food addiction represents a substance use disorder is based on several studies that have produced evidence of biological and behavioral changes in response to highly palatable food that parallels addiction criteria (Ifland *et al.*, 2015; Schulte *et al.*, 2017). It is suggested that these changes are a result of the exposure to this kind of foods activating the mesolimbic reward-related pathway of the brain (N. D. Volkow *et al.*, 2011; Smith and Robbins, 2013; Lindgren *et al.*, 2018). A recent systematic review, examining the validity of food addiction, concluded that a large number of existing articles support food addiction as a diagnostic construct. Amongst the 35 articles (52 studies), the majority of them found evidence for symptoms related to brain reward dysfunction and impaired control, followed by evidence for supplemental characteristics consistent with addiction, including genetic susceptibility, substance sensitization and cross-sensitization, and impulsivity (Gordon *et al.*, 2018).

Not all foods are equally implicated in addictive-like eating behavior. Foods with added fat and refined carbohydrates such as sugar have been shown to be consumed in a more addictive manner and craved more intensely than less refined foods (Schulte *et al.*, 2015; Gordon *et al.*, 2018). It has been suggested that sugar could be regulated as a substance of abuse due to the negative health outcomes similar to reported in alcohol use disorder at individual and societal levels (Lustig *et al.*, 2012). However, some authors disagree in this point arguing that the evidence of sugar addiction remains unconvincing (Westwater *et al.*, 2016). On the other hand, data from human studies suggest that is

the combination of sweet and fat more than sugar itself, which is more associated with addictive symptoms (Markus *et al.*, 2017; Pursey *et al.*, 2017). Thus, a single macronutrient is not necessary for maladaptive eating, but rather the combination of macronutrients in highly palatable caloric food supraphysiological activates the brain reward circuitry modifying consummatory behaviors (Fletcher and Kenny, 2018).

On the contrary, some researchers are more cautious about the food addiction concept arguing that it should be more appropriate to call eating addiction and being classified as a behavioral disorder (Hebebrand *et al.*, 2014). This statement is based on the unconfirmed connotation about food contains chemical substances that can lead to the development of a substance use disorder. Behavioral addiction is not related to any substance of abuse although shares some features with substance-induced addiction (American Psychiatric Association, 2013). This argument is contradicted by other authors suggesting that the addictive-like behavior towards highly palatable food could involve both a behavior (eating) and a substance (food). A similar dichotomy has been also seen in other substance use disorders such as tobacco addiction (Gordon *et al.*, 2018). In the treatment of tobacco use disorder, behavioral modification is required due to the strong connection between the effects of the nicotine and the act of using it. Nonetheless, nicotine is the principal driver of the addiction and is therefore classified as a substance use disorder. In parallel to other substance use disorders, food addiction could involve both behavioral

and substance-related symptoms although the addictive of the highly palatable foods are more closely to criteria for substance use disorder (Gordon *et al.*, 2018).

Based on these controversies, critics and proponents agree that more research is needed. Therefore, the work presented in this thesis intends to provide new neurobiological evidence confirming the validity of food addiction as a substance use disorder. Nevertheless, it seems widely accepted that adopting an addiction perspective on food and eating has practical implications for the prevention and treatment of eating disorders and obesity (Meule, 2019).

3. Neurobiology of food addiction and eating disorders

3.1. Food intake control

The regulation of food intake comprises close relationships between homeostatic and non-homeostatic hedonic factors, which balance ensures the initiation and the maintenance of eating behavior (Onaolapo and Onaolapo, 2018). The homeostatic control or energy balance is regulated through the control exerted on both energy intake and energy expenditure that maintain body weight and metabolic function. Homeostatic and hedonic systems are activated during all feeding situations. The degree to which each process is activated may depend on the type of food and the physiological state of the subject (Rossi and Stuber, 2018). Reward-related signals can override homeostatic signals, mainly contributing to the consumption of additional foods above the body's energy requirement leading to eating disorders (Caron and Richard, 2017).

3.1.1. Homeostatic regulation of food intake

A complex physiological control system is involved in the maintenance of the energy balance. This system contains afferent signals from the periphery about the state of the energy stores and efferent signals from the brain that affect energy intake and expenditure (Sandoval *et al.*, 2008). This control is integrated by numerous interactions between the gastrointestinal tract, the adipose tissue, and the central nervous system and has influences from behavioral, sensorial, autonomic, nutritional and endocrine mechanisms (Abdalla, 2017).

Appetite control includes short-term and long-term regulation. The short-term signals determine the beginning and the end of a meal (hunger and satiation) and the interval between meals (satiety). The long-term signals arise from tissue stores (adipose tissue) and help to regulate the body energy depots finally coordinating our eating behavior (Abdalla, 2017).

3.1.1.1. Food intake cycle

After the ingestion of a meal, the gastrointestinal tract, containing chemo- and mechano- receptors, sends information to the brain about the amount of food ingested and its nutrient content via sensory input (vagus nerve to the nucleus of the solitary tract) providing the "satiety signals". After digestion, when nutrients have been metabolized in the peripheral tissue or crossed directly the blood-brain barrier, the long-term signals from adipose tissue signals reach the arcuate nucleus of the hypothalamus. Additionally, a large number of products from digestion and components responsible for their metabolism are integrated and converged in the brain informing about the metabolic state resulting from food consumption (Figure 4) (Hopkins *et al.* 2016).

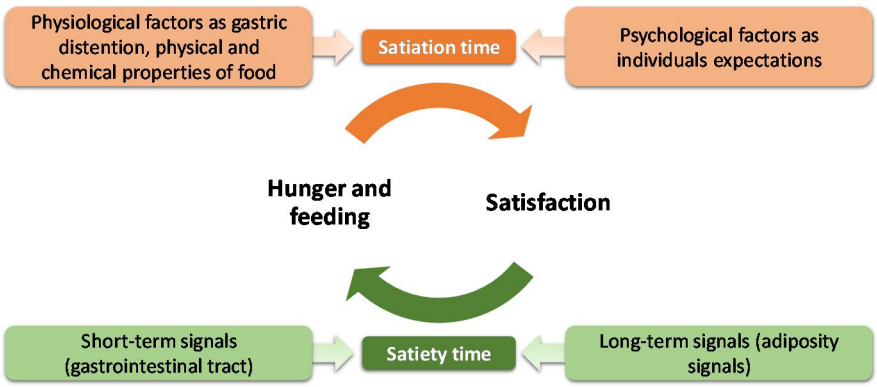

Figure 4. **Food intake cycle and its components** (Modified from Abdalla, 2017).

3.1.1.2. Central regulation

Hypothalamus and brainstem are essential parts of the homeostatic energy balance regulatory system.

The **hypothalamus** plays a major role in the appetite control being the relay center from afferent signals from gastrointestinal tract: sensory information about the filling of stomach, chemical signals of satiety from nutrients in the blood, signals from gastrointestinal hormones, hormonal signals from adipose tissue, and signals from the cerebral cortex (taste, smell and sight of the food). The hypothalamus processes all this information and sends efferent signals for the food intake control. Many nuclei are integrated into the hypothalamus: the arcuate nucleus, the paraventricular nucleus, the dorsomedial nucleus, the ventromedial nucleus and the lateral hypothalamic area (Wynne *et al.*, 2005).

In the **arcuate nucleus,** several hormones released from the gastrointestinal tract an adipose tissue converge to regulate food intake and energy expenditure. It contains two types of neurons that project to other hypothalamic areas involved in appetite control: neurons coexpressing neuropeptide Y and agouti-related peptide (AgRP) and neurons coexpressing pro-opiomelanocortin (POMC) - the precursor of melanocyte peptides stimulating hormone, α-, β-, γ- MSH - and cocaine- and amphetamine-regulated transcript (CART). The neuropeptide Y/AgRP positive neurons stimulate food intake whereas the POMC/CART positive neurons suppress feeding (Abdalla, 2017) (Figure 5).

The **lateral hypothalamus** performs the role of feeding center by initiating the motor drives to search for food (Rossi *et al.*, 2019). In contrast, the **ventromedial,** the **paraventricular** and the **dorsomedial** nucleus perform the role of satiety center (Mishra *et al.*, 2017). Specifically, the ventromedial nucleus receives POMC neuronal projections from the arcuate nucleus. POMC neurons from the arcuate nucleus play a role in activating BDNF neurons in the ventromedial nucleus to decrease food intake. Finally, the **dorsomedial nucleus** also contains a high level of neuropeptide Y and α-MSH terminals originating in the arcuate nucleus and its destruction results in hyperphagia and obesity (Abdalla, 2017) (Figure 5).

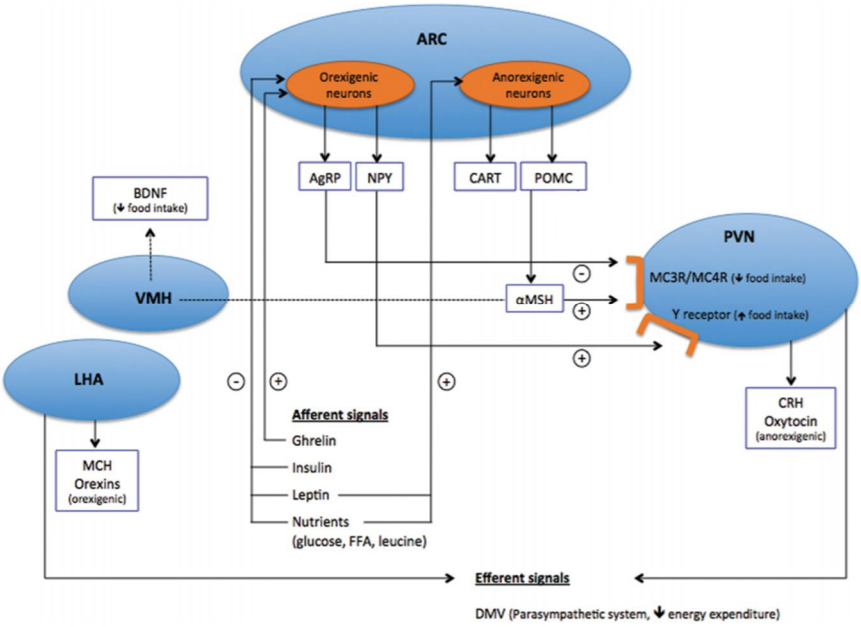

Figure 5. Simplified scheme of regulation of energy homeostasis by the hypothalamus. ARC, arcuate nucleus; PVN, paraventricular nucleus; VMH, ventromedial hypothalamus; LHA, lateral hypothalamic area; AgRP, agouti-related peptide; NPY, neuropeptide Y; CART, cocaine-amphetamine-related transcript; POMC, proopiomelanocortin; α-MSH, alpha-melatonin stimulating hormone; BDNF, brain-derived neurotrophic factor; MCH, melanin-concentrating hormone; CRH, corticotropin-releasing hormone; DMV, dorsal motor nucleus of the vagus (Haliloglu and Bereket, 2015).

3.1.1.3. Peripheral regulation

Peripheral signals including chemicals released by gastric stimuli, by food processing in the gastrointestinal tract and by adipose tissue are involved in the peripheral control of appetite (Mishra *et al.*, 2017). Many of them are peptide neurotransmitters which receptors are highly expressed in the hypothalamic feeding and satiety centers. These neurotransmitters are generally classified as:

- **Orexigenic substances that stimulate feeding:** neuropeptide Y, AgRP, melatonin concentrating hormone, orexin A and B, endorphins, ghrelin, cortisol, among others.

- **Anorexigenic substances that inhibit feeding:** α-MSH, leptin, serotonin, CRH, norepinephrine, insulin, glucagon-like peptide, cholecystokinin, CART, peptide YY, among others.

Energy homeostasis depends on brain reliability to integrate and generate an adequate response to these peripheral hormonal and nutritional signals. The main hormones affecting food intake include ghrelin, an orexigenic peptide, and the anorexigenic hormones insulin and leptin (Abdalla, 2017). Briefly:

- **Ghrelin** is an orexigenic gut peptide secreted mainly from the stomach. It is considered the "hunger" hormone responsible for meal inhibition due to its pre-pandrial elevation whereas these levels fall after meals. It is involved in the short-term regulation of food intake and long-term regulation of body weight through decreasing fat utilization (Castañeda *et al.*, 2010).

- **Insulin** is a peptide secreted from beta cells of the pancreas. It is involved in glucose metabolism stimulating glucose uptake by peripheral tissues. Insulin also

circulates in the bloodstream in proportion to white fat deposits serving as a sensor of body fat content to the hypothalamus (Considine *et al.*, 1996). Insulin receptors can be broadly found in the arcuate nucleus of the hypothalamus together with anorexigenic POMC and orexigenic NPY/AgRP expressing neurons. Insulin inhibits NPY/AgRP peptide production in the ARC while enhancing POMC expression (Dodd and Tiganis, 2017).

- **Leptin** is a peptide secreted mainly by the adipose tissue and has a key role in the energy homeostasis (Klok *et al.*, 2007). The levels of leptin in the blood positively correlated with the amount of body fat. During periods of fasting, leptin secretion is reduced and after meals is increased (Friedman, 2004). Leptin produces its anorexigenic effect in the arcuate nucleus via inhibition of neuropeptide Y/AgRP neurons and activation of POMC/CART neurons leading to reduced food intake and increased energy expenditure (Abdalla, 2017).

The inability to detect energy-storage fluctuations due to inadequate sensing of metabolic signals has been associated with obesity (Caron and Richard, 2017). Several studies have shown that obesity causes profound changes to the energy balance centers of the hypothalamus which results in the loss of central leptin (Volkow *et al.*, 2013) and insulin sensitivity (Williams, 2012). Moreover, obesity-induced central

ghrelin resistance in neural circuits regulating behavior, and impaired ghrelin secretion from the stomach (Zigman *et al.*, 2016).

3.1.2. Hedonic regulation of food intake

The decision to eat is not only influenced by the internal homeostatic signals but also by non-homeostatic factors, such as food palatability and environmental cues, contributing to the hedonic feeding (Volkow *et al.*, 2013; Kure Liu *et al.*, 2019). In the **hedonic regulation**, the corticolimbic appetite network plays a crucial role. This network includes cortical areas constituting the executive system and subcortical limbic regions forming the reward system that all together exert a decisional control on food intake (Caron and Richard, 2017).

3.1.2.1. The brain executive system and the decision to eat

The brain executive system integrates the activity of the prefrontal cortex (PFC) and is essential for conscious and voluntary eating. This system is influenced by the adjacent somatosensory, gustatory and olfactory cortices that collect the sensory information from the oral cavity and digestive tract associated with the organoleptic properties of food. The dysfunction of the executive system causes impulsive behaviors leading to eating disorders and obesity (Caron and Richard, 2017).

3.1.2.2. The brain reward system and the desire and pleasure to eat

The brain executive system interacts with both adjacent cortical areas and with subcortical limbic structures establishing the motivational and the pleasure value of food. The main neurotransmitter implicated in

this reward system is DA (Solinas *et al.*, 2018). Food intake enhances DA release in this circuit mediating the pleasurable aspects of the eating (N. D. Volkow *et al.*, 2011).

In the limbic circuit, two interconnected components of the brain DA reward circuitry are clearly involved: the ventral tegmental area (VTA) and the nucleus accumbens (NAc). These two areas express peptides and hormonal peripheral receptors, such as glucagon-like peptide -1, ghrelin, leptin, insulin, orexin, and melanocortin receptors (Volkow *et al.*, 2013). Therefore, several hormones and neuropeptides involved in energy homeostasis are directly modulating the DA reward system indicating an important cross-talk between the homeostatic and hedonic systems.

In the VTA, leptin inhibits DA neuron activity and decreases food intake (Domingos *et al.*, 2011), whereas ghrelin increases VTA DA activity and promotes food intake (Skibicka *et al.*, 2011). Both direct modulation of VTA DA neurons by hormones and inputs to VTA from brain areas involved in metabolic functions are implicated in this regulation. An example of this regulation is the lateral hypothalamus that provides major direct innervation of VTA. Optogenetic stimulation of the lateral hypothalamus-VTA projection produces a compulsive sugar seeking behavior despite negative consequences (Nieh *et al.*, 2015). On the other hand, the metabolic signals from the hypothalamus to the NAc modulate the motivation, whereas the direct and indirect projection from NAc to the hypothalamus may explain the capability of the

mesolimbic processes to hijack the homeostatic regulatory circuits and drive up energy intake (Hopkins *et al.* 2016).

In the reward system, the NAc DA signaling integrates the incentive salience of food-related stimuli ("**wanting**") and hedonic ("**liking**") aspects of the rewarding process associated with eating. The circuits implicated in food wanting and liking are the same as those implicated in drug intake (Volkow *et al.*, 2017). These responses are controlled by the DA projections from the VTA (Caron and Richard, 2017). Liking and wanting seem to have separate roles in promoting food overconsumption. In terms of liking, some individuals with risk of weight gain experience an exaggerated hedonic response to palatable foods (enjoy more the food). Processes of wanting may enhance the vulnerability to augment body weight through increased reactivity towards cues signaling the availability of food. Thus, liking seems important in establishing the motivational properties of food, but once these are retained it is the up-regulation of wanting in an obesogenic environment "insensitivity to homoeostatic signals but over-reactivity to external cues" that promotes overconsumption (Hopkins *et al.* 2016).

Therefore, the NAc is a critical brain node between the cortical executive system and the autonomic hypothalamic circuits. The NAc integrates information from the PFC and gustatory circuits as well as signals emerging from viscera. NAc also sends reward-related information to the lateral hypothalamus, which in turn receives learning-related inputs from the hippocampus and amygdala and is a

key modulator of the mesocorticolimbic dopaminergic pathway (Figure 6).

3.1.3. Dysregulation of food intake control in highly palatable food exposure

As it has mentioned above, there are multiple signaling pathways that ensure that food is consumed when needed. The consumption of "standard" food mainly generates information on its energy content through different peripheral signals that are transported via afferents of the vagus nerve to the nucleus of the solitary tract and through receptors located in the hypothalamus and other autonomic and limbic brain regions causing consumption to cease. However, a different scenario is apparent with repeated access to highly palatable food. With the ingestion of palatable food, taste sensing is different than with standard food. Indeed, information is transmitted to the reward circuit, leading to the activation of reward mediators like DA, endocannabinoids, and endogenous opioids. The reward circuit connections with appetite-controlling neurons in the hypothalamus increase the expression of hunger peptides such as neuropeptide Y and orexins while blunting the signaling of satiety peptides like insulin, leptin, and cholecystokinin. Therefore, some individuals may eventually override the inhibitory processes that signal satiety when food is highly palatable and begin to consume compulsive large amounts of food despite biological needs. This loss of control and compulsive pattern of food intake is similar to the drug intake patterns

seen in addiction and has led to the description of obesity as a form of food addiction (Figure 6) (Hopkins *et al.* 2016; Volkow *et al.*, 2013a).

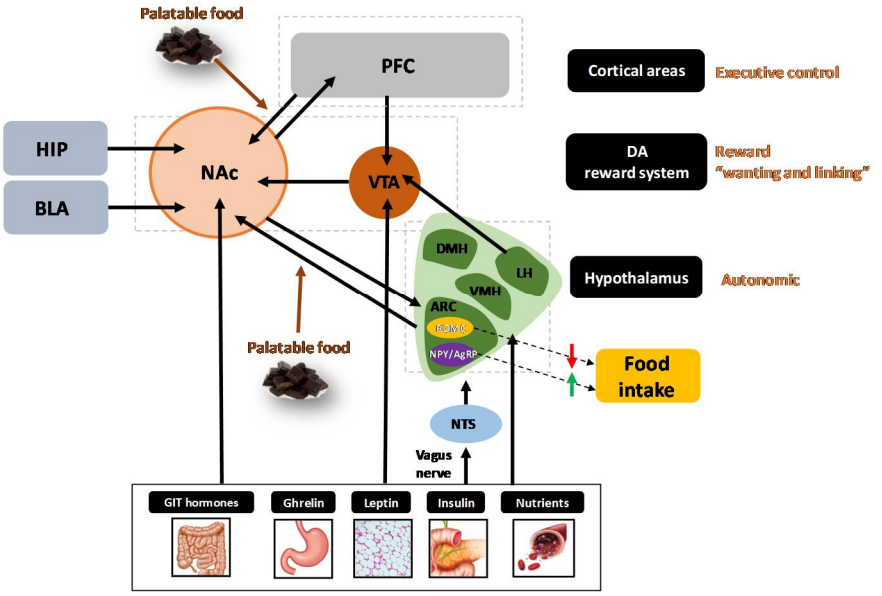

Figure 6. **Schematic representation of the highly interconnected system that affects the intake of food.** It includes food-responsive peptides and hormones, energy homeostatic structures in the hypothalamus, the core of the dopamine (DA) reward system in the nucleus accumbens and ventral tegmental area, and various cortical areas in charge of processing affect, motor, and cognitive information. NTS, nucleus solitary tract; ARC, arcuate nucleus; DMH, dorsomedial nucleus; VMH, ventromedial nucleus; LH, lateral hypothalamic area; NAc, nucleus accumbens; PFC, prefrontal cortex; VTA, ventral tegmental area; HIP, hippocampus; BLA, basolateral amygdala; GIT, gastrointestinal tract. (Modified from Volkow *et al.*, 2013a; Caron and Richard, 2017).

3.2. The brain's reward circuitry

The rewarding effect produced by natural rewards such as food, water, and sex is a consequence of their action in the brain reward system. Within this system, the **mesolimbic pathway**, comprising dopaminergic neurons in the VTA that project to NAc has a key role in the **positive reinforcement**. The VTA-NAc pathway mediates the recognition and the evaluation of rewards in the environment and the promotion of goal-directed behavior, resulting in the acquisition of the reward and the initiation of their consumption (Koob and Le Moal, 2008). Importantly, this endogenous system is also recruited by all drugs of abuse to exert their rewarding effects. Early work has shown that all known drugs of abuse increase extracellular levels of DA in the NAc (Di Chiara and Imperato, 1988) and other studies suggested that DA critically contributes to the codification of the motivational value and silence of a given stimulus (Bromberg-Martin *et al.*, 2010).

Additionally, the DA VTA neurons also innervate other areas of the limbic system, including several regions of the PFC, amygdala (central and basolateral parts) and hippocampus among others. All these regions are interconnected involving glutamatergic, GABAergic, cholinergic and dopaminergic transmission leading to a highly complex network (Figure 7). Brain reward regions have been assigned to specific behavioral functions. Thus, frontal cortical regions mediate control of executive functions, amygdala contributes to the formation of associative reward- and fear-related memories, and hippocampus is crucial for declarative memory functions. Therefore, the sensory and

emotional information coming from each of these limbic circuitries are converged and integrated into the NAc, which in turn activate and/or inhibit extrapyramidal motor systems to produce motivational actions (Russo and Nestler, 2013; Parsons and Hurd, 2015).

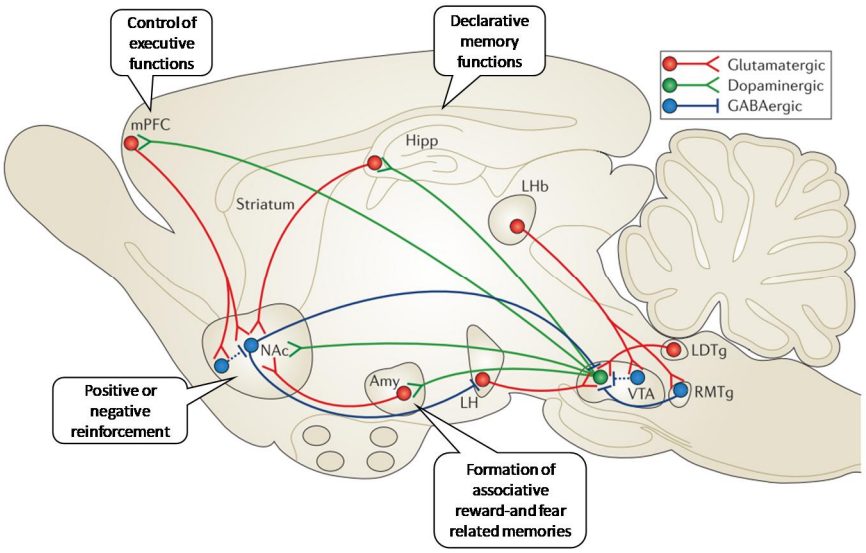

Figure 7. The mesocorticolimbic system circuitry. A simplified schematic diagram of the mesocorticolimbic system circuitry in rodent brain highlighting the major dopaminergic, glutamatergic and GABAergic connection to and from the ventral tegmental area (VTA) and nucleus accumbens (NAc). Amy, amygdala; Hipp, hippocampus; LH, lateral hypothalamus; mPFC, medial prefrontal cortex; LHb, lateral habenula; LDTg, lateral dorsal tegmentum; RMTg, rostromedial tegmentum (Adapted from Russo and Nestler, 2013).

On the other hand, these same circuits also contribute to the **negative-reinforcement** mechanism that promotes behaviors for avoiding aversive states. Exposition to aversive conditions such as chronic pain, unavoidable shock, certain patterns of over or under-eating, and withdrawal from addictive drugs produces a decrease of DA levels in the NAc contributing to aversive states. The role of the NAc in aversive states is supported by pharmacological studies in which manipulation

of this area produces aversion (Carlezon and Thomas, 2009). Importantly, negative reinforcement mechanisms related to palatable food or long-term drug abstinence are mediated in part by stress signaling systems involving the extended amygdala (Parsons and Hurd, 2015).

To better understand this complex circuitry, the cytoarchitecture, the microcircuitry and the principal connections of the main brain reward regions in aspects relevant to food addiction, learned from drug addiction, are summarized in this section.

3.2.1. Ventral tegmental area

The VTA is a heterogeneous brain area composed by dopaminergic projection neurons (~60%), GABAergic interneurons and GABAergic projection neurons (~30-35%), and a smaller proportion of glutamatergic neurons (2-3%) (Margolis *et al.*, 2012). Dopaminergic neurons express tyrosine hydroxylase and release DA, although there are some dopaminergic neurons that coexpress both tyrosine hydroxylase and the GABA synthesizing enzyme glutamic acid decarboxylase 65Kd isoform (GAD65) releasing GABA together with DA in the synapses, resulting in an inhibition of the activity of the NAc (Tritsch *et al.*, 2012). Conversely, a subset of dopaminergic neurons coexpresses both tyrosine hydroxylase and the vesicular glutamate transporter 2 leading to the release of glutamate together with DA (Yamaguchi *et al.*, 2011). These findings highlight the complexity of VTA cytoarchitecture.

The VTA has two principal DA output pathways, one projecting to the NAc (mesolimbic) and other projecting to the PFC (mesocortical) and additional regions, including amygdala and hippocampus. Most studies have focused on the mesocorticolimbic pathways since the stimulation of these DA neurons with the subsequent release of DA in projection sites (notably in NAc), produces reinforcement. This reinforcement is modulated by GABAergic projection from VTA to NAc and lateral habenula (Stamatakis *et al.*, 2013) (Figure 8).

The VTA receives excitatory inputs from several brain regions including glutamatergic projections from the laterodorsal tegmental nucleus, the lateral habenula, and the PFC. The projections from the laterodorsal tegmental nucleus preferentially synapse on DA VTA neurons projecting to NAc and its activation triggers reward. In contrast, enhancing glutamatergic lateral habenula neurons that innervate DA VTA neurons projecting to PFC induce aversive behavior (Lammel *et al.*, 2012). Moreover, the VTA receives inhibitory inputs of GABAergic projections from the rostromedial tegmental nucleus or "tail" of the VTA exerting an inhibitory control over DA VTA-NAc pathway (Cooper *et al.*, 2017). The rostromedial tegmental nucleus activity is enhanced by the excitatory projections from lateral habenula and decreased glutamate levels in the rostromedial tegmental nucleus reduce the release of GABA in the VTA disinhibiting the DA VTA-NAc neurons promoting reward (Pistillo *et al.*, 2015). Other brain regions, such as the NAc, amygdala, ventral pallidum and lateral hypothalamus also send projections to the VTA conforming with the explained afferents

and efferents a complex local microcircuit inside the mesocorticolimbic circuit (Figure 8).

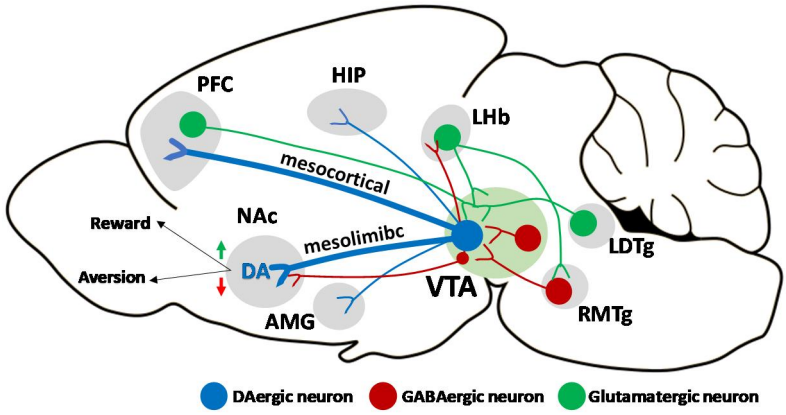

Figure 8. **Schematic representation of the complex VTA microcircuitry showing the main outputs and inputs of this area**. PFC, prefrontal cortex; HIP, hippocampus; LHb, lateral habenula; LDTg, laterodorsal tegmental nucleus; RMTg, rostromedial tegmental nucleus; VTA, ventral tegmental area; AMG, amygdala; NAc, nucleus accumbens (Adapted from Cooper *et al.*, 2017).

3.2.2. Nucleus accumbens

The NAc is a major component of the ventral striatum and mediates motivation and reward-related behaviors constituting a key node of the mesolimbic dopamine circuitry. The NAc is divided into two functional subregions known as the core (central part) and the shell (surrounding medially, ventrally and laterally the core) with different anatomical connectivity and presumed behavioral roles (Figure 9). The **core** has been thought to be responsible for the acquisition of reward–cue associations, responses to motivational stimuli, impulsive choices and initializing motor actions, whereas the **shell** has been proposed to

be more involved in reward prediction, affective processing and drug relapse (Di Chiara, 2002; Salgado and Kaplitt, 2015) (Figure 9).

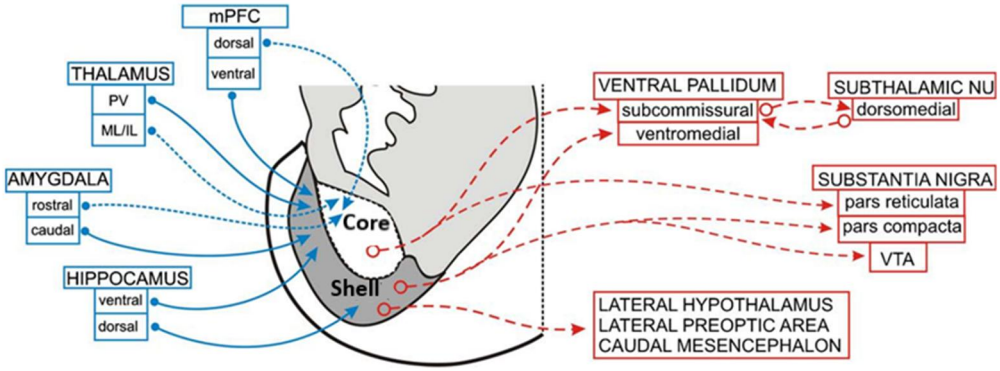

Figure 9. **Schematic diagram of the inputs and outputs of the shell and core of the nucleus accumbens**. Dopaminergic, serotonergic, and noradrenergic inputs have been omitted from the drawing. ML/IL, midline and intralaminar thalamic nuclei; mPFC, medial prefrontal cortex; PV, paraventricular thalamic nucleus; VTA, ventral tegmental area (Basar *et al.*, 2010).

The principal population of neurons in the NAc consists of GABAergic medium spiny neurons (MSNs) comprising ~95% of the total cells located in this area, the remaining ~5% is composed by GABAergic and cholinergic interneurons. The MSNs are largely subdivided into two subtypes based on the preferentially DA-like receptors that they expressed: dopamine type-1 receptor (D_1R)-expressing MSN that also contains dynorphin and D_2R-expressing MSN that also contains enkephalin.

In the **dorsal striatum,** the D1-MSNs form the direct striatonigral pathway (ultimately increasing thalamocortical drive) whereas the D2-MSNs constitute the indirect striatopallidal pathway (ultimately decreasing thalamocortical drive) (Klawonn and Malenka, 2019). **Direct**

pathway MSNs extend axonal projections to the internal part of the globus pallidus (GPi) and the substantia nigra pars reticulata (SNpr) inhibiting the GABAergic neurons in these areas. This inhibition of the SNpr leads to a disinhibition of the thalamic glutamatergic neurons, which receive SNpr input and project to the cortex promoting movement. Conversely, **indirect pathway MSNs** project indirectly to the SNpr via the external part of the globus pallidus (GPe) and the subthalamic nucleus. The inhibition of the GABAergic projections to the subthalamic nucleus from GPe results in a disinhibition of the glutamatergic projections from the subthalamic nucleus area to the SNpr/GPi output nuclei. Finally, the activation of the GABAergic neurons in SNpr/GPi inhibits the thalamus reducing movement (Gerfen and Surmeier, 2011) (Figure 10). This is the classic model widely studied in the dorsal striatum. Recent reports revealed that this model is oversimplified and propose a model in which the two pathways are functionally and structurally intertwined due to intrastriatal connections (Calabresi *et al.*, 2014). Accordingly, a similar organization as in the dorsal striatum has been assumed in the NAc of the **ventral striatum**, but with the ventral pallidum instead of the GPe as a relay station in the D2-MSN indirect pathway. It has not been yet clarified if the ventral pallidum projects to the subthalamic nucleus or directly to the VTA/SNpr. Some authors suggested that projections from the basal ganglia to the subthalamic nucleus derive largely from the GPe and not include the ventral pallidum (De Deurwaerdère *et al.*, 2013; Mannella *et al.*, 2013; Hamani *et al.*, 2017) (Figure 10).

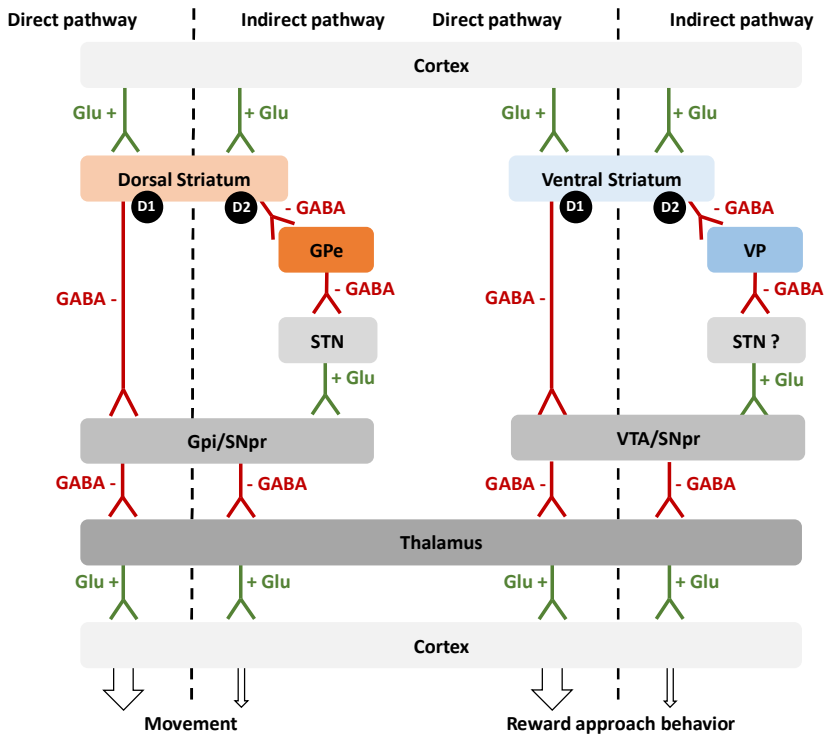

Figure 10. **Schematic representation of the canonical view for the direct and indirect pathway in the dorsal striatum (left) and ventral striatum (right)**. GPe and GPi, external and internal globus pallidus; VP, ventral pallidum; SNpr, substantia nigra pars reticulata; STN, subthalamic nucleus; D1 and D2 dopaminergic receptors. Excitatory projections in green and inhibitory projections in red (Adapted from Gerfen and Surmeier, 2011; Mannella *et al.*, 2013).

However, current research suggested that the classic dichotomy between the roles of D1-MSNs and D2-MSNs in the NAc must also be questioned. Recent works using optogenetics and tracing tools found that a significant proportion of D1-MSNs project to the ventral pallidum comprising the classical indirect pathway while some D2-MSNs project directly to the thalamus comprising the defined direct pathway (Figure 11). Thus, D1 MSNs projecting to the ventral pallidum could participate in an "indirect pathway"-like manner, whereas D2 MSNs could be

involved in a "direct pathway"-like manner, highlighting the ventral pallidum as a central hotspot of the reward circuitry (Kupchik *et al.*, 2015; Kupchik and Kalivas, 2017; Klawonn and Malenka, 2019).

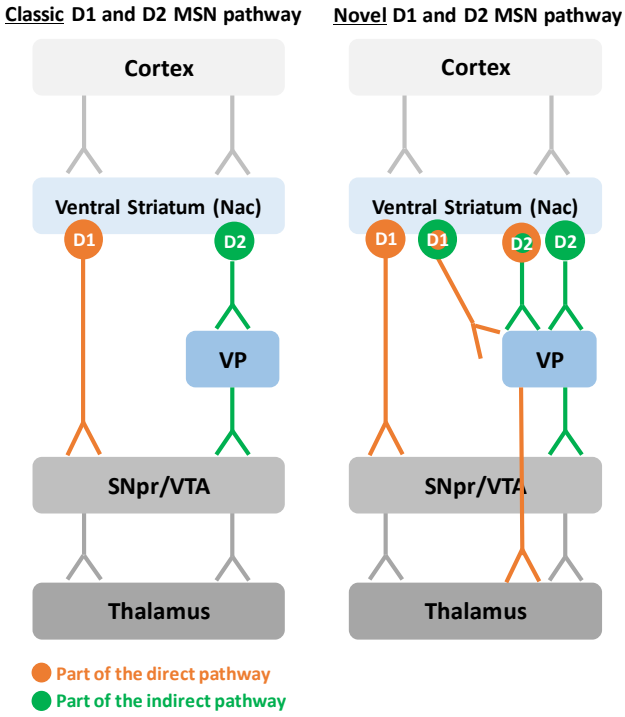

Figure 11. **Schematic diagram of NAc D1 and D2 MSN anatomical connectivity emphasizing the differences between the classic conceptualization of indirect and direct pathways and a novel view.** NAc, nucleus accumbens; VP, ventral pallidum; SNr, substantia nigra pars reticulata; VTA, ventral tegmental area. (Adapted from Kupchik *et al.*, 2015; Klawonn and Malenka, 2019).

Therefore, the major efferents of the NAc are to the ventral pallidum and other brain areas, such as substantia nigra, VTA, hypothalamus, and brainstem. Accurately examination reveals the presence of two distinct dopaminergic NAc-ventral pallidum circuits based on the NAc topography. The NAc core projects primarily to the dorsolateral portion

of the ventral pallidum, which in turns projects to subthalamic nucleus and SNpr forming the dopaminergic innervation of the striatum. The shell mainly innervates the ventromedial ventral pallidum division, which contains reciprocal connection with the PFC and the VTA, sending dopaminergic projections to mesocortical sites (Salgado and Kaplitt, 2015) (Figure 12).

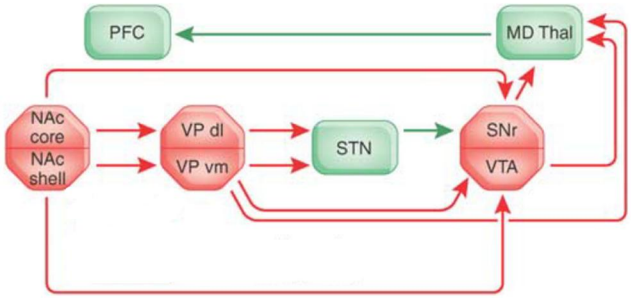

Figure 12. **Distinct dopaminergic nucleus accumbens-ventral pallidum circuits based on NAc topography.** Only major projections are shown. Red indicates inhibitory structures and pathways, whereas green indicates excitatory connections. MD Thal, mediodorsal thalamic nucleus; NAc, nucleus accumbens; PFC, prefrontal cortex; SNr, substantia nigra zona reticulata; STN, subthalamic nucleus; VP dl/vm, ventral pallidum, dorsolateral, and ventromedial; VTA, ventral tegmental area (Adapted from Sesack and Grace, 2010).

The NAc shell projections to the VTA create long-loop feedback that regulates DA neurons activity indicating that the modulation of MSNs NAc activity is bidirectional (Carr *et al.*, 2000; Xia *et al.* , 2011; Yang *et al.*, 2018). Recent studies demonstrate that NAc neurons synapse onto both VTA GABA and DA neurons in the VTA forming an indirect and direct feedback loop. With respect to the **direct loop**, the MSNs in the medial part of the NAc shell directly inhibit DA VTA neurons suppressing behavioral output. In the **indirect loop**, MSNs from the lateral part of the NAc shell synapse with VTA GABAergic neurons,

leading to disinhibition of DA neurons projecting back to the NAc lateral shell (Figure 13). Activation of this NAc pathway increases firing of the VTA DA neurons that enhance reward-related bursting and could mediate the maladaptive increased DA activity produced by drugs of abuse (Yang *et al.*, 2018). This ascending spiral allows limbic associated structures to influence transmission in successively more motor-related parts of basal ganglia (NAc to dorsal striatum) (Klawonn and Malenka, 2019).

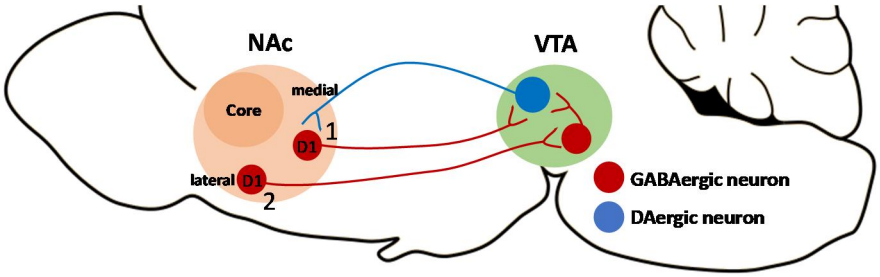

Figure 13. **Simplified diagram of the feedback connectivity between NAc and VTA. (1) The direct feedback loop** in which medial shell NAc D1 MSNs synapse on medial VTA DA neurons that project back to the medial NAc suppressing behavioral output. **(2) The indirect feedback loop** in which medial shell NAc D1 MSNs synapse on medial VTA DA neurons that project back to the medial NAc promoting reward-related behaviors. NAc, nucleus accumbens; VTA, ventral tegmental area (Based on Yang *et al.*, 2018).

The NAc MSNs in addition to the VTA receives inputs from other cortical and subcortical structures, such as the PFC, amygdala, hippocampus, and thalamus (Sesack and Grace, 2010). These inputs project to specific cellular targets within NAc subregions transferring different types of information. There is evidence that a single MSN receives inputs from several afferents structures (Stuber *et al.*, 2012).

Overall, these findings suggest that the NAc is a critical node of circuitry that translates motivation to action, although the specific neurobiological mechanism underlying this behavior is not well understood. Further studies considering the connectivity of individual populations of MSNs based on their anatomical localization, the targets to which they project, and their molecular properties are needed.

3.2.3. Prefrontal cortex

The PFC is a brain area involved in several executive functions including regulation of cognitive, emotional and motivational processes. Among all these functions are those associated with control behavior: such as response inhibition, planning, attention, and decision-making (Miller and Cohen, 2001). Dysregulation of these functions leads to a loss of self-control driving to compulsive food intake, drug use and addiction (Goldstein and Volkow, 2011).

The cytoarchitecture of the mPFC consists mainly of excitatory glutamatergic pyramidal projection neurons, which represent 80% of the total population, and GABAergic inhibitory interneurons representing the remaining 20%. Both can be subdivided into different cell types based on morphological, physiological and molecular properties. Specifically, **pyramidal neurons** located in layer (L) V of the mPFC can be divided in two subtypes: thick tufted, subcortically projecting cells and thin tufted, colossally projecting cells. On the other hand, two types of **interneurons** have been described: the perisomatic targeting fast-spiking parvalbumin interneurons and the dendritic

targeting non-fast spiking somatostatin interneurons (Figure 14). Both interneurons types exert strong control over local circuitry. While fast-spiking interneurons tonically inhibit pyramidal neurons, the non-fast spiking interneurons are involved in modulating the activity of fast-spiking interneurons (Druga, 2009). Optogenetic studies revealed that subcortically projecting pyramidal neurons are preferentially inhibited by fast-spiking parvalbumin interneurons (Anthony T. Lee *et al.*, 2014; Dembrow and Johnston, 2014). Interestingly, recent studies provided evidence for the first time for the existence of GABAergic projection neurons from the mPFC to subcortical structures, such as NAc, transmitting aversive signals (A. T. Lee *et al.*, 2014).

The mPFC has a **laminar organization** similar to other parts of the cortex. The pyramidal neurons located in LII, III, V and VI extend their axons vertically towards the deep layers of the cortex and project their apical and basal dendrites respectively to the more superficial and deep layers. The pyramidal neurons located in superficial layers (LII/III) are mainly cortico-cortical neurons taking part in intracortical circuits with other pyramidal and GABAergic neurons. In contrast, the pyramidal neurons located in deep layers (LV/VI) project to subcortical areas including VTA and NAc. Furthermore, pyramidal neurons in LV and VI receive projections from VTA DA neurons, while pyramidal neurons in LII, III and V receive functional inputs from other cortical areas, thalamus, BLA and hippocampus (Figure 14).

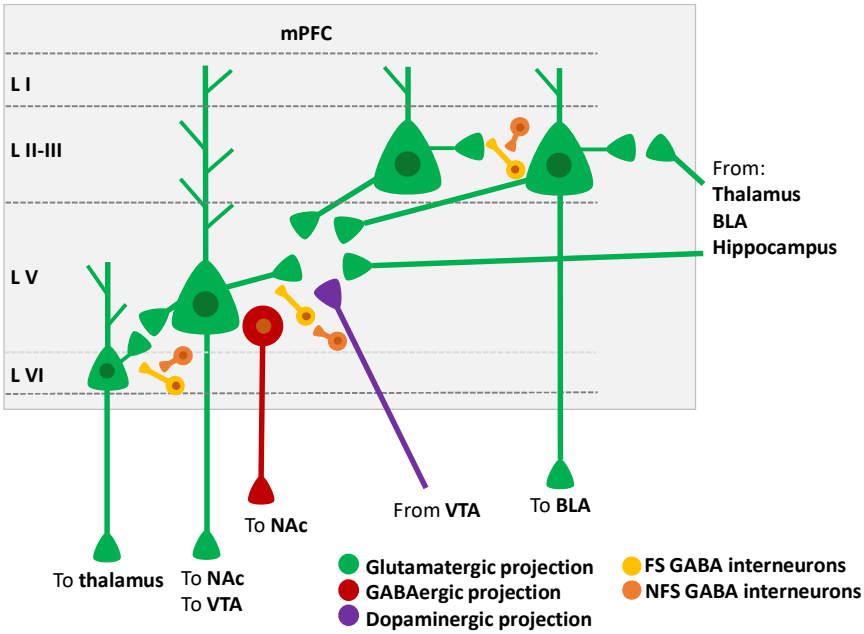

Figure 14. Simplified diagram of the connectivity in the mPFC. The pyramidal neurons in superficial layers (LII/III) are mainly cortico-cortical neurons. The pyramidal neurons in deep layers (LV /VI) are cortico-subcortical neurons manly projecting to VTA and NAc. Pyramidal neurons in LV and VI receive projections from VTA DA neurons while pyramidal neurons in LII, III and V receive functional inputs from other cortical areas, thalamus, BLA and hippocampus. NAc, Nucleus accumbens; VTA, ventral tegmental area; BLA, basolateral amygdala; FS, fast-spiking, NFS, non-fast spiking (Adapted from Pistillo *et al.*, 2015).

Thus, mPFC integrates and relay information from several structures and may evaluate the salience and motivational significance of food- and drug-associated contexts and stimuli (Carr *et al.*, 2000; Douglas and Martin, 2004).

Within the rodent mPFC, different **areas** can be defined along a dorsal to the ventral axis: the medial precentral area, the anterior cingulate cortex, the prelimbic cortex (PL), the infralimbic cortex (IL) and the ventral orbital cortices. These structures are usually grouped in a dorsal

component (dmPFC) encompassing the anterior cingulate cortex and PL, and in a ventral component (vmPFC) containing the IL and ventral orbital cortex (Heidbreder and Groenewegen, 2003). Although the mPFC subregions are reciprocally interconnected, the dorsal and ventral portions of the rodent mPFC have dissociable connectivity with several key regions implicated in addiction. Indeed, the **dorsal mPFC (PL)** projects predominantly to NAc core, central and basolateral (BLA) amygdala, whereas the **ventral mPFC (IL)** innervates almost exclusively the NAc shell, medial, basomedial, central and cortical nuclei of the amygdala. The two subregions of the mPFC also differ in their patterns of cortico-cortical, cortico-thalamus and cortico-hypothalamus connectivity (Figure 15). This clear segregation between PL versus IL is an imperfect approach. Indeed, ventral regions of the PL tend to innervate both core and shell regions of the NAc as do dorsal parts of the IL, indicating that mPFC projections typically follow a dorsal-ventral gradient (Figure 15c). However, the anatomical, neurochemical and functional differences support the view that the PL and IL mPFC have dissociable roles in various behaviors, including goal-directed behavior and drug seeking (Jasinska *et al.*, 2015; Moorman *et al.*, 2015).

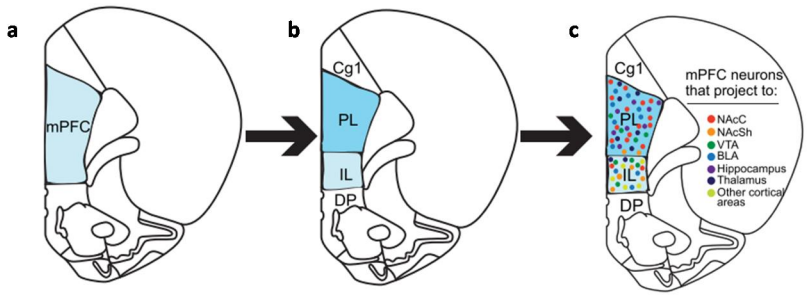

	Striatum	Amygdala	Cortex	Thalamus	Hypothalamus	Brainstem
PL projections	• NAc core • NAc shell (ventral) • Caudat-putamen	• CeA • BLA	• ACC • PL • IF • MO • Insular cortex	• MD • IMD • PVT	• PF • LH	• VTA • SN • LC • PAG • Raphe
IL projections	• NAc shell • Caudat-putamen	• Medial • Basomedial • Cortical • CeA	• ACC • PL • IF • MO • Insular cortex • Piriform cortex • Entorhinal cortex	• MD • IMD • PVT	• DMH • LH • PF • PH	• VTA • SN • LC • PAG

Figure 15. Schematic summarizing the projections of PL and IL to reward-related regions. (a) mPFC as a unified structure. (b) Structural distinctions within the mPFC. (c) mPFC projections typically follow a dorsal-ventral gradient. ACC, anterior cingulate cortex; BLA, basolateral amygdala; CeA, central amygdala; IL, infralimbic cortex; IMD, intermediodorsal thalamus; LC, locus coeruleus; LH; lateral hypothalamus; MD, mediodorsal thalamus; MO, medial orbital cortex; NA, nucleus accumbens; PAG, periaqueductal gray; PF, perifornical area of the hypothalamus; PH, posterior hypothalamus; PL, prelimbic cortex; PVT, paraventricular thalamus; SN, substantia nigra; VTA, ventral tegmental area. (Adapted from Moorman *et al.*, 2015).

The classical functional dichotomy between PL and IL postulates that the PL area promotes natural and drug reward seeking, whereas the IL inhibits it. As a consequence, the PL area plays an important role in executing behaviors, while IL appears to be more involved in response inhibition (Moorman *et al.*, 2015). Studies using drug self-administration reinstatement paradigms, support this model reporting that the pharmacological inactivation of **PL** effectively blocks stress,

drug-priming and cue-induced reinstatement of cocaine seeking (McFarland and Kalivas, 2001; Moorman *et al.*, 2015). Similar to pharmacological inactivation, photoinhibition of PL neurons attenuated cocaine and cocaine-prime induced reinstatement (Stefanik *et al.*, 2013) and decreases stress-induced relapse of palatable food seeking (Calu *et al.*, 2013). On the other hand, several studies indicated the involvement of **IL** in the suppression of cocaine seeking, since IL inactivation enhanced lever pressing in late extinction of cocaine self-administration (Peters *et al.*, 2008b). Conversely, activation of this region with glutamate agonists following extinction suppressed cocaine-induced reinstatement (Peters *et al.*, 2008a).

However, the model that PL serves to promote behavior and IL suppress it represents an overly simplistic framework. Compelling evidence suggested that PL has an inhibitory role in regulating reward-seeking behaviors. Pharmacological inactivation of the PL, using GABA receptor agonists, reduced the ability of a footshock-associated conditioned stimulus to decrease cocaine responding (Limpens *et al.*, 2015). Interestingly, PL inactivation also increased punishment resistance in animals responding for sucrose, indicating that PL is necessary for punishment-induced suppression of responding for both drug and natural rewards (Limpens *et al.*, 2015). Furthermore, it has been demonstrated that prolonged cocaine self-administration decreased the excitability of PL pyramidal neurons using a model of self-administration with punishment-conditioning in which rats were first exposed to an extended drug-self administration training followed

by aversive footshock associated with drug-infusion. This reduction was more pronounced in shock-resistant rats than those sensitive to the punishment. This endophenotype in punishment resistant rats was restored using optogenetic stimulation of PL decreasing responding for cocaine during footshock sessions (Chen *et al.*, 2013). This result is supported by the finding that photoinhibition of PL pyramidal neurons enhanced cocaine self-administration and attenuated reinstatement of cocaine-seeking in rats that were subjected to a high-frequency cocaine intake schedule (Martín-García *et al.*, 2014).

Similarly, the IL is not only responsible for suppression seeking behavior. Indeed, IL inactivation attenuated cocaine prime-induced reinstatement and rats with an IL-lesioned exhibited a decreased reinstatement after cocaine abstinence (Pelloux *et al.*, 2013). With respect to natural rewards, IL inactivation decreased food pellet seeking and had no effect on the expression of extinction (Sangha *et al.*, 2014).

These apparent conflicting findings of the role of the PL and IL mPFC in drug seeking could be answered by key methodological differences between the two main experimental paradigms used. PL appears to facilitate behavior of drug seeking during traditional self-administration and reinstatement paradigms, whereas appears to suppress behavior during self-administration with punishment conditioning paradigms. Regarding reinstatement models, the mPFC manipulations are following a cocaine extinction when the effects of cocaine have ceased. This timing is important because at this point DA

transmission is at normal or even reduced levels. In contrast, the mPFC manipulations in self-administration with punishment-conditioning paradigms, are performed in the course of cocaine delivery when DA neurotransmission is enhanced to supraphysiological levels by the cocaine action.

Human studies have provided clues in clarifying these conflict results. Although the homology between human and rodent PFC is not completely understood, it is now accepted that the mPFC is relatively comparable across species taking into account similarities in connections and functions (Jasinska *et al.*, 2015). The human dorsolateral PFC (dlPFC) is equivalent to the rodent PL area and the vmPFC corresponds to the rodent IL area (Koob and Volkow, 2016) (Figure 16).

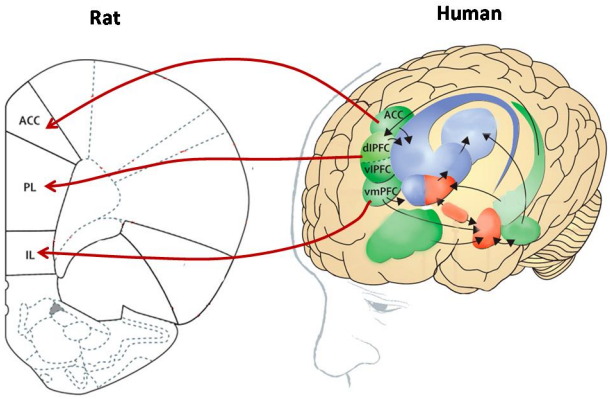

Figure 16. Correspondence between rat and human medial frontal regions. ACC, anterior cingulate cortex; PL, prelimbic cortex; IL, infralimbic cortex; dlPFC, dorsolateral prefrontal cortex; vlPFC, ventrolateral prefrontal cortex; vmPFC, ventromedial prefrontal cortex (Modified from Koob and Volkow, 2016).

Neuroimaging studies showed that the dlPFC is one of the key areas which activity increased in response to specific cocaine-related cues and is associated with a high risk of relapse (Wexler *et al.*, 2001; Marhe

et al., 2013). These findings are in agreement with preclinical models of cocaine reinstatement, suggesting that dlPFC activity is dominated by cue-reactivity, which reflected learned associations between drug cues, drug seeking and drug taking. Additionally, fMRI studies showed reduced activation in the dlPFC of cocaine users in response inhibition tasks (Crunelle *et al.*, 2012). These individuals present cognitive deficits, including impaired cognitive-control performance. These last findings are also congruent with preclinical studies combining self-administration and punishment conditioning and with the well-established role of the PL in the expression of conditioned fear-related behaviors, in which PL neurons fire during expression of conditioned fear responses (Burgos-Robles *et al.*, 2009). Therefore, the aggravation of cocaine seeking by an impaired dorsal mPFC could be explained by a dorsal mPFC activity dominated by inhibitory control processes, which reflect a learned association between drug cues and aversive footshock (Jasinska *et al.*, 2015). Altogether these findings suggest that the PL has a key role in associative learning, both associating the environmental cue or the punishment with the reward (Jasinska *et al.*, 2015).

Considering the complexity surrounding the mPFC areas involved in reward seeking, future research is required to focus on specific networks and not in the entire area to fully understand the mechanisms underpinning inhibitory control.

3.3. Modulation of the reward system

The brain reward system can be modulated by dopaminergic and endocannabinoid signaling (explain in detail below) and by the opioid system among others. For instance, the endogenous opioid system composed by endogenous opioids (endorphins, enkephalins, and dynorphins) through opioid receptors (mu, delta, and kappa receptors) also modulates the mesolimbic DA system (Trigo *et al.*, 2010). The opioid system is implicated in assigning hedonic values to rewards and in integrating information related with rewards to guide decision-making and execution of goal-directed behavior (Volkow *et al.*, 2019).

3.3.1. Dopaminergic signaling

DA is a neurotransmitter that has attracted an enormous amount of attention since its discovery 70 years ago. Neuroscientists investigated the influences that DA exerts on behavioral and neural circuits and the cellular and molecular underlaying of such effects (Beaulieu and Gainetdinov, 2011). DA signaling plays an important role in multiple central nervous system functions, such as voluntary movement, feeding, affect, decision making, attention, learning, working memory and reward. Considering the diversity of critical functions of DA, it is not surprising that multiple human disorders have been linked to dopaminergic dysfunctions including Parkinson's disease, Tourette's syndrome, schizophrenia, obsessive-compulsive disorder, and addiction (Tritsch and Sabatini, 2012).

3.3.1.1. Components of the dopaminergic system

DA neurons

DA neurons are located in three main areas of the midbrain: the retrorubral field, the SNc, and the VTA. Four major DA pathways have been identified: the **nigrostriatal pathway** conferred by DA neurons from SNc to the dorsal striatum, mainly involved in the control of movement and habits. The **mesolimbic** and the **mesocortical pathways** formed by DA neurons from the VTA to NAc and PFC respectively, implicated in the reward system and modulate reinforcing, learning and motivation as previously mentioned. The **tuberoinfundibular pathway** constituted by cells from the arcuate and periventricular nucleus of the hypothalamus projecting to the pituitary. This pathway controls the release and synthesis of pituitary hormones, primarily prolactin (Baik, 2013; Solinas *et al.*, 2018) (Figure 17). However, an overlap in their function has been revealed since the NAc is involved in action selection and the dorsal striatum in reinforcing learning (Wise, 2009).

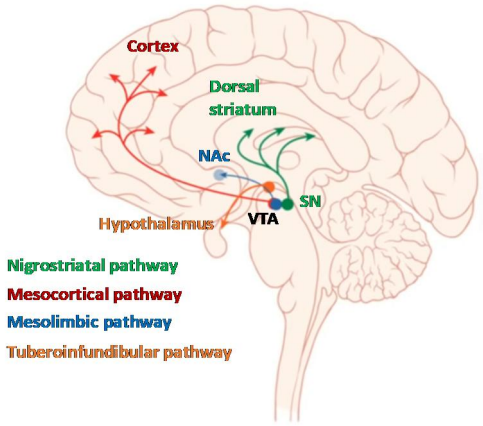

Figure 17. Dopaminergic pathways in the brain. Major four dopaminergic pathways are presented: nigrostriatal pathway, mesolimbic pathway, mesocortical pathway and the tuberoinfundibular pathway. VTA, ventral tegmental area; SN, substantia nigra; NAc, nucleus accumbens.

DA neurons display different activity states: active (firing) or silent (non-firing). When DA neurons are firing, they can fire in a stable irregular **tonic mode** (low frequency, 1-8 Hz) or in a transient (<500 msec) **phasic mode** (high frequency, >15 Hz) with bursts of action potentials. The spontaneously firing at low frequencies suggest that each neuron provides a basal DA tone to many target neurons, which is important for rapid sensitivity to external stimuli. Changes in firing from low frequencies to burst phasic firing at high frequencies occur by exposure to salient (reinforcing, novel, unexpected or aversive) stimuli and are involved in reinforcement learning (Volkow *et al.*, 2017). Tonic firing is generated by intrinsic pace-maker membrane properties of DA neurons and causes the release of DA (in the range of nM) from extrasynaptic release sites. These low levels of DA are sufficient to induce an activation of the high-affinity DA receptors (autoreceptors), which determinates motivational arousal. In contrast, phasic spiking is dependent on glutamate receptor activation and voltage-gated ionic channels and results in a high extracellular DA release (in the range of µM) in the synaptic cleft, which stimulates the low-affinity postsynaptic DA receptors resulting in response to behaviorally salient stimuli (Dreyer *et al.*, 2010). DA is then rapidly removed from the synapse by the DA transporter (DAT) and the signal is terminated.

DA receptor subtypes

DA mediates its physiological actions by interacting with DA receptors belonging to the large family of G protein-coupled receptors (GPCRs). These distinct but closely related DA receptors are commonly divided

into two sub-families based on their structural, pharmacological and signaling properties: **D_1-like DA receptors** subfamily involving the D_1 and D_5 receptor, and **D_2-like DA receptor** subfamily involving D_2, D_3 and D_4 receptors (Jaber *et al.*, 1996). The individual members of the same subfamily share common structural characteristics but have sequence variations that determine differences in their affinity for ligands and coupling to signal transduction pathways. The affinity of D_2-like receptors for DA is generally reported to be 10- to 100- fold higher than D_1-like receptors, with D_3 and D_4 receptors displaying the highest sensitivity for DA and D_1 receptors the lowest. However, D_1 and D_2 receptors can exist in both high and low affinity states, and they have similar nanomolar affinities for DA in their high affinity states (Beaulieu and Gainetdinov, 2011) (Table 1).

The D_1- and D_2-like receptors are genetically different with regard to the presence or absence of introns in their coding sequences. Whereas the D_1-like subfamily genes do not contain introns, the genes that encode for the D_2-like subfamily have several introns. The D_2R gene (*DRD2*) contains exons that allow the generation of two splicing variants, termed D_2S and D_2L (long and short, respectively). These two alternatively spliced isoforms differ in the presence of an additional 29 amino acids in the third intracellular loop (Khan *et al.*, 1998). These variants of the D_2R have distinct levels of expression with the D_2L mRNA being expressed at higher levels than the shorter variant (Usiello *et al.*, 2000). Moreover, D_2S has been shown to be mostly expressed presynaptically and to be involved in autoreceptor functions, whereas

D_2L seems to be predominantly a postsynaptic isoform (Beaulieu and Gainetdinov, 2011) (Table 1).

Table 1. Basic characteristics of DA receptors (Modified from Tritsch and Sabatini, 2012).

	D_1-LIKE FAMILY		**D_2-LIKE FAMILY**		
DA receptor subtype	D_1R	D_5R	D_2R	D_3R	D_4R
Gene name	*Drd1a*	*Drd5*	*Drd2*	*Drd3*	*Drd4*
Number of introns	0	0	6	5	3
Splice variants	No	No	Yes (D_2S, D_2L)	Yes	Yes
Affinity for DA (µm)	1.0-5.0	0.2-2.0	0.2-2.0	0.02-0.2	0.01-0.1
G protein coupling	$G\alpha_s$, $G\alpha_{olf}$	$G\alpha_s$, $G\alpha_q$	$G\alpha_i$, $G\alpha_0$	$G\alpha_i$, $G\alpha_0$	$G\alpha_i$, $G\alpha_0$

DA receptor distribution

DA receptors are highly expressed in the central nervous system and periphery. The two most abundant receptor subtypes expressed in the brain are the D_1 and D_2 receptors, with D_1R displaying the most widespread distribution and highest expression levels. Both receptors are most prominently found in areas where DA fibers innervate, being dorsal striatum, NAc and olfactory tubercle the principal recipient structures of the midbrain. They are also found in other forebrain structures including cortex (Figure 18). With respect the receptor distribution in the cell, no differences were reported between D1 and D2 receptors. Indeed, both are localized presynaptically in nerve terminals and axonal varicosities, as well postsynaptically in dendritic shafts and spines (Bentivoglio and Morelli, 2005; Tritsch and Sabatini, 2012).

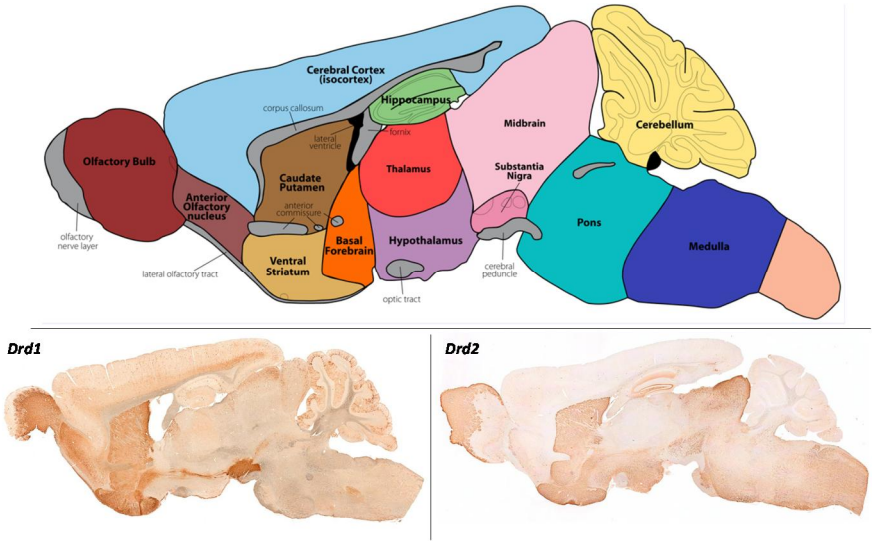

Figure 18. Distribution of *Drd1* and *Drd2* mRNA expression in mouse brain. EGFP marker in Tg (Drd1-EGFP) X60Gsat/Mmmh and in Tg (Drd2-EGFP) S118Gsat/Mmnc (Obtained from Gensat (2018, May 15). Retrieved from http://www.gensat.org/imagenavigator).

In the **striatum,** D_1 and D_2 receptors are largely segregated into distinct MSN neuronal populations as previously described. DA receptors are coexpressed with glutamate receptors on dendritic spines allowing the DA signaling the modulation of the glutamate transmission (Tritsch and Sabatini, 2012). Moreover, presynaptic D_2R are also present on the terminals of DA afferents including glutamatergic cortical and thalamic afferents that innervate MSN and interneurons (Sesack *et al.*, 1994), and in a small number D_1R in presynaptic glutamatergic terminals (Pistillo *et al.*, 2015).

In the cerebral cortex, we focus on the **PFC** due to its involvement in executive functions and because is the principal cortical recipient of DA afferents. DA receptors in the PFC are abundant in the cingulate, PL and

IF cortices in pyramidal neurons, interneurons and glial cells through LII to LVI. In contrast to the striatum, only a fraction of the total neurons expresses DA receptors indicating that a considerable number of cells are not directly modulated by DA.

With regard to the different cortical layers, the expression of D_1R is similar in deep layers than in superficial layers, whereas D_2R is essentially localized in LV of the mPFC. **D_1R** mRNA is expressed in approximately 20% of layer LII/III and in 38% of LV pyramidal cells. In these neurons, D_1Rs are mainly located in pyramidal cells, but they are proportionally more widespread and homogeneously expressed within interneurons suggesting a predominant inhibitory role of D_1R in the cortical PFC output via D_1R on GABAergic interneurons (Santana and Artigas, 2017). Thus, D_1R mRNA is present in 30-60% of all interneurons compared to the 10-20% in the pyramidal neurons. By contrast, **D_2R** mRNA is sparsely detected in superficial layer pyramidal neurons (5% in LII/III) and is more abundant in LV (25%) and LVI (13%) pyramidal cells (Santana *et al.*, 2009). In contrast, the distribution of both D_1R and D_2R transcripts in GABAergic neurons was quite homogenous across layers, with the only exception of D_2R-positive GABAergic cells in LVI (17% vs. 5 and 8% in LII--III and V, respectively (Santana *et al.*, 2009) (Figure 19). D_2R distributes in a smaller fraction compared to D_1R in both glutamatergic and GABAergic cells, indicating that D_1R is the most widespread and strongly expressed receptor in PFC.

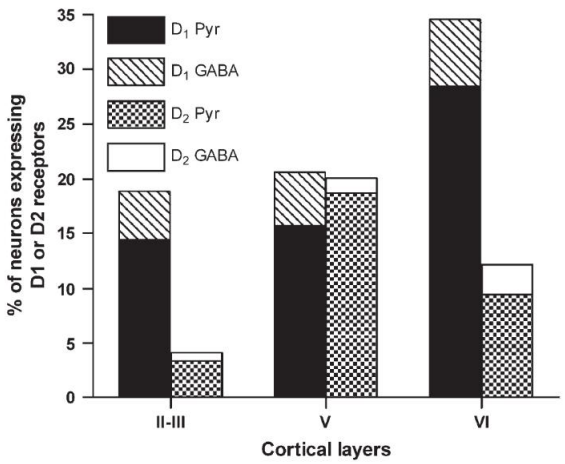

Figure 19. Relative distribution of D_1R and D_2R mRNAs in pyramidal and GABAergic neurons in the mPFC in the different layers. Note that these values are the proportions of all pyramidal and GABAergic neurons containing one or other transcripts (Santana *et al.*, 2009).

3.3.1.2. Dopaminergic receptor signaling

D_1- and D_2-like receptor subfamilies differ functionally in the intracellular signaling pathways that they modulate. All DA receptors activate heterotrimeric G proteins, but the second messenger pathways and effector proteins activated by both receptors mediate opposite effects.

D_1-like receptors are generally coupled to $G\alpha_{s/olf,}$ whereas D_2-like receptors are coupled to $G\alpha_{i/o}$. Without DA, the DA receptors are constituting an inactive trimeric complex form by the association of the βγ-complex to the α-subunit bounded to GDP. When DA arrives, the GDP release and the GFP binds to the α-subunit driven to the disassociation of the trimeric complex. Subsequently, α_s-subunit of the D_1R stimulates adenylyl cyclase leading to the production of the second

messenger cyclic adenosine monophosphate (cAMP) whereas α_i-subunit of the D_2R inhibits cAMP production. The formation of cAMP triggers a signaling cascade through the activation of protein kinase A (PKA). (Pierce *et al.*, 2002; Beaulieu and Gainetdinov, 2011). PKA has several substrates such as voltage-gated potassium (K^+), sodium (Na^+) and calcium (Ca^{2+}) channels, ionotropic glutamate, GABA receptors and transcription factors mediating the effects of DA receptor stimulation. One of the major targets of PKA is the DA and cAMP-regulated phosphoprotein (DARPP-32), a multifunctional protein highly expressed in the striatum and cortical areas that modulates downstream signal transduction pathways in response to multiple neurotransmitters including DA. When DARPP-32 is phosphorylated by PKA in response to D_1R activation, DARPP-32 amplifies PKA signaling by inhibiting protein phosphatase 1, which counteracts PKA's actions. By contrast, dephosphorylation by the calmodulin-dependent protein phosphatase 2B upon D_2R stimulation converts DARPP-32 into a potent inhibitor of PKA signaling (Beaulieu and Gainetdinov, 2011; Tritsch and Sabatini, 2012) (Figure 20).

In addition to cAMPA/PKA-regulated signaling, DA receptors can modulate intracellular Ca^{2+} levels by acting on ion channels. Specifically, βγ-subunits activate phospholipase C (PLC) after the stimulation of D_2R. Activation of PLC leads to the production of inositol triphosphate (IP_3) and diacylglycerol and subsequently increased mobilization of intracellular Ca^{2+} levels in response to IP_3. D_2R βγ-subunits are also implicated in the regulation of N-type Ca^{2+} channels

and G protein-coupled inwardly rectifying potassium channels (GIRKs) producing an inhibitory effect in neurons, suppressing firing (Lüscher and Slesinger, 2010) (Figure 20).

On the other hand, DA receptors do not signal exclusively through heterotrimeric G proteins and may also engage in G protein-independent signaling events. Thus, D_1R and D_2R can alter membrane trafficking of Ca^{2+} channels as well as N-methyl-D-aspartate (NMDA) and $GABA_A$ receptors through direct protein-protein interactions or downstream of tyrosine kinase activation (Beaulieu and Gainetdinov, 2011) (Figure 20).

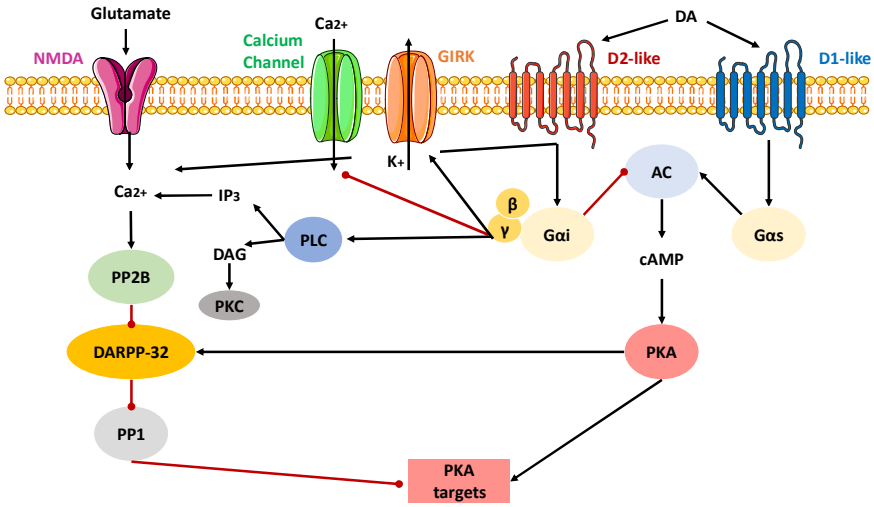

Figure 20. Intracellular DA signaling pathways. Schematic of signaling networks cAMP/PKA-dependent and Gβγ-dependent regulated by D1- and D2-like receptor responding neurons. Black and red arrows depict activation and inhibition, respectively. NMDA, N-methyl-D-aspartate; PP2B, protein phosphatase 2B; DARPP-32, DA and cAMP-regulated phosphoprotein; PP1, protein phosphatase 1; IP_3, inositol triphosphate; DAG, diacylglycerol, PLC, phospholipase C; GIRK, G protein-coupled inwardly rectifying potassium channels; AC, adenylyl cyclase; cAMP, cyclic adenosine monophosphate; PKA, protein kinase.

Finally, DA receptors can experience desensitization in response to extensive exposure to agonists and can undergo resitization when an agonist does not activate them for a prolonged period of time. The desensitization is produced by the phosphorylation of G protein-coupled receptor kinases, which recruit arrestins promoting the receptor internalization from the cellular membrane due to its binding to clathrin (Laporte *et al.*, 2002).

3.3.1.3. The dopaminergic system in food addiction and eating disorders

Dysfunction in the dopaminergic system has been related to food addiction and eating disorders due to the involvement of this system in food reward and eating behaviors. A strong correlation has been suggested between adaptations in the DA system and compulsive eating behavior, one of the main features of food addiction (DiFeliceantonio and Small, 2019). Thus, animals given “cafeteria diet”, consisting of a selection of highly palatable and energy-dense food, display compulsive eating behavior and decreased D_2R expression in the striatum. Moreover, lentivirus-mediated knockdown of striatal D_2R rapidly accelerated the development of addiction-like reward deficits and the onset of compulsive-like food seeking in rats with extended access to palatable high-fat food (Johnson and Kenny, 2010). The implication of the DA system is also supported by the increased reinstatement of food seeking behavior induced by the administration of D_2R agonists (Ball *et al.*, 2011). These findings in rodents were consistent with reports in humans indicating that obesity is associated

with a downregulation of striatal D_2R associated with a dysfunction of cortical areas (Volkow *et al.*, 2017).

Data generated from animal models of binge eating show a dysregulation of the mesolimbic DA system. Rats that are bingeing on sucrose displayed an increase in D_1R binding in the NAc and a decrease in D_2R binding in the dorsal striatum (Colantuoni *et al.*, 2001). Similar findings with a paradigm of restricted access to sucrose observed decreased D_2R binding and upregulation in DA transporter (Bello *et al.*, 2002; Avena and Bocarsly, 2012).

All these studies suggest a potential pharmacological DA targeting treatment for eating disorders. Most of them were focused on the D_2R in striatal areas modulating food reward and motivation.

3.3.2. Endocannabinoid signaling

The endocannabinoid system is a neuromodulatory system involved in many physiological functions including reward function. The endocannabinoid system is composed by the cannabinoid receptors, their endogenous ligands known as endocannabinoids and the enzymes involved in their synthesis and degradation.

3.3.2.1. Components of the endocannabinoid system

Cannabinoid receptors

Endogenous and exogenous cannabinoids bind at least to two major types of cannabinoid receptors, **cannabinoid type-1 receptor (CB_1R)** and **cannabinoid type-2 receptor (CB_2R)**. They are both GPCRs mainly

coupled to the inhibitory $G_{i/o}$ protein (Childers and Deadwyler, 1996). CB_1R is localized preferentially in the central nervous system being the most G protein-coupled receptor expressed in the adult brain (Burns *et al.*, 2007). The brain regions with the highest levels of CB_1R expression include hippocampus, olfactory bulb, cerebellum and basal ganglia. Moderate CB_1R expression is found in the cerebral cortex, amygdala, hypothalamus, and parts of the brainstem. Whereas regions as the thalamus and the ventral horn of spinal cord have low CB_1R expression (Zou and Kumar, 2018) (Figure 21).

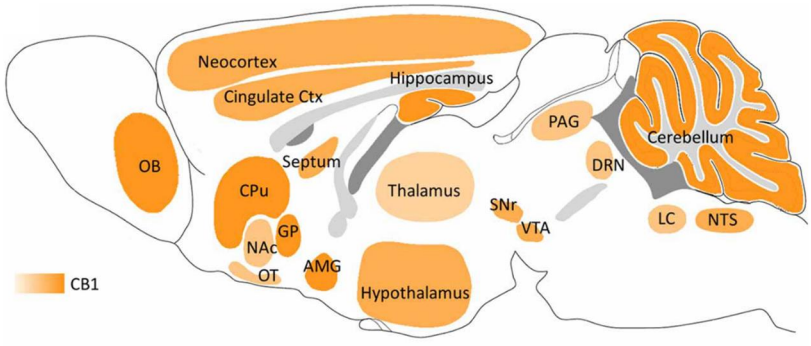

Figure 21. Schematic representation of the main areas expressing CB_1R. The main areas involved in the mesolimbic pathway express this endocannabinoid receptor (Flores *et al.*, 2013).

Furthermore, CB_1R has been described in peripheral tissues including fat tissue, gastrointestinal tract, cardiovascular system, liver, pancreas, immune system, among others (Busquets Garcia *et al.*, 2016) (Figure 22). At cellular localization, several studies confirmed a high expression of CB_1R on presynaptic terminals (Tsou *et al.*, 1998). However, the localization of CB_1R at postsynaptic sites cannot be discarded since

some studies reported post-synaptic mediated self-inhibition in the cortex (Marinelli *et al.*, 2009). Recent studies discovered that CB_1R also localized in intracellular compartments as lysosomes and mitochondria, presumably forming a subpopulation with pharmacological properties distinct from their plasma membrane-localized counterparts (Zou and Kumar, 2018). Additionally, CB_1R is expressed in lower extend in glial cells including astrocytes, oligodendrocytes and microglia (Stella, 2009; Busquets-Garcia *et al.*, 2018).

In contrast, CB_2R expression is low in the central nervous system but this receptor is highly expressed in peripheral immune cells and tissues as spleen, bones and skin (Atwood and Mackie, 2010) (Figure 22). In the central nervous system, CB_2R expression is mainly restricted to microglia and endothelial cells. However, recent studies demonstrate the expression of CB_2R (Van Sickle *et al.*, 2005) in neurons and its functional involvement in drug reward (Onaivi *et al.*, 2012).

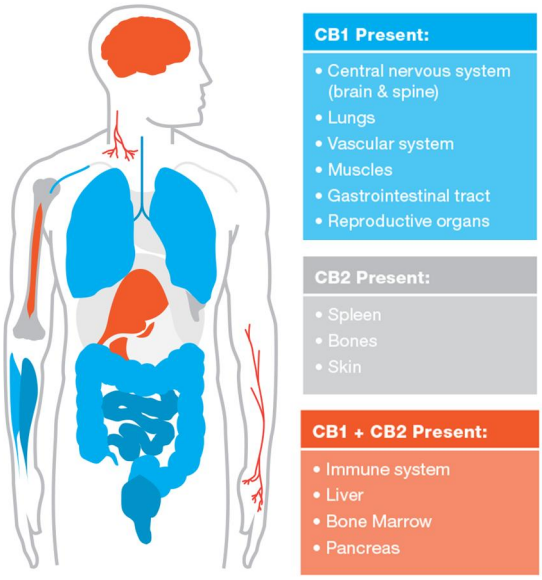

Figure 22. Schematic representation of the peripheral distribution of CB_1R and CB_2R. The localization of these receptors in different peripheral locations highlights their involvement in several physiological functions.

Pharmacological evidence indicates the existence of other possible cannabinoid receptors including the transient receptor potential vanilloid receptor 1 (Di Marzo and De Petrocellis, 2010), G protein-coupled receptor (GPR) 55, GPR18, the sphingosine-1-phosphate lipid receptors GPR3, GPR6 and GPR12 (Morales *et al.*, 2017b) and the peroxisome proliferator-activated receptors (O'Sullivan, 2009).

Endocannabinoid ligands

The two best-characterized endocannabinoids ligands are N-arachidonoylethanolamide (anandamide, **AEA**) and 2-arachidonoylglycerol (**2-AG**). These endoccanabinoids are derivates of arachidonic acid, resembling lipid transmitters, conjugated with

ethanolamine to form fatty acid amides, or with glycerol to form monoacylglycerols. Due to their lipid nature, endocannabinoids are not stored in vesicles. They are synthesized "on demand" by multiple pathways from lipid precursors present in cell membranes and immediately released through Ca^{2+}-dependent mechanisms. Thus, endocannabinoid signaling is vastly dependent on the state of synaptic activity (Alger and Kim, 2011).

AEA and 2-AG both exert agonist activity at CB_1R and CB_2R. AEA binds with a slightly higher affinity to CB_1R than to CB_2R, exhibits low efficacy agonist at both receptors, acting as a partial agonist. However, 2-AG has equal affinity for both receptors and acts as a full agonist exhibiting greater efficacy than AEA (Pertwee *et al.*, 2010) (Table 2).

Apart from the endogenous cannabinoids, there are natural and synthetic compounds that bind to the cannabinoid receptors. The most abundant **natural cannabinoids** (phytocannabinoids) present in the *Cannabis sativa* plant are Δ^9-tetrahydrocannabinol (Δ^9-THC) and cannabidiol. Δ^9-THC is the main psychoactive component of the marijuana acting as a partial agonist of CB_1R and CB_2R, whereas cannabidiol is not psychoactive and its affinity for CB_1R and CB_2R is very low (Morales *et al.*, 2017a). **Synthetic cannabinoids** have also been designed with different selectivity profiles for cannabinoid receptors including mixed agonists for both receptors, selective CB_1R and CB_2R agonists, and selective CB_1R and CB_2R antagonists. The agonists most used with affinity for both receptors are WIN55,212-2, HU-210 and CP55,940. The antagonists block activation of cannabinoid receptors by

either endogenous or exogenous cannabinoids in a manner. The most used CB1R-selective competitive antagonists are rimonabant (SR141716A), taranabant (MK-0364), AM281 and LY320135. However, the majority of these molecules also act as inverse agonists, producing inverse cannabimimetic effects in the absence of agonists (Martín-García *et al.*, 2010; Pertwee *et al.*, 2010) (Table 2).

Table 2. Cannabinoid receptor ligands and their Ki values for the *in vitro* displacement of a tritiated compound (i.e [$_3$H] CP55,940, [$_3$H]SR141716A, [$_3$H]WIN55,212-2) from specific binding sites on rat, mouse or human CB_1R and CB_2R. (Adapted from Pertwee *et al.*, 2010).

CANNABINOID RECEPTOR LIGANDS	Ki (nM)	
	CB1R	CB2R
Agonists with similar affinity for CB1R and CB2R		
(−)-Δ^9-THC	5.05–80.3	3.13–75.3
HU-210	0.06–0.73	0.17–0.52
CP55,940	0.5–5.0	0.69–2.8
R-(+)-WIN55,212-2	1.89–123	0.28–16.2
AEA	61–543	279–1940
2-AG	58.3, 472	145, 1,400
Agonists with higher affinity for CB1R		
ACEA	1.4, 5.29	195, >2,000
Arachidonylcyclopropylamide	2.2	715
R-(+)-methAEA	17.9–28.3	815–868
Noladin ether	21.2	>3,000
Agonists with higher affinity for CB2R		
JWH-133	677	3.4
HU-308	>10000	22.7
JWH-015	383	13.8
AM1241	280	3.4
CB1R-Selective Competitive Antagonists		
Rimonabant (SR141716A)	1.8–12.3	514–13,200
AM251	7.49	2,290
AM281	12	4,200
LY320135	141	14,900
Taranabant	0.13, 0.27	170, 310
NESS 0327	0.00035	21
O-2050	2.5, 1.7	1.5
CB2R-Selective Competitive Antagonists		
SR144528	50.3–>10,000	0.28–5.6
AM630	5152	31.2
JTE-907	2370	35.9
Others		
Cannabidiol	4350->10,000	2399->10,000
Cannabinol	120-1130	96-301

3.3.2.2. Cannabinoid type-1 receptor signaling

CB_1R is coupled to $G_{i/o}$ and its activation inhibits adenylyl cyclase and the cAMP production. Subsequently, activation of CB_1R modulates various types of ion channels and enzymes in a cAMP-dependent or -independent manner.

Postsynaptic neuronal depolarization opens voltage-dependent Ca^{2+} channels, and the resulting Ca^{2+} influx triggers the enzymatic synthesis of 2-AG. Alternatively, activation of certain G_q-coupled receptors particularly group 1 metabotropic glutamate receptors (mGluRs) and M1/M3 muscarinic acetylcholine receptors (mAChRs), triggers the release of endocannabinoids in a Ca^{2+}-independent manner likely involving activation of PLC. The resulting endocannabinoid is then released postsynaptically and travels retrogradely to act on presynaptic CB_1Rs from the same or a neighboring synapse to inhibit transmitter release (Kano *et al.*, 2009; Lau *et al.*, 2017) (Figure 23). Multiple studies demonstrate that the activation of CB_1R inhibits neurotransmitter release (Schlicker and Kathmann, 2001). Thus, the endocannabinoid system contributes to multiple forms of synaptic plasticity at different synapses. The suppression of the neurotransmitter release after the CB_1R activation can be transient (seconds) leading to endocannabinoid-mediated short-term depression (eCB-STD), or persistent (minutes to hours) leading to endocannabinoid-mediated long-term depression (eCB-LTD). There are two main forms of eCB-STD; the depolarization-induced suppression of inhibition (DSI) and depolarization-induced

suppression of excitation (DSE) in GABAergic and glutamatergic synapses, respectively (Castillo *et al.*, 2012).

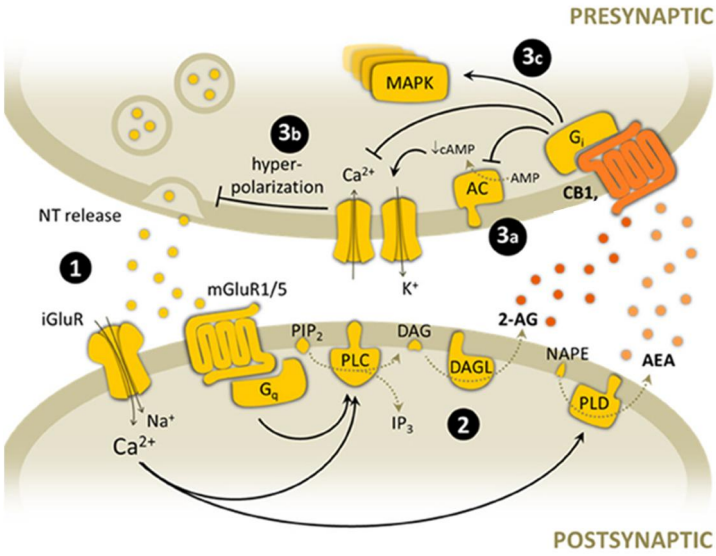

Figure 23. **Endocannabinoid-mediated synaptic signaling.** (1) Glutamate is released from presynaptic terminals and stimulates both ionotropic and metabotropic glutamate receptors, leading to postsynaptic depolarization through Ca^{2+} entrance and G_q-protein activation. (2) High Ca^{2+} concentration stimulates endocannabinoid synthesis through PLC and PLD. 2-AG synthesis is also mediated by Gq-protein activation. (3) Endocannabinoids are released to the synaptic cleft and activate CB_1 presynaptic receptor. Some of the main downstream consequences of CB_1R activation and subsequent Gi-protein stimulation are: (3a) inhibition of AC activity, (3b) membrane hyperpolarization after modulation of K^+ and Ca^{2+} channels, and subsequent inhibition of NT release, (3c) activation of protein kinase cascades such as MAPK pathway. NT, neurotransmitter; iGluR, ionotropic glutamate receptor; mGluR, metabotropic glutamate receptor; PIP2, phosphatidylinositol bisphosphate; DAG, diacylglycerol; 2-AG, 2-arachidonoylglycerol; NAPE, N-arachidonoyl-phosphatidylethanolamine; AEA, anandamide; PLC, phospholipase C; DAGL, diacylglycerol lipase; PLD, phospholipase D; AC, adenyl cyclase; cAMP, cyclic AMP; MAPK, mitogen-activated protein kinase (Modified from Flores *et al.*, 2013).

3.3.2.3. Endocannabinoid modulation of brain reward system

CB_1R is present in the main structures of the mesocorticolimbic system, where exert widespread modulatory influences on excitatory and inhibitory signaling and controls reward processing and food intake (Parsons and Hurd, 2015).

At the cellular level, dopaminergic neurons in the VTA, MSNs in the NAc and pyramidal neurons within the PFC are under the local influence of GABAergic and glutamatergic inputs modulated by the endocannabinoid system activity. The activation of CB_1R present on axon terminals of GABAergic neurons in the VTA leads to the inhibition GABA transmission (DSI), and the removal of this inhibitory input on DA neurons leads to increased excitation of DA VTA neurons (D'Addario *et al.*, 2014). The activation of CB_1R also decreases excitatory glutamatergic transmission (DSE) in the VTA and NAc, mainly regulating the activity of neurons projecting from the PFC (Melis *et al.*, 2004). Interestingly, DSE is augmented by D_2R activation while it is partially blocked by D_2R antagonist, suggesting an important role of DA modulating the endocannabinoid signaling (Melis *et al.*, 2004). In accordance, eCB-LTD and inhibitory LTD is expressed at these synapses in the PFC and eCB-iLTD is facilitated by D_2R agonism (Chiu *et al.*, 2010). Excitatory corticostriatal neurons linking the PFC and NAc are critical in mediating reward-related behaviors. Therefore, eCB-LTD of cortical pyramidal neurons may result in hypofunction of the corticostriatal circuit (Lau *et al.*, 2017).

Endocannabinoids within the mesocorticolimbic system has a prominent role in regulating food intake (Busquets-Garcia *et al.*, 2015). Exogenous AEA and 2-AG both increase extracellular DA levels in the NAc in a CB_1-dependent manner eliciting hyperphagia (Solinas *et al.*, 2006). Moreover, CB_1R antagonism attenuated the DA release evoked by the presentation of a novel and palatable food (Soria-Gómez *et al.*, 2009). Despite the well characterized orexigenic effect of endocannabinoids, some researchers revealed an opposing effect on food intake depending on excitatory or inhibitory synapses. Thus, endocannabinoids acting via CB_1R on glutamatergic terminals in the NAc induce hyperphagia, while their actions at CB_1R on GABAergic terminals in the NAc produce hypophagia (Bellocchio *et al.*, 2010). Therefore, the final effect of endocannabinoids on food intake depends on the functional balance between its actions on inhibitory GABAergic versus excitatory glutamatergic transmission (Bellocchio *et al.*, 2010).

On the other hand, the endocannabinoid system can control food intake through the modulation of sensory perception such as palatability and olfaction, leading to an increase in food intake. Local pharmacological and genetic manipulations revealed that cortical feedback projection to the main olfactory bulb crucially regulates food intake via CB_1R (Soria-Gómez *et al.*, 2014).

3.3.2.4. The endocannabinoid system in food addiction and eating disorders

The widespread role of the endocannabinoid system as a modulator of both homeostatic and hedonic aspects of food intake prompted

investigations into possible alterations of this system in eating disorders and obesity. Enhanced levels of AEA were found in patients with anorexia nervosa and binge eating disorder (Di Marzo *et al.*, 2001; Monteleone *et al.*, 2005). Human studies have associated the levels of CB_1R mRNA and CB_1R protein with eating disorders. Thus, PET studies revealed increased receptor levels in the insula and inferior frontal and temporal cortex in anorexia nervosa patients (Gérard *et al.*, 2011). Moreover, human genetic studies reported a positive association between eating disorders and specific polymorphisms of genes encoding for different components of the endocannabinoid system, such as CB_1R (Monteleone *et al.*, 2009). Based on these findings, it has been hypothesized that the dysregulated endocannabinoid tone of eating disorders patients may represent an adaptative response aimed at maintaining energy balance by potentiating internal orexigenic signals and facilitating the rewarding properties of food intake (Monteleone and Maj, 2013; D'Addario *et al.*, 2014).

Several preclinical and clinical observations have also shown an association between obesity and hyperactivity of the endocannabinoid system manifested as overproduction of endocannabinoids or/and upregulation of cannabinoid receptors in central and peripheral tissues involved in energy homeostasis (Di Marzo and Matias, 2005). Therefore, much attention has been focused on the pharmacological antagonism of this system to restore normal endocannabinoid tone aiming for the reduction of body weight and the maintenance of

obesity (Rinaldi-Carmona *et al.*, 1994; D'Addario *et al.*, 2014; Lau *et al.*, 2017).

On the other hand, little is known about the role of the endocannabinoid system in food addiction. A recent study using a validated food addiction mouse model performed in our laboratory found that long-term operant training to obtain highly palatable food produced adaptative changes at epigenetic and protein levels in the endocannabinoid system (Mancino *et al.*, 2015). Specifically, we observed a significant reduction in DNA methylation at CB_1R gene (*Cnr1*) promoter in PFC, which was associated with upregulation of gene expression and the subsequent increase in CB_1R protein in mice classified as food addicted. The involvement of the CB_1R in the food addictive behavior was corroborated using pharmacological and genetic approaches. Administration of rimonabant reduced the percentage of animals that reached the addiction scores. In accordance, the genetic deletion of the CB_1R in constitutive CB_1KO mice decreased operant seeking behavior and these KO mice did not reach the criteria for addiction (Mancino *et al.*, 2015). We hypothesized that the CB_1R may modulate the primary glutamatergic neuronal output of PFC ultimately affecting brain reward processes and enhancing extracellular DA levels in the NAc (Mancino *et al.*, 2015). Future studies are needed to elucidate whether this hypothesis is correct and to investigate the specific cell-type in which CB_1R is exerting the addictive-like behavior effect.

4. Dynamics in the transition to addiction: stages of the food addiction cycle

Addiction can be conceptualized in three stages that interact with each other forming a recurring cycle that worsens over time ending with the pathological state of compulsive intake. This transition to controlled intake to loss of control involves neuroplastic changes in the brain reward, stress, and executive function systems (Koob and Volkow, 2010, 2016). Analogously to drug addiction, the three key, and not mutually exclusive elements of compulsive eating are habitual overeating, overeating to relieve a negative emotional state and overeating despite negative consequences that are related to three major neurocircuits involved in reward learning, emotional processing, and inhibitory control respectively. Although these processes involved different brain areas and several interconnected networks, the three major regions comprised are the basal ganglia, the extended amygdala and the PFC (Moore *et al.*, 2017, 2018) (Figure 24) (Table 3).

4.1. Habitual overeating: maladaptive habit formation

Maladaptive habit responding is initiated with the association of environmental stimuli with food availability in the phenomenon called **conditioned reinforcement**. With the repeated pairing of a cue with the food, the learned cue itself becomes salient in the phenomenon termed **incentive salient** (Koob and Volkow, 2016). Both conditioned reinforcement and incentive salience can strongly increase the want to eat and maintained food seeking even in the absence of food presentation or in the absence of physiological needs, forming the

habit (Velázquez-Sánchez *et al.*, 2015; Moore *et al.*, 2017). Thus, the habit formation is the end result of an adaptive learning process where voluntary actions become habitual through the reinforcement of these behaviors (Everitt and Robbins, 2005).

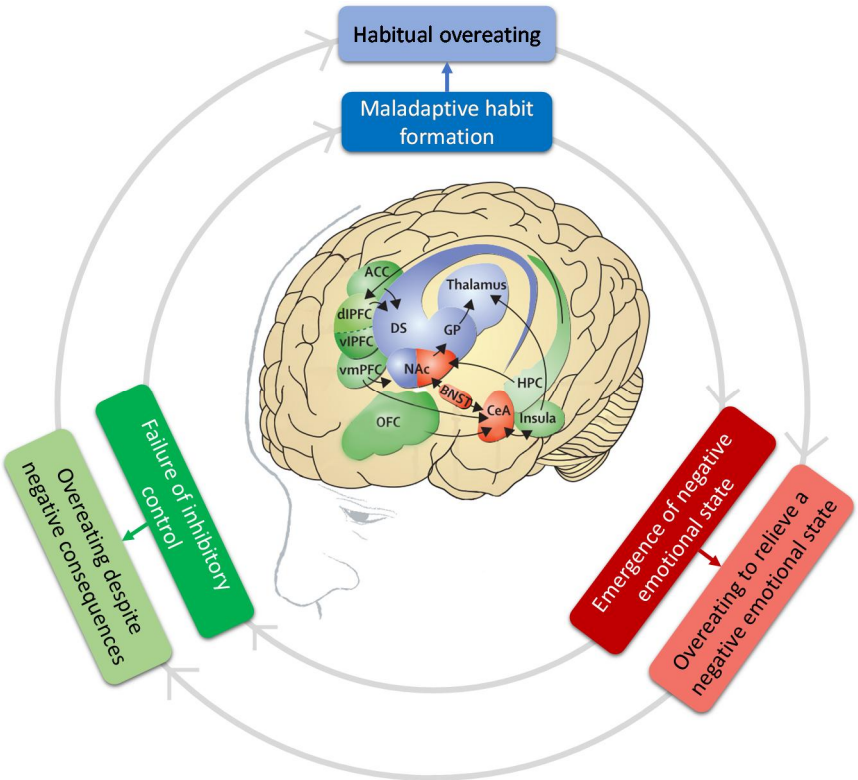

Figure 24. Model of the addiction cycle conceptualized in three stages with the corresponding brain areas involved, in which each dysfunction contributes to the compulsive overeating. The overall neurocircuitry correspond to three functional domains: habitual overeating (reward and incentive salience: basal ganglia [blue]), overeating to relieve a negative emotional state (negative emotional states and stress: extended amygdala [red]), and overeating despite negative consequences (craving, impulsivity, and executive function: PFC, insula, and allocortex [green]). (Adapted from Koob and Volkow, 2016; Moore *et al.*, 2017).

Food-associated stimuli are enough to maintain compulsive seeking behavior associated with food craving. In an animal model of operant conditioning maintained by palatable food paired with a cue light, rats exhibited higher active lever responding and not reduced responding in the presence of the conditioned punishment compared to control rats exposed to chow food (Velazquez-Sanchez 2015). Related with this result, compulsive palatable food seeking behavior has been reported in mice in continued responding on a food-paired lever during a period signaled of non-availability (Mancino *et al.*, 2015).

The outcome devaluation procedures are usually used to measure habits formation in scientific research. Rats exposed intermittently to obesogenic diet (sweetened condensed milk which is high in sugar and fat) for a long period of time showed no devaluation effect, failing to adjust responding according to the current value of the outcome and reflecting evidence of habitual performance (Corbit, 2016).

It is hypothesized that the transition from controlled actions to more habit-based behaviors of responding involves the shift from action-outcome ventrally dependent learning systems to dorsally dependent habit systems (Stahl, 2013). As behavior is repeatedly executed, the role of glutamate inputs from the PFC and amygdala into the NAc becomes less important in favor of glutamate projecting from sensory-motor cortical areas to the dorsal striatum (Everitt and Robbins, 2005). Several recent findings suggest that diet can promote this shift in striatal circuits from medial to lateral, and thus goal-directed to habitual systems (Corbit, 2016). Neuroimaging studies have been

found reduced activation of the caudate nucleus of the striatum (involved in goal-directed actions) and augmented activity of the putamen (involved in habit responding) to palatable food taste, promoting impulsive eating in obese subjects as compared with healthy weight controls (Babbs *et al.*, 2013; Moore *et al.*, 2017) (Figure 24) (Table 3).

4.2. Overeating to relieve a negative emotional state: emergence of a negative affect

As individuals progress towards compulsive intake of palatable food, the hedonically rewarding properties of the food may hold less importance in favor to food intake for preventing or ameliorating negative states (e.g, anxiety, depression, irritability…) that are experienced when preferred foods are not available (Parylak *et al.*, 2011). In this framework, this stage is considered the "**dark side**" of the addiction cycle (Koob, 2013).

Human studies reported that switching from a high-fat diet to a lower-fat diet after one month of eating high-fat diet, increased anger and hostility (Wells *et al.*, 1998). In agreement, dietary restraint after overeating resulted in negative emotions such as irritability, nervousness, and intense anxiety (Greeno and Wing, 1994). Thus, repeated overconsumption of palatable foods produces long-term neuroadaptations in brain reward and stress pathways that ultimately promote depressive or anxious responses when those foods are no longer available (Parylak *et al.*, 2011). On the hand, depressive and anxiety-like traits may confer vulnerability to eating disorders and to

some forms of obesity. Thus, binge eaters have greater rates of psychiatric diagnoses and show increased prevalence of major depression, bipolar disorder and anxiety disorders (Rosenbaum and White, 2015).

The withdrawal-induced negative affect is underpinning by two processes: (I) within-system neuroadaptations and (II) between-system neuroadaptations.

Within-system neuroadaptations involve neurotransmitter changes in systems implicated in the reinforcing effects of food, producing a decreased reward function signaling characterized by loss of motivation for all rewards. Thus, high-fat and high-fat sugar diets induce alterations in dopaminergic systems with downregulation of D_2Rs in the striatum and reduction of DA basal levels in the NAc. This is consistent with the lower availability of D_2Rs reported in obese individuals compared to non-obese controls and this reduction correlated directly with BMI (Wang *et al.*, 2001). Striatal D_2Rs availability also correlates with lower glucose metabolism of the prefrontal brain regions (Nora D. Volkow *et al.*, 2008).

Between-system neuroadaptations involve the recruitment of brain stress system in the extended amygdala which is not directly involved in the positive rewarding effects but is recruited and dysregulated by chronic activation of the reward system (Moore *et al.*, 2017). Both, the hypothalamic-pituitary-adrenal axis and the brain stress system mediated by corticotropin-releasing factor are activated in this stage. Rats withdrawn from intermittent access to palatable food exhibited

increased anxiety and depressive-like behavior during withdrawal accompanied by increased expression of corticotropin-releasing factor in the central amygdala (Cottone *et al.*, 2009). Translated from the drug addiction field, the purpose of these neuroadaptations is to try to overcome the chronic presence of the perturbing substance, limiting the reward and restoring the normal function. Based on that, the concept "**anti-reward system**" was established as an opponent-like process (Koob, 2013).

In summary, the neurobiological substrates underlying this stage are the within-system neuroadaptations (downregulation of reward neurotransmission) and between-system neuroadaptations (recruitment of the brain anti-reward stress systems during food withdrawal) contributing to the emergence of a negative emotional state, and that relief of anxiety or stress can drive compulsive eating behavior (Moore *et al.*, 2017, 2018) (Figure 24) (Table 3).

4.3. Overeating despite aversive consequences: failure of inhibitory control

Compulsive behaviors towards palatable food imply dysfunctions in multiple frontostriatal circuitries resulting in loss of inhibitory control. Loss of control over food seeking and taking leads to continue food use despite many incurring negative consequences under which behaviors would typically be suppressed (Deroche-Gamonet *et al.*, 2004). The overeating persists despite the adverse events, such as physical, psychological and social problems resulting in an intention to attempt

to diet and to avoid triggering foods. However, the majority relapse into unhealthy eating habits (Moore *et al.*, 2017).

PFC plays a crucial role in this stage. Two opposing systems within the PFC have been classically postulated: a Go system and a Stop system. While the **Go system** involves the dlPFC-striatal circuit driving craving and re-engaging habits, the **Stop system** involves the vmPFC-striatal circuit inhibiting this drive through the assessment of the incentive value choices and suppression of emotional responses to stimuli. However, a recently published study identified two other functional frontostriatal circuits, the orbitofrontal cortex-striatal conforming the Go system and the PL (dlPFC in humans)-striatal conforming the Stop system (Chen *et al.*, 2013; Hu *et al.*, 2019). These frontostriatal circuits dynamically change over the course of addiction showing a higher orbitofrontal cortex-striatal and lower PL-striatal connectivity (Hu *et al.*, 2019). The apparent contradictory result of the dlPFC has been already discussed in the previously PFC section (3.2.3) suggesting an associative learning role of this area as a possible explanation. Besides, there is an unbalanced between these two systems in the progression of the addictive disorder. On one side, prefrontal areas are hyperresponsive to food cues, whereas on the other side a general hypoactivation of prefrontal circuits comprised in inhibitory control outcomes in the disinhibition of the basal ganglia and amygdala stress systems (Koob and Volkow, 2016).

The compulsive-behavior towards palatable food has been modeled in laboratory animals. For instance, animals continue to consume

palatable food even in the presence of an electric shock, conditioned stimulus that signals an electric shock or aversive conditions (Deroche-Gamonet *et al.*, 2004; Everitt *et al.*, 2008; Mancino *et al.*, 2015; Velázquez-Sánchez *et al.*, 2015) (Figure 24) (Table 3).

Table 3. A summary of the features of each element of compulsive eating behavior (Adapted from Moore *et al.*, 2017).

Elements of compulsive eating behavior	Neurobiological mechanisms	Characteristic behavior	The most implicated brain area
Habitual overeating	Aberrant reward learning	Inability to reduce eating or seeking behavior following a decrease in food value or contingency	Basal ganglia
Overeating to relieve a negative emotional state	Affective habituation	Eating to cope with decreased sensitivity to reward	Basal ganglia
	Affective withdrawal	Eating to cope with negative affect (eg, anxiety and stress)	Extended amygdala
Overeating despite negative consequences	Decreased inhibitory control	Eating persist in conditions where it would normally be suppressed	Prefrontal cortex

5. Complex multifactorial nature of food addiction and eating disorders: gene and environment interaction

Food addiction and eating disorders are complex multifactorial diseases that are the result of the effect of multiple genes in combination with multiple environmental factors and the interaction between them. These multiple factors impact in the brain development and function influencing behavior and leading to different individual's vulnerability or resilience to develop the disorder (Hamer, 2002). This vulnerability includes intrinsic factors (sex, age, age at the first use, personality traits, genetic, comorbidity with other psychopathological conditions among others) and extrinsic factors (socioeconomic status, adverse life events, addictive-substance availability among others) (Molle *et al.*, 2017). The relative importance of these factors varies across the lifespan and at different stages of the disease (Ducci and Goldman, 2012).

In the case of food addiction, the multifactorial nature of this disorder could explain why the vast majority of people that are in contact with highly palatable food (addictive substance) do not become addicted (Piazza and Deroche-Gamonet, 2013). Equally as drugs of abuse, repetitive exposure to the substance induces long-lasting neuroadaptive changes, in individuals who are vulnerable to addiction, which further promote food-seeking behaviors and ultimately lead to persistent an uncontrolled pattern of use (Kalivas and O'Brien, 2008). Thus, food addiction could result from a pathological response to highly

palatable food in a few individuals by a vulnerable biological phenotype.

5.1. Genetic mechanisms of food addiction and eating disorders

The genetic mechanisms of multifactorial diseases indicate that the inheritance of the disorder has a polygenetic component (Volkow and Muenke, 2012). This makes difficult to determine a person's risk of inheriting or passing on these disorders. However, a **multifactorial threshold model** has been postulated (Reich *et al.*, 1975). In this model, it is assumed that a number of different genes along with a number of environmental variables act as risk and protective factors for the development of the disease that are considered as a single entity known as "liability". The liabilities of all individuals in a population form a continuous variable that is normally distributed among the population. The individual is affected if the combined effects of genetic and environmental influences push an individual's liability across a certain threshold level (Figure 25).

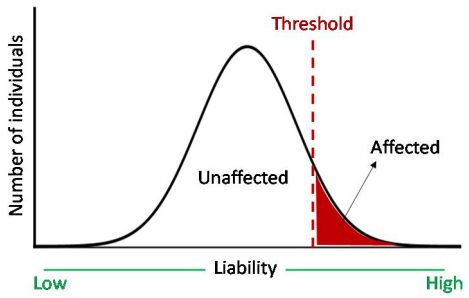

Figure 25. Multifactorial threshold model. The liability distribution for a multifactorial disease. An individual must exceed a threshold on this distribution to be affected with the disease.

Different genetic factors have been described to be important determinants for the risk or resilience of a psychiatric disorder. The genetic polymorphisms involved in addiction have been broadly studied and importantly there is increasing evidence suggesting that genes implicated in drug addictive behaviors may also be associated with food addiction and obesity (Heber and Carpenter, 2011). Since food intake and all substance of abuse exert their rewarding effects by increasing DA in the NAc, genetic variations affecting the DA system have attached most attention (Volkow and Muenke, 2012).

The most studied polymorphism is the A1 allele for the dopamine D_2R gene (*Taq*1A). The *Taq*1A polymorphism is located more than 10 kilobase-pairs downstream from the coding region of the *DRD2* gene or in the coding gene for the neighboured *ANKK1* gene (Neville *et al.*, 2004). Individuals carrying the A1 allele of the *Taq*1A polymorphism (rs1800497) have been associated with the concept of "Reward deficiency syndrome" consisting in a hypodopaminergic state due to a compromised D_2R and with reduced levels of D_2R density compared with other individuals. Therefore, the lack of D_2R causes individuals to have a high risk for multiple addictive, impulsive and compulsive behaviors due to a possible compensatory performance for insufficient DA activity. Subsequently, direct associations have been reported between *Taq*1A A1 allele with obesity and comorbid substance use disorders (Blum *et al.*, 1996, 2000).

Other polymorphisms have been associated with addiction and obesity related with the DA system such as DA receptors genes for DA

receptors type 2, 3 and 4 (*DRD2*, *DRD3*, and *DRD4*) as well as the DA transporter (*DAT1*) gene and genes for enzymes associated with DA degradation as catechol-o-methyl-transferase (COMT) (Lindgren *et al.*, 2018).

Despite these findings, it was only a few years ago that specific genome-wide association studies (GWAS) were performed in females having food addiction identified by the YFAS (Cornelis *et al.*, 2016). The results show an enrichment for gene members of the MAPK signaling pathway, but no candidate single nucleotide polymorphisms or a gene for drug addiction was significantly associated with food addiction. They associated this negative result to the limited study power (Cornelis *et al.*, 2016).

Recent studies have begun to recognize the importance of considering the simultaneous involvement of multiple genes in the regulation of pathways by taking into account epistatic interactions among polymorphic loci. Epistasis is used to describe nearly any set of complex interactions among genetic loci (Phillips, 2008). Nikolova *et al*. were the first to use a biologically founded “multilocus genetic profile score”, a composite genetic index reflecting the cumulative effect of multiple polymorphic loci of known functionality on a specific signaling mechanism (Nikolova *et al.*, 2011). Thus, the simultaneous consideration of multiple functional loci allows for the inclusion of polymorphisms with nonsignificant independent effects, which only collectively account for significant proportions of variability. Specifically, they set up a multilocus genetic profile representing the

cumulative impact of functional polymorphisms on DA signaling (comprising *DAT*, *DRD2*, *DRD4,* and *COMPT* genes), which individually have been associated with variation in striatal DA signaling, that can be used to explain individual differences in reward-related ventral striatum variability. They found that the multilocus genetic profile score accounted for a greater proportion of variance in ventral striatum reactivity than did each locus considered independently (Nikolova *et al.*, 2011).

A study employing this genetic methodology to the food addiction learning, investigated whether functional genetic markers associated with elevated DA signaling distinguished between those with YFAS-diagnosed food addiction and non-affected controls (Davis *et al.*, 2013). They found a significantly increased DA signaling in food addiction group compared to controls supporting a reward-based causal model progressing from an inherent biological susceptibility to increased risk for overeating, and ultimately to develop an addiction to hyperpalatable food (Davis *et al.*, 2013). In accordance, recent work revealed that higher polygenic scores approximating DA signaling predicted higher food addiction symptoms and BMI via the relatively blunted reward-related activity of the ventral striatum. This last study was performed in lean individuals indicating that emerging symptoms of food addiction and risk for obesity may have identifiable biological correlates in lean individuals. Thus, risk-related neural and genetic biomarkers that predict subclinical symptoms of food addiction may be

useful for early identification and prevention of weight gain and obesity (Romer *et al.*, 2019).

Regarding other eating disorders such as binge eating disorder, specific studies using the same approach of multilocus genetic profile including six functional markers on four DA genes found a similar result. Binge eating disorder group showed a significantly higher multilocus genetic profile score than obese non-binge eating disorder controls indicating greater DA signaling strength in the striatum and higher responsiveness to reward in binge eating disorder participants (Davis, 2015).

Based on the growing evidence that the DA reward circuit can be modulated by the endocannabinoid system, different reports suggest that the genomic heterogeneity of the endocannabinoid-related genes may influence substance abuse and overeating vulnerability. Most research has been focused on the *CNR1* and *FAAH* genes. Thus, the presence of the rs1049353 mutant CB_1 allele is associated with severe alcoholism and heroin abuse (Parsons and Hurd, 2015). Moreover, the CB_1 single nucleotide polymorphisms rs1049353 showed associations with increased BMI and fat mass due to affecting the stability of mRNA or protein translation in a way that alters CB_1R function decreasing agonist affinity (Doris *et al.*, 2019). However, the specific role of the *CNR1* in the vulnerability of the individual for developing addiction and the underlying mechanisms is not still understood.

5.2. Epigenetic mechanisms of food addiction and eating disorders

Epigenetic mechanisms are candidates for the study of psychiatric disorders that are caused by the interactions between genetic factors and the environment. The term **epigenetics** is defined as a series of biochemical processes through which changes in gene expression are achieved throughout the lifecycle of an organism without a change in DNA sequence (Jaenisch and Bird, 2003). Thus, epigenetic mechanisms can be viewed as the vehicle through which the environment interacts with an individual's genome to determine all aspects of function in health and disease (Nestler, 2014). Certain epigenetic changes resulting from behavioral experience or random developmental events underlie permanent changes in brain function, which could confer vulnerability to addiction and can be inherited (Nestler and Lüscher, 2019).

Epigenetic mechanisms include diverse types of post-translational modifications of histones, methylation of DNA itself, and, more recently, non-coding RNAs such as microRNAs (miRNAs).

5.2.1. Histones modifications

Histone tails may be post-translationally and covalently modified by acetylation, methylation, phosphorylation, ubiquitination, among others. These modifications modulate in a reversible manner the degree of compaction of the chromatin leading to either an open (enable gene expression) or close chromatin state (repress gene expression) (De Sa Nogueira *et al.*, 2018). Precisely, **acetylation** generally promotes the decondensation of chromatin and increases

gene activity by negating the positive charge of lysine residues in histone tails and increases the spacing between nucleosomes (Figure 26). In turn, histone **methylation** can either promote or repress gene activity, depending on the residue undergoing methylation. Different enzymes are involved in the covalent modifications of histone tails: histone acetyltransferases catalyze acetylation and histone deacetylases catalyze deacetylation, while histone methyltransferases catalyze methylation and histone demethylases catalyze demethylation. The functional consequences of histone modifications are facilitated in part by certain proteins that bind to specific modified residues and affect transcriptional changes (Nestler, 2014).

Drug intake modulates histone acetylation and methylation, which has consequences on gene expression or repression explaining some behavioral responses to the drug (Nestler, 2014). Thus, chronic cocaine treatment induces H3 acetylation in the promoters of *BDNF* (brain-derived neurotrophic factor) and cyclin-dependent kinase-5 genes, which have all been implicated in regulating the motivational properties of cocaine. Other authors found a downregulation of two histone lysine dimethyltransferase in NAc induced by chronic cocaine exposure. Genetic models of these proteins were able to modify neuron morphology in the NAc and enhance preference for cocaine (Maze *et al.*, 2010). Finally, selective deletion of this histone lysine dimethyltransferase in *Drd2* neurons resulted in the unsilencing of transcriptional programs normally specific to *Drd1* neurons. Therefore,

the authors proposed a new role for histone modification in contributing to neuronal subtype identity (Maze *et al.*, 2014).

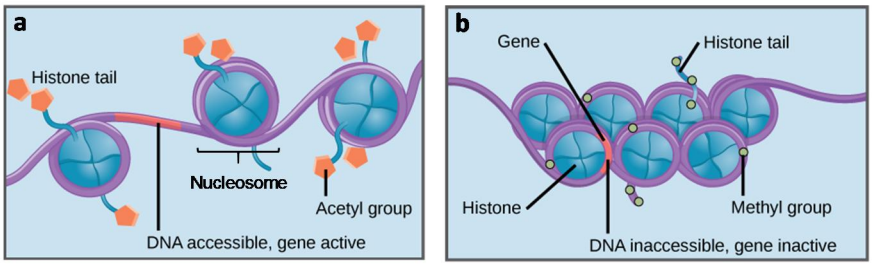

Figure 26. Epigenetic changes can alter the nucleosome position to allow gene transcription. a. Histone acetylation results in loose packing of nucleosomes allowing the binding of transcription factors to DNA and gene expression. **b.** Methylation of DNA and sometimes histones cause nucleosomes to pack tightly together limiting the binding of transcriptomic factors to DNA and suppressing gene expression (Modified from Clark *et al.*, 2018).

5.2.2. DNA methylation

DNA methylation is viewed as a more stable epigenetic change compared to histone tail modifications, in which most of histone modifications are considered reversible. This modification plays a critical role in the establishment and maintenance of cell identity as differentiation during development (Bogdanović and Lister, 2017).

DNA methylation corresponds to the addition of a methyl group to the carbon C5 position of cytosine predominantly at GpC sites. This modification, when occurring in the promoter region, is mostly associated with transcriptional repression (Figure 26). It can either present the association of DNA-binding factors with their target sequence or bind to methyl-CpG-binding proteins to recruit transcriptional corepressors to modify the surrounding chromatin into a silenced state. DNA methylation is catalyzed by DNA

methyltransferases involved in the maintenance of methylation (type 1) or in de novo methylation (type 3). Demethylation processes are performed by ten-eleven translocation enzyme, which catalyzes the hydroxylation of the methylated cytosine (Nestler, 2014).

DNA methylation is altered by drugs of abuse. Expression of DNA methyltransferases-3 in NAc is differentially altered by acute or chronic cocaine exposure and a local knockdown of this protein in NAc increases behavioral response to cocaine, whereas overexpression has the opposite effect (LaPlant *et al.*, 2010). A current challenge is to determine the cell-type specificity of observed epigenetic alterations. A study investigating the DNA-methylation cell- specificity in addiction reveals an increased hypermethylated gene region in genes enriched preferentially in glutamatergic, but not in GABAergic, neurons (Kozlenkov *et al.*, 2017). These results are in accordance with the reduced glutamate transmission reported in the frontal cortex after cocaine exposure (De Sa Nogueira *et al.*, 2018).

5.2.3. Non-coding RNA: microRNA

The complete sequencing of the mammalian genome reveals that several mRNAs that are not translated into proteins (non-coding RNAs) play regulatory roles in cell function. The most studied are miRNAs. miRNAs are length 20-25 nucleotides and act as post-transcriptional regulators that bind to complementary sequences in the 3' untranslated region of their target mRNAs to repress translation or alter mRNA stability and degradation (O'Brien *et al.*, 2018). The complementary base-pairing between miRNA and their target mRNA is

imprecise allowing one single miRNA the regulation of hundreds of protein-coding genes. It is well known that miRNAs are important in brain development, but also have a key role in adult brain function. miRNAs are located in somatodendritic mature neurons and can be translated to synaptic dendrites operating locally to control aspects of synapse development and plasticity (Schratt, 2009).

The biogenesis of miRNAs is a multistep process. They are transcribed by RNA polymerase II leading to the generation of primary miRNA transcripts, which are cleaved in the nucleus by the microprocessor complex, which includes the proteins Drosha and DGCR8. The cleavage product is a precursor miRNA hairpin that is exported to the cytoplasm by an exportin 5-dependent pathway. There, the precursor miRNA is further processed by the RNase Dicer to an intermediate miRNA duplex. The activity of Dicer can be modulated by accessory proteins as FMR1. Depending on the thermodynamic characteristics of the miRNA duplex, one strand (the leading strand) is loaded into a multi-protein complex (miRNA-induced silencing complex, miRISC), whereas the other strand (the passenger strand) is usually degraded. The resulting miRNA-associated miRISC is guided to target mRNAs owing to the extensive, but imperfect pairing of the miRNA, to target sequences that are preferentially located within the 3' untranslated regions of the mRNA. This interaction leads to translational repression and/or degradation of the target mRNA. Important components of miRISC with regard to synaptic function include Argonaute and the helicases MOV10 and DDX6. In addition, accessory RNA-binding proteins (FMR1

and PUM2) are thought to modulate the activity of miRISC in neurons (Schratt, 2009) (Figure 27).

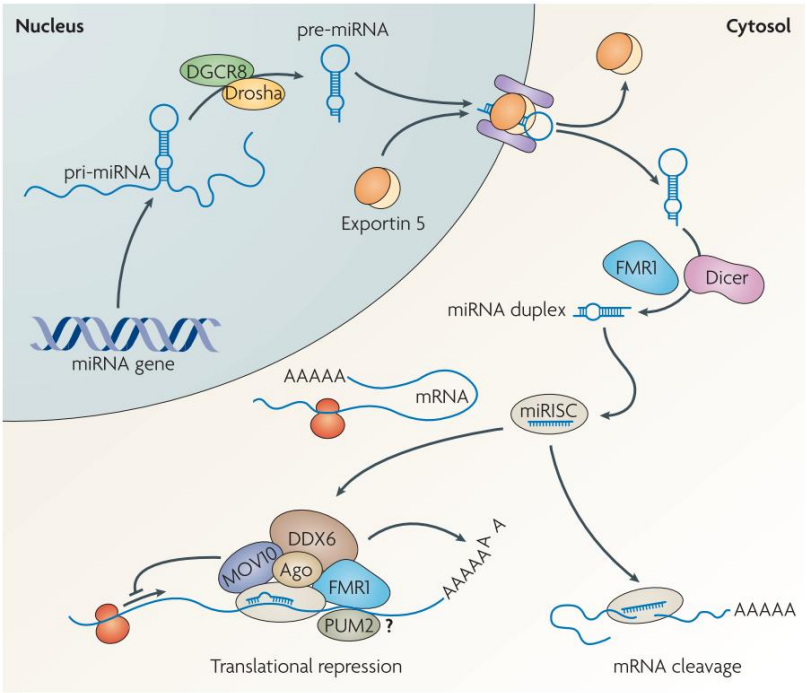

Figure 27. Diagram explaining the miRNA biogenesis. miRNA, microRNA; Pol II, RNA polymerase II; pri-miRNAs, primary miRNA; pre-miRNA, precursor miRNA; miRISC, miRNA-induced silencing complex; Ago, Argonaute (Schratt, 2009).

miRNAs are subject to regulation by neuronal activity at multiple levels. Several promoters of neural miRNAs are occupied by classical activity-regulated transcription factors, such as CREB and MEF2 which couple Ca^{2+}-regulated signaling cascades to the transcriptional machinery (Gebert and MacRae, 2019).

Based on the important role of miRNAs in synaptic plasticity and the emerging appreciation that maladaptive neuroplasticity mechanisms

drive addiction, it is not surprisingly the association of several miRNAs with the addictive-behavior. Multiple miRNAs are reported to be up- or downregulated by drugs of abuse (Doura and Unterwald, 2016). miR-181a, miR-1, and miR-124 are increased and decreased respectively after cocaine exposure. miR-132 and miR-212 are enriched in neurons in a CREB-dependent manner activated by cAMP during cocaine exposure (Hollander *et al.*, 2010). Thus, extended daily access to cocaine self-administration produced an increase of CREB phosphorylation in the dorsal striatum and this effect was amplified by overexpression of miR-212 that in turn reduced cocaine self-administration (Hollander *et al.*, 2010).

An efficient pharmacological approach for silencing miRNAs in vivo, called antagomir, have been developed to study the effects of miRNA-directed regulation on gene expression (Krützfeldt *et al.*, 2005). AntagomiRs are chemically modified, cholesterol-conjugated single-stranded RNAs. These oligos of about 21–23 nucleotides fully complement the miRNAs and effectively compete with miRNA target mRNAs with a stronger binding to the miRNA-associated gene silencing complexes (miRNA-RISCs) (Krützfeldt *et al.*, 2005).

Importantly, the majority of miRNAs are located intracellularly, but a significant number of miRNAs have been observed in the extracellular parts, including blood. This has been attached much attention to use circulating miRNAs as biomarkers for disease. To date, some studies have been performed in comparing circulating miRNAs between

smokers, alcoholics and methamphetamine users versus controls obtaining promising results (Smith and Kenny, 2018).

In spite of these studies in the drug addiction framework, no specific studies have been yet published, to my knowledge, investigating the epigenetic changes during food addiction. In our previous study (Mancino *et al.*, 2015), we only evaluated the epigenetic mark of a target gene (CB_1R gene) at a DNA methylation level. A wide epigenetic study in animals with loss of control towards highly palatable food will be of interest to define the miRNAs alterations during these processes.

6. Animal models of food addiction and eating disorders

Animal models have led to significant leaps in understanding the pathophysiology of several diseases including eating disorders and addiction. It is noteworthy that animal models do not totally emulate all human conditions due to the complexity and multifactorial nature of this kind of disorders, but important features can be reliably measured having variables controlled (Belin and Deroche-Gamonet, 2012). The validity of an animal model is evaluated by three types of validators: construct, face and predictive validity. **Construct validity** is how well the mechanism used to induce the disease phenotype in animals reflects the disease etiology in humans. **Face validity** is how well a model replicates the diseases phenotype (anatomical, biochemical, neuropathological or behavioral features) in humans. Finally, **predictive validity** signifies that a model responds to treatments in a way that predicts the effects of those treatments in humans and measures how well a model can be used to predict currently unknown aspects of the disease in humans (Nestler and Hyman, 2010).

Several animal models of different eating disorders and addiction have been generated through diverse means, including selective breeding, genetic engineering, brain lesions, and environmental manipulations. In the last years, optogenetics and chemogenetics manipulations of specific circuits have produced interesting and promising useful approaches. Based on the main topics of this thesis, the food addiction and binge eating mouse models are now explained in detail.

6.1.Food addiction mouse model

A first food addiction mouse model with face validity was generated by Mancino *et al* at 2015. This is an operant conditioning model that exposed mice to long-term operant training to obtain palatable food. Importantly, this model permits to distinguish different subpopulations of mice vulnerable or resilient to food addiction (Mancino *et al.*, 2015).

The **operant conditioning model** is based on the instrumental learning process through which the strength of a behavior is modified by reinforcement or punishment (Sanchis-Segura and Spanagel, 2006). An operant box is used to conduct drug or food operant self-administration. These chambers are equipped with an active and inactive lever/nose pokes, responding on the active lever/nose poke will activate a pump/dispenser delivering the reinforcer (drug or food), while responding on the inactive lever/nose pokes has no consequences. The active responding is paired with stimuli such as a light or a tone, which facilitates the operant behavior (Figure 28). The most common schedules of reinforcement used in drug self-administration are the fixed ratio (FR) and the progressive ratio (PR) schedules. Under a FR schedule, the reinforcer is delivered every time that a pre-established number of responses are performed. Usually, there is a time out period (10 s) after each pellet delivery or drug infusion, where operant responses are not rewarded to avoid drug overdose. The PR schedule to assess the motivational effects for the reward is used. In this schedule, the required ratio to deliver the reinforcer increases following a pre-established progression. The

maximal ratio that an animal is willing to do to obtain one single pellet or infusion is called the "breaking point". Thus, the breaking point is considered to be a measure of the motivation for the reinforcer and can be compared with other reinforcers to assess relative reinforcing efficacy or strength. Operant conditioning self-administration procedures are considered to be the most valid and reliable models of human drug/food consumption (Sanchis-Segura and Spanagel, 2006).

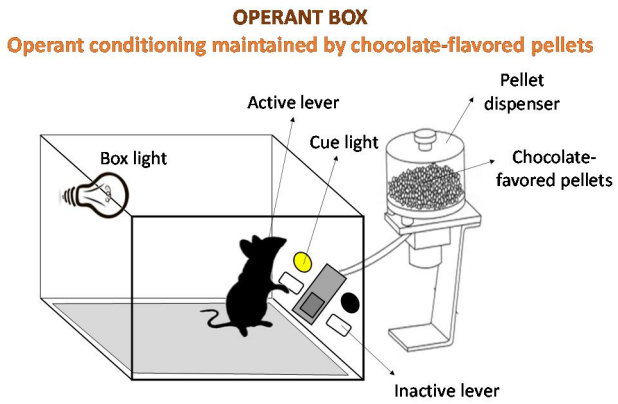

Figure 28. Scheme of an operant box to perform operant conditioning maintained by chocolate flavored-pellets. The chamber is provided with two levers. Responses on the active lever will deliver a food pellet and activate a light (cue), while responses of the inactive lever will have no consequences.

Our food addiction mouse model (Mancino *et al.*, 2015) was adapted from that previously described for cocaine addiction in mice by (Deroche-Gamonet *et al.*, 2004). The cocaine addiction model was the first multi-symptomatic model of addiction, instead of a mere drug self-administration model, based on the DSM-IV clinical criteria. This model provides a unique tool to identify a percentage of drug-exposed rats that shift from controlled to compulsive self-administration, despite

equal cocaine intake, highlighting the interindividual differences (Deroche-Gamonet *et al.*, 2004).

In the **DSM-IV** (1994), the diagnosis of drug addiction was human-centered in contrast to the previous DSM-III (1980) in which the diagnosis was focused on the physical effects produced by the long-term exposure to drugs of abuse, tolerance, and withdrawal. A notable change was produced in the DSM-IV because the criteria of tolerance and withdrawal were not necessary or sufficient for the diagnosis of addiction and add five criteria focused on the loss of control over the drug taking. The five loss of control criteria can be grouped into three major behavioral aspects: persistence to response (difficulty to limit drug use), motivation (extremely strong motivation for the drug) and resistance to punishment (maintaining drug used despite awareness of negative consequences) (American Psychiatric Association, 1994). Deroche-Gamonet *et al* evaluated these three hallmarks of substance dependence in rats after a prolonged cocaine self-administration period to classify rats as addicted and non-addicted based on the scores of each criterion above a certain threshold (Belin and Deroche-Gamonet, 2012).

Remarkably, the emerging of the last DSM version (2013), the **DSM-5**, did not alter the three main addictive dimensions. The major change was the combination of two separate categories of abuse and dependence into a single category, Substance Use Disorders with 11 criteria with the addition of the *craving* criterion and the removal of the *legal problems*. It was introduced the concept of different severities

depending on the criteria achieved: 0–1, unaffected; 2–3, mild; 4–5, moderate; ≥6, severe. Only severe substance use disorder with a substantial loss of self-control is synonymous with the term *addiction* (Volkow *et al.*, 2016). In the DSM-5, symptoms of tolerance and withdrawal occurring during medical treatment with prescribed medications do not count when diagnosing a substance use disorder in order to avoid the mislabelling of patients as dependent or addicted. Finally, DSM-5 includes for the first time behavioral addiction (gambling disorder) as a new category, indicating that these addictions activate reward systems similar to those activated by drugs of abuse and produced some behavioral symptoms that appear comparable to those produced by the substance use disorders (American Psychiatric Association, 2013; Compton *et al.*, 2013; Korrekturen, 2014; Robinson and Adinoff, 2016).

As it was previously mentioned, the concept of food addiction not included in the DSM-5 is currently diagnosed by the validated tool YFAS 2.0 (Schulte and Gearhardt, 2017). This questionnaire is adapted from the substance use disorders criteria in the DSM-5. Notably, the food addiction mouse model evaluates the three addiction criteria which summarize the hallmarks of addiction based on DSM-IV, specified in DSM-5, and now included in the food addiction diagnosis through the YFAS 2.0 (Table 4).

The **food addiction mouse model** consists on a long period of operant conditioning maintained by chocolate-flavored pellets (118 sessions) in which the three food addiction criteria were evaluated in two time

points (early and late period): (I) persistence to response when food is signaled as not available, (II) high motivation for the food and (III) resistance to punishment, keep seeking and taking the food despite negative consequences. In the late period, mice were categorized in food addicted or non-addicted depending on the number of positive criteria that they have met. An animal was considered positive for an addiction criterion when the score of the specific behavioral test was above the 75th percentile of the normal distribution of the chocolate group (Mancino *et al.*, 2015).

The research performed using this model indicated that is a valid model with face and predictive validity. Animals considered food addicted (2-3 criteria) show high scores of each of the three addiction criteria than mice considered as non-addicted (0 criteria). Addicted mice represented ~20% of the population exposed to palatable food, an incidence similar to that reported in humans (19.9%, Pursey *et al.*, 2014). This percentage was decreased by the rimonabant treatment. These results highlight the importance of the interaction between a vulnerable phenotype and chronic palatable food exposure in the development of compulsive food self-administration. Thus, the food addiction mouse model is a reliable model to investigate the neurobiological mechanisms underlying the vulnerability or the resilience to make the transition from controlled to compulsive palatable food intake.

Table 4. **Diagnostic items of drug use related disorders in DSM-IV and DSM5 and of food addiction in YFAS 2.0, with their corresponding criteria measured in the mouse model of food addiction** (Modified from Piazza and Deroche-Gamonet, 2013; Moore *et al.*, 2017)**.** *Certain foods: sweets, starches, salty, fatty and sugary foods.

	DSM-IV	DSM-5	YFAS 2.0	Animal models
	Substance-related disorders	Substance-related and addictive disorders	Food addiction	Mice model of food addiction (2015)
	Substance abuse	Substance use disorders with severity	**Self-report** asking about "certain foods"*	3 main addictive domains
Diagnosis	At least 1 of these 4 criteria	At least of the 11 criteria (2-3 mild, 4-5 moderate, ≥6 severe)	Clinically significant or distress and 2 or more of the criteria (2–3 mild, 4–5 moderate, and ≥6 severe)	At least 2 of the 3 criteria
Criteria / Questions	1. Recurrent failure in major role obligations	1. Recurrent failure in role obligations	1. Recurrent failure in role obligation	
	2. Use in physically hazardous situations	2. Use in physically hazardous situations	2. Use in physically hazardous situations	
	3. Recurrent substance-related legal problems			
	4. Continued use despite social or interpersonal problems	3. Continued use despite social or interpersonal problems	3. Continued use despite social or interpersonal problems	
	Substance dependence			
	3 out of these 7 criteria			
Criteria / Questions	1. Tolerance	4. Tolerance	4. Tolerance	
	2. Withdrawal	5. Withdrawal	5. Withdrawal	
	3. Consumed more (larger amount and for a longer period) than planned	6. Consumed more (larger amount and for a longer period) than planned	6. Consumed more (larger amount and for a longer period) than planned	1. Persistence to response (difficulty to limit food use)
	4. Unable to cut down or stop	7. Unable to cut down or stop	7. Unable to cut down or stop	
		8. Craving	8. Craving	
	5. Great deal of time spent	9. Great deal of time spent	9. Great deal of time spent	2. Motivation (strong motivation for the food)
	6. Important social, work or recreational activities are given up because of use	10. Important social, work or recreational activities are given up because of use	10. Important social, work or recreational activities are given up because of use	
	7. Use despite knowledge of physical/emotional consequences	11. Use despite knowledge of physical/emotional consequences	11. Use despite knowledge of physical/emotional consequences	3. Resistance to punishment (keep taking the food despite negative consequences)

6.2.Binge eating mouse model

Several animal models have been developed to study binge eating behavior. Some models produce voluntary binge eating in sated animals by offering limited access to palatable food, others incorporate a cyclic periods of food deprivation and feeding to stimulate animals to binge eat when palatable food is presented and others used stressors such as footshock to precipitate binge eating (Avena and Bocarsly, 2012). Thus, the majority of the models typically use food restriction, stress and limited access to palatable diets. However, these models have some drawbacks. Food deprivation increases locomotor activity and corticosterone levels, and these models do not cause stable binge-like eating patterns in a short period of time. Consequently, some laboratories develop a rapid and relatively simple model of binge-eating behavior in mice that do not require food deprivation nor the application of exogenous stressors (Cottone *et al.*, 2009; Czyzyk *et al.*, 2010).

Animals following this model of binge eating are exposed to *ad libitum* access to standard food and to intermittent access to palatable food only during 24h/48h. Thus, a binge cycle involved 6/5 days of access to chow only followed by 24 h/48 h free-choice access to palatable and chow. The binge eating behavior is analyzed measuring the food intake at 2.5 h, 24 h, and 48 h during the free-choice period. The human pathology is characterized by consuming a large amount of food typically high calories, fat and sugar, in a discrete period of time. These main features are mimic in this mouse model of binge eating indicated

by significantly stably increased intake of palatable food in the first 2.5 h and because usually the palatable food presented is high energy diet (73% more fat and 43% more sucrose than standard food) (Czyzyk *et al.*, 2010) or cafeteria diet (composed of an equivalent mixed of four popular brand chocolate bars highly consumed in humans) (Gutiérrez-Martos *et al.*, 2017). This model has predictive validity since some pharmacological agents with clinical efficacy in binge eating disorder reduce binge eating in this model. However, there are other characteristics of the human pathology that are not presented in this mouse model, such as changes in serum corticosterone levels or anxiety and depressive-like behaviors (Novelle *et al.*, 2018).

Structural plasticity changes in the NAc have been found in this model and the activation of microglia and neuroinflammatory processes play an important role in the development of overeating (Gutiérrez-Martos *et al.*, 2017). Therefore, this binge-eating approach could be an interesting model to evaluate how the endocannabinoid system contributes to overeating.

6.3.Chemogenetic and optogenetic approaches

The recent development of optogenetics and chemogenetics has revolutionized systems in neuroscience by allowing excitation and inhibition of specific neuronal subpopulations and neuronal circuits to study the neurobiological mechanisms of clinical disorders (Vlasov *et al.*, 2018).

Optogenetics involves the introduction of genes encoding for photoactivatable ion channels (opsins) in targeted cells to enable the depolarization or hyperpolarization depending on the specific opsin employed: channelrhodopsin-2 for depolarizing neurons and halorhodopsin for hyperpolarizing neurons. One key advantage of optogenetics is the ability to have precise temporal control (milliseconds range) of neuronal activity, although a permanent intracranial implant is required for the delivery of light pulses (Aston-Jones and Deisseroth, 2013).

In turn, **chemogenetics** refers to the insertion of designer receptors exclusively activated by designer drugs (DREADDs) to provide a lock-and-key approach to selectively modulate neuronal function. Unlike optogenetics, chemogenetics does not offer a high temporal resolution, but allows sustained neuronal excitation or inhibition for a long time in a noninvasive manner since intracranial implants are not required. The DREADDs are GPCRs modified from muscarinic receptors and include Gs, Gq and Gi varieties. When expressed in neurons, DREADDs are not sensitive to endogenous ligands, but are sensitive to a “designer drug”, clozapine N-oxide (CNO), which is an inert and inactive clozapine metabolite (Urban and Roth, 2015).

In the case of the human M3 muscarinic DREADD receptor coupled to Gq (hM3Dq), only two point mutations (Y3.33C and A5.46G) to the human muscarinic receptor 3 were needed to achieve the mutant hM3Dq with (I) nanomolar potency for CNO, (II) insensitivity to the endogenous ligand acetylcholine, and (III) low levels of constitutive

activity. The stimulation of the hM3Dq DREADD by CNO undergoes burst firing in a Gq-coupling dependent manner and faithfully mimics the signaling of the native M3 muscarinic receptors activated by acetylcholine (Alvarez-Curto *et al.*, 2011). Overexpression of hM3Dq in pancreatic cells (Guettier *et al.*, 2009), hepatocytes (Hua Li *et al.*, 2013), neurons (Alexander *et al.*, 2009) and astrocytes (Agulhon *et al.*, 2013) does not increase basal activity, indicating an absence of constitutive activity in these in vivo contexts.

Since hM3Dq is a GPCR, it could be the subject of the typical regulatory processes of these kinds of proteins, such as phosphorylation, desensitization, internalization or downregulation. Thus, prolonged activation of hM3Dq by CNO could lead to a decreased response due to desensitization and/or downregulation of the receptor (Roth, 2016). However, a study indicates that the chronic administration of CNO, consecutive daily doses, does not modify the effects on potentiation of locomotor activity in rats with an overexpression of hM3Dq in hippocampal pyramidal neurons (Alexander *et al.*, 2009). Likewise, repeated doses of CNO are capable to preserve an effective activation of hM3Dq in hypothalamic neurons, as measured by feeding response in vivo (Krashes *et al.*, 2011, 2013).

On the other, since Y3.33 and A5.46 are conserved residues, the Gi DREADD was also created using the same point mutations in both the M2 and M4 muscarinic receptors (hM2Di, hM4Di) (Armbruster *et al.*, 2007). The hM4Di produces a downstream signaling cascade leading to the neuron silencing by activating the GIRKs as Gi-coupled GPCRs do.

The overexpression of hM4Di activated by CNO in hippocampal pyramidal neurons induces hyperpolarization and silences spontaneous and depolarization-evoked firing (Armbruster *et al.*, 2007). Several studies demonstrate the utility of silencing the neuronal firing to identify the neuronal circuits involved in a particular behavior or neurophysiological response. For example, the inhibition of AgRp-expressing neurons in the arcuate nucleus of the hypothalamus by activated hM4Di inhibited feeding (Krashes *et al.*, 2011).

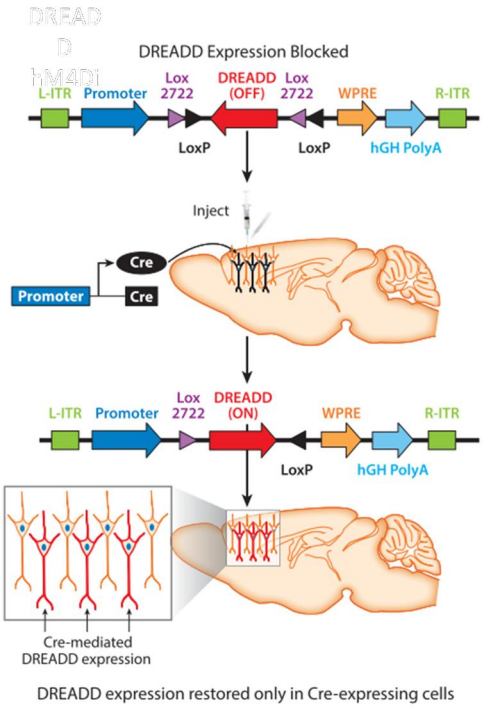

Figure 29. Cell-type DREADD expression specificity approach. Schematic of a DREADD virus in which the DREADD is in an inverse orientation until the virus infects neurons that express Cre recombinase (black). The viral construct contains a promoter, usually hSyn, and the DREADD gene in an inverse orientation flanked by two repeating loxP sites. To obtain cell-type specific expression, the virus is microinjected into mice that express the Cre recombinase gene under the control of a cell-type specific promoter. The Cre recombinase cuts both loxP sites, thus correcting the orientation of the DREADD for proper expression and allowing for the selective expression of the DREADD receptor only in Cre-expressing neurons (red) (Adapted from Urban and Roth, 2015).

DREADDs are typically introduced to neurons by viral vectors. A variety of options are available to achieve cell-type DREADD expression specificity. Several studies used the Cre-loxP approach (Kuhlman and

Huang, 2008). This strategy employs two pairs of heterotypic, antiparallel loxP-type recombination sites, which undergo an inversion of the coding sequence followed by the excision of two sites. Injecting an adeno-associated virus (AAV) encoding DREADDs flanked by two repeating loxP sites, with cell-type specific Cre recombinase allows a cell-type specific expression in mice (Krashes *et al.*, 2011) (Figure 29).

Other viral approaches to achieve cell-type specificity is to include cell-type specific promoters in the AAV or to use genetically modified mice expressing Cre-recombinase in a specific cell population. Finally, a combinatorial viral strategy using a retrograde AAV targeting axonal projections combined with the DREADD AAV is used to target a precise neuronal network (Roth, 2016) (Figure 30).

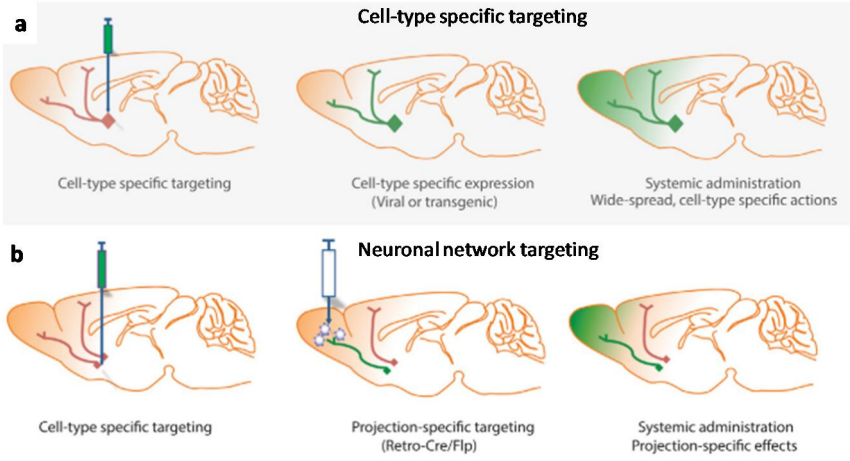

Figure 30. Potential approaches for cell-specific and neuronal network (projection-specific) modulation of neuronal activity using DREADDs. a, The standard approach whereby DREADDs are expressed in a cell-type-specific manner (either virally or transgenically) **b**, How a combination of cell-type-specific expression (e.g., localized injection of AAV-loxP-hSyn-DREADD) and projection-specific infusion of CAV-Cre or retrograde AAV allows for the projection-specific expression and activation of DREADDs (Adapted from Roth, 2016).

Recently, some publications suggested that DREADDs-mediated behavior could be induced by the metabolized clozapine rather than by the CNO, as revealed by the high and low affinity for DREADDs respectively, and supported by the finding that CNO lacks brain penetrance (Gomez *et al.*, 2017). Clozapine, as an antipsychotic drug, could potentially lead to important undesirable side effects. However, DREADDs require very low subthreshold clozapine doses for their selective activation and these findings still encourage researchers to use DREADD technology. To overcome these limitations a second-generation DREADD agonists, as Compound 21 (Chen *et al.*, 2015), JHU37152 and JHU37160 were recently developed with high in vivo DREADD potency for the last two (Bonaventura *et al.*, 2018). However, the new ligands have not been yet validated in the different DREADD experimental approaches.

7. Therapeutics for food addiction and eating disorders

Treatments aiming to control overeating are clinically relevant due to the rising rates of food addiction and binge eating disorder contributing to the obesity pandemic (Figure 31).

Nowadays, the most effective weight loss therapy in obesity is the bariatric surgery, which produces a weight loss of 15% or more of initial weight and is associated with reduced mortality and improvements in comorbid diseases. Pre-bariatric patients have more prevalence of food addiction than other obese individuals and it is associated with more frequent food-cravings and higher attentional impulsivity (Meule *et al.*, 2014). After bariatric surgery, 93% of subjects who were identified with food addiction before the surgery no longer met criteria according to the YFAS (Pepino *et al.*, 2014). However, there are well-described unfavorable surgical consequences requiring additional surgery, and gastrointestinal and nutritional problems are important long-term concerns. The nutritional and metabolic consequences of bariatric surgery require monitoring and micronutrient supplementation for lifelong (Madura *et al.*, 2012). Thus, bariatric surgery is restricted to obese individuals with high BMI (BMI>35) and particular clinical characteristics that difficult the application of other pharmacotherapy approaches.

7.1.Pharmacological treatments

The history of pharmacological treatments for obesity is dismal since several approved drugs were later withdrawn due to poor safety profiles and side effects. Even, the drugs not withdrawn are approved only for short-term use under 12 weeks (Davis *et al.*, 2014) (Figure 31).

Amphetamines and appetite suppressants were prescribed several decades ago. However, adverse reactions including cardiovascular effects and abuse potential limited their usefulness (Bersoux *et al.*, 2017). Drugs that could suppress appetite without the potential for abuse were then developed. **Sibutramine**, a norepinephrine and serotonin reuptake inhibitor, was approved for weight loss in 1997. Increases of blood pressure and heart rate among other side effects resulted in the withdrawn from both the United States and European markets (Padwal and Majumdar, 2007). On the other, the preclinical literature induced a wide range of promising pharmacological strategies that aim to target modulators of the brain reward system. One important brain reward modulator is the endocannabinoid system, which controls appetite and consumption of food. The CB_1R antagonist, **rimonabant**, was approved in Europe and more than 30 countries worldwide in 2006 for the treatment of obesity (Rinaldi-Carmona *et al.*, 1994). While effective in inducing weight loss, this drug was withdrawn from clinical use just 2 years later due to psychiatric side effects, including anxiety, depression and suicidal ideas (Christensen *et al.*, 2007). Afterward, new neutral CB_1R antagonists and/or peripherally restricted CB_1R antagonists unable to cross the

blood-brain barrier have been developed (D'Addario *et al.*, 2014). Alternatively, pharmacological modulators of endocannabinoids synthesis, rather than CB_1R blockade, could provide a more physiological approach to treat obesity.

One current available drug for obesity, approved in 1999, is **orlistat**, an inhibitor of gastrointestinal lipase reducing the absorption of dietary fat. It has been shown to be modestly useful in reducing the symptoms of binge and decreasing body weight. Orlistat is currently considered a good choice because of its safe cardiovascular risk profile and beneficial effects on lipids levels. However, unpleasant side effects have been described including diarrhea and excess gas (Rössner *et al.*, 2000).

Additional approved anti-obesity drugs are based on the arguments indicating that the neurobiological mechanisms between food addiction, obesity, and drug addiction are mostly overlapped. This leads to the proposal of new treatments for obesity and food addiction by using drugs already proven successful in the treatment of drug addiction (Lindgren *et al.*, 2018). **Naltrexone** is an opioid antagonist preferentially acting on mu opioid receptor, currently used for treating alcohol and opioid addiction. Naltrexone use has been revealed to significantly diminish food intake in normal-weight volunteers and to decrease the subjective liking of foods, mainly highly palatable foods. Moreover, naltrexone reduces reward activation in normal volunteers seeing and tasting chocolate (Lee and Fujioka, 2009). On the other, **bupropion** is a norepinephrine-dopamine reuptake inhibitor leading to an increase DA activity, it was developed as an antidepressant and

currently approved to smoking cessation. The combination of these two drugs sold under the brand name, **Contrave**, has been proposed to be a new anti-obesity treatment. Contrave administration reduces body weight (5% or more) after 56 weeks of treatment in 48% of obese participants (Greenway *et al.*, 2010). Moreover, Contrave blunted hypothalamic activation to food cues and enhanced activation of brain regions involved in inhibitory control, internal awareness and memory (Wang *et al.*, 2014).

Other medications have been FDA-approved for the treatment of obesity with relevant implications for the current and future treatment of food addiction. These drugs are lorcaserin and topiramate. **Lorcaserin** targets the serotonin 5HT2C receptor in the brain inducing satiety while **topiramate** is an antiepileptic medication with GABAergic activity and antagonizes AMPA/kainate glutamate receptors agonist activity decreasing appetite and weight. Topiramate also acted as anti-binge eating and anti-purging being useful in the treatment of binge eating disorder. A clinical study reported that prolonged administration of topiramate induces a marked reduction in the frequency of binge episodes with significant weight loss (Milano *et al.*, 2013).

7.2.Non-pharmacological treatments

7.2.1. Behavioral therapies

The behavioral therapies such as cognitive behavioral intervention could be a good non-pharmacological alternative taking into account

that food and drug addictive behaviors are the result, in part, of maladaptive eating or substance patterns. These psychosocial interventions are focused on challenging and changing unhelpful cognitive distortions, such as thoughts, beliefs, attitudes, and behaviors, improving emotional regulation, and the development of personal coping strategies that target solving current problems (McHugh *et al.*, 2010; Jacob and Isaac, 2012; Castelnuovo *et al.*, 2017; Linardon *et al.*, 2017). It is usually recommended a combination of behavioral therapies with pharmacological ones.

7.2.2. Brain stimulation therapeutics

The circuit-based therapeutics could be invasive as deep brain stimulation or non-invasive, such as repetitive transcranial magnetic stimulation (rTMS) and transcranial direct current stimulation (tDCS).

Deep brain stimulation

Deep brain stimulation is an invasive non-lesional neurosurgical procedure with surgical implantation of current passing electrodes for the electrical stimulation of discrete brain regions. It is well established as a safe and efficacious treatment for Parkinson's disease (Honey *et al.*, 2017) and has been employed more recently as a potential treatment for several circuit-based neuropsychiatric conditions, including obsessive-compulsive disorder (Alonso *et al.*, 2015) and major depression (Cleary *et al.*, 2015). However, deep brain stimulation provides a general stimulation and this weak specificity not offers the selectivity of preclinical optogenetic approaches (Cooper *et al.*, 2017). To solve this problem, a combinatorial approach with deep brain

stimulation and pharmacological adjuvant that helps to eliminate opposing effects from the general stimulation has been proposed in the addiction field. Critically, in preclinical models, this approach was sufficient to reverse the cocaine-induced changes in synaptic plasticity and cocaine locomotor sensitization in cocaine-exposed mice (Creed *et al.*, 2015).

Deep brain stimulation strategy has been also used in preclinical and clinical obesity studies. Thus, the stimulation of specific hypothalamic regions (homeostatic center) and NAc (reward system) in women resulted in weight loss and a reduction in BMI (Harat *et al.*, 2016). These results pointed out the possibilities of deep brain stimulation in the treatment of obesity, food addiction, and other eating disorders. However, a number of further studies are necessary to better determine the possible side effects and deep brain stimulation effectiveness in this field.

Repetitive transcranial magnetic stimulation and transcranial direct current stimulation

rTMS and tDCS are non-invasive stimulation strategies without surgical intervention. **rTMS** passes brief current pulses through a coil over the scalp to generate an electromagnetic field that inhibits (low frequency, <5 Hz rTMS) or activates (high frequency, >5 Hz rTMS) target neurons, while **tDCS** delivers weak electrical current to brain regions through electrodes placed on the scalp to either depolarize (anodal tDCS) or hyperpolarize (cathodal tDCS) resident neurons.

Most studies to date, have employed high-frequency rTMS and tDCS targeting the dlPFC in order to increase neuronal excitability and cortical activity improving executive control. dlPFC is known to exert top-down control due to its connectivity with the limbic circuit (Volkow *et al.*, 2013). Obese subjects and drug abusers show a decreased dlPFC activity associated with compulsive behaviors (Lindgren *et al.*, 2018). Recent studies using high-frequency rTMS of the dlPFC reported reduced cocaine use and cravings in patients with cocaine use disorder (Terraneo *et al.*, 2016). In accordance, a reduction in food cravings and weight loss was observed in a cohort of obese subjects after 5 weeks of high-frequency dlPFC rTMS (Ferrulli *et al.*, 2019). In the same line, several studies stimulating the dlPFC with tDCS in obese patients observed a decrease in food cravings (Lee *et al.*, 2018).

The possible efficacy of high-frequency rTMS of dlPFC in treating addiction-like behavior towards drugs or food might be explained by the induction of long-term neuroplastic changes modulating cortical excitability. The long-term plasticity is produced at dlPFC, the primary activation site, and may have an effect on subcortical areas, the secondary activation sites, due to the release of a wide variety of neurotransmitters. Indeed, high-frequency rTMS of dlPFC induces a sustained increase of DA levels in the human ventral striatal complex (Diana *et al.*, 2017).

These findings suggest a potential role of rTMS and tDCS in the treatment of obesity, food addiction, and addiction, given its safety-feasibility profile and lack of serious side effects. More studies are

required to define stimulation parameters, the frequency of the treatment, and the long-term persistence of any beneficial effects.

7.2.3. Neurofeedback strategies

Other non-pharmacological approaches include neurofeedback strategies. These strategies train patients to regulate their own brain activity using real-time feedback from functional magnetic resonance imaging or electroencephalography (Hammond, 2011). The goal is to promote normalized brain activity via associative learning and provide patients with coping strategies to modify psychological states. A few small studies have found positive results with neurofeedback in subjects with substance use disorders and overeating, the majority of them focused on treat craving (Schmidt *et al.*, 2017; Volkow and Boyle, 2018). Although these treatments are still in very preliminary stages, in combination with pharmacological or behavioral interventions could potentially help to enhance treatment efficacy (Volkow and Boyle, 2018).

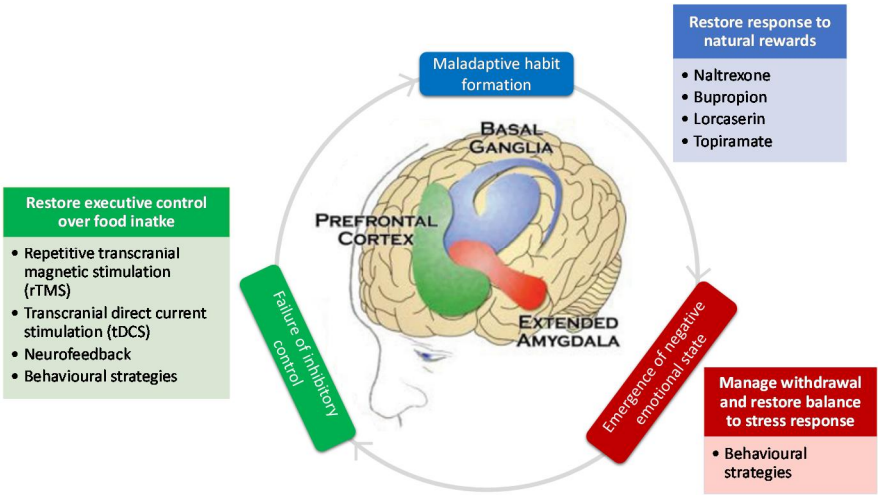

Figure 31. The three stages of the food addiction cycle with the main brain regions implicated and possible pharmacological or non-pharmacological strategies to restore them (Modified from Volkow and Boyle, 2018).

Basic research focused on understanding the neurobiological mechanisms of food addiction and eating disorders, trying to identify the specific brain-circuits involved, would allow the identification of new targets for prevention and treatment of specific disease's endophenotypes in a personalized manner.

Objectives

General objective

The general objective of this thesis is to study the neurobiological mechanisms involved in the loss of control over food intake underlying the food related addictive disorders.

Objective 1: To study the neurobiological mechanisms underlying the resilience and the vulnerability to develop food addiction: focus on the endocannabinoid and dopamine systems.

Chapter 1: A specific top-down cortical pathway controls resilience versus vulnerability to develop food addiction.

Objective 2: To study the differential epigenetic signatures of the food addiction resilient and vulnerable phenotypes. Modulation of microRNAs as potential therapeutic targets.

Chapter 2: Characterizing the differential epigenetic profile of vulnerable and resilient phenotypes to develop food addiction.

Objective 3: To investigate the role of the endocannabinoid system in the binge eating disorder and the emotional manifestations associated.

Chapter 3: CB_1R in $CAMKII\alpha^+$ neurons is involved in the loss of control over palatable food intake in a binge eating mouse model

Results

Laura Domingo-Rodriguez*, Inigo Ruiz de Azua*, Eduardo Dominguez, Eric Senabre, Sami Kummer, Mohi Navandar, Sarah Baddenhausen, Clementine Hofmann, Raul Andero, Susanne Gerber, Mara Dierssen, Beat Lutz#, Elena Martín-García#, Rafael Maldonado#.

A specific top-down cortical pathway controls resilience versus vulnerability to develop food addiction.

Under second review in Nature Communications.

* Equal contribution

Equal seniority

Chapter 1

A specific top-down cortical pathway controls resilience versus vulnerability to develop food addiction

1.1.Abstract

Food addiction is linked to obesity and eating disorders and is characterized by a loss of behavioral control and compulsive food intake. Using a food addiction mouse model, we found that a lack of CB_1R in dorsal telencephalic glutamatergic neurons prevents the development of food addiction, which was associated with enhanced glutamatergic transmission in the mPFC. In contrast, chemogenetic-induced decrease of neuronal activity in the mPFC- NAc projections produced compulsive food seeking. Transcriptomic analysis and genetic manipulation identified that increased D_2R expression in the mPFC-NAc pathway promoted this addictive phenotype. Our study unravels a new neurobiological mechanism underlying resilience and vulnerability to develop food addiction, which is expected to pave ways for novel and efficient interventions to battle this disorder.

1.2.Materials and methods

Animals

Male mice, aged 2-4 months, were housed individually in a temperature- and humidity-controlled laboratory conditions (21 ± 1ºC, 55 ± 10%) maintained with food and water *ad libitum.* Mice were tested during the dark phase of a reverse light cycle (lights off at 8.00 a.m and on at 20.00 p.m). Firstly, we used Glu-CB1-KO mice ($CB1^{floxed/floxed;\ Nex\text{-}Cre/+}$ mice), lacking

CB_1R in dorsal telencephalic glutamatergic neurons, and their wild-type (WT) littermates in C57BL/6N background (Marsicano *et al.*, 2002; Monory *et al.*, 2006; Bellocchio *et al.*, 2010; Martín-García *et al.*, 2016). Secondly, we used Nex-Cre/+ mice expressing Cre recombinase in dorsal telencephalic glutamatergic neurons (Goebbels *et al.*, 2006) and also WT JAX™ C57BL/6J (C57BL/6J) mice purchased from Charles River (France). All experimental protocols were performed in accordance with the guidelines of the European Communities Council Directive 2010/63/EU and approved by the local ethical committee (Comitè Ètic d'Experimentació Animal-Parc de Recerca Biomèdica de Barcelona, CEEA-PRBB). In agreement, maximal efforts were made to reduce the suffering and the number of mice used.

Behavioral experiments

Operant behavior apparatus

Mouse operant chambers (Model ENV-307A-CT, Med Associates, Georgia, VT, USA) were used for operant responding maintained by chocolate-flavored pellets. The operant chambers were equipped with two retractable levers, one randomly selected as the active lever and the other as the inactive. Pressing on the active lever resulted in a food pellet delivery paired with a stimulus-light (associated-cue), located above the active lever, and while pressing on the inactive lever had no consequences. A food dispenser equidistant between the two levers permitted the delivery of food pellets when required. The floor of the chambers was a grid floor that served to deliver electric food shocks in the session of shock-test and served as a contextual cue in the session of shock-associated cue, the day after the shock session. During the rest of self-administration sessions, a

metal sheet with holes was placed above the grid floor. Thus, mice could discriminate between different contexts. The chambers were made of aluminum and acrylic and were housed in sound- and light-attenuated boxes equipped with fans to provide ventilation and white noise.

Food pellets

During the operant conditioning sessions, after active responding by lever pressing, animals received a 20 mg chocolate-flavored pellet, which is a highly palatable isocaloric pellet (TestDiet, Richmond, IN, USA). These pellets had a similar caloric value (3.44 kcal/g: 20.6% protein, 12.7% fat, 66.7% carbohydrate) of standard maintenance diet provided to mice in their home cage (3.52 kcal/g: 17.5% protein, 7.5% fat, 75% carbohydrate) with some slight differences in their composition: addition of chocolate flavor (2% pure unsweetened cocoa) and modification in the sucrose content. Indeed, although the carbohydrate content was similar in the standard diet (75%) and in highly palatable isocaloric pellets (66.7%), the proportion of sucrose content in standard diet food was 8.3% and in highly palatable isocaloric pellets 50.1%.

Self-administration session

The beginning of each self-administration session was signaled by turning on a house light placed on the ceiling of the chamber during the first 3 s. Daily self-administration sessions maintained by chocolate-flavored pellets lasted 1 h or 2 h and were composed by 2 pellet periods (25 min and 55 min) separated by a pellet-free period (10 min). During the pellet periods, pellets were delivered contingently after an active response paired with a stimulus light (cue light). A time-out period of 10 s was established after

each pellet delivery, where the cue light was off, and no reinforcer was provided after responding on the active lever. Responses on the active lever and all the responses performed during the time-out period were recorded. During the pellet-free period, no pellet was delivered, and this period was signaled by the illumination of the entire self-administration chamber. In the operant conditioning sessions, mice were under FR1 schedule of reinforcement (one lever-press resulted in one pellet delivery) followed by an increased FR to 5 (FR5) (five lever-presses resulted in one pellet delivery) for the rest of the sessions. As previously described (Martín-García *et al.*, 2011), the criteria for the achievement of the operant responding were acquired when all of the following conditions were met: (1) mice maintained a stable responding with less than 20% deviation from the mean of the total number of reinforcers earned in three consecutive sessions (80% of stability); (2) at least 75% responding on the active lever; and (3) a minimum of 5 reinforcers per session. After each session mice were returned to their home cages.

Three addiction criteria

Three behavioral tests were used to evaluate the food addiction criteria as recently described (Mancino *et al.*, 2015) and adapted from cocaine addiction in rats (Deroche-Gamonet *et al.*, 2004). These three criteria summarized the hallmarks of addiction based on DSM-IV (Deroche-Gamonet *et al.*, 2004), specified in DSM-5 and now included in the food addiction diagnosis through the YFAS 2.0 (Gearhardt *et al.*, 2016).

Persistence to response: Non-reinforced active responses during the pellet free period (10 min), when the box was illuminated and signaling the

unavailability of pellet delivery, were measured as persistence of food-seeking behavior. On the 3 consecutive days before the PR mice were scored.

Motivation: The PR schedule of reinforcement was used to evaluate the motivation for the chocolate-flavored pellets. The response required to earn one single pellet escalated according to the following series: 1, 5, 12, 21, 33, 51, 75, 90, 120, 155, 180, 225, 260, 300, 350, 410, 465, 540, 630, 730, 850, 1000, 1200, 1500, 1800, 2100, 2400, 2700, 3000, 3400, 3800, 4200, 4600, 5000, and 5500. The maximal number of responses that the animal performs to obtain one pellet was the last event completed, referred to as the breaking point. The maximum duration of the PR session was 5 h or until mice did not respond on any lever within 1 h.

Compulsivity: Total number of shocks in the session of shock test (50 min) performed after the PR test, when each pellet delivered was associated with a punishment, were used to evaluate compulsivity-like behavior, previously described as resistance to punishment (Deroche-Gamonet *et al.*, 2004; Mancino *et al.*, 2015). Mice were placed in a self-administration chamber without the metal sheet with holes and consequently with the grid floor exposed (contextual cue). In this shock-session, mice were under a FR5 schedule of reinforcement during 50 min with two scheduled changes: at the fourth active lever-response mice received only an electric footshock (0.18 mA, 2 s) without pellet delivery and at the fifth active lever-response, mice received another electric footshock with a chocolate-flavored pellet paired with the cue light. The schedule was reinitiated after

10 s pellet delivery (time-out period) and after the fourth response if mice did not perform the fifth response within a min.

Attribution of the three addiction criteria

After performing the three behavioral tests to measure the food addiction behavior, mice were categorized in addicted or non-addicted animals depending on the number of positive criteria that they had achieved. An animal was considered positive for an addiction criterion when the score of the specific behavioral test was above the 75th percentile of the normal distribution of the chocolate control group. Mice that achieved 2 or 3 addiction criteria were considered addicted animals and mice that achieved 0 or 1 addiction criteria were considered non-addicted animals.

Impulsivity

Non-reinforced active responses during the time-out periods (10 s) after each pellet delivery were measured as impulsivity-like behavior indicating the inability to stop a response once it is initiated (Koob and Volkow, 2010). The three consecutive days before the PR were considered.

Shock-induced conditioned suppression

Non-reinforced active responses during the following session after the shock-session were measured for the aversive associative learning. Mice were placed in the self-administration chamber during 50 min with the same grid floor used during the shock-session. However, during this session, pressing the active lever had no consequences, no shock, no chocolate-flavored pellets, and no cue-light.

Locomotor activity

Locomotor activity was evaluated by using individual locomotor activity boxes (10.8 cm width × 20.3 cm length × 18.6 cm high, Imetronic, Pessac, France) equipped with infrared sensors to detect locomotor activity and an infrared plane to detect rearings. The boxes were provided with a removable cage, a sliding floor, a trough and a bottle. Mice were placed in the boxes during 2 h and the kinetics of the total activity (number of beam breaks) was recorded in blocks of 10 min.

Drugs

For the surgery procedure, ketamine hydrochloride (Imalgène; Merial Laboratorios S.A.) and medetomidine hydrochloride (Domtor; Esteve, Spain) were mixed and dissolved in sterile 0.9% physiological saline and administered intraperitoneally (i.p., 75 mg/kg and 1 mg/kg of body weight respectively) to anesthetize the mice. After surgery, anesthesia was reversed by a subcutaneous (s.c.) injection of atipamezole hydrochloride (Revertor; Virbac, Spain; 2.5 mg/kg of body weight) dissolved in sterile 0.9% physiological saline. In addition, mice received an i.p. injection of gentamicine (Genta-Gobens; LaboratoriosNormon, Spain; 1 mg/kg of body weight) and a s.c. injection of meloxicam (Metacam; BoehringerIngelheim, Rhein; 2 mg/kg of body weight) both dissolved in sterile 0.9% physiological saline.

For the activation of the inhibitory hM4Di-DREADD, CNO (Enzo Life Sciences, NY) was administered using Alzet osmotic minipumps (Model 2004; alzet, Cupertino, CA) filled previously with CNO (diluted in 0.9% sterile saline; 5 mg/mL) or saline. The osmotic minipump was implanted

s.c. in the back of the mice under brief isofluorane anesthesia. Minipumps delivered a constant s.c. flow rate of 0.25 µl/h for 28 days.

For electrophysiological studies, we used WIN55,212-2 5 µM (Sigma-Aldrich, Spain), rimonabant 4 µM (Sanofi-Aventis, Spain), quinpirole hydrochloride 2 µM (Sigma-Aldrich, Spain) and DA hydrochloride 10 µM (Sigma-Aldrich, Spain).

Surgery and virus vector microinjection

General surgical procedures

Mice were anesthetized as reported in the drugs section and placed into a stereotaxic apparatus for receiving the AAV intracranial injections. All the injections were made through a bilateral injection cannula (33-gauge internal cannula, Plastics One, UK) connected to a polyethylene tubing (PE-20, Plastics One, UK) attached to a 10 µl microsyringe (Model 1701 N SYR, Cemented NDL, 26 ga, 2 in, point style 3, Hamilton company, NV). The displacement of an air bubble inside the length of the polyethylene tubing that connected the syringe to the injection needle was used to monitor the microinjections. The volume [0.2 µl per site in PL, 0.4 µl per site in NAc core] was injected at a constant rate of 0.05 µl/min (PL) or 0.1 µl/min (NAc core) by using a microinfusion pump (Harvard Apparatus, Holliston, MA) for 4 min. After infusion, the injection cannula was left in place for an additional period of 10 min to allow the fluid to diffuse and to prevent reflux, and then it was slowly withdrawn during 10 additional min. We used the following coordinates to target our injections according to Paxinos and Franklin (Paxinos, G. and Franklin, 2001): (PL) AP +1.98 mm, L ±0.3 mm, DV -2.3 mm; (NAc core) AP +1.34 mm, L ±1 mm, DV -4.6 mm.

Viral vectors

We used the following vectors: AAV-hM4Di-DREADD (AAV8-hSyn-DIO-hM4D(Gi)-mCherry,1.21E+13 gc/ml) and AAV-control-DREADD (AAV8-hSyn-DIO-mCherry, 1.19E+13 gc/ml) from Viral Vector Production Unit of Universitat Autònoma de Barcelona, AAV-retrograde-Cre (AAV pmSyn1-EBFP-Cre; 6×10^{12} vg/mL) from Addgene (viral prep # 51507-AAVrg), AAV-D_2R (AAV2/1-hSyn-DIO-SF-D_2R(L)-IRES-mVenus, 1.23E+13 gc/ml), the plasmid was a gift from Christoph Kellendonk and Jonathan Javitch's lab (Gallo *et al.*, 2018), and the corresponding AAV-control (AAV1/2-hSyn-floxstop-hrGFP, 7.69E+11 gc/ml) was from Beat Lutz's lab. For the inhibition of glutamatergic neurons in the PL subregion, a bilateral injection targeting the PL was performed in Nex-Cre mice. Mice received an injection of 0.2 µl per site of the AAV-hM4Di-DREADD or 0.2 µl per site of the AAV-control-DREADD. For the specific inhibition of the projecting neurons from PL to NAc core, two bilateral injections were performed in WT C57BL/6J mice, one targeting the PL and the other the NAc core. Mice received an injection of 0.2 µl per site of the AAV-hM4Di-DREADD into PL and an injection of 0.4 µl per site of the AAV-retrograde-Cre into the NAc core. For the overexpression of D_2R in the PL-NAc core projecting neurons, two bilateral injections were performed in WT C57BL/6J mice, one targeting the PL and the other the NAc core. Mice received bilateral injections of 0.2 µl of the AAV-D_2R or 0.2 µl per site of the AAV-control into PL and bilateral injections of 0.4 µl of the AAV-retrograde-Cre into the NAc core.

Experimental design

In the first experiment (Figure 33), Glu-CB1-KO mice (n=58) and WT mice (n=56) were trained under FR1 schedule of reinforcement during 6 sessions, followed by 112 sessions of FR5 to self-administer chocolate-flavored pellets. The three addiction criteria (1) persistence to response, (2) motivation, and (3) compulsivity were evaluated at two different time points in each mouse. The first time point was the early period (sessions 1-18 of FR5) and the second time point was the late period (sessions 95-112 of FR5). For the *in vitro* electrophysiological recordings, we used naïve Glu-CB1-KO mice (n=3-5) and their WT littermates (n=3-5) (see section *In vitro* electrophysiology in brain slices).

For the inhibition of the glutamatergic transmission in PL subregion (Figure 43), mice followed the same behavioral procedure described for the early period in the first experiment with some variations due to the surgical AAV injection (Figure 46**Figure 43**). In particular, Nex-Cre mice were trained to acquire the operant conditioning maintained by chocolate-flavored pellets under FR1 (2 sessions) and FR5 (2 sessions) schedule of reinforcement followed by the surgery for injecting Cre-dependent AAVs carrying the DREADD (DREADD approach). After bilateral intracranial injection of the AAV-hM4Di-DREADD in the PL, the expression of the AAV was allowed during the period of 4 weeks. At the beginning of this period, mice were under FR5 (4 sessions) to recover the basal levels of operant responding. At the end of these 4 weeks, an osmotic minipump filled with CNO or saline was s.c. implanted in the back of each mouse. Subsequently, during the chronically CNO-induced activation of the expressed hM4Di receptors,

mice were under FR5 scheduled sessions followed by the measurement of the three addiction criteria. To verify the viral expression, mice were perfused at the end of the experiment, and the fluorescent reporter mCherry was visualized in brain slices using a Leica DMR microscope equipped with a digital camera Leica DFC 300FX (10x objectives). In a subset of injected mice, *in vitro* electrophysiology recordings were used to verify CNO induced suppression of neuronal activity (see section *In vitro* electrophysiology in brain slices). For the specific inhibition of the projecting neurons from PL to NAc core (Figure 51), mice followed a similar experimental design as described above with a modification in the surgical intervention. In this experiment, a dual viral approach was performed to selectively silence the PL neurons that project to NAc core (retro-DREADD approach): bilateral intracranial injection of AAV-hM4Di-DREADD targeting the PL and of AAV-retrograde-Cre targeting the NAc core. To verify viral expression, mice were perfused at the end of the experiment and the fluorescent reporter mCherry was visualized in brain slices, as previously described. Cre-recombinase expression was detected by immunofluorescence using an anti-Cre recombinase antibody (see section Immunofluorescence studies). Same as in the previous experiment, *in vitro* electrophysiology recordings were used in a subset of injected mice to verify CNO induced suppression of neuronal activity (see section *In vitro* electrophysiology in brain slices).

For the transcriptomic analysis, mice were sacrificed immediately after the last FR5 session of the food addiction procedure and mPFC was extracted to perform RNA-sequencing (see section RNA-sequencing).

For the overexpression of D_2R in PL-NAc core pathway (

Figure **65**), mice followed the same behavioral and surgical procedure with a dual vector approach similar to that described in the previous experiment with slight modifications: (I) AAV-D_2R or AAV-control was injected in the PL, (II) the surgical intervention for the osmotic minipump filled with CNO was not required and (III) an immunofluorescence assay was performed after the perfusion of the mice using an anti-GFP antibody that visualized the mVenus and GFP reporters of the AAVs injected in PL and against Cre recombinase to visualize the injection site of the retrograde AAV in the NAc core and the retrograde transport to the PL (see section Immunofluorescence studies). Equally to previous experiments, *in vitro* electrophysiology recordings were used in a subset of injected mice to verify that overexpression of D_2R induced the suppression of neuronal activity by using D_2R agonists, quinpirole and DA (see section *In vitro* electrophysiology in brain slices).

In vitro electrophysiology in brain slices

Animals were sacrificed and brains were quickly removed obtaining coronal slices (300 µm) with vibratome (Leica VT1200S) upon the presence of low-Na^+ cutting solution (composition in mM: Sucrose 212, NaHCO3 27, Dextrose 10, CaCl2 2.2, MgSO4 2.2, KCl 2, NaH2PO4 1.5; pH 7.4 when saturated with 95% O2 + 5% CO2). Afterwards, slices were incubated (40 min/34°C) in artificial cerebrospinal fluid (ACSF; composition in mM: NaCl 124, KCl 2.5, NaHCO3 26, CaCl2 2, MgCl2 1, NaH2PO4 1.25, glucose 10; pH 7.4 when saturated with 95% O2 + 5% CO2). Visualization of brain slices was performed with an upright microscope (BX51WI, Olympus), outfitted

with x4 lens, x40 water immersion lens, Nomarsky optics and mercury lamp with adequate filters for blue (470-490nm) and green (533-580nm) light stimulation. L5 pyramidal neurons were recognized by their position along the cortical column, soma shape and presence of apical dendrite and electrophysiological properties.

Voltage-clamp and current-clamp electrophysiological recordings were performed by using a Multiclamp 700B amplifier (Axon Instruments), filtered at 1-2 kHz and digitized at 20 kHz with a 16 bits Axon Digidata 1550B (Axon Instruments). Protocols design and data acquisition were performed with pClamp9.2 software (Axon Instruments). Borosilicate patch pipettes (1.5mm o.d., 0.86 mm i.d., with inner filament; Harvard Apparatus) were used after pulled (P-97, Sutter Instrument). Pipette resistance was calculated with pClamp software and was estimated among 8-10 MΩ. Electrical DC pulses were applied with a DS3 Isolated Stimulator (Digitimer) using a theta-glass pipette filled with ACSF solution. All recordings were performed at RT (21-23°C).

mEPSC detection in layer 5 pyramidal neurons of Glu-CB1-KO mice

Miniature excitatory postsynaptic currents (mEPSC) were recorded in L5 pyramidal neurons of PL-mPFC by doing voltage-clamp somatic whole-cell recordings. Patch pipettes were filled with intracellular solution (composition in mM: 130 mM K-gluconate, 5 mMKCl, 5mMNaCl, 5 mM EGTA, 10mM HEPES, 2 mM Mg-ATP, 0.2 mM Na-GTP; pH 7.2 adjusted with KOH; 285–295mOsm). mEPSC recorded in voltage-clamp configuration holding membrane potential at -68 mV (theoretic Nernst equilibrium potential for Cl-≈ -68mV). The previously described ACSF was used as an

extracellular solution adding 2 µM of the selective Na^+ channels blocker tetrodotoxine (Abcam) for mEPSC isolation, 10 min after obtaining records, to isolate miniature currents. mEPSC frequency was estimated in 120 s recording.

Paired-Pulse facilitation recordings in layer 5 of Glu-CB1-KO mice

Synaptic facilitation is a form of short-term plasticity that enhances synaptic transmission for less than a second (Jackman and Regehr, 2017) (Figure 32). Facilitation runs counter to the natural tendency of synapses to weaken during repeated activation, a phenomenon known as depression that can result from depletion of the readily releasable pool of synaptic vesicles and a decrease in neurotransmitter release. However, facilitation counteracts depression by increasing the probability of release in a frequency-dependent manner at some synapses with specialized mechanisms that boost neurotransmitter release even as the pool of available synaptic vesicles decreases (Jackman and Regehr, 2017).

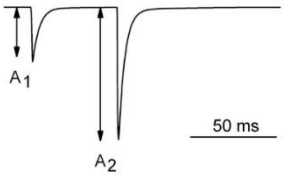

Figure 32. Synaptic facilitation. Illustrated excitatory postsynaptic currents evoked by a pair of pulses delivered at a 50 ms interval. Facilitation increases the amplitude of the second response approximately 2-fold (Jackman and Regehr, 2017).

Synaptic facilitation was achieved by applying consecutive electrical stimulus with a 50 ms interpulse interval in L2/3 of mPFC. The evoked field-excitatory postsynaptic potentials (fESPS) were recorded in L5 with ACSF filled patch pipette. Once the evoked fEPSP were stabilized, at least 50 consecutive responses were recorded. Synaptic facilitation was estimated

as the ratio among second response amplitude (P2) respect the first response amplitude (P1). Electrical stimulus (0.06 Hz) was the 50% of the intensity needed to evoke the maximal fEPSP amplitude.

Layer 5 evoked fEPSP pharmacological modulation

A single fEPSP was evoked on L5 by stimulating on L2/3 as previously described. Once fEPSP was stable, 50 consecutive responses were recorded to stablish the baseline fEPSP amplitude. Each pharmacological application was perfused in the recording chamber for 20 min while recording evoked fEPSP. The effect of WIN55,212-2 5 µM (Sigma-Aldrich, Spain) and rimonabant 4 µM (Sanofi-Aventis, Spain) in the fEPSP amplitude was calculated by averaging the last 10 evoked fEPSP.

Pharmacological modulation of L5 pyramidal neurons properties of mPFC

Somatic current-clamp whole-cell recordings were obtained in the presence of ACSF and pharmacological treatment. Intracellular solution composition (in mM) was: KMeSO4 135, KCl 10, HEPES 10, NaCl 5, ATP-Mg 2.5, GTP-Na 0.3; pH adjusted to 7.3 by adding KOH. Hyperpolarizing and depolarizing square current pulses were applied (from -200 pA to 300 pA; Δ25 pA; 1s duration). Resistance was obtained from the first depolarizing pulse. Rheobase was calculated by applying a ramp hyperpolarizing current-pulses (from 150 pA-300 pA; 1.5 s duration). hM4Di-mCherry positive neurons modulation was estimated after 10 min of perfusing recording chamber with CNO 10 µM (Enzo Life Sciences, NY) diluted in ACSF. DA hydrochloride 10 µM (Sigma-Aldrich, Spain) and quinpirole hydrochloride 2 µM (Sigma-Aldrich, Spain) modulation of D_2R-mVenus and

GFP positive neurons was performed after 10 min perfusing recording chamber.

RNA sequencing

RNA extraction

Tissue collection was performed immediately after the last FR5 session. After decapitation, the brains were removed from the skulls and processed rapidly on ice. The mPFC was isolated according to the following coordinate from Paxinos and Franklin 2001 (Paxinos, G. and Franklin, 2001) (AP +1.98 mm) and the samples were placed in individual tubes, frozen on dry ice, and stored at −80°C until RNA isolation for the RNA-sequencing. The remaining brain parts from the same animals were frozen on dry ice and stored at −80°C.

Total RNA from mPFC was extracted using a miRNeasy Mini kit for subsequent RNA-seq analysis and RT-PCR validation. Briefly, tissues were homogenized in QIAzol Lysis Reagent and, after adding chloroform, the aqueous phase was collected and microRNA and total RNA were extracted by using miRNeasy Mini kit (Qiagen, 217004).

Library preparation and total RNA-sequencing

Further evaluation of the RNA, RNA library generation, and sequencing were carried out by StarSEQ GmbH (Mainz, Germany). Sequencing was performed on an Illumina NextSeq 500 sequencer with High Output chemistry and minimum output of 60 million single end reads (75 bp) per sample.

Total RNA (750-1000 ng/sample) was rRNA depleted by Ribo-Zero rRNA Removal Kit (Human/Mouse/Rat) from Illumina. For sequencing library generation, the NEBNext Ultra II Directional RNA Library Kit was used. Resulting RNA libraries were size selected to a median insert size of 300 bp.

RNAseq data analysis

RNA sequencing for WT and Glu-CB1-KO mice were performed under addicted and non-addicted conditions. RNA-seq output was received as raw files in fastq format. To check the quality of the individual sequenced sample, we used FASTQC version v0.10.5. Quality check followed by alignment using TopHat version v2.1. (Trapnell *et al.*, 2010) to the mouse genome (mm^9) with default parameters. Further, mapped reads were considered for read count per gene using HTSeq version 0.9. (Anders *et al.*, 2015). HTSeq output (read counts per gene) were normalized and differential gene expression analysis was performed using R package DESeq (Anders and Huber, 2010) with FDR rate of 0.1. Variability between the addicted and non-addicted mice was determined using principal component analysis from plot function of DEseq package. p-value was calculated using nbinomTest function from DEseq package. Differential expression analysis was performed between addicted and non-addicted mice. Similarly, we performed differential expression analysis between WT and Glu-CB1-KO. Genes with > 1.5 log2 fold change and p-value < 0.01 between addicted and non-addicted and WT vs Glu-CB1-KO with read count > 40 in either condition were considered as differentially expressed genes. Further, it was visualized with a volcano plot using R (Anders and Huber, 2010; Trapnell *et al.*, 2010; Anders *et al.*, 2015).

RT-PCR validation

RNA was reverse transcribed using High Capacity RNA-to-cDNA kit (Applied Biosystems, 4390778). Primers for Taqman® Gene Expression Assay were purchased from Applied Biosystems. Real-time PCR analysis was carried out with the following primers (gene name: probe code): *Actb*: Mm02619580_g1; *Adora2a*: Mm00802075_m1; *Cnr1*: Mm00432621_s1; *Drd2*: Mm00438545_m1; *Drd1*: Mm02620146_s1; *Fos*: Mm01302932_g1; *Gpr88*: Mm02620353_s1; *Npas4*: Mm01227866_g1; *Tbp*: Mm01277042_m1; *Usp11*: Mm00455198_m1. Relative expression of mRNAs was determined after normalization with housekeeping genes using the ΔΔCt method.

Immunofluorescence studies

Tissue preparation for immunofluorescence

Mice were deeply anesthetized by i.p. injection (0.2 ml/10 g of body weight) of a mixture of ketamine/medetomidine prior to intracardiac perfusion with 4% paraformaldehyde in 0.1 M Na_2HPO_4/ 0.1 M NaH_2PO_4 buffer, pH 7.5, delivered with a peristaltic pump at 30 ml per min for 2 min. Subsequently, brains were extracted and post-fixed with 4% PFA for 24 h and transferred to a solution of 30% sucrose at 4 °C. Coronal frozen sections (30 µm) of the PL and NAc core were obtained on a freezing microtome and stored in a 5% sucrose solution at 4°C until use.

Immunofluorescence

Free-floating slices were rinsed in 0.1 M PB, blocked in a solution containing 3% normal goat serum and 0.3% Triton X-100 in 0.1M PB (NGS-T-PB) at

room temperature for 2 h, and incubated overnight at 4ºC in the same solution with the primary antibody to anti-Cre recombinase (1:500, mouse, MAB3120, Merck Millipore) or anti-GFP (1:500, rabbit, GTX20290, GeneTex). On the next day, after 3 rinses in 0.1 M PB, sections were incubated with the secondary antibody AlexaFluor-488 donkey anti-mouse (1:500, Life Technologies) or AlexaFluor-488 donkey anti-rabbit (1:500, Life Technologies) at room temperature in NGS-T-PB for 2 h. After incubation, sections were rinsed and mounted immediately after onto glass slides coated with gelatine in Fluoromount mounting medium.

Image analysis

The stained sections of the brain were analyzed with Leica TCS SP5 CFS (fixed stage) upright confocal microscope with two non-descanned HyD detectors. The images were processed using the ImageJ analysis software.

Fluorescence in situ hybridization

Double fluorescence *in situ* hybridization experiments were performed on coronal cortical sections and mPFC (PL and IL) and NAc were analyzed using FITC labeled riboprobe for *Cre* recombinase and digoxigenin labeled riboprobe for dopamine D_2 receptor gene (*Drd2*) to detect *Cre*/*Drd2* double positive neurons to confirm the presence of both the endogenous *Drd2* mRNA and the mRNA of the injected *Cre* recombinase gene in the targeted cells. This cell population in the mPFC was analyzed in three AAV-retrograde-Cre injected WT C57BL/6J animals to determine the overlapping expression *of Drd2* and of retrogradely traveled *Cre* recombinase-expressing virus. Slides with 6 parallel coronal sections of 3 animals, injected with AAV-retrograde–Cre were analyzed, containing NAc,

PL and IL cortex (and striatum), the sections covering cortical region 2.10 – 1.18 mm anterior to bregma.

Adult WT C57BL/6J mice, injected in weeks 10-14 were sacrificed 4 weeks after injection by cervical dislocation. Brains were removed, snap-frozen on dry ice and stored at -80°C. After removing from -80°C, brains were mounted on Tissue Freezing Medium (Leica Biosystems) and 18 µm-thick coronal sections were cut from the frozen forebrain on a cryostat Leica CM3050 S, dried on a 42°C warming plate and stored at -20°C until used.

Both digoxigenin and fluorescein isothiocyanate labeled riboprobes were used. The DNA template for *Drd2* probe was originally generated by RT-PCR from cDNA derived from total mouse brain, previously reported(Hermann *et al.*, 2002). GenBank accession number, primer sequences and length of probe are listed therein. For a riboprobe specific for *Cre* recombinase RNA, we isolated the stretch of cDNA from *Cre* recombinase sequence of the AAV-retrograde-Cre (Addgene vector AAV pmSyn1-EBFP-Cre) using a forward primer which contains at the 5' end also the EcoR1 recognition sequence as well as 5 nucleotides at the very 5'end (fw primer 5'-ACTATGAATTCCGAGTGATGAGGTTCGCAAG-3') and the reverse primer containing at the 5' end the XhoI recognition sequence preceded by 5 nucleotides (rev primer 5'-AACTACTCGAGCCGGTATTGAAACTCCAGCG-3') resulting in a 867 bp product. PCR products were cloned into pBluescript KS^- and used as templates for riboprobe synthesis as described. The identity of subcloned fragments was checked by sequencing. Linearized template DNA was column purified (PCR purification kit, Invitrogen), resuspended in diethyl pyrocarbonate (DEPC)-treated H_2O at a concentration of 1 µg/µl,

and stored at -20°C. For both probes *in vitro* transcription was carried out for 3 h at 37°C in a total volume of 20 µl containing 2 µg of linearized plasmid with inserts of desired genes *Drd2* or *Cre recombinase*. Restriction enzymes (New England Biolabs) used for linearization and RNA polymerases used for each probe were as described (Hermann *et al.*, 2002): *Cre recombinase* antisense: EcoRI, T3; *Cre recombinase* sense: XhoI, T7; *Drd2* antisense: BamHI, T3; Drd2 sense: Eco RI, T7. Pretreatment, hybridization and visualization of signals in fluorescent *in situ* hybridization procedure was carried out as described (Zimmermann *et al.*, 2018). Digoxigenin labeled *Drd2*riboprobe was used at a final concentration of 1000 ng/ml hybridization mix, FITC-labeled *Cre recombinase* riboprobe at 800 ng/ml.

Statistical analysis

All statistical comparisons were performed with SPSS (IBM, version 25). Comparisons between two groups were analyzed by Student t-test or U Mann-Whitney depending on the distribution defined by the Kolmogorov-Smirnov normality test. ANOVA with repeated measures was used when required to test the evolution over time. Two-way ANOVA by subsequent post hoc analysis (Fisher PLSD) was used for multiple group comparison. The Pearson correlation coefficient was used to analyze the relationship between values in each addiction criteria and the final criteria achieved. All results were expressed as individual values with the median and the interquartile range. A p-value <0.05 was used to determine statistical significance. The sample sizes were similar to those reported in previous

publications (Mancino *et al.*, 2015). Supplementary tables 1-6 provided a complete report of the statistical results for the data described in the figures.

1.3. Results

Loss of CB_1R in dorsal telencephalic glutamatergic neurons leads to resilience to develop food addiction

Given that CB_1R plays a crucial role in the modulation of glutamatergic transmission (Monory *et al.*, 2006), we explored the function of this receptor in food addiction. Glu-CB1-KO mice lacking CB_1R in dorsal telencephalic glutamatergic neurons and their WT littermates were exposed to the recently established operant model of food addiction (Mancino *et al.*, 2015). Glu-CB1-KO (n=58) and WT mice (n=56) were trained under a FR1 schedule of reinforcement during 6 sessions followed by 112 sessions under FR5 to obtain chocolate-flavored pellets as reinforcers (Figure 33 and Methods). A large cohort of mice was used in this experiment to select extreme resilient and vulnerable subpopulations for transcriptomic studies (see below).

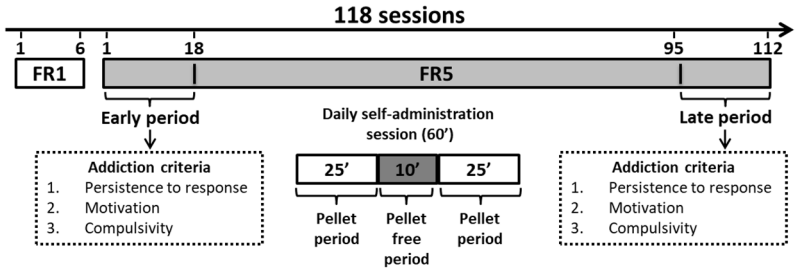

Figure 33. Experimental design of the food addiction mouse model. Mice were trained for chocolate-flavored pellets under a fixed ratio (FR) 1 schedule of reinforcement on 1 h daily sessions for 6 days followed by 112 days on a FR5. Each session was composed by 2 pellets session (25 min) of normal delivered pellets separated by a pellet free period (10 min) in which pressing the active lever has no pellet delivery. In the FR5, 2 time points were considered, early and late period to measure the addictive-like behavior: (1) persistence to response, (2) motivation and (3) compulsivity.

In FR1, both genotypes increased the number of reinforcers across sessions without significant differences indicating similar levels of acquisition of the operant conditioning learning. When the effort to obtain one single pellet was increased to FR5, the progressive increase of the number of reinforcers was reduced in Glu-CB1-KO as compared to WT (Figure 34), finally leading to a reduced number of reinforcers over the entire FR5 period (genotype effect, $P<0.001$; interaction genotype x sessions, $P<0.001$, Figure 34). This result indicated that palatable pellets were less reinforcing for the mutants since the early period suggesting that this trait could be a predisposing protective factor. Animals that responded less than 25% of all FR5 sessions and did not achieve the acquisition criteria were excluded from the remaining experimental sequence: Glu-CB1-KO (14.7%), WT (6.7%).

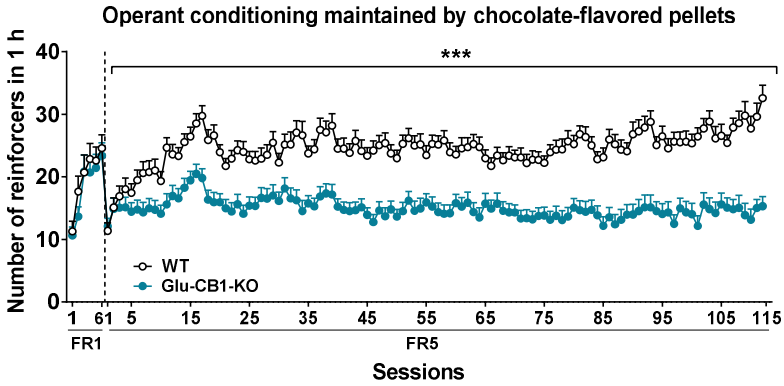

Figure 34. Reduced number of reinforcers during 1 h of operant training sessions maintained by chocolate-flavored pellets in Glu-CB1-KO compared to WT mice (± S.E.M, repeated measures ANOVA, genotype effect *** $P<0.001$; total number of mice was 56 for WT, and 58 for Glu-CB1-KO; statistical details are included in Supplementary Table1).

In the early period, a significant genotype difference was only observed in the criterion of compulsivity, evaluated by the number of active responses associated with a footshock delivery. A suppressed response in front of negative consequences was revealed in Glu-CB1-KO mice compared to WT mice ($P<0.05$, Figure 35c). In contrast, non-significant genotype differences were found in the persistence to response, as evaluated by the number of non-reinforced active responses during the pellet free period, and in motivation, defined by the breaking point obtained during the PR schedule (Figure 35a-b). In the late period, Glu-CB1-KO mice showed significantly less persistence to response, reduced motivation, and decreased compulsivity in seeking for highly palatable food compared to WT mice, revealing a resilient phenotype of these mutants to develop food addiction ($P<0.01$, Figure 35d-f).

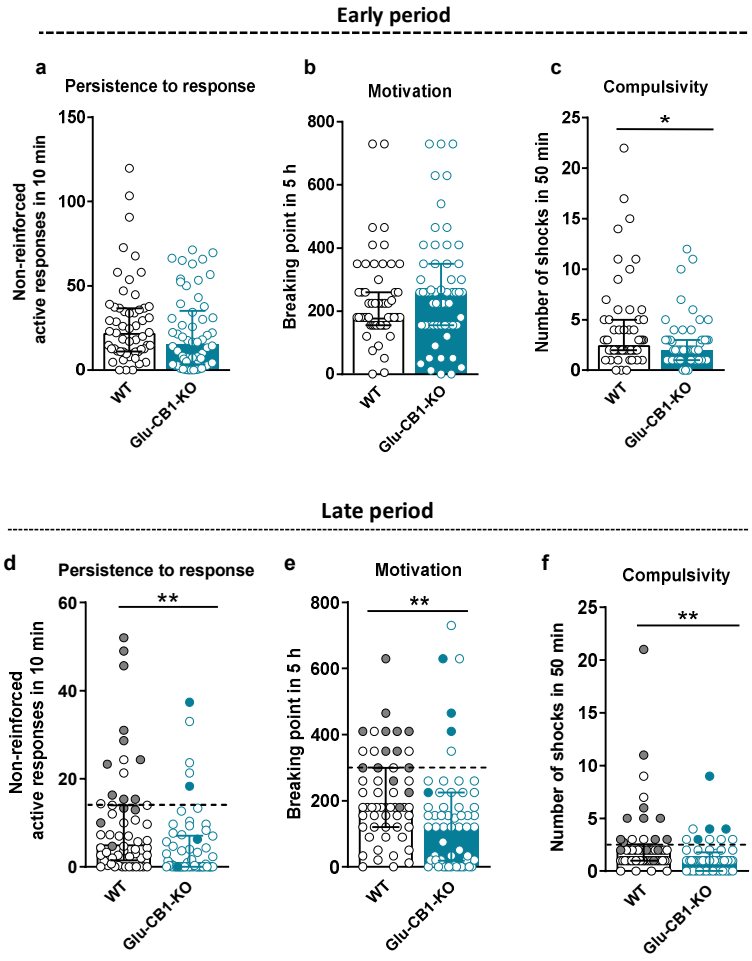

Figure 35. Behavioral tests of the three addiction criteria in both genotypes at the early (a-c) and late (d-f) period (individual data with interquartile range). **a,d**, **Persistence to response.** Total number of non-reinforced active responses during three consecutive daily 10-min of pellet free period. **b,e, Motivation.** Breaking point achieved in 5 h of PR schedule. The breaking point refers to the maximal effort that an animal is willing to do to earn one pellet. **c,f, Compulsivity**. Number of shocks that mice received in 50 min in the shock test in which each pellet delivery was associated with a footshock (0.18 mA). The dashed horizontal line indicated the 75th percentile of distribution of WT mice, it is used as the threshold to consider a mouse positive for one criterion. Addicted mice in grey filled circles for WT and blue for Glu-CB1-KO mice (U-Mann-Whitney, *P< 0.05, **P< 0.05; the total number of mice was 56 for WT, and 58 for Glu-CB1-KO; statistical details are included Supplementary Table1).

Two additional factors of vulnerability to addiction, the behavioral trait of impulsivity and sensitivity to aversive associative learning, were also evaluated. The impulsivity was measured by the inability to stop an action once initiated (responding during the time-out period after each pellet delivery, 10 s). Glu-CB1-KO mice showed significantly less impulsivity than WT mice only in the late period (P<0.01, Figure 36a). The aversive associative learning was tested by the ability of the shock-associated cue to suppress pellets seeking the day after the shock-test. Here, in both early and late periods, Glu-CB1-KO mice showed a significantly increased learning with high suppression of food seeking compared to WT mice (P<0.01, Figure 36b).

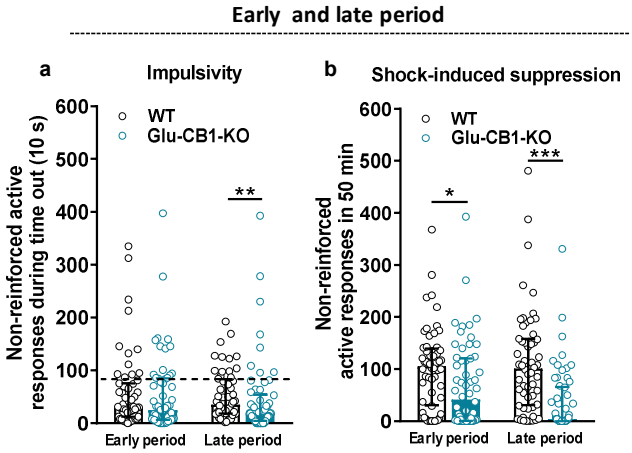

Figure 36. **Behavioral tests of impulsivity and shock-induced suppression in the early and late period represented by individual values with the median and the interquartile range. a**, **Impulsivity**. Number of non-reinforced active lever-presses during three consecutive daily time out (10 s) after each pellet delivery (U-Mann-Whitney, ** P<0.01). **b**, **Shock-induced suppression**. Number of non-reinforced active responses in 50 min in the following session after the shock test with the same discriminative stimulus (grid floor) as shock test in which pressing the active lever had no consequences: no shock, no chocolate-flavored pellets and no cue-light (U-Mann-Whitney, ** P<0.01, *** P<0.001, total number of mice was 56 for WT, and 58 for Glu-CB1-KO; statistical details are included in Supplementary Table1).

We individually categorized mice in addicted (covering 2-3 criteria) or non-addicted using the results of three food addiction criteria in the late period, as previously reported (Mancino *et al.*, 2015). Only 6.9% of the Glu-CB1-KO mice achieved 2-3 criteria and were considered addicted compared with the 25.0% of WT mice (P<0.01, Figure 37).

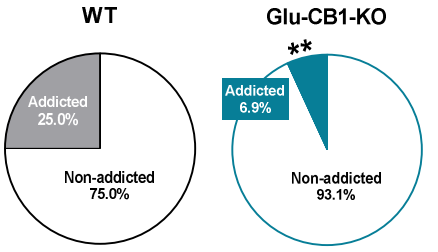

	Non-addicted		Addicted	
	0 crit	1 crit	2 crit	3 crit
WT	50.0%	25.0%	19.6%	5.4%
Glu-CB1-KO	74.1%	19.0%	5.2%	1.7%

Figure 37. **Reduced percentage of mice categorized as addicted in Glu-CB1-KO group at the late period** (Chi-square **P<0.01; the total number of mice was 56 for WT, and 58 for Glu-CB1-KO; statistical details are included in Supplementary Table1).

Of note, Glu-CB1-KO mice strongly decreased the likelihood to develop food addiction. Positive correlations were found between the number of criteria in both mutant and WT mice and the intensity of each criterion (Figure 38a-c), and a small percentage of mutant mice achieved similar high extreme values in 2-3 criteria as WT mice (Figure 38d-h). Thus, the deletion of the CB_1R in dorsal telencephalic glutamatergic neurons is a conducive factor for the prevention to develop food addiction but as expected in a multifactorial disease it is not enough to totally stop the transition to addiction.

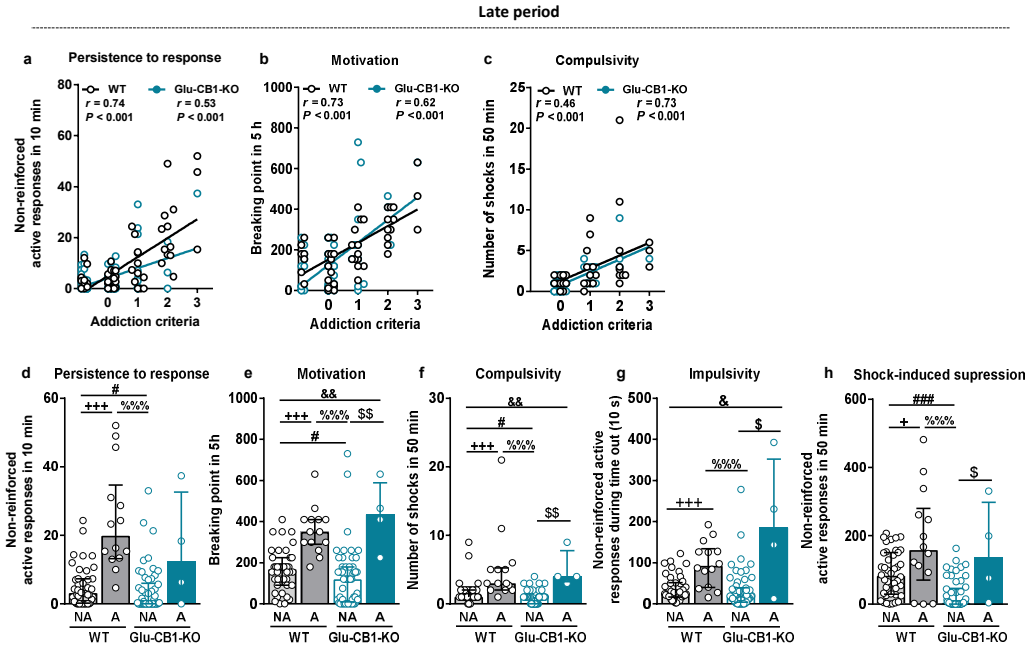

Figure 38. **a-c, Correlations**. Pearson correlations between individual values of addiction criteria and **a,** non-reinforced active responses in 10 min, **b**, breaking point in 5 h, **c**, number of shocks in 50 min**. d-h, Behavioral tests of the three addiction criteria, impulsivity and shock-induced suppression in the late period represented by individual values and bars with median and the interquartile range for the four groups classified as addicted (A) and non-addicted (NA) mice in both genotypes**. **d**, Persistence to response. **e**, Motivation. **f**, Compulsivity. **g**, Impulsivity. **h**, Shock-induced suppression (U Mann-Whitney, + *P*< 0.05, +++ *P*< 0.001 WT NA vs WT A, # *P*< 0.05, ### *P*< 0.001 WT NA vs Glu-CB1-KO NA, & *P*< 0.05, && *P*< 0.01 WT NA vs Glu-CB1-KO A, %%% *P*< 0.001 WT A vs Glu-CB1-KO NA, $ *P*< 0.05, $$ *P*< 0.01 Glu-CB1-KO NA vs Glu-CB1-KO A; the total number of mice was 56 for WT, and 58 for Glu-CB1-KO; statistical details are included in Supplementary Table1).

To study if the resilient phenotype of the Glu-CB1-KO mice was influenced by the body weight, we measured the evolution of the body weight during the whole experimental sequence of 24 weeks, the total average of body weight separately in the early and in the late period and the correlations between the body weight and the 3 addiction criteria (Figure 39). The lack of significant differences between genotypes in the early period indicates

that this variable is not a predisposing factor in the development of the addictive-like behavior. In the late period, although the body weight differences between genotypes emerged, the correlations between body weight and the 3 addiction criteria were not significant indicating that the body weight variable is not explaining the lower persistence to response, motivation and compulsivity found in the Glu-CB1-KO mice.

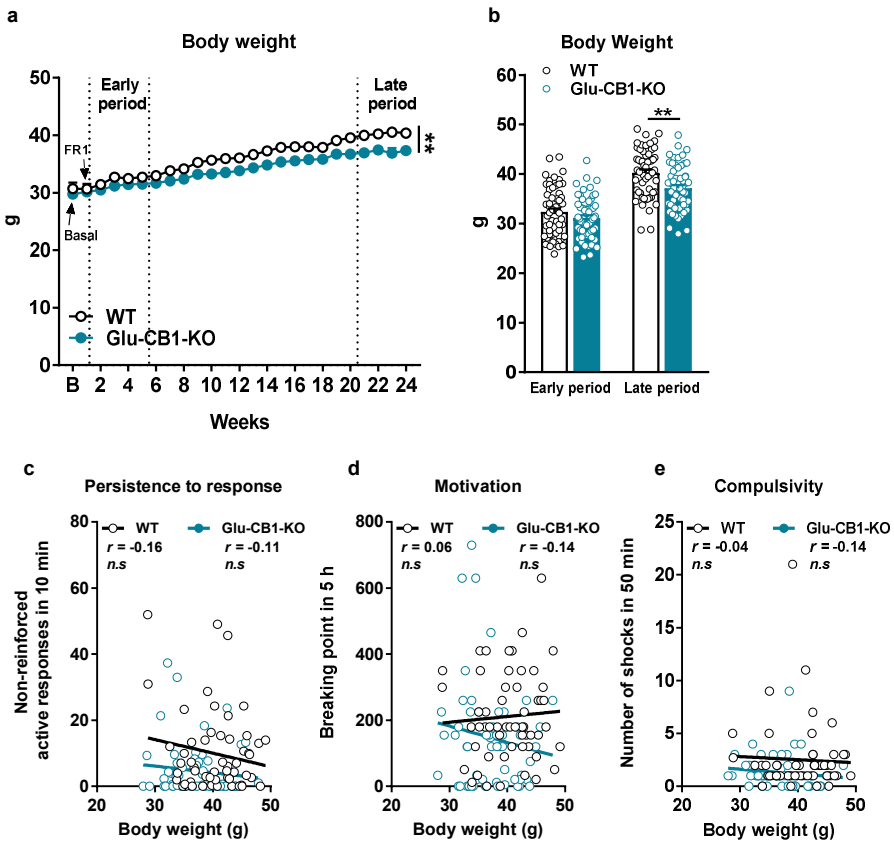

Figure 39. Body weight. **a**, Weekly measures of body weight in grams (Repeated measures ANOVA, Genotype effect $^{**}P<0.01$). **b**, Mean body weight of the early period and late period (t-test, $^{**}P<0.01$). **c-e**, Correlation between the body weight (g) and the 3 addiction criteria in both genotypes. **c,** persistence to response. **d,** Motivation. **e**, Compulsivity (The total number of mice was 56 for WT, and 58 for Glu-CB1-KO Statistical details are included in Supplementary Table1).

Increased synaptic excitatory transmission on glutamatergic mPFC neurons in Glu-CB1-KO

Considering that the activation of presynaptic CB_1R on glutamatergic neurons is supposed to suppress vesicular release of glutamate (Kano *et al.*, 2009), and given the notion that increased neuronal activity of the mPFC may regulate the development of addiction (Goldstein and Volkow, 2011), we applied *ex vivo* electrophysiological experiments to uncover the consequences of CB_1R deletion in glutamatergic transmission in mPFC. In naïve mutant mice, we quantified the frequency of mEPSCs in L5 pyramidal neurons of the PL area of the mPFC that project to subcortical regions. These neurons, by performing whole-cell recordings in brain slices in the presence of 2 μM tetrodotoxine, are a readout of the number of neurotransmitter vesicles release (Riga *et al.*, 2014). We found that mEPSCs frequency was increased in Glu-CB1-KO compared to WT mice, suggesting an enhanced probability of glutamate vesicle release by the presynaptic terminals of pyramidal neurons projecting to L5 that could be independent of presynaptic voltage Ca^{2+} ion channels ($P<0.05$, Figure 40a). Then, we studied the synaptic facilitation in order to determine whether Ca^{2+}-dependent synaptic transmission was affected in Glu-CB1-KO mice. We applied a paired pulse facilitation (PPF) protocol with a 50 ms interstimulus interval in mPFC L2/3 glutamatergic axons and recorded evoked local fEPSP in L5. We found higher synaptic facilitation (increased PPF ratio) in Glu-CB1-KO than in WT mice, indicating that the lack of CB_1R in glutamatergic terminals produced an augmented Ca^{2+}-dependent synaptic transmission

suggesting an increased glutamate release leading to enhanced activation of L5 pyramidal neurons (*P*<0.05,Figure 40b).

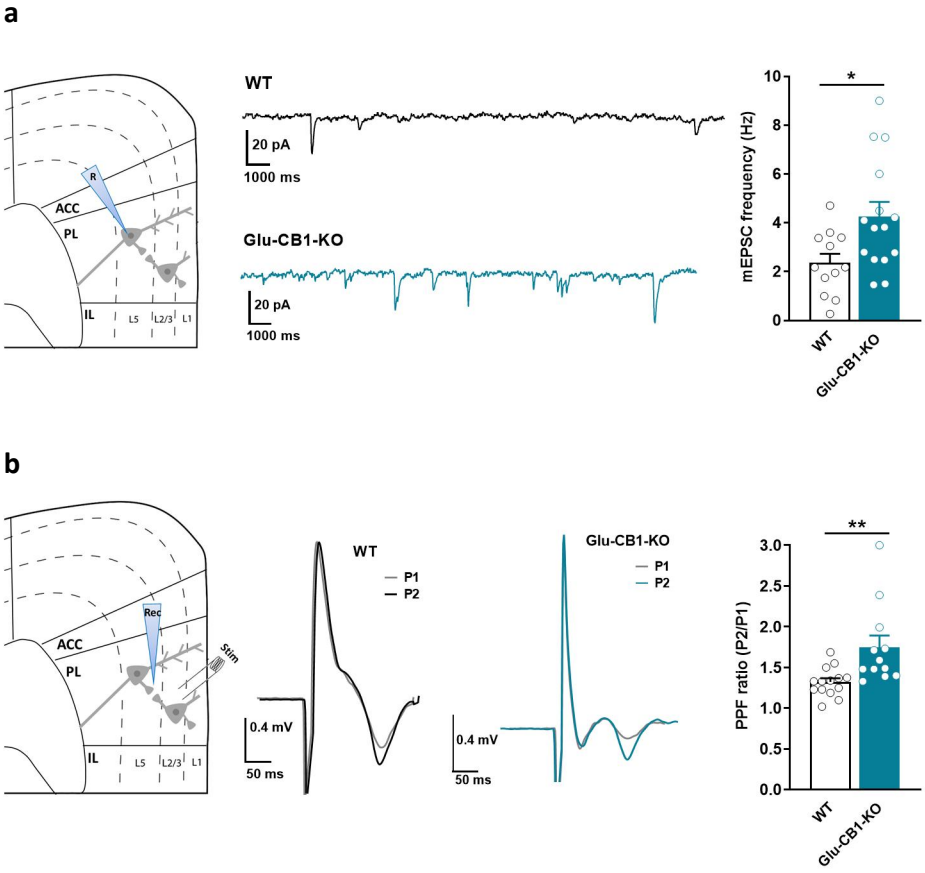

Figure 40. a, Representative recordings of miniature excitatory postsynaptic currents (mEPSCs) detection in L5 pyramidal neurons of mPFC (left). Increased mEPSC frequency in Glu-CB1-KO compared to WT (t-test **P*<0.05; 11-15 cells from 4 animals per genotype; right). **b, Paired pulse facilitation (PPF).** Representative overlapped recordings of L5 field excitatory postsynaptic potential (fEPSP) before (P1) and after (P2) stimulating twice in layer 2/3 with an interpulse interval of 50 ms (left). Increased paired pulse facilitation ratio (P2/P1) in Glu-CB1-KO compared to WT (t-test **P*<0.05; 12-14 slices from 5 animals per genotype; right; mean ± S.E.M; statistical details are included in Supplementary Table 2).

Taken together these results indicated an enhanced spontaneous and action potential dependent synaptic transmission and activation of L5 neurons. Additionally, we validated the functional deletion of CB_1R signaling at glutamatergic presynaptic terminals in the mPFC of Glu-CB1-KO mice by studying the modulation of the amplitude of single L5 fEPSP evoked by electrical stimulation on L2/3 in the presence of the CB1 agonist WIN55, 212-2 (5 µM). As expected, the fEPSP amplitude evoked was strongly reduced in the WT mice after WIN55,212-2 application compared to the baseline before treatment, indicating a functional activation of CB_1R signaling. In contrast, L5 fEPSP amplitude was not diminished in the Glu-CB1-KO animals (genotype x treatment, $P<0.05$, Figure 41).

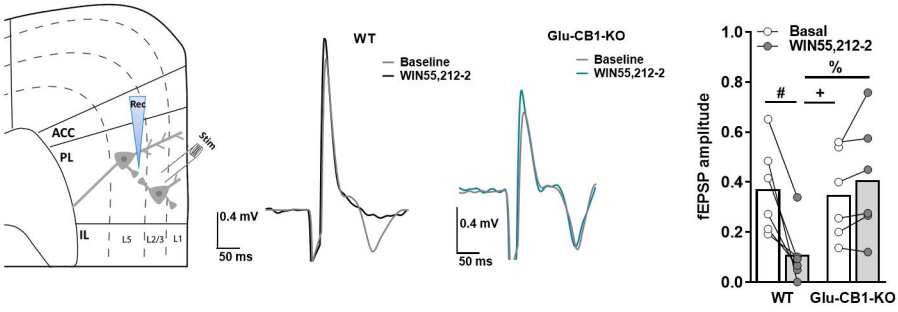

Figure 41. Representative overlapped recordings of the modulation of fEPSP amplitude before and after application of the CB_1R agonist WIN55,212-2 (5 µM) compared to basal conditions for WT and Glu-CB1-KO (left). Quantification of the amplitude variation of the fEPSP for WT and Glu-CB1-KO (6 slices from 3 animals per genotype; right; # $P<0.05$ WT basal vs WT WIN, + $P<0.05$ WT WIN vs Glu-CB1-KO basal, % $P<0.05$ WIN-treated WT vs Glu-CB1-KO; data was presented as a mean and individual values; statistical details are included in Supplementary Table 2).

As a further demonstration, we completely blocked WIN55,212-2 inhibitory effect in mPFC synaptic transmission by applying the selective CB_1R antagonist rimonabant (4 µM; Figure 42).

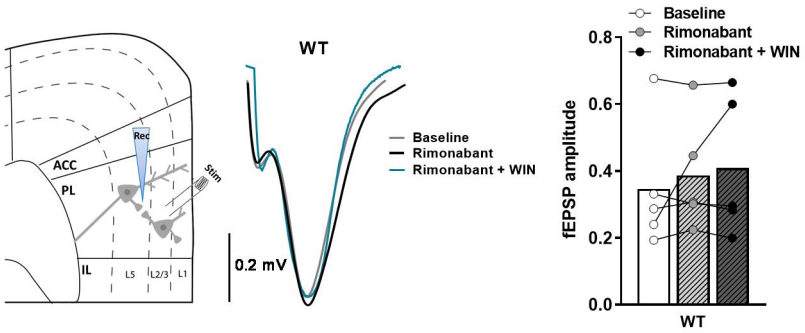

Figure 42. Representative recording of field excitatory postsynaptic potential (fEPSP) in baseline conditions and in the presence of rimonabant (4 µM) and rimonabant (4 µM) + WIN55,212-2 (5 µM) in WT mice (5 slices from 3 mice; left). Quantification of the fEPSP amplitude variation respect to baseline conditions in response to rimonabant (4 µM), and rimonabant (4 µM) + WIN55,212-2 (5 µM; data was presented as a mean and individual values; statistical details are included in Supplementary Table 2).

Overall, we obtained a functional confirmation of the absence of the CB_1R in the Glu-CB1-KO mice and demonstrated the modulatory effect of CB_1R in excitatory glutamatergic transmission in PL, which participates in the enhanced inhibitory control of food operant seeking behavior observed in the Glu-CB1-KO mice.

Chemogenetic inhibition of glutamatergic PL neurons promotes food addiction

Based on our above observations, we hypothesized that hypoactivity of glutamatergic transmission in mPFC would promote addictive-like behavior in WT mice when exposed to the palatable food addiction model. We used a chemogenetic approach to selectively reduce the activity of all the glutamatergic neurons in the PL. We selectively expressed the hM4Di-DREADD in glutamatergic neurons by bilateral injections of a Cre-dependent AAV expressing hM4Di-DREADD (AAV8-hSyn-DIO-hM4D(Gi)-

mCherry) into the PL of Nex-Cre mice (Figure 43a). Nex-Cre mice express the Cre recombinase specifically in dorsal telencephalic glutamatergic neurons. Monitoring of mCherry expression allowed to verify injection sites (Figure 43b).

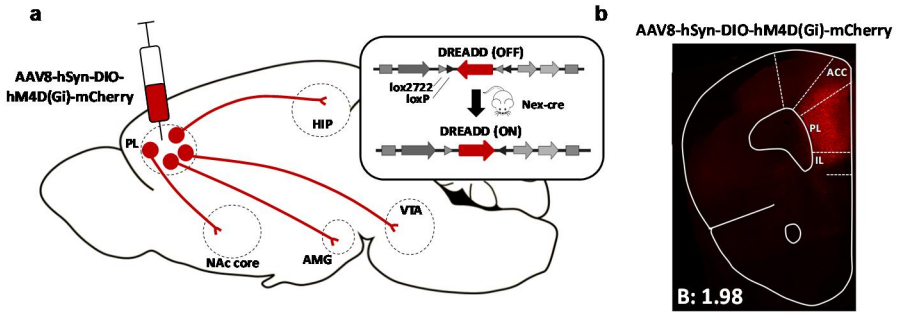

Figure 43. a, Scheme of viral strategy for selective hM4Di-mCherry expression in glutamatergic PL neurons**. b**, Representative immunofluorescence image of Cre-dependent hM4Di-mCherry detected at PL injection site. NAc, nucleus accumbens; HIP, hippocampus; AMG, amygdala; VTA, ventral tegmental area; ACC, anterior cingulate; PL, prelimbic; IL, infralimbic.

Next, we aimed at validating our approach by using whole-cell current clamp recordings in L5 of visually identified hM4Di-expressing PL neurons in the presence of the selective exogenous ligand CNO. We observed reduced excitability of identified hM4Di-expressing PL glutamatergic neurons. CNO application blocked current-evoked action potential firing caused by decreased membrane resistance ($P< 0.05$, Figure 44a-b). No significant differences in the firing rate, membrane resistance nor in rheobase were found when CNO was applied in mPFC slices of mice not expressing the hM4Di receptors, suggesting that these CNO-induced effects were selectively mediated by hM4Di receptor activation (Figure 45a-c).

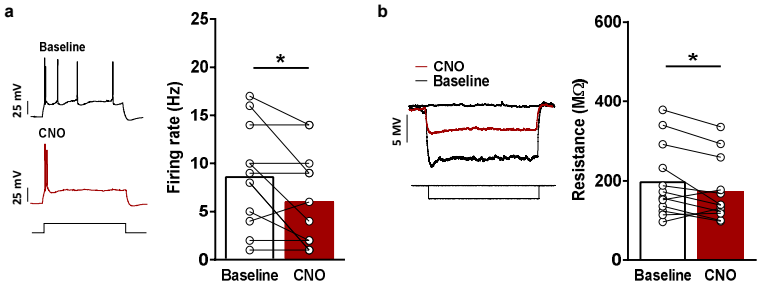

Figure 44. a, Firing rate. Representative recordings showing evoked (200 pA) action potential in visualized hM4Di-mCherry expressing neurons in the L5 at baseline and after CNO (10 µM) application (left). Decreased firing rate after CNO application (mean and individual values, paired t-test *P<0.05; 12 cells from 7 animals; right). **b, Membrane resistance**. Representative recordings showing decreased voltage response to a depolarizing current square pulse of 25 pA (1 s duration) after CNO (10 µM) application compared to baseline in visualized neurons of Nex-Cre mice injected with Cre-dependent AAV-hM4Di-mCherry in L5 (left). Quantification of the membrane resistance (MΩ) at baseline and after CNO (10 µM) application (mean and individual values; Wilcoxon test, *P<0.05; 12 cells from 5 animals; statistical details are included in Supplementary Table 3)**.**

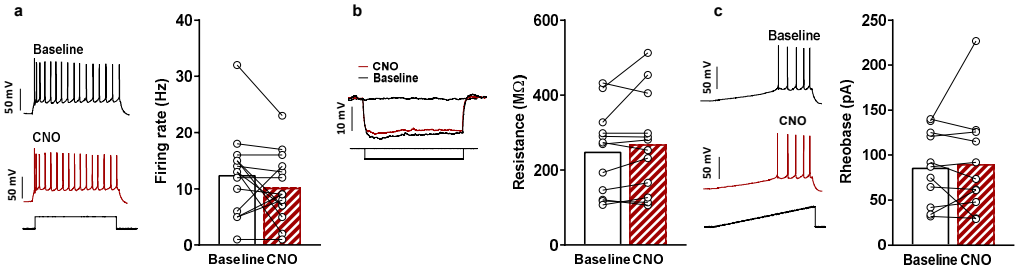

Figure 45. a-c, Electrophysiological recordings from WT mice injected with AAV-control-mCherry in PL L5 visualized neurons at baseline and after CNO (10 µM) application a, Firing rate. Representative recordings showing evoked (200 pA) action potential after CNO application (left). Quantification of the firing rate (Hz) (14 cells from 4 animals; right). **b, Membrane resistance**. Representative recordings showing no differences in voltage response to a depolarizing current square pulse of 25 pA (1 s duration) after CNO application (left). Quantification of the membrane resistance (MΩ) (14 cells from 4 animals; right). **c, Rehobase**. Representative recordings showing the equally required current to elicit the first action potential after CNO application. The current ramp was of 150 pA and 1.5 s duration (left). Quantification of the current required (pA) for firing (14 cells from 4 animals; right; mean and individual data; statistical details are included in Supplementary Table 3).

Therefore, we expected to induce a vulnerable phenotype in those mice expressing inhibitory DREADD in PL when chronically induced hypoactivity of excitatory glutamate transmission using CNO minipumps, leading to the development of food addiction already in the early training period. We trained Nex-Cre mice (n=27) to self-administer chocolate-flavored pellets in the operant chambers under FR1 (2 sessions) and FR5 (2 sessions) schedule of reinforcement before AAV injection and under FR5 (4 sessions) after injection to recover the basal levels of responding (Figure 46). Then, an osmotic minipump filled with CNO (n=14) or saline (n=13) was s.c. implanted in the back of each mouse. During the chronic CNO exposure (4 weeks, 0.25 µl/h) with the subsequent inhibition of the glutamatergic PL neurons, mice underwent FR5 sessions for 4 weeks, and the 3 food addiction criteria were evaluated in the last week.

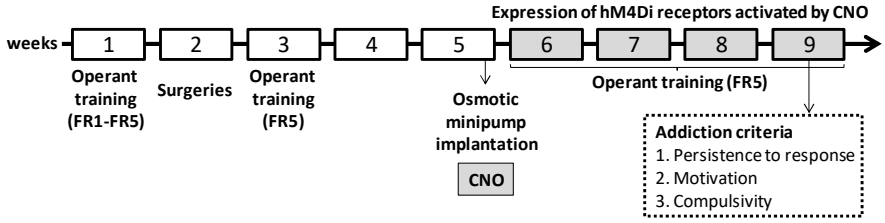

Figure 46. Timeline of the experimental sequence of the early period of food addiction mouse model. Mice were trained to acquire the operant conditioning maintained by chocolate-flavored pellets under FR1 (2 sessions) and FR5 (3 sessions) schedule of reinforcement followed by the surgery for injecting Cre-dependent AAVs carrying the hM4Di-DREADD. After the surgery, the expression of the AAV was allowed for the period of 4 weeks. At the beginning of this period, mice were under FR5 (4 sessions) to recover the basal levels of responding and at the end of the period, an osmotic minipump filled with CNO was implanted. During the chronically inhibition of CNO-induced activation of the expressed hM4Di receptors, mice were under FR5 sessions followed by the measurements of the 3 addiction criteria.

No significant differences between CNO and saline treated mice without inhibitory DREADD expression were found in operant responding (Figure 47a-d), discarding unspecific effects of CNO. In addition, no effect of CNO was found in other parameters, such as body weight, food intake and locomotor activity in mice expressing the inhibitory DREADD (Figure 47e-g).

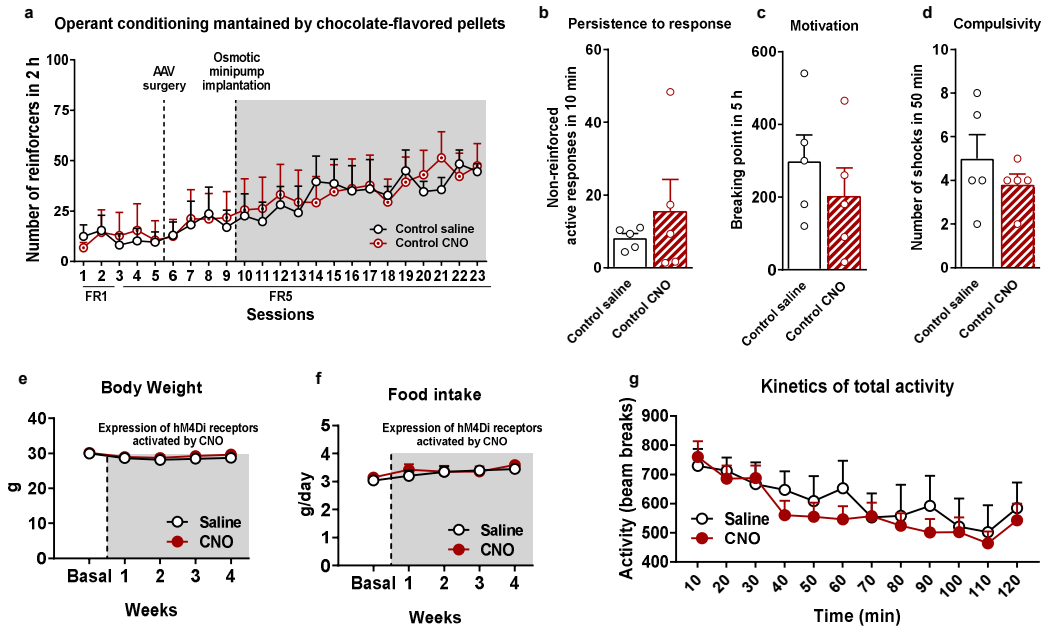

Figure 47. a-d, Lack of CNO-induced effects in mice injected with AAV-control-DREADD either treated with saline (n=5) or CNO (n=5). a, Operant conditioning maintained by chocolate-flavored pellets. **b**, Persistence to response. **c,** Motivation. **d,** Compulsivity. **e-g, Additional variables to measure the effects of chronically CNO administration in Nex-Cre mice expressing hM4Di receptors in PL (saline n=13, CNO n=14). e,** Body weight. Weekly measures of body weight in grams for the saline and CNO groups. **f,** Food intake. Weekly measures of regular chow food intake provided to mice in their home cage in grams per day for both groups. **g,** Kinetics of total activity. Locomotor activity measured by beam breaks represented in 10-min blocks during 2 h in both groups (statistical details are included in Supplementary Table 3).

Nex-Cre mice expressing hM4Di receptor activated chronically by CNO showed the same number of reinforcers obtained in the daily sessions of the operant conditioning maintained by chocolate-flavored pellets compared to saline treated animals (Figure 48).

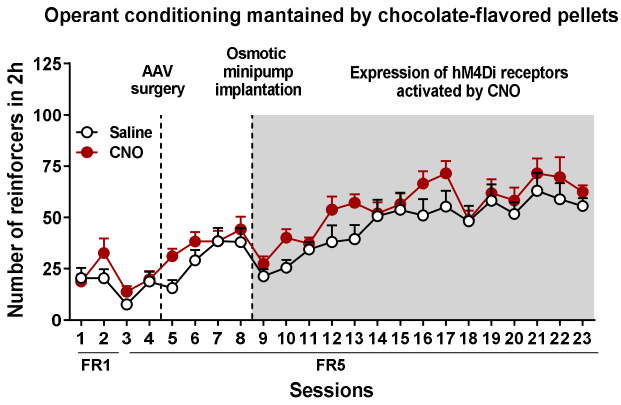

Figure 48. Number of reinforcers during operant training maintained by chocolate-flavored pellets (mean ± S.E.M; repeated measures ANOVA, treatment effect $^{**}P<0.01$; n=13 for saline treated mice and n=14 for CNO treated mice; statistical details are included in Supplementary Table 3).

With regards to the addiction criteria, no differences were obtained in persistence to response, motivation nor compulsivity between CNO and saline treated animals (Figure 49a-c). Even so, when analyzing the distribution of the individual values, 60.0% of hM4Di expressing mice were above or equal to the 75th percentile threshold of the control group in motivation and compulsivity criteria. In agreement, 42.8% of mice with the inhibition of glutamatergic PL neurons accomplished the criteria of addiction as compared to 15.4% of saline treated mice ($P<0.01$, Figure 49d), suggesting that a decreased excitability of glutamatergic transmission in PL neurons, which most likely project to other distinct brain areas, is involved in the development of this addictive behavior.

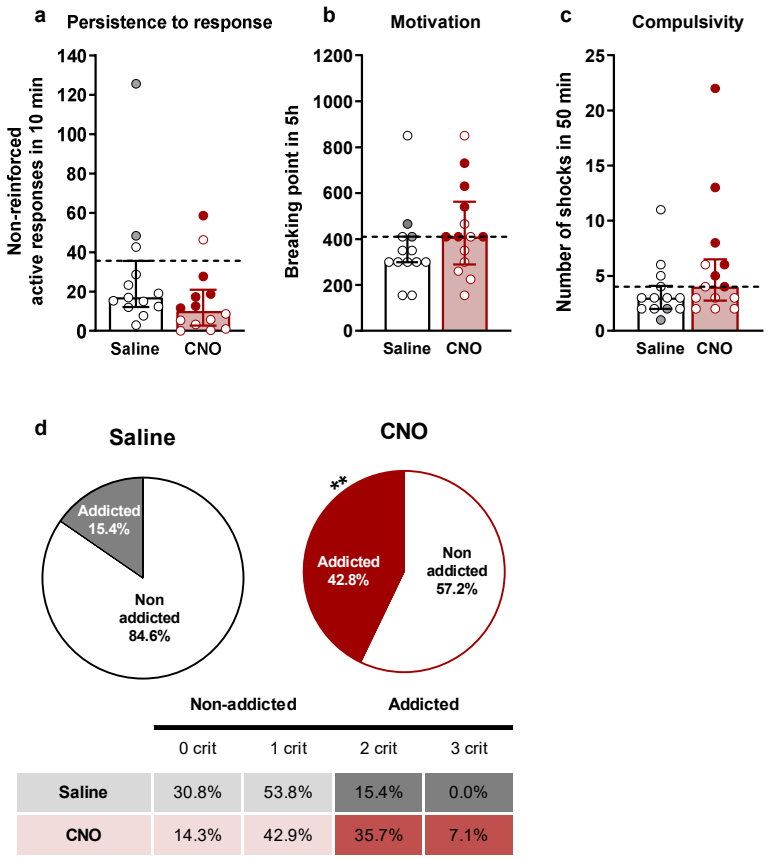

Figure 49. a-c, Behavioral tests of the three addiction criteria in the early period (individual values with the median and the interquartile range). The 75th percentile of the distribution of saline-treated mice is indicated by the dashed horizontal line. Addicted mice in grey filled circles for saline treated mice and red for CNO treated mice. **d,** Increased percentage of CNO treated mice classified as food addicted animals (Chi-square ***P*<0.01; n=13 for saline treated mice and n=14 for CNO treated mice; statistical details are included in Supplementary Table 3).

Positive correlations showed that the intensity of the three food addiction criteria was proportional to the number of criteria met by the subject in CNO group and in the persistence to response in saline group (Figure 50a-f).

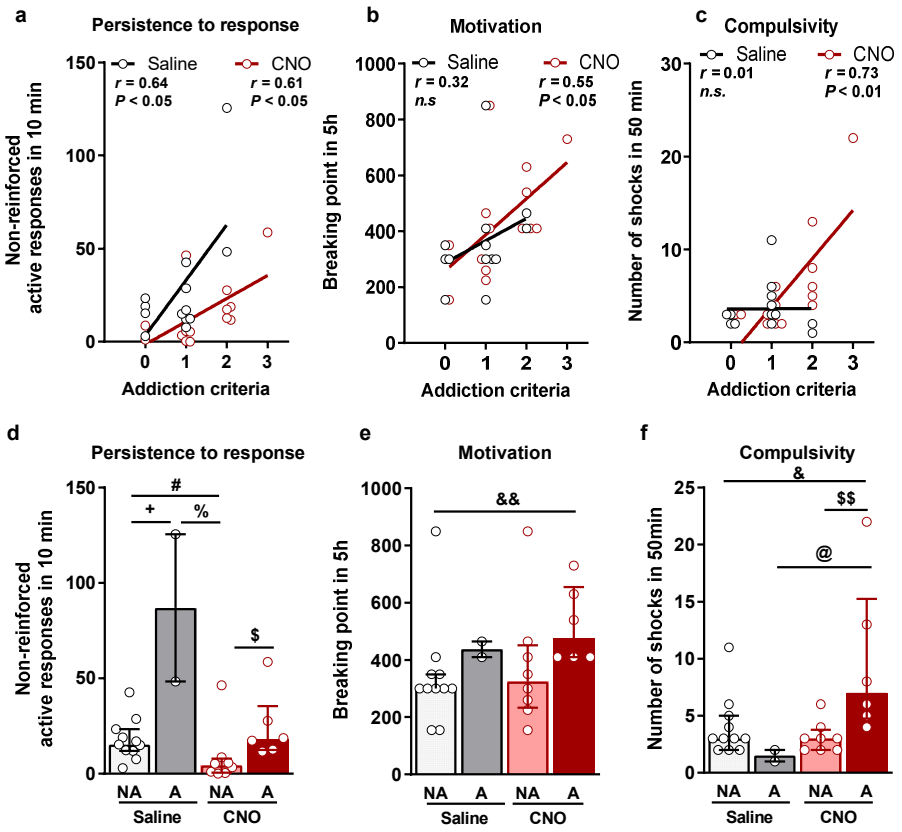

Figure 50. a-c, Correlations. Pearson correlations between individual addiction criteria and **a,** non-reinforced active responses in 10 min, **b,** breaking point in 5 h, **c,** number of shocks in 50 min. **d-f, Behavioral tests of the three addiction criteria represented by individual values and bars with median and the interquartile range for the four groups classified as addicted and non-addicted mice in both experimental treatment groups** (saline n=13, CNO n=14). **d**, Persistence to response. **e,** Motivation. **f**, Compulsivity. (U Mann-Whitney, + *P*<0.05 saline NA vs saline A; # *P*<0.05 saline NA vs CNO NA, && *P*<0.01 saline NA vs CNO A; % *P*<0.05 saline A vs CNO NA; @ *P*<0.05 saline A vs CNO A, $ *P*<0.05, $$ *P*<0.01 CNO NA vs CNO A. Statistical details are included in Supplementary Table 3).

Chemogenetic inhibition of PL-NAc core projection leads to loss of inhibitory control and compulsive behavior towards highly palatable food

As shown above, decreased excitatory transmission in PL promotes food addiction-like behavior and PL neurons send projections widely to multiple brain areas. Next, we asked which specific projection is involved in the loss of behavioral control. To answer this question, we adopted a combined chemogenetic and a retrograde AAV variant approach (Tervo *et al.*, 2016) that enables the retrograde tagging of neuronal projections. We injected two AAVs: AAV-hM4Di-DREADD (AAV8-hSyn-DIO-hM4D(Gi)-mCherry) into PL and AAV-retrograde-Cre (AAV-pmSyn-EBFP-Cre) into the NAc core (Figure 51a). Thus, hM4Di receptors expression only occurred in PL neurons that directly projected to the NAc core. mCherry and Cre recombinase were visualized by immunofluorescence to verify the injection site of the AAVs and the retrograde transport of Cre (Figure 51b).

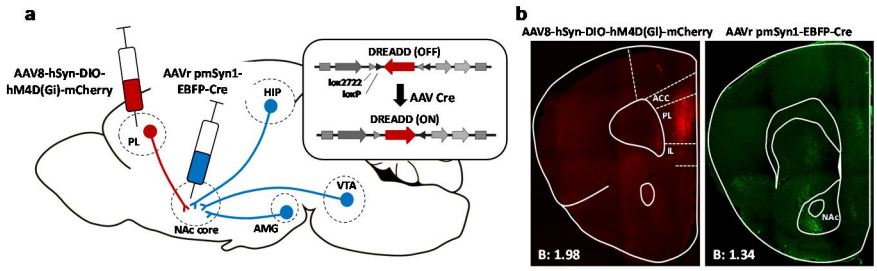

Figure 51. a, Scheme of combinatorial viral strategy for selective hM4Di-mCherry expression in PL-NAc core neurons. **b,** Representative immunofluorescence image of Cre-dependent hM4Di-mCherry detected at PL injection site (left) and Cre recombinase at NAc core (right). NAc, nucleus accumbens; HIP, hippocampus; AMG, amygdala; VTA, ventral tegmental area; ACC, anterior cingulate; PL, prelimbic; IL, infralimbic.

Whole-cell current clamp recordings performed in PL L5 of visually identified hM4Di-expressing PL-NAc core neurons confirmed that CNO activation of hM4Di receptor inhibited the activity of PL-NAc core neurons confirmed that CNO activation of hM4Di receptor inhibited the activity of PL-NAc neurons. Indeed, CNO bath application decreased membrane resistance and subsequently blocked current-evoked action potential firing frequency (*P*<0.05, Figure 52a-b). Furthermore, the current needed to evoke one single action potential was higher when the CNO was applied as compared to the baseline (Figure 52c). This effect was hM4Di receptor specific because no significant differences in the firing rate, membrane resistance nor in rheobase were found when CNO was applied in mPFC slices of mice not expressing the hM4Di receptors (Figure 45a-c).

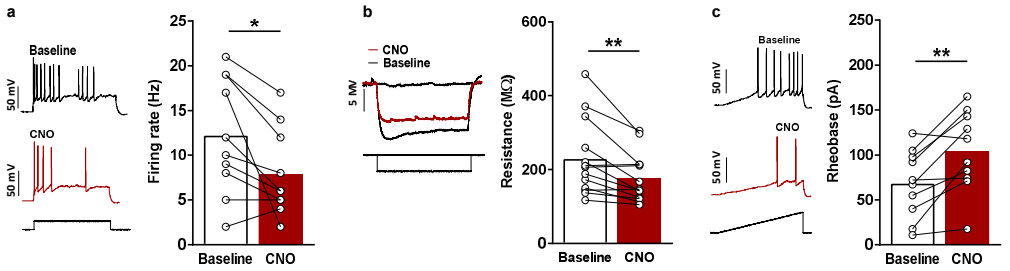

Figure 52. a, Firing rate. Representative recordings showing evoked (200 pA) action potential in hM4Di-mCherry layer 5 neurons at baseline and after CNO (10 µM) application (left). Decreased firing rate after CNO application (mean and individual values; paired t-test **P*<0.05; 10 cells from 4 animals; right). **b, Membrane resistance.** Representative recordings showing decreased voltage response to a depolarizing current square pulse of 25 pA (1 s duration) after CNO application (left). Quantification of the membrane resistance (MΩ) (13 cells from 3 animals; paired t-test, ***P*<0.01; right)**. c, Rehobase.** Representative recordings showing the increased required current to elicit the first action potential after CNO application. The current ramp was of 150 pA and 1.5 s duration (left). Quantification of the current required (pA) for firing (10 cells from 3 animals; paired t-test, ***P*< 0.01; right; statistical details are included in Supplementary Table 4)**.**

Using this approach, we expected that selective inhibition of the PL-NAc core projections would decrease the inhibitory control during food operant training, and thereby promoting a more susceptible phenotype to develop addiction-like behavior. We performed the early food addiction protocol in mice treated chronically with CNO (n=22) or saline (n=12) (Figure 53).

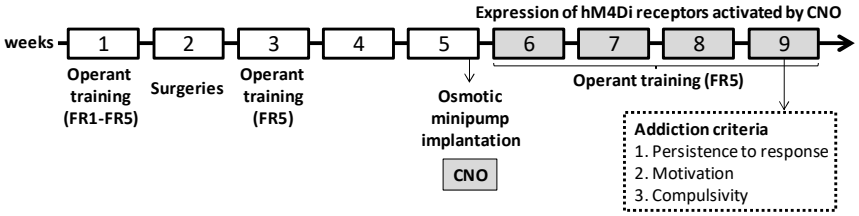

Figure 53. **Timeline of the experimental sequence of the early period of food addiction mouse model.** Mice were trained to acquire the operant conditioning maintained by chocolate-flavored pellets under FR1 (2 sessions) and FR5 (3 sessions) schedule of reinforcement followed by the surgery for injecting Cre-dependent AAVs carrying the hM4Di-DREADD at PL and the AAV-retrograde-Cre targeting NAc core. After the surgery, the expression of the AAV was allowed for the period of 4 weeks. At the beginning of this period, mice were under FR5 (4 sessions) to recover the basal levels of responding and at the end of the period, an osmotic minipump filled with CNO was implanted. During the chronically inhibition of CNO-induced activation of the expressed hM4Di receptors, mice were under FR5 sessions followed by the measurements of the 3 addiction criteria.

No differences were found in the number of reinforcers in the daily training sessions between CNO and saline treated mice during the operant conditioning maintained by chocolate-flavored pellets, indicating that the inhibition of PL-NAc core projection did not affect the reinforcing effects of these pellets (Figure 54). In contrast, this specific manipulation of the PL-NAc projection produced a robust increase in the food addiction compulsivity criterion ($p<0.01$, Figure 55c). Thus, mice with chronic inhibition of PL-NAc core projection could not stop responding for chocolate-flavored pellets in the shock test, receiving a higher number of

shocks compared to the saline group. The lack of significant differences in the persistence to response and motivation highlights that the PL-NAc core projection was selectively involved in the loss of control leading to compulsive food seeking (*P*<0.01, Figure 55a-b).

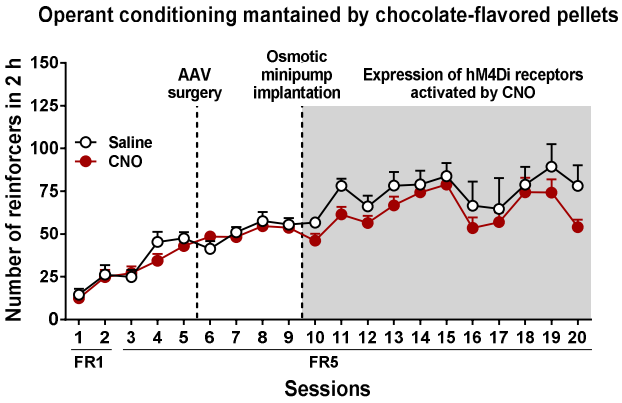

Figure 54. Number of reinforcers during operant training sessions maintained by chocolate-flavored pellets (mean ± S.E.M); n=12 for saline treated mice vs 22 for CNO treated mice; statistical details are included in Supplementary Table 4).

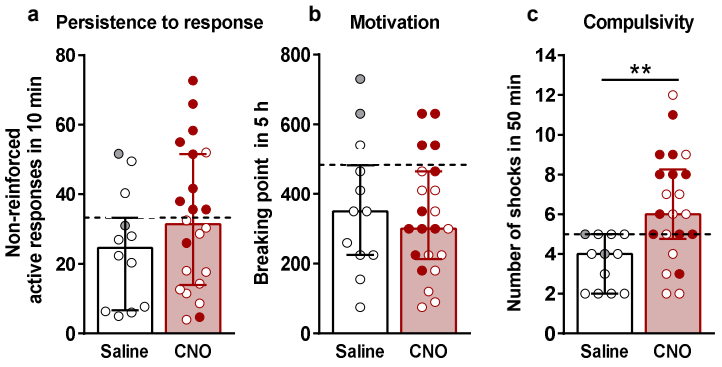

Figure 55. a-c, **Behavioral tests of the 3 addiction criteria showing increased compulsivity in CNO treated mice**. **a,** Persistence to response. **b,** Motivation. **c,** compulsivity. The 75th percentile of the distribution of mice treated with saline is indicated by the dashed horizontal line. Addicted mice in grey filled circles for saline treated mice and red for CNO treated mice (individual values with the median and the interquartile range, U-Mann-Whitney **P<0.01; n=12 for saline treated mice vs 22 for CNO treated mice; statistical details are included in Supplementary Table 4).

The increased compulsivity could not be explained by an unspecific effect of CNO, since no significant differences of CNO on the 3 addiction criteria were detected in chronically treated mice not expressing the inhibitory DREADD (Figure 47a-d). In addition, no side effects of CNO were observed on body weight, food intake or locomotor activity in these mice (Figure 56a-c).

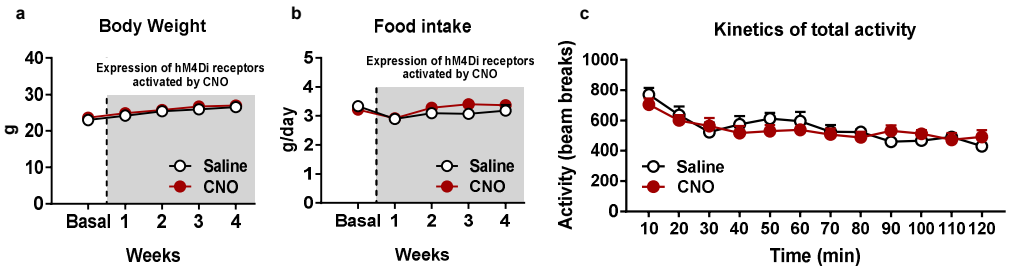

Figure 56. a-c, Additional variables to measure the effects of chronic CNO treatment in mice expressing hM4Di receptors in PL-NAc core projection neurons a, Body weight. Weekly measures of body weight in grams for the saline and CNO groups. **b,** Food intake. Weekly measures of regular chow food intake provided to mice in their home cage in grams per day for both groups. **c,** Kinetics of total activity. Locomotor activity measured by beam breaks represented in 10-min blocks during 2 h in both groups (saline n=12 and CNO n=22; statistical details are included in Supplementary Table 4).

We observed that our manipulation produced a vulnerable phenotype to develop food addiction, as shown by the fact that the majority of CNO treated animals (77.3%) were above the 75th percentile of the compulsivity criterion. Using the categorization based on the three criteria, a highly significant percentage of the CNO-treated mice (50.0%) was considered addicted as compared to the control animals (16.7%, P<0.001, Figure 57). Finally, a positive correlation between the number of criteria reached and

the values of each addiction criterion was found in CNO group in the 3 criteria and in saline group in the criteria of compulsivity (Figure 58a-f). Thus, we demonstrated that the specific inhibition of the PL neurons projecting to the NAc core is a crucial factor that confers vulnerability to develop food addiction.

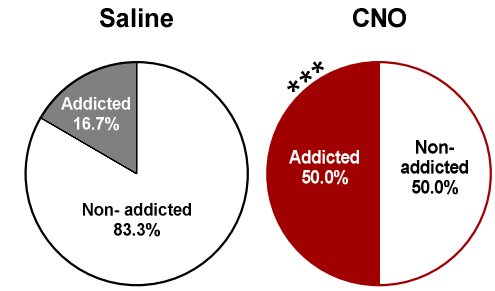

	Non-addicted		Addicted	
	0 crit	1 crit	2 crit	3 crit
Saline	33.3%	50.0%	16.7%	0.0%
CNO	22.7%	27.3%	45.4%	4.6%

Figure 57. Increased percentage of CNO treated mice classified as food addicted animals (Chi-square ***P<0.001; n=12 for saline treated mice vs 22 for CNO treated mice; statistical details are included in Supplementary Table 4).

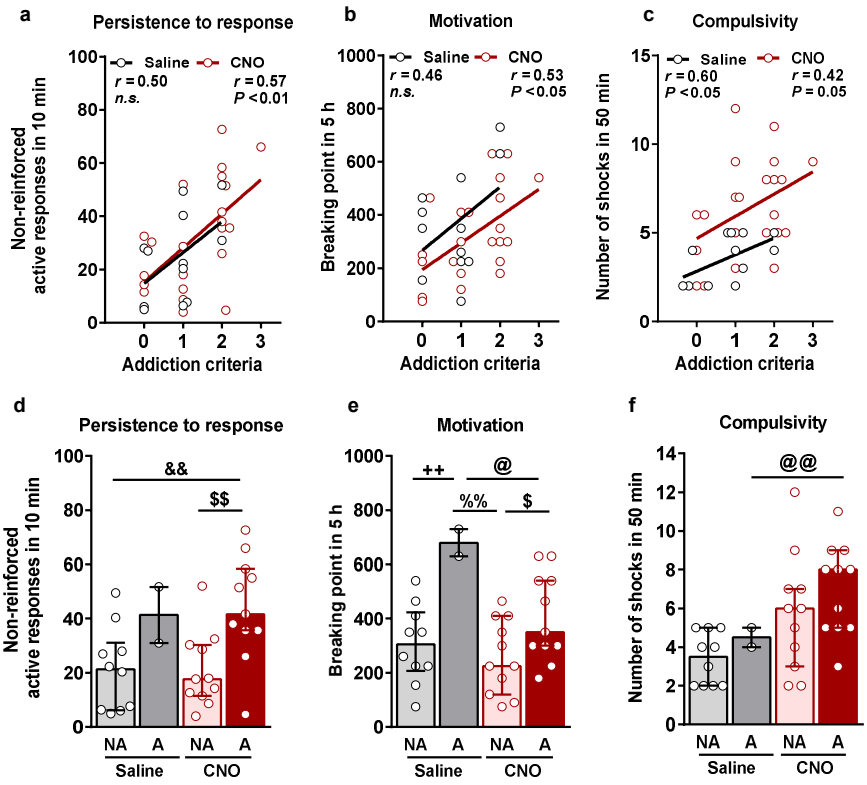

Figure 58. a-c, Correlations. Pearson correlations between individual addiction criteria and **a,** non-reinforced active responses in 10 min, **b,** breaking point in 5 h, **c,** number of shocks in 50 min. **d-f**, **Behavioral tests of the three addiction criteria represented by individual values and bars with median and the interquartile range for the four groups classified as addicted (A) and non-addicted (NA) mice in both treatment groups**, **d,** Persistence to response. **e,** Motivation. **f,** Compulsivity. (U Mann-Whitney, ++ *P*< 0.01 saline NA vs saline A, && *P*< 0.01 saline NA vs CNO A, %% *P*< 0.01 saline A vs CNO NA, @ *P*< 0.05, @@ *P*< 0.01 saline A vs CNO A, $ *P*< 0.05, $$ *P*< 0.01, CNO NA vs CNO A; saline n=12, CNO n=22; statistical details are included in Supplementary Table 4).

Transcriptomic analysis reveals an upregulation of the Drd2 gene expression in mPFC of addicted mice independently of the CB_1R genotype

To characterize gene expression signatures for food addiction, we performed whole transcriptome analysis of mPFC samples of addicted and

non-addicted WT and Glu-CB1-KO mice, classified on the bases of the performance at the late period (n=4-6). We selected both WT and Glu-CB1-KO mice displaying similar extreme values in the 3 addiction criteria (Figure 59a-c). In these mice, non-significant differences were observed in pellet intake between addicted and non-addicted mice in the last FR5 session, immediately before tissue collection (Figure 59d). Therefore, we assume that changes in gene expression would be related to the addiction phenotype and not to the amount of pellet intake during the training sessions.

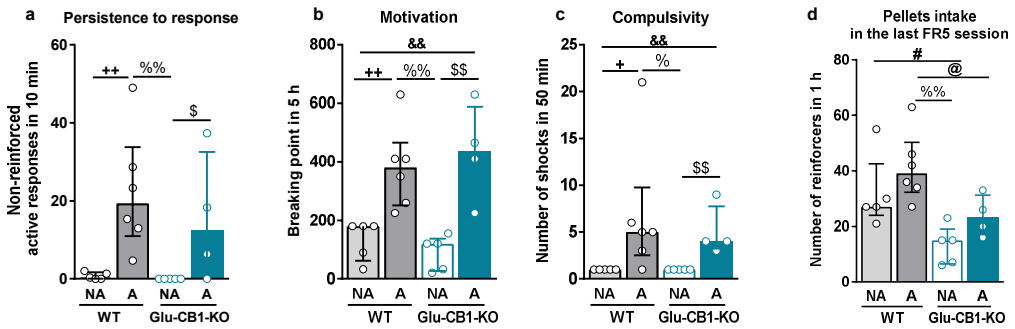

Figure 59. **a-c**, **Behavioral tests of the three addiction criteria during the late period for those mice selected for RNA-seq in each of the four groups, addicted (A) and non-addicted (NA) mice in both genotypes. a,** Persistence to response. **b,** Motivation. **c,** Compulsivity. **d,** Pellet intake in the last FR5 session before sample collection (individual values and bars with median and the interquartile range; n=5 WT NA, n=6 WT A, n=5 Glu-CB1-KO NA, n=4 Glu-CB1-KO NA; (+ *P*<0.05, ++ *P*<0.01 WT NA vs WT-A, # *P*<0.05 WT NA vs Glu-CB1-KO NA, && *P*<0.01 WT NA vs Glu-CB1-KO A, % *P*<0.05, %% *P*<0.01 WT A vs Glu-CB1-KO NA, @ *P*<0.05, WT A vs Glu-CB1-KO A, $ *P*<0.05, $$ *P*<0.05 Glu-CB1-KO NA vs Glu-CB1-KO A; statistical details are included in Supplementary Table 5).

To determine overall transcriptional changes in the addicted versus non-addicted mice, we applied principal component analysis, revealing the variation between the samples. Two overlapping clusters were observed,

allowing a general separation of the addicted from non-addicted mice (Figure 60).

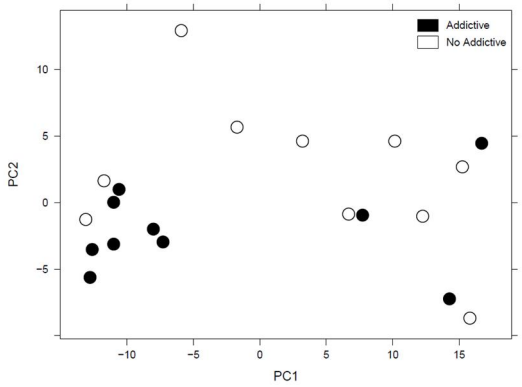

Figure 60. Principle component analysis (PCA) showing variation between addicted and non-addicted mice (Statistical details are included in Supplementary Table 5).

Upon performing differential gene expression analysis, the volcano plot of the RNA-seq data analysis showed a rather small number of differentially expressed genes between non-addicted and addicted mice: 20 genes were significantly upregulated, whereas 47 genes were downregulated (Figure 61a). Interestingly, *Drd2* (dopamine receptor type 2), *Adora2a* (adenosine receptor 2a), *Gpr88* (orphan G-protein coupled receptor 88), and *Drd1* (dopamine receptor type 1) mRNA were found to be strongly upregulated in the addicted mice. These four differentially expressed genes were selected for technical validation by qPCR. The results confirmed the up-regulation of *Drd2*, *Adora2a*, *Gpr88,* and *Drd1* mRNAs in addicted mice ($P < 0.05$, Figure 61b).

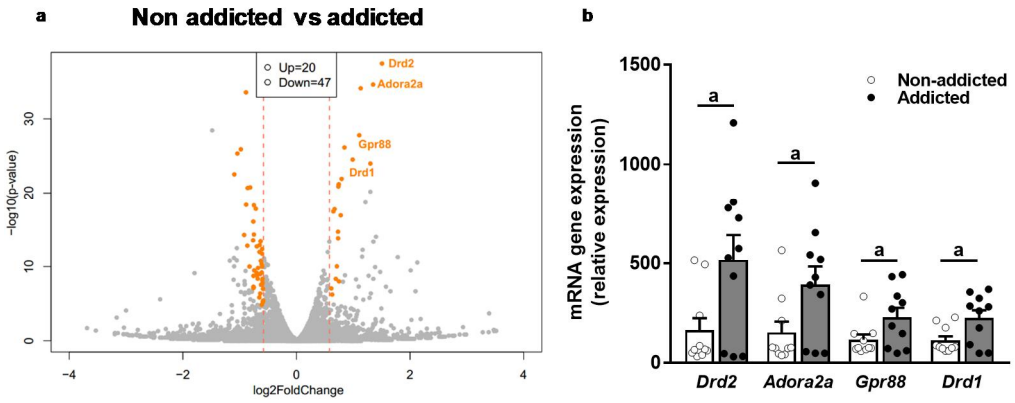

Figure 61. a, Volcano plot of the RNA-seq data analysis. The cutoff of 1.5 fold change and significantly expressed genes in addicted mice compared to non-addicted mice are highlighted in orange; **b, Quantitative real time PCR of selected genes** (a *P*<0.05 non-addicted vs addicted; statistical details are included in Supplementary Table 5).

As expected, no changes were found in housekeeping genes between non-addictive and addictive samples (Figure 62a-c), validating RNA-seq data analysis.

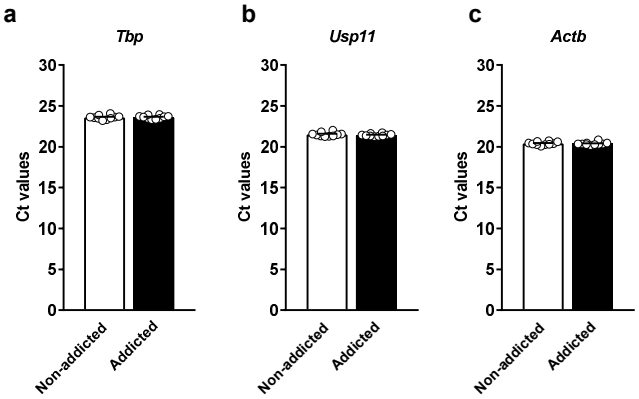

Figure 62. Ct values for housekeeping genes (Statistical details are included in Supplementary Table 5).

Furthermore, RNA-seq data analysis also showed differential expressed genes between WT and Glu-CB1-KO mice: 14 genes were significantly

upregulated, whereas 20 genes were downregulated (Figure 63a). Technical validation by qPCR confirmed that *Cnr1* (cannabinoid type 1 receptor gene) was downregulated as expected, and *Fos* (c-fos) was also downregulated in mutants ($P<0.05$, $P<0.001$, Figure 63b). Interestingly, c-fos has been extensively used as a molecular marker of neuronal activity, implicating an enhanced neuronal activity in mPFC of WT compared to Glu-CB1-KO mice. In fact, *Fos* mRNA levels correlate with the increased number of reinforcers in WT as compared with Glu-CB1-KO immediately prior to sample collection (Figure 59d). A non-significant difference was found for *Npas4* mRNA, encoding the transcription factor neuronal PAS containing protein 4. This result confirmed the observation that *Npas4* was not differentially expressed according to established thresholds of RNA seq analysis (Figure 63b).

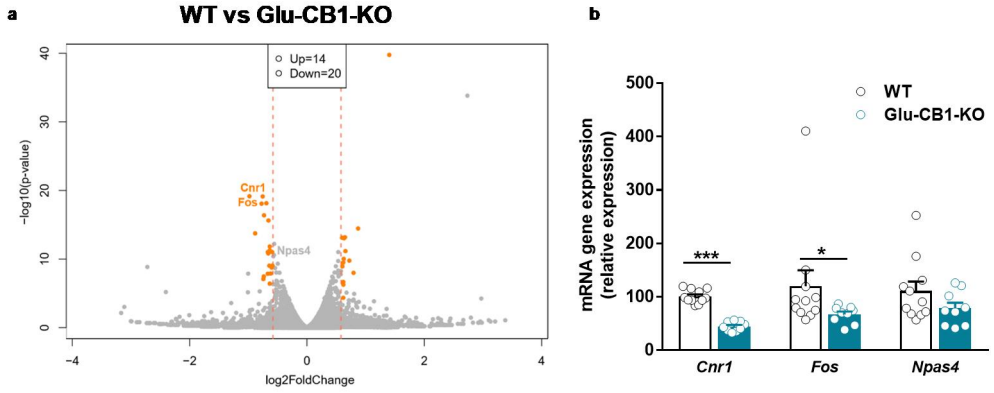

Figure 63. **a, Volcano plot of the RNA-seq data analysis.** The cutoff of 1.5 fold change and significantly expressed genes in Glu-CB1-KO compared to WT are highlighted in orange. **b, Quantitative real time PCR of selected genes** (**P*<0.05, ****P*<0.001 WT vs Glu-CB1-KO; statistical details are included in Supplementary Table 5).

In summary, transcriptomic data analysis shed new lights into the gene expression signature in mPFC related to food addiction, suggesting

molecular mechanisms associated with the loss of control of palatable food intake. As we found that *Drd2* gene is the most significantly upregulated gene in addicted mice, we hypothesized that this upregulation could play a key role in the development of food addiction-like behavior, irrespective of the presence or absence of CB_1R.

Overexpression of Drd2 in PL-NAc core projections promotes loss of inhibitory control towards highly palatable food

Based on the above findings, we tested whether the selective overexpression of *Drd2* in the PL-NAc core projections induces the loss of inhibitory control for palatable food self-administration. Using these experimental conditions, we aimed at mimicking the upregulation of the *Drd2* gene observed in addicted mPFC after long-term exposure to highly palatable food operant training. First, we confirmed low endogenous *Drd2* mRNA expression in PL by *in situ* hybridization (Figure 64a).

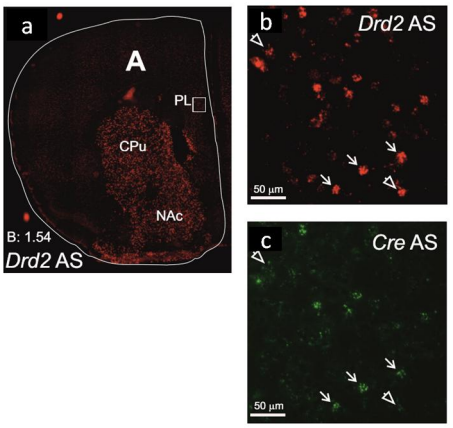

Figure 64.a, Overview of Drd2 mRNA localization (red) in caudate putamen (CPu), NAc and PL at bregma of approx. 1.54 mm, as detected by *in situ* hybridization. **b,** Enlarged view of the area shown in a, revealing Drd2 mRNA localization in PL, and **c,** Cre mRNA (green). Arrows: Cells with colocalization of Drd2 and Cre mRNA; arrowheads: Cells expressing only Drd2 mRNA.

For specific overexpression in PL-NAc core projections, we used a dual viral vector approach with an AAV-D2R (AAV-hSyn-DIO-D2L-mVenus, n=13) and

AAV-control (AAV-Syn1-Stop-GFP, n=12) injected into PL, and an AAV-retrograde-Cre (AAV-pmSyn-EBFP-Cre) injected into the NAc core (Figure 65a). We first verified the injection site of the viruses by immunofluorescence against mVenus and Cre recombinase (Figure 65b).

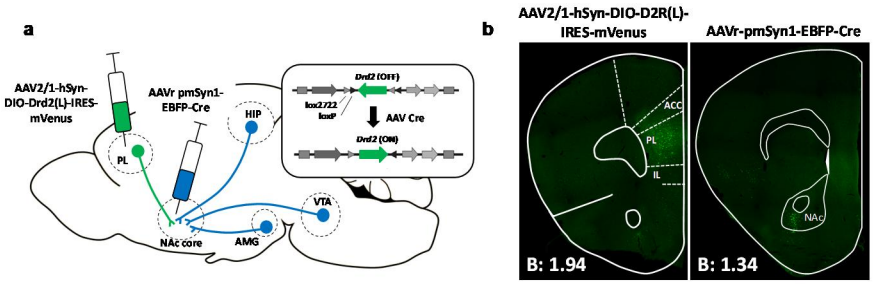

Figure 65. a, Scheme of combinatorial viral strategy for selective D_2R-mVenus expression in PL-NAc core projecting neurons. **b**, Representative immunofluorescence image showing Cre-induced D_2R-mVenus protein at PL injection site (left) and Cre recombinase protein at NAc core injection site (right). NAc, nucleus accumbens; HIP, hippocampus; AMG, amygdala; VTA, ventral tegmental area; ACC, anterior cingulate; PL, prelimbic; IL, infralimbic.

We also confirmed by *in situ* hybridization that retrogradely expressed *Cre* recombinase mRNA is present in PL, and that importantly this mRNA is coexpressed with the endogenous *Drd2* mRNA in PL (Figure 64b-c), indicating that our approach of *Drd2* overexpression is selectively targeted to a fraction of *Drd2*-positive PL-NAc core projection neurons. The functional consequence of *Drd2* overexpression was first investigated by electrophysiology. We performed *in vitro* whole cell recordings in brain slices using the D_2R selective agonist quinpirole to confirm that the overexpression of D_2R decreased the excitability of PL-NAc core projection neurons. Quinpirole (2 µM) application significantly increased rheobase and reduced membrane resistance and firing rate in response to a 150 pA current square pulse ($P<0.05$, $P<0.01$, Figure 66).

No differences were observed in control PL L5 pyramidal neurons, suggesting that the D_2R overexpression was responsible for this inhibitory effect despite the fact that D_2R is also endogenously expressed in mPFC of control mice (Figure 67a-c). A similar reduction in membrane resistance, firing rate and increased rheobase was observed after the application of the endogenous agonist DA (10 µM) (*P*<0.05, *P*<0.01, *P*<0.001, Figure 67d-i).

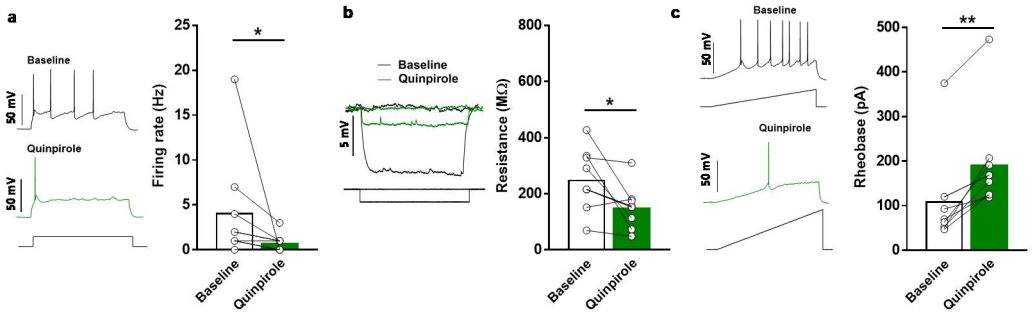

Figure 66. **a**, **Firing rate.** Representative recordings showing evoked (150 pA) action potential in D_2R-mVenus-expressing neurons in layer 5 at baseline and after quinpirole (2 µM) application (left). Decreased firing rate (Hz) after quinpirole (2 µM) application (mean and individual values; paired t-test **P*<0.05, 9 cells from 3 animals overexpressing D_2R; right). **b, Membrane resistance.** Representative recordings showing decreased voltage response to a depolarizing current square pulse of 25 pA (1 s duration) after quinpirole application (left). Quantification of the membrane resistance (MΩ) (9 cells from 3 animals; paired t-test, **P*< 0.05; right)**. c, Rehobase.** Representative recordings showing the increased required current to elicit the first action potential after quinpirole application. The current ramp was of 150 pA (above), 250 pA (below) and 1.5 s duration (left). Quantification of the current required (pA) for firing (9 cells from 3 animals; Wilcoxon test, ***P*< 0.01; right; statistical details are included in Supplementary Table 6).

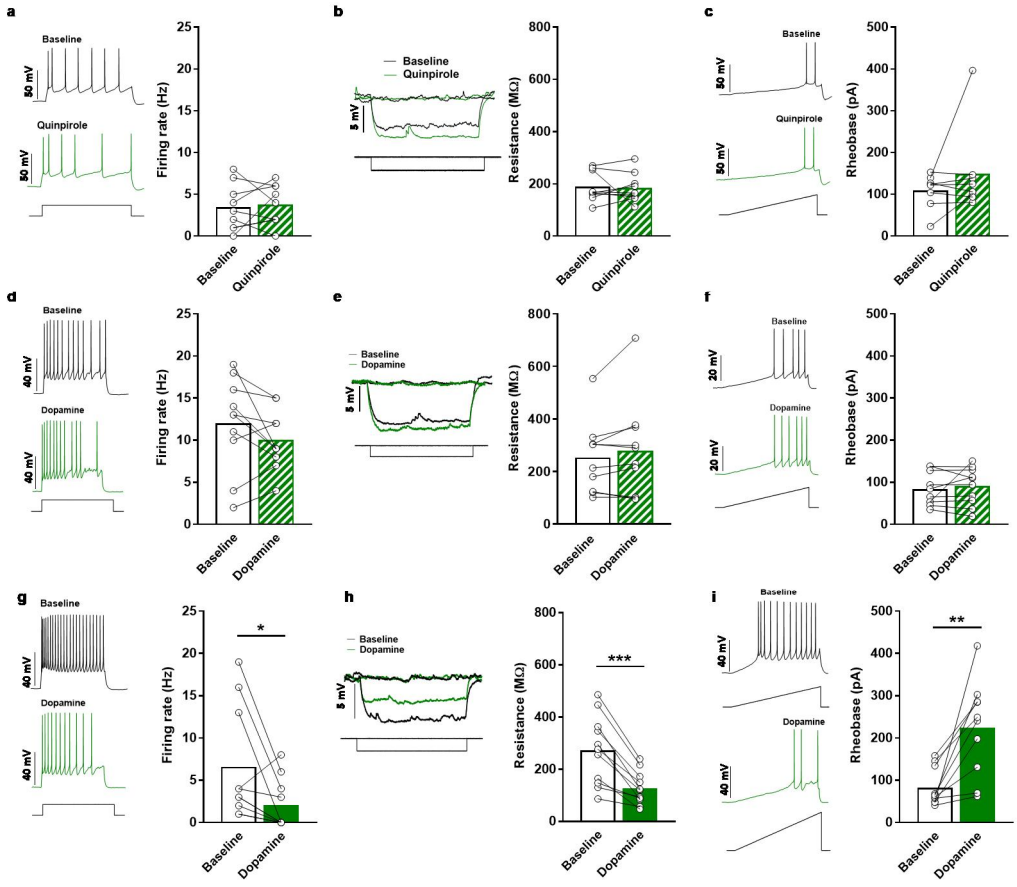

Figure 67. a-f, Electrophysiological recordings from WT mice injected with AAV-control-GFP in PL layer 5 visualized neurons at baseline and after quinpirole (2 µM) or dopamine (10 µM) application represented as mean and individual data. a,d, Firing rate. Representative recordings showing evoked (150 pA) action potential after quinpirole or dopamine application (left). Quantification of the firing rate (Hz) (9-10 cells from 3 animals; right). **b,e, Membrane resistance**. Representative recordings showing no differences in voltage response to a depolarizing current square pulse of 25 pA (1 s duration) after quinpirole or dopamine application (left). Quantification of the membrane resistance (MΩ) (9-10 cells from 3 animals; right). **c,f, Rehobase**. Representative recordings showing the equally required current to elicit the first action potential after quinpirole or dopamine application. The current ramp was of 150 pA and 1.5 s duration (left). Quantification of the current required (pA) for firing. (9-10 cells from 3 animals; right;). **g-i**, **Electrophysiological recordings from WT mice injected with AAV-D_2R-mVenus in PL layer 5 visualized neurons at baseline and after dopamine (10 µM) represented as mean and individual data. g, Firing rate**. Representative recordings showing evoked (150 pA) action potential after dopamine

application (left). Quantification of the firing rate (Hz) (Wilcoxon, *P<0.05; 11 cells from 3 animals; right). **h, Membrane resistance**. Representative recordings showing decreased voltage response to a depolarizing current square pulse of 25 pA (1 s duration) after dopamine application (left). Quantification of the membrane resistance (MΩ) (11 cells from 3 animals; paired t-test, ***P< 0.001; right). **i, Rehobase.** Representative recordings showing the increased required current to elicit the first action potential after dopamine application (left). The current ramp was of 150 pA (above), 250 pA (below) and 1.5 s duration. Quantification of the current required (pA) for firing (11 cells from 3 animals; Wilcoxon test, **P< 0.01; right; statistical details are included in Supplementary Table 6).

For the behavioral analysis, we used a food addiction procedure in the early period similar to the experiments shown above (Figure 68).

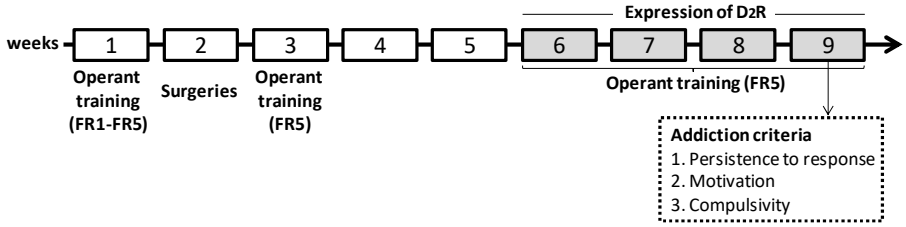

Figure 68. Scheme of combinatorial viral strategy for selective D_2R-mVenus expression in PL-NAc core projecting neurons. Mice were trained to acquire the operant conditioning maintained by chocolate-flavored pellets under FR1 (2 sessions) and FR5 (3 sessions) schedule of reinforcement followed by the surgery for injecting Cre-dependent AAV-D_2R in PL and the AAV-retrograde-cre targeting NAc core. After the surgery, the expression of the AAV was allowed for the period of 4 weeks. At the beginning of this period, mice were under FR5 (4 sessions) to recover the basal levels of responding. During the overexpression of D_2R, mice were under FR5 sessions followed by the measurements of the 3 addiction criteria.

We found that overexpression of D_2R in PL-NAc core projection neurons produced compulsive behavior towards highly palatable food, despite harmful consequences in the shock test, presumably by endogenous DA. This manipulation only affected the compulsivity addiction criterion, since no differences were found in the persistence to response, motivation nor reinforcement (P<0.05, Figure 69a-d). A subset of 57.1% of manipulated mice was above the 75th percentile threshold of the control group in the

compulsivity criterion, and this result was not found in the other addiction criteria.

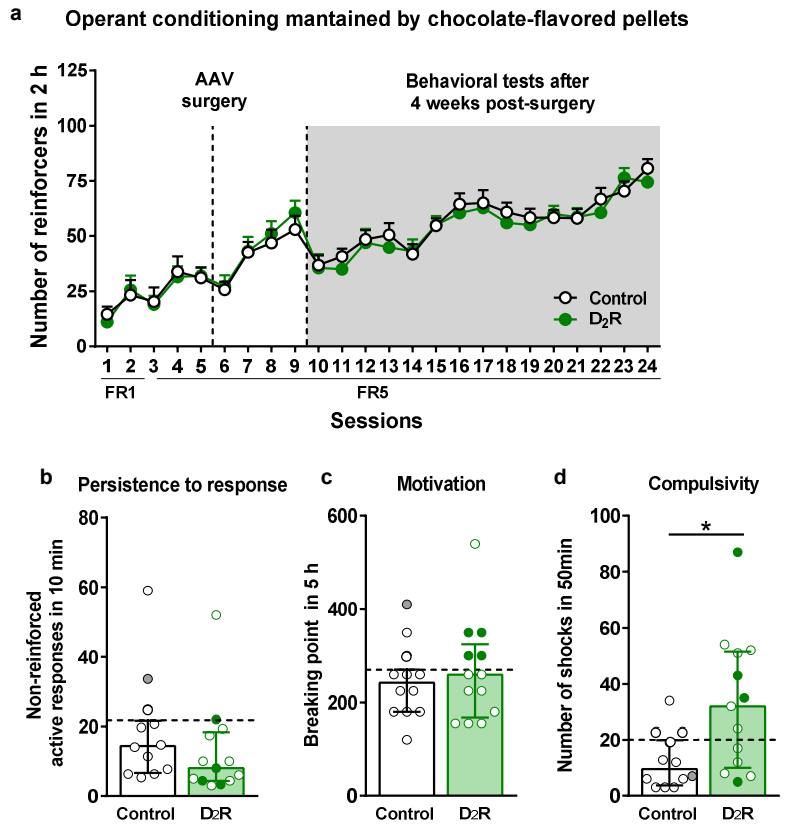

Figure 69. **a**, Number of reinforcers during operant training sessions maintained by chocolate-flavored pellets. **b-d**, Behavioral tests of the three addiction criteria in the early period showed increased compulsivity in mice overexpressing D_2R. **b**, Persistence to response. **c,** Motivation. **d,** Compulsivity. The 75th percentile of the distribution of control mice is indicated by the dashed horizontal line. Addicted mice in grey filled circles for control and green for D_2R mice (Individual values with the median and the interquartile range, t-test *P<0.05; n= 12 for control mice, and 13 for D_2R; statistical details are included in Supplementary Table 6).

Finally, the percentage of D_2R overexpressing mice that achieved 2-3 addiction criteria was 30.8% compared to 8.3% in control mice (P<0.01, Figure 70).

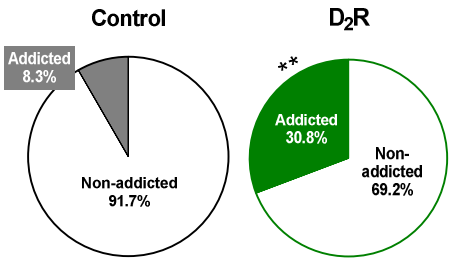

	Non-addicted		Addicted	
	0 crit	1 crit	2 crit	3 crit
Control	33.4%	58.3%	8.3%	0.0%
D_2 R	15.4%	53.9%	30.8%	0.0%

Figure 70. Increased percentage of mice overexpressing D_2R classified as food addicted animals (Chi-square $^{**}P<0.01$; n= 12 for control mice, and 13 for D_2R; statistical details are included in Supplementary Table 6).

A positive correlation between the number of criteria reached and the values obtained in each criterion was found in all the groups (Figure 71a-f). No differences were found in additional variables such as body weight, food intake and locomotor activity after D_2R overexpression (Figure 71g-i). To conclude, we revealed that overexpression of D_2R allowed that DA via D_2Rs decreased the excitability of PL-NAc core projections, conveying the vulnerability to develop food addiction.

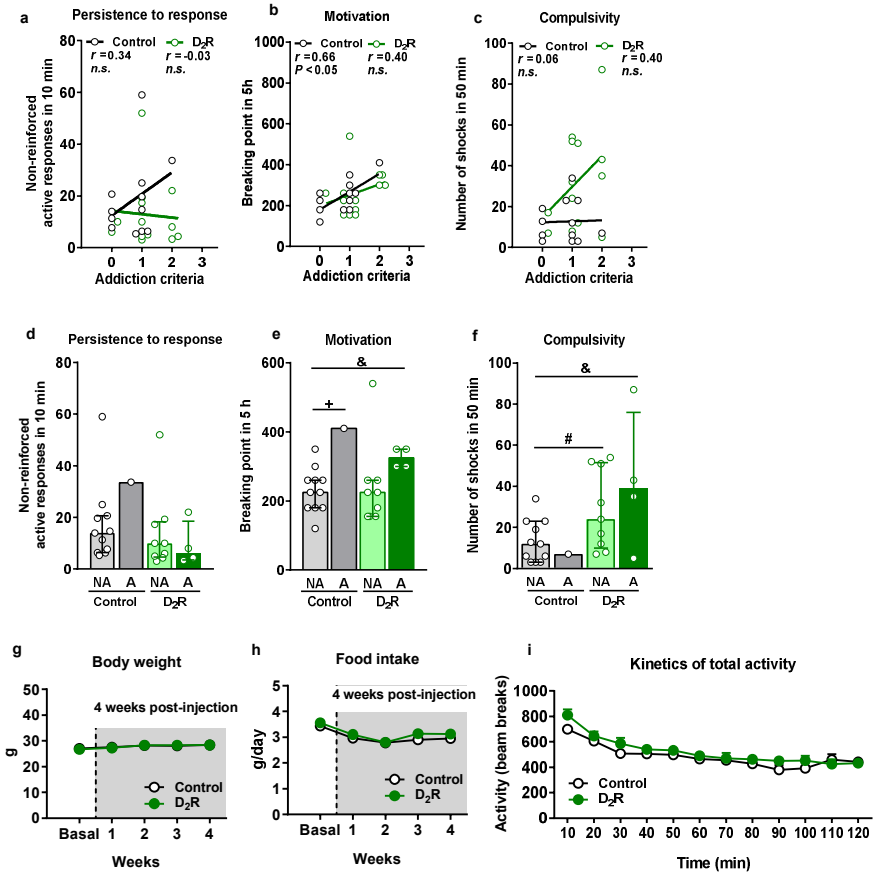

Figure 71. a-c, **Correlations**. Pearson correlations between individual addiction criteria and **a,** non-reinforced active responses in 10 min, **b,** breaking point in 5h, **c,** number of shocks in 50 min. **d-f, Behavioral tests of the three addiction criteria represented by individual values and bars with median and the interquartile range for the four groups classified as addicted (A) and non-addicted (NA) mice in both injected groups**. **d,** Persistence to response. **e,** Motivation. **f,** Compulsivity. **g-i, Control variables to measure the effects of D_2R overexpression in mice overexpressing D_2R in PL-NAc core projection neurons**. **g,** Body weight. Weekly measures of body weight in grams for both injected groups. **h,** Food intake. Weekly measures of regular chow food intake provided to mice in their home cage in grams per day for both groups. **i,** Kinetics of total activity. Locomotor activity measured by beam breaks represented in 10-min blocks during 2 hours in both injected groups. (AAV-control mice, n=12; AAV-D_2R mice, n=13; U Mann-Whitney +P<0.05 control NA vs control A, # P<0.05 control NA vs D_2RNA, & P<0.05 control NA vs D_2RA; statistical details are included in Supplementary Table 6).

Supplementary Table 1

Figure number	Statistical analysis	Factor name	Statistic value	P-value
Figure 34	Repeated measures ANOVA	**FR1 (Sessions 1-6)**		
		Genotype	$F_{(1,112)} = 0.33$	n.s
		Sessions	$F_{(5,560)} = 29.00$	$P < 0.001$
		Genotype x Sessions	$F_{(5,560)} = 0.62$	n.s
		FR5 (Sessions 1-112)		
		Genotype	$F_{(1,112)} = 36.72$	$P < 0.001$
		Sessions	$F_{(111,12432)} = 5.38$	$P < 0.001$
		Genotype x Sessions	$F_{(111,12432)} = 3.53$	$P < 0.001$
Figure 35a-c	Kolmogorov-Smirnov	**Early period**		
		Persistence to response	$K\text{-}S = 0.15$	$P < 0.001$
		Motivation	$K\text{-}S = 0.19$	$P < 0.001$
		Compulsivity	$K\text{-}S = 0.27$	$P < 0.001$
	U Mann-Whitney	**Early period**		
		Persistence to response	$U = 1320.00$	n.s.
		Motivation	$U = 1384.50$	n.s.
		Compulsivity	$U = 1242.50$	$P < 0.05$
Figure 35d-f	Kolmogorov-Smirnov	**Late period**		
		Persistence to response	$K\text{-}S = 0.25$	$P < 0.001$
		Motivation	$K\text{-}S = 0.16$	$P < 0.001$
		Compulsivity	$K\text{-}S = 0.28$	$P < 0.001$
	U Mann-Whitney	**Late period**		
		Persistence to response	$U = 1043.50$	$P < 0.01$
		Motivation	$U = 1035.50$	$P < 0.01$
		Compulsivity	$U = 1071.00$	$P < 0.01$
Figure 36a	Kolmogorov-Smirnov	**Early period**		
		Impulsivity	$K\text{-}S = 0.22$	$P < 0.001$
		Late period		
		Impulsivity	$K\text{-}S = 0.21$	$P < 0.001$
	U Mann-Whitney	**Early period**		
		Impulsivity	$U = 1464.00$	n.s
		Late period		
		Impulsivity	$U = 1159.50$	$P < 0.01$
Figure 36b	Kolmogorov-Smirnov	**Early period**		
		Shock-induced suppression	$K\text{-}S = 0.14$	$P < 0.001$
		Late period		
		Shock-induced suppression	$K\text{-}S = 0.20$	$P < 0.001$
	U Mann-Whitney	**Early period**		
		Shock-induced suppression	$U = 1178.50$	$P < 0.05$
		Late period		
		Shock-induced suppression	$U = 697.00$	$P < 0.001$
Figure 37	Chi-square	Genotype	$C\text{-}S = 7.06$	$P < 0.01$
Figure 38a-c	Pearson correlation	**WT**		
		Non-reinforced active responses in 10 min and addiction criteria	$r = 0.74$	$P < 0.001$
		Breaking point in 5h and addiction criteria	$r = 0.73$	$P < 0.001$
		Compulsivity and addiction criteria	$r = 0.46$	$P < 0.001$
		Glu-CB1-KO		
		Non-reinforced active responses in 10 min and addiction criteria	$r = 0.53$	$P < 0.001$
		Breaking point in 5h and addiction criteria	$r = 0.73$	$P < 0.001$
		Compulsivity and addiction criteria	$r = 0.46$	$P < 0.001$

Figure 38d-h	Kolmogorov-Smirnov	Persistence to response	*K-S* = 0.25	*P* < 0.001
		Motivation	*K-S* = 0.16	*P* < 0.001
		Compulsivity	*K-S* = 0.28	*P* < 0.001
		Impulsivity	*K-S* = 0.21	*P* < 0.001
		Shock-induced suppression	*K-S* = 0.21	*P* < 0.001
	U Mann-Whitney	**Persistence to response**		
		WT NA vs WT A	*U* = 40.50	*P* < 0.001
		WT NA vs Glu-CB1-KO NA	*U* = 866.50	*P* < 0.05
		WT NA vs Glu-CB1-KO A	*U* = 52.00	n.s.
		WT A vs Glu-CB1-KO NA	*U* = 42. 00	*P* < 0.001
		WT A vs Glu-CB1-KO A	*U* = 19.00	n.s.
		Glu-CB1-KO NA vs Glu-CB1-KO A	*U* = 57.50	n.s.
		Motivation		
		WT NA vs WT A	*U* = 52.50	*P* < 0.001
		WT NA vs Glu-CB1-KO NA	*U* = 803.50	*P* < 0.05
		WT NA vs Glu-CB1-KO A	*U* = 10.00	*P* < 0.01
		WT A vs Glu-CB1-KO NA	*U* = 52.50	*P* < 0.001
		WT A vs Glu-CB1-KO A	*U* = 18.50	n.s.
		Glu-CB1-KO NA vs Glu-CB1-KO A	*U* = 14.50	*P* < 0.01
		Compulsivity		
		WT NA vs WT A	*U* = 80.00	*P* < 0.001
		WT NA vs Glu-CB1-KO NA	*U* = 814.50	*P* < 0.05
		WT NA vs Glu-CB1-KO A	*U* = 7.50	*P* < 0.01
		WT A vs Glu-CB1-KO NA	*U* = 61.50	*P* < 0.001
		WT A vs Glu-CB1-KO A	*U* = 21.50	n.s.
		Glu-CB1-KO NA vs Glu-CB1-KO A	U = 4.00	*P* < 0.01
		Impulsivity		
		WT NA vs WT A	*U* = 102.00	*P* < 0.001
		WT NA vs Glu-CB1-KO NA	*U* = 878.50	n.s.
		WT NA vs Glu-CB1-KO A	*U* = 33.00	*P* < 0.05
		WT A vs Glu-CB1-KO NA	*U* = 107.00	*P* < 0.001
		WT A vs Glu-CB1-KO A	*U* = 17.00	n.s.
		Glu-CB1-KO NA vs Glu-CB1-KO A	*U* = 37.00	*P* < 0.05
		Shock-induced suppression		
		WT NA vs WT A	*U* = 185.50	*P* < 0.05
		WT NA vs Glu-CB1-KO NA	U = 439.50	*P* < 0.001
		WT NA vs Glu-CB1-KO A	*U* = 61.50	n.s.
		WT A vs Glu-CB1-KO NA	*U* = 125.00	*P* < 0.001
		WT A vs Glu-CB1-KO A	*U* = 26.00	n.s.
		Glu-CB1-KO NA vs Glu-CB1-KO A	*U* = 36.50	*P* < 0.05
Figure 39a-e	Repeated measures ANOVA	**Body weight**		
		Genotype	$F_{(1,112)}$ = 7.02	*P* < 0.01
		Sessions	$F_{(23,2576)}$ = 231.81	*P* < 0.001
		Genotype x Sessions	$F_{(23,2576)}$ = 4.44	*P* < 0.001
	Kolmogorov-Smirnov	Early period	*K-S* = 0.07	n.s.
		Late period	*K-S* = 0.06	n.s.
	Paired t-test	Early period	*t* = 4.23	n.s
		Late period	*t* = 0.19	*P* < 0.01
	Pearson correlation	**WT**		
		Non-reinforced active responses in 10 min and addiction criteria	*r* = -0.16	n.s
		Breaking point in 5h and addiction criteria	*r* = 0.06	n.s
		Compulsivity and addiction criteria	*r* = -0.04	n.s
		Glu-CB1-KO		
		Non-reinforced active responses in 10 min and addiction criteria	*r* = -0.11	n.s
		Breaking point in 5h and addiction criteria	*r* = -0.14	n.s
		Compulsivity and addiction criteria	*r* = -0.14	n.s

Supplementary Table 2

Figure number	Statistical analysis	Factor name	Statistic value	P-value
Figure 40a	Kolmogorov-Smirnov	mEPSC	$K\text{-}S$ = 0.13	n.s.
	T-test (Equal variances assumed)	mEPSC	T = -2.57	$P < 0.05$
Figure 40b	Kolmogorov-Smirnov	PPF	$K\text{-}S$ = 0.28	P < 0.001
	U Mann-Whitney	PPF	U = 19.00	$P < 0.05$
Figure 41	Two-way ANOVA	**fEPSP**		
		Genotype	$F_{(1,20)} = 3.45$	n.s
		Treatment	$F_{(1,20)} = 1.89$	n.s
		Genotype x Treatment	$F_{(1,20)} = 4.69$	$P < 0.05$
	Fisher PLSD posthoc	WT basal x WT WIN		$P < 0.05$
		WT basal x Glu-CB1-KO basal		n.s.
		WT basal x Glu-CB1-KO WIN		n.s
		WT WIN x Glu-CB1-KO basal		$P < 0.05$
		WT WIN x Glu-CB1-KO WIN		$P < 0.05$
		Glu-CB1-KO basal x Glu-CB1-KO WIN		n.s.
Figure 42	Kolmogorov-Smirnov	Baseline	$K\text{-}S$ = 0.33	$P < 0.05$
		Rimonabant	$K\text{-}S$ = 0.28	$P < 0.05$
		Rimonabant + WIN	$K\text{-}S$ = 0.30	n.s
	Friedman test	Chi-square	$C\text{-}S$ = 0.4	n.s

Supplementary Table 3

Figure number	Statistical analysis	Factor name	Statistic value	*P*- value
Figure 44a-b	Kolmogorov-Smirnov	Firing rate Baseline	$K\text{-}S$ = 0.15	n.s.
		Firing rate CNO	$K\text{-}S$ = 0.21	n.s.
	Paired t-test	Firing rate	t = 2.66	$P < 0.05$
	Kolmogorov-Smirnov	Resistance baseline	$K\text{-}S$ = 0.21	n.s.
		Resistance CNO	$K\text{-}S$ = 0.25	$P < 0.05$
	Wilcoxon test	Resistance	Z = -2.12	$P < 0.05$
Figure 45a-c	Kolmogorov-Smirnov	Firing rate baseline	$K\text{-}S$ = 0.19	n.s.
		Firing rate CNO	$K\text{-}S$ = 0.18	n.s.
		Resistance baseline	$K\text{-}S$ = 0.19	n.s.
		Resistance CNO	$K\text{-}S$ = 0.17	n.s.
		Rheobase baseline	$K\text{-}S$ = 0.17	n.s.
		Rheobase CNO	$K\text{-}S$ = 0.20	n.s.
	Paired t-test	Firing rate	t = 1.50	n.s.
		Resistance	t = -1.50	n.s.
		Rheobase	t = -0.37	n.s.

Figure 47a-d	Repeated measures ANOVA	**FR1 (Sessions 1-2)**		
		Treatment	$F_{(1,8)} = 0.14$	n.s
		Sessions	$F_{(8,64)} = 0.87$	n.s
		Treatment x Sessions	$F_{(8,64)} = 0.16$	n.s
		FR5 (Sessions 6-9)		
		Treatment	$F_{(1,8)} = 0.03$	n.s
		Sessions	$F_{(8,64)} = 2.45$	$P < 0.05$
		Treatment x Sessions	$F_{(8,64)} = 0.23$	n.s
		FR5 (Sessions 10-23)		
		Treatment	$F_{(1,8)} = 0.01$	n.s
		Sessions	$F_{(13,104)} = 2.15$	$P < 0.05$
		Treatment x Sessions	$F_{(13,104)} = 0.45$	n.s
	Kolmogorov-Smirnov	**Addiction criteria**		
		Persistence to response	$K\text{-}S = 0.33$	$P < 0.01$
		Motivation	$K\text{-}S = 0.16$	n.s.
		Compulsivity	$K\text{-}S = 0.28$	$P < 0.05$
	U Mann-Whitney	**Addiction criteria**		
		Persistence to response	$U = 12.50$	n.s.
	t-test (Equal variances assumed)	Motivation	$t = 0.89$	n.s.
	U Mann-Whitney	Compulsivity	$U = 9.50$	n.s.
Figure 47e-g	Repeated measures ANOVA	**Body Weight**		
		Treatment	$F_{(1,27)} = 0.61$	n.s
		Weeks	$F_{(4,108)} = 7.46$	$P < 0.001$
		Treatment x Weeks	$F_{(4,108)} = 0.44$	n.s
		Food Intake		
		Treatment	$F_{(1,27)} = 0.16$	n.s
		Weeks	$F_{(3,81)} = 1.08$	n.s
		Treatment x Weeks	$F_{(3,81)} = 0.45$	n.s
		Kinetics of total activity		
		Treatment	$F_{(1,16)} = 0.21$	n.s
		Time	$F_{(11,176)} = 11.20$	$P < 0.001$
		Treatment x Time	$F_{(11,176)} = 0.84$	n.s
Figure 48	Repeated measures ANOVA	**FR1 (Sessions 1-2)**		
		Treatment	$F_{(1,25)} = 0.70$	n.s
		Sessions	$F_{(1,25)} = 4.01$	n.s
		Treatment x Sessions	$F_{(1,25)} = 4.16$	n.s
		FR5 (Sessions 3-8)		
		Treatment	$F_{(1,25)} = 1.34$	n.s
		Sessions	$F_{(5,125)} = 29.85$	$P < 0.001$
		Treatment x Sessions	$F_{(5,125)} = 1.69$	n.s
		FR5 (Sessions 9-23)		
		Treatment	$F_{(1,24)} = 2.16$	n.s
		Sessions	$F_{(14,350)} = 12.82$	$P < 0.001$
		Treatment x Sessions	$F_{(14,350)} = 0.75$	n.s
Figure 49a-c	Kolmogorov-Smirnov	Persistence to response	$K\text{-}S = 0.71$	$P < 0.001$
		Motivation	$K\text{-}S = 0.88$	$P < 0.01$
		Compulsivity	$K\text{-}S = 0.68$	$P < 0.001$
	U Mann-Whitney	Persistence to response	$U = 57.00$	*n.s*
		Motivation	$U = 64.50$	*n.s.*
		Compulsivity	$U = 61.50$	*n.s.*
Figure 49d	Chi square	Treatment	$C\text{-}S = 8.12$	$P < 0.01$

Figure 50a-c	Pearson correlation	**Saline**		
		Non-reinforced active responses in 10 min and addiction c	r = 0.64	P < 0.05
		Breaking point in 5h and addiction criteria	r = 0.32	n.s.
		Compulsivity and addiction criteria	r = 0.01	n.s.
		CNO		
		Non-reinforced active responses in 10 min and addiction c	r = 0.61	P < 0.05
		Breaking point in 5h and addiction criteria	r = 0.56	P < 0.05
		Compulsivity and addiction criteria	r = 0.74	P < 0.01
Figure 50d-f	Kolmogorov-Smirnov	Persistence to response	*K-S* = 0.71	P < 0.001
		Motivation	*K-S* = 0.88	P < 0.01
		Compulsivity	*K-S* = 0.68	P < 0.001
	U Mann-Whitney	**Persistence to response**		
		Saline NA vs Saline A	U = 00.00	P < 0.05
		Saline NA vs CNO NA	U = 16.00	P < 0.05
		Saline NA vs CNO A	U = 26.00	n.s.
		Saline A vs CNO NA	U = 0.00	P < 0.05
		Saline A vs CNO A	U = 1.00	n.s.
		CNO NA vs CNO A	U = 5.00	P < 0.05
		Motivation		
		Saline NA vs Saline A	U = 2.50	n.s.
		Saline NA vs CNO NA	U = 40.50	n.s.
		Saline NA vs CNO A	U = 7.50	P < 0.01
		Saline A vs CNO NA	U = 4.00	n.s.
		Saline A vs CNO A	U = 4.50	n.s.
		CNO NA vs CNO A	U = 10.50	n.s.
		Compulsivity		
		Saline NA vs Saline A	U = 1.50	n.s.
		Saline NA vs CNO NA	U = 36.50	n.s.
		Saline NA vs CNO A	U = 8.50	P < 0.05
		Saline A vs CNO NA	U = 1.50	n.s.
		Saline A vs CNO A	U = 0.00	P < 0.05
		CNO NA vs CNO A	U = 3.00	P < 0.01

Supplementary Table 4

Figure number	Statistical analysis	Factor name	Statistic value	P-value
Figure 52a	Kolmogorov-Smirnov	Firing rate baseline	*K-S* = 0.19	*n.s.*
		Firing rate CNO	*K-S* = 0.22	n.s.
	Paired t-test	Firing rate	t = 2.94	P < 0.05
Figure 52bc	Kolmogorov-Smirnov	Resistance baseline	*K-S* = 0.19	n.s.
		Resistance CNO	*K-S* = 0.19	n.s.
		Rheobase baseline	*K-S* = 0.17	n.s.
		Rehobase CNO	*K-S* = 0.15	n.s.
	Paired t-test	Resistance	t = 3.58	P < 0.01
		Rehobase	t = -4.05	P < 0.01

Figure 54	Repeated measures ANOVA	**FR1 (Sessions 1-2)**		
		Treatment	$F_{(1,32)} = 0.15$	n.s
		Sessions	$F_{(8, 256)} =$	$P < 0.001$
		Treatment x Sessions	$F_{(8, 256)} = 0.01$	n.s
		FR5 (Sessions 3-9)		
		Treatment	$F_{(1,32)} = 0.22$	n.s
		Sessions	$F_{(8, 256)} =$	$P < 0.001$
		Treatment x Sessions	$F_{(8, 256)} = 1.64$	n.s
		FR5 (Sessions 10-20)		
		Treatment	$F_{(1,15)} = 0.55$	n.s
		Sessions	$F_{(10,150)} = 6.37$	$P < 0.001$
		Treatment x Sessions	$F_{(10,150)} = 0.91$	n.s
Figure 55a-c	Kolmogorov-Smirnov	Persistence to response	$K\text{-}S = 0.09$	n.s
		Motivation	$K\text{-}S = 0.11$	n.s
		Compulsivity	$K\text{-}S = 0.17$	$P < 0.05$
	t-test (Equal variances assumed)	Persistence to response	$t = 1.16$	n.s.
		Motivation	$t = -0.56$	n.s.
	U Mann-Whitney	Compulsivity	$U = 48.50$	$P < 0.01$
Figure 56 a-c	Repeated measures ANOVA	**Body Weight**		
		Treatment	$F_{(1,32)} = 0.65$	n.s
		Weeks	$F_{(3,96)} = 43.38$	$P < 0.001$
		Treatment x Weeks	$F_{(3,96)} = 0.41$	n.s
		Food Intake		
		Treatment	$F_{(1,16)} = 0.44$	n.s
		Weeks	$F_{(3,48)} = 4.68$	$P < 0.001$
		Treatment x Weeks	$F_{(3,48)} = 0.71$	n.s
		Kinetics of total activity		
		Treatment	$F_{(1,17)} = 0.07$	n.s
		Time	$F_{(11,187)} = 9.04$	$P < 0.001$
		Treatment x Time	$F_{(11,187)} = 1.14$	n.s
Figure 57	Chi square	Treatment	$C\text{-}S = 17.60$	$P < 0.001$
Figure 58ac	Pearson correlation	**Saline**		
		Non-reinforced active responses in 10 min and addiction criteria	$r = 0.50$	n.s.
		Breaking point in 5h and addiction criteria	$r = 0.46$	n.s.
		Compulsivity and addiction criteria	$r = 0.60$	$P < 0.05$
		CNO		
		Non-reinforced active responses in 10 min and addiction criteria	$r = 0.57$	$P < 0.01$
		Breaking point in 5h and addiction criteria	$r = 0.51$	$P < 0.05$
		Compulsivity and addiction criteria	$r = 0.45$	$P < 0.05$

Figure 58d-h	Kolmogorov-Smirnov	Persistence to response	*K-S* = 0.10	n.s
		Motivation	*K-S* = 0.13	n.s
		Compulsivity	*K-S* = 0.20	*P* < 0.001
	t-test (Equal variances assumed)	**Persistence to response**		
		Saline NA vs Saline A	*t* = -1.69	n.s.
		Saline NA vs CNO NA	*t* = 0.05	n.s.
		Saline NA vs CNO A	*t* = -2.97	*P* < 0.01
		Saline A vs CNO NA	*t* = 1.91	n.s.
		Saline A vs CNO A	*t* = -0.19	n.s.
		CNO NA vs CNO A	*t* = -3.23	*P* < 0.01
		Motivation		
		Saline NA vs Saline A	*t* = -3.50	*P* < 0.01
		Saline NA vs CNO NA	*t* = 0.92	n.s.
		Saline NA vs CNO A	*t* = -1.49	n.s.
		Saline A vs CNO NA	*t* = 4.32	*P* < 0.01
		Saline A vs CNO A	*t* = 2.30	*P* < 0.05
		CNO NA vs CNO A	*t* = -2.46	*P* < 0.05
	U Mann-Whitney	**Compulsivity**		
		Saline NA vs Saline A	*U* = 5.50	n.s.
		Saline NA vs CNO NA	*U* = 27.00	n.s.
		Saline NA vs CNO A	*U* = 8.00	n.s.
		Saline A vs CNO NA	*U* = 10.0	*P* < 0.01
		Saline A vs CNO A	*U* = 3.50	n.s.
		CNO NA vs CNO A	*U* = 34.00	n.s.

Supplementary Table 5

Figure number	Statistical analysis	Factor name	Statistic value	P-value
Figure 59a-d	Kolmogorov-Smirnov	Persistence to response	*K-S* = 0.26	*P* < 0.01
		Motivation	*K-S* = 0.17	n.s.
		Compulsivity	*K-S* = 0.29	*P* < 0.001
		Pellets intake in the last FR5 session	*K-S* = 0.14	n.s .
	U Mann-Whitney	**Persistence to response**		
		WT NA vs WT A	*U* = 0.00	*P* < 0.01
		WT NA vs Glu-CB1-KO NA	*U* = 7.50	n.s.
		WT NA vs Glu-CB1-KO A	*U* = 3.50	n.s.
		WT A vs Glu-CB1-KO NA	*U* = 0.00	*P* < 0.01
		WT A vs Glu-CB1-KO A	*U* = 9.00	n.s.
		Glu-CB1-KO NA vs Glu-CB1-KO A	*U* = 2.50	*P* < 0.05
	t-test (Equal variances assumed)	**Motivation**		
		WT NA vs WT A	*t* = -3.52	*P* < 0.01
		WT NA vs Glu-CB1-KO NA	*t* = 1.06	n.s.
		WT NA vs Glu-CB1-KO A	*t* = - 3.70	*P* < 0.01
		WT A vs Glu-CB1-KO NA	*t* = 4.20	*P* < 0.01
		WT A vs Glu-CB1-KO A	*t* = -0.52	n.s.
		Glu-CB1-KO NA vs Glu-CB1-KO A	*t* = 4.33	*P* < 0.01
	U Mann-Whitney	**Compulsivity**		
		WT NA vs WT A	*U* = 2.50	*P* < 0.05
		WT NA vs Glu-CB1-KO NA	*U* = 12.50	n.s.
		WT NA vs Glu-CB1-KO A	*U* = 0.00	*P* < 0.01
		WT A vs Glu-CB1-KO NA	*U* = 2.50	*P* < 0.05
		WT A vs Glu-CB1-KO A	*U* = 10.50	n.s.
		Glu-CB1-KO NA vs Glu-CB1-KO A	*U* = 0.00	*P* < 0.01
	t-test (Equal variances assumed)	**Pellets intake in the last FR5 session**		
		WT NA vs WT A	*t* = -1.20	n.s.
		WT NA vs Glu-CB1-KO NA	*t* = 2.81	*P* < 0.05
		WT NA vs Glu-CB1-KO A	*t* = 1.10	n.s.
		WT A vs Glu-CB1-KO NA	*t* = 4.47	*P* < 0.01
		WT A vs Glu-CB1-KO A	*t* = 2.51	*P* < 0.05
		Glu-CB1-KO NA vs Glu-CB1-KO A	*t* = 2.20	n.s.
Figure 61b	Kolmogorov-Smirnov	*Drd2*	*K-S* = 0.27	*P* < 0.01
		Adora2a	*K-S* = 0.27	*P* < 0.001
		Gpr88	*K-S* = 0.22	*P* < 0.05
		Drd1	*K-S* = 0.25	*P* < 0.01
	t-test (Equal variances assumed)	*Drd2*	*t* = -2.56	*P* < 0.05
		Adora2a	*t* = -2.30	*P* < 0.05
	t-test (Equal variances not assumed)	*Gpr88*	*t* = -2.11	*P* < 0.05
		Drd1	*t* = -2.51	*P* < 0.05
Figure 62a-c	Kolmogorov-Smirnov	*Tbp*	*K-S* = 0.10	n.s.
		Usp11	*K-S* = 0.17	n.s.
		Actb	*K-S* = 0.17	n.s.
	t-test (Equal variances assumed)	*Tbp*	*t* = -0.27	n.s.
		Usp11	*t* = 0.94	n.s.
		Actb	*t* = 0.38	n.s.
Figure 63b	Kolmogorov-Smirnov	*Cnr1*	*K-S* = 0.18	n.s.
		Fos	*K-S* = 0.33	*P* < 0.001
		Npas4	*K-S* = 0.18	n.s.
	assumed)	*Cnr1*	*t* = 11.20	*P* < 0.001
	U Mann-Whitney	*Fos*	*U* = 22	*P* < 0.05
	assumed)	*Npas4*	*t* = 1.49	n.s.

Supplementary Table 6

Figure number	Statistical analysis	Factor name	Statistic value	*P*- value
Figure 66a	Kolmogorov-Smirnov	Firing rate baseline	$K\text{-}S$ = 0.30	$P < 0.05$
		Firing rate Quinpirole	$K\text{-}S$ = 0.30	$P < 0.05$
	Paired t-test	Firing rate	Z = -2.41	$P < 0.05$
Figure 66b-c	Kolmogorov-Smirnov	**Quinpirole - D2R**		
		Resistance baseline	$K\text{-}S$ = 0.18	n.s.
		Resistance Quinpirole	$K\text{-}S$ = 0.24	n.s.
		Rheobase baseline	$K\text{-}S$ = 0.35	$P < 0.01$
		Rheobase Quinpirole	$K\text{-}S$ = 0.34	$P < 0.01$
	Paired t-test	Resistance	t = 2.79	$P < 0.05$
	Wilcoxon test	Rheobase	Z = -2.67	$P < 0.01$
Figure 67a-c	Kolmogorov-Smirnov	**Quinpirole - Control**		
		Firing rate baseline	$K\text{-}S$ = 0.14	n.s.
		Firing rate Quinpirole	$K\text{-}S$ = 0.24	n.s.
		Resistance baseline	$K\text{-}S$ = 0.27	n.s.
		Resistance Quinpirole	$K\text{-}S$ = 0.16	n.s.
		Rheobase baseline	$K\text{-}S$ = 0.25	n.s.
		Rheobase Quinpirole	$K\text{-}S$ = 0.38	$P < 0.01$
	Paired t-test	Firing rate	t = -0.37	n.s.
		Resistance	t = 0.23	n.s.
	Wilcoxon test	Rheobase	Z = -0.70	n.s.
Figure 67d-i	Kolmogorov-Smirnov	**Dopamine - Control**		
		Firing rate baseline	$K\text{-}S$ = 0.17	n.s.
		Firing rate Dopamine	$K\text{-}S$ = 0.12	n.s.
		Resistance baseline	$K\text{-}S$ = 0.19	n.s.
		Resistance Dopamine	$K\text{-}S$ = 0.20	n.s.
		Rheobase baseline	$K\text{-}S$ = 0.18	n.s.
		Rheobase Dopamine	$K\text{-}S$ = 0.16	n.s.
	Paired t-test	Firing rate	t = 1.13	n.s.
		Resistance	t = -1.47	n.s.
		Rheobase	t = -0.70	n.s.
	Kolmogorov-Smirnov	**Dopamine - D2R**		
		Firing rate baseline	$K\text{-}S$ = 0.35	$P < 0.01$
		Firing rate Dopamine	$K\text{-}S$ = 0.35	$P < 0.01$
		Resistance baseline	$K\text{-}S$ = 0.16	n.s.
		Resistance Dopamine	$K\text{-}S$ = 0.21	n.s.
		Rheobase baseline	$K\text{-}S$ = 0.33	$P < 0.01$
		Rheobase Dopamine	$K\text{-}S$ = 0.15	n.s.
	Wilcoxon test	Firing rate	Z = -2.01	$P < 0.05$
	Paired t-test	Resistance	t = 6.00	$P < 0.001$
	Wilcoxon test	Rheobase	Z = -2.80	$P < 0.01$
Figure 69a	Repeated measures ANOVA	**FR1 (Sessions 1-2)**		
		AAV PL	$F_{(1,23)}$ = 0.01	n.s
		Sessions	$F_{(1,23)}$ = 12.19	$P < 0.001$
		AAV PL x Sessions	$F_{(1,23)}$ = 0.72	n.s
		FR5 (Sessions 3-9)		
		AAV PL	$F_{(1,23)}$ = 0.07	n.s
		Sessions	$F_{(6,184)}$ = 25.58	$P < 0.001$
		AAV PL x Sessions	$F_{(6,184)}$ = 0.43	n.s
		FR5 (Sessions 10-24)		
		AAV PL	$F_{(1,23)}$ = 0.25	n.s
		Sessions	$F_{(14,322)}$ = 20.23	$P < 0.001$
		AAV PL x Sessions	$F_{(14,322)}$ = 0.45	n.s

Figure 69b-d	Kolmogorov-Smirnov	Persistence to response	*K-S* = 0.19	*P* < 0.05
		Motivation	*K-S* = 0.16	n.s
		Compulsivity	*K-S* = 0.17	n.s
	U Mann-Whitney	Persistence to response	*U* = 47.00	n.s.
	t-test (Equal variances assumed)	Motivation	*t* = -0.52	n.s.
		Compulsivity	*t* = -2.77	*P* < 0.05
Figure 70	Chi square	AAV PL	*C-S* = 8.57	*P* < 0.001
Figure 71a-c	Pearson correlation	**Control**		
		Non-reinforced active responses in 10 min and addiction criteria	*r* = 0.34	*P* < 0.05
		Breaking point in 5h and addiction criteria	*r* = 0.66	*P* < 0.05
		Compulsivity and addiction criteria	*r* = 0.06	n.s.
		D2R		
		Non-reinforced active responses in 10 min and addiction criteria	*r* = -0.03	*P* < 0.05
		Breaking point in 5h and addiction criteria	*r* = 0.40	n.s.
		Compulsivity and addiction criteria	*r* = 0.40	n.s.
Figure 71d-f	Kolmogorov-Smirnov	Persistence to response	*K-S* = 0.19	P < 0.05
		Motivation	*K-S* = 0.16	n.s
		Compulsivity	*K-S* = 0.17	n.s
	U Mann-Whitney	**Persistence to response**		
		Control NA vs Control A	*U* = 1.00	n.s.
		Control NA vs D2R NA	*U* = 33.00	n.s.
		Control NA vs D2R A	*U* = 13.00	n.s.
		Control A vs D2R NA	*U* = 1.00	n.s.
		Control A vs D2R A	*U* = 0.00	n.s.
		D2R NA vs D2R A	*U* = 14.50	n.s.
	T-test (Equal variances assumed)	**Motivation**		
		Control NA vs Control A	*t* = -2.66	*P* < 0.05
		Control NA vs D2R NA	*t* = -0.20	n.s.
		Control NA vs D2R A	*t* = -2.80	*P* < 0.05
		Control A vs D2R NA	*t* = 1.34	n.s.
		Control A vs D2R A	*t* = 2.63	n.s.
		D2R NA vs D2R A	*t* = -1.37	n.s.
		Compulsivity		
		Control NA vs Control A	*t* = 0.57	n.s.
	t-test (Equal variances not assumed)	Control NA vs D2R NA	*t* = -2.27	*P* < 0.05
		Control NA vs D2R A	*t* = -2.70	*P* < 0.05
	t-test (Equal variances assumed)	Control A vs D2R NA	*t* = -1.05	n.s.
		Control A vs D2R A	*t* = -0.94	n.s.
		D2R NA vs D2R A	*t* = -0.96	n.s.
Figure 71g-i	Repeated measures ANOVA	**Body Weight**		
		AAV PL	$F_{(1,23)}$ = 0.00	n.s
		Weeks	$F_{(3,69)}$ = 11.29	*P* < 0.001
		AAV PL x Weeks	$F_{(3,69)}$ = 0.53	n.s
		Food Intake		
		AAV PL	$F_{(1,23)}$ = 1.24	n.s
		Weeks	$F_{(3,69)}$ = 4.23	*P* < 0.05
		AAV PL x Weeks	$F_{(3,69)}$ = 0.65	n.s
		Kinetics of total activity		
		AAV PL	$F_{(1,22)}$ = 1.33	n.s
		Time	$F_{(11,242)}$ = 28.15	*P* < 0.001
		AAV PL x Time	$F_{(11,242)}$ = 1.09	n.s

Laura Domingo-Rodriguez*, Judith Cabana-Domínguez*, Laura Pineda-Cirera, Aurelijus Burokas, Noèlia Fernàndez-Castillo, Bru Cormand#, Elena Martín-García#, Rafael Maldonado#.

Characterizing the differential epigenetic profile in vulnerable and resilient phenotypes to develop food addiction.

Under preparation.

* Equal contribution

Equal seniority

Chapter 2

Characterizing the differential epigenetic profile of vulnerable and resilient phenotypes to develop food addiction.

2.1.Abstract

Food addiction is a multifactorial disorder produced by the interactions between gene networks and multiple environmental factors. Thus, epigenetic mechanisms are excellent candidates for understanding the neurobiological mechanisms underlying the vulnerable and the resilient phenotype to develop food addiction. In this study, genetically similar inbred mice underwent a food addiction mouse model and two extreme subpopulations of food addicted and non-addicted mice were identified. Four phenotypic traits as factors of vulnerability to addiction were assessed to classify mice in a quantitative addiction scale. In the extreme subpopulations of addicted and non-addicted mice, we evaluated the microRNAs and DNA methylation profiling at genome-wide level of the mPFC, a key area involved in the inhibitory control. We found 11 differentially expressed microRNAs and genomic hypomethylated regions in *Drd2, Adora2a, Gpr88* and *Drd1* genes. Thus, these epigenetic signatures are contributing to the development of the loss of behavioral control pointing out miRNAs and methylation modulators as a novel therapeutic target.

2.2.Materials and methods

Animals

Experiments were performed in male C57BL/6J inbred mice (Charles River Laboratories, Lyon, France), aged 2 months. Mice were housed and maintained in the same conditions described in the previous chapter. All experimental protocols were performed in accordance with the guidelines of the European Communities Council Directive 2010/63/EU and approved by the local ethical committee (Comitè Ètic d'Experimentació Animal-Parc de Recerca Biomèdica de Barcelona, CEEAPRBB).

Behavioral experiments

Food pellets

During the operant conditioning sessions, after active responding by lever pressing, animals received a 20 mg **standard pellet** (TestDiet, Richmond, IN, USA) or a 20 mg **chocolate-flavored pellet** (highly isocaloric pellet, TestDiet, Richmond, IN, USA). The standard pellet formula was similar to the standard maintenance diet provided to mice in their home cage (24.1% protein, 10.4% fat, 65.5% carbohydrate, with a caloric value of 3.30 kcal/g). Highly palatable isocaloric pellets presented a similar caloric value of standard pellets with modifications in the sucrose and sugars content as was described in the previous chapter.

Behavioral tests to evaluate 4 phenotypic traits considered as factors of vulnerability to addiction

Impulsivity: Non-reinforced active responses during the time-out periods (10 s) after each pellet delivery were measured as impulsivity-like behavior indicating the inability to stop a response once it is initiated. The three consecutive days before the PR test were considered.

Cognitive flexibility: Measured in a reversal test. The reversal test was a normal training self-administration session, but the active and the inactive levers were reversed. A mouse is considered to discriminate when at least 75% of the responses are on the same lever.

Appetitive associative learning: We used the cue-induced food seeking test, in which a 90 min session was divided in two periods: 60 min + 30 min. In the first 60 min period, all lever-presses were not reinforced (active and inactive lever-presses producing no scheduled consequences). In the subsequent 30 min, the white cue light, associated with pellet delivery during a normal self-administration session, was illuminated contingently for 30 min according to an FR5. To signal the change in the schedule, the cue light was presented twice non-contingently and for 4 s.

Aversive associative learning: Non-reinforced active responses during the following session after the shock-session were measured for the aversive associative learning. Mice were placed in the self-administration chamber for 50 min with the same grid floor used during the shock-session. However, during this session, pressing the active

lever had no consequences, no shock, no chocolate-flavored pellets and no cue-light.

Experimental design

Mice were trained to obtained chocolate-flavored pellets (n=51) or standard pellets (n=7) in operant boxes during 98 sessions in 1 h-daily sessions (Figure 72). The operant boxes and the self-administration sessions were accurately described in the chapter before. Mice were under FR1 during 6 sessions followed by 92 sessions under FR5. The food addiction-like behavior was evaluated in an early period (1-14 sessions) and a late period (82-92 sessions), by the three food addiction criteria: (1) persistence to response, (2) motivation and (3) compulsivity. Importantly, 4 additional phenotypic traits as factors of vulnerability to addiction, impulsivity, cognitive flexibility, appetitive associative learning and sensitivity to aversive associative learning, were also evaluated. At the end of the late period, animals were classified as food-addicted or non-addicted depending on the number of the three initially evaluated addiction criterion achieved. After the categorization, we classified mice in a quantitative addiction scale using the score values obtained in the three addiction criteria and in the 4 phenotypic traits considered as factors of vulnerability to addiction. It is explained in detail in the results section.

Finally, the most severe 6 addicted mice and 6 non-addicted mice exposed to chocolate-flavored pellets were used to evaluate the differential changes in microRNAs and DNA methylation underlying the loss of control toward palatable food. The behavioral test to evaluate

food addiction criteria and the attribution of the criteria are explained in the previous chapter. Blood samples were extracted before and after the experimental sequence.

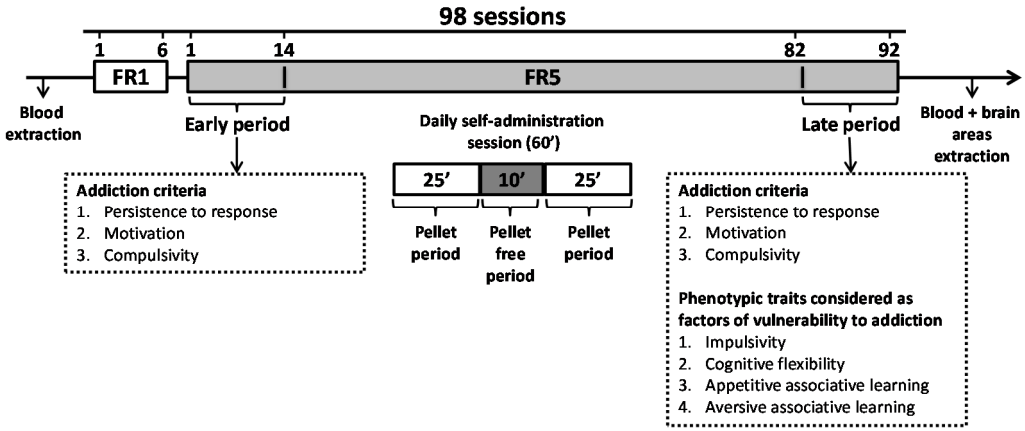

Figure 72. Timeline of the experimental sequence of the food addiction mouse model. Mice were trained for chocolate-flavored pellets or standard pellets under a fixed ratio (FR) 1 schedule of reinforcement on 1 h daily sessions for 6 days followed by 92 days on a FR5. Each session was composed by 2 pellets session (25 min) of normal delivered pellets separated by a pellet free period (10 min) in which pressing the active lever has no pellet delivery. In the FR5, 2 time points were considered, early and late period to measure the addictive-like behavior: (1) persistence to response, (2) motivation and (3) compulsivity. At the late period 4 additional phenotypic traits as factors of vulnerability to addiction were evaluated: (1) impulsivity, (2) cognitive flexibility, (3) appetitive associative learning and (4) aversive associative learning.

Epigenetic studies

At the end of the behavioral experiment, mice were sacrificed by decapitation, the brains were removed and mPFC and NAc were isolated to the following coordinates from Paxinos and Franklin (Paxinos, G. and Franklin, 2001): mPFC, AP+1.98 mm and NAc, AP+1.54. The samples were placed in individual tubes, frozen on dry ice and

stored at -80ºC until genomic DNA and RNA isolation for the methylomic and miRNA studies.

The study of miRNAs and DNA methylation was carried out with the collaboration of Bru Cormand laboratory (Departament de Genètica, Microbiologia i Estadística, Facultat de Biologia, Universitat de Barcelona, Spain).

MiRNAs

Total RNA from mPFC was extracted using a miRNeasy Mini kit (Qiagen, 217004) and the quality of the samples was confirmed by Bioanalyzer system. The RNA samples were sent to the Center for Genomic Regulation (CRG, Barcelona, Spain) for the sequencing analysis of small RNAs. The small RNA library was generated by kit NEBNext® Ultra™ DNA Library Prep Kit. Sequencing was performed by Illumina HiSeq 2500 System. Finally, the bioinformatic analysis was done by the OASIS2 pipeline.

DNA methylation profiling by Methyl-CpG-Binding Domain Sequencing (MBD-seq)

Genomic DNA was isolated using the AllPrep DNA/RNA/miRNA Universal Kit (Qiagen, Melbourne, VIC, Australia) from mPFC and NAc. DNA quality, MBD enrichment, library generation (TruSeq Nano DNA Kit) and sequencing has been done by Macrogen Inc. (Korea). DNA integrity was confirmed by agarose gel electrophoresis and quantified by Picogreen (Invitrogen, Carlsbad, CA, USA) using Victor 3 fluorometry. MBD enrichment was performed using the MethylMiner Methylated

DNA Enrichment Kit. Library preparation was carried out with Truseq DNA nano (350pb) kit (Illumina) and finally sequenced on an Illumina HiSeq4000 (2x100pb).

Differentially methylated regions analysis

Raw data read quality was analyzed with FastQC and cleaned of adapters or low quality reads using Trimmomatic 0.36 accordingly to the following parameters: LEADING:3 TRAILING:3 SLIDINGWINDOW:4:20 MINLEN:36. Subsequently, reads were mapped against the *mus musculus* genome of reference (GRCm38/mm10) with Bowtie2. MEDIPS R package have been used to identify differential methylated regions according to the following parameters: uniq=1e-3, extend=100, shift=0, ws=100 min, RowSum = 6. Multiple quality controls through MEDIPS software have been done to ensure reliable and reproducible results: saturation analysis, correlation between samples, sequence pattern coverage and CpG enrichment. Finally, we have analyzed the DNA methylation patterns considering 5 Kb up/downstream from all the protein coding genes. Methylation patterns of food addicted mice have been compared to the ones from non-addicted mice and differentially methylated regions have been classified depending on their location.

Statistical analysis

All statistical comparisons were performed with SPSS (IBM, version 25). Comparisons between two groups were analyzed by Student t-test or U Mann-Whitney depending on the distribution defined by the Kolmogorov-Smirnov normality test. ANOVA with repeated measures

was used when required to test the evolution over time. The Pearson correlation coefficient was used to analyze the relationship between values in the additional test of vulnerability to addiction and the final criteria achieved. A *P* value <0.05 was used to determine statistical significance. The sample sizes were similar to those reported in previous publications (Mancino *et al.*, 2015).

2.3.Results

Mice underwent a food addiction protocol as previously described (Mancino *et al.*, 2015). Mice were trained 6 sessions under FR1 followed by 92 sessions of FR5 to obtain chocolate-flavored pellets (n=51) or standard pellets (n=7) as a control (Figure 72). During the acquisition of operant responding under FR1, both groups of mice obtained the same number of pellets. In FR5, the chocolate group showed a higher number of reinforcers compared to standard group (repeated measures ANOVA; pellets effect *P*<0.001, pellets x sessions *P*<0.001; Figure 73a-b). This significant difference is maintained among all FR5 sessions indicating that chocolate-flavored pellets have strength reinforcing effects than standard pellets.

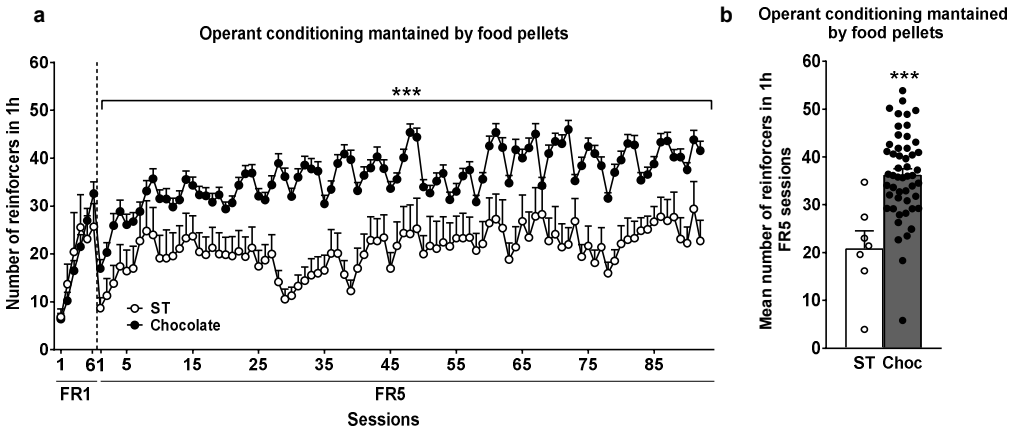

Figure 73. Operant conditioning maintained by chocolate-flavored pellets or standard pellets. a, Mice trained with chocolate pellets increased the number of reinforcers in 1 h FR5 daily sessions compared to mice trained with standard pellets (mean ± S.E.M; repeated measures ANOVA; pellets effect *** $P<0.001$, pellets x sessions $P<0.001$). **b,** Mean number of reinforcers in 1h of the total FR5 sessions (mean ± S.E.M; t-test *** $P<0.001$; n=51 mice trained with chocolate pellets, n=7 mice trained with standard pellets; ST, standard).

We tested both groups for the three behaviors used to evaluate the addiction criteria during an early and a late FR5 period. In the early period, only significant differences were showed in the persistence to response criterion between mice trained with chocolate and standard pellets (t-test $P<0.05$, Figure 74a-c). In turn, in the late period, chocolate trained mice presented higher persistence to response (U Mann-Whitney $P<0.05$, Figure 74d), augmented motivation (U Mann-Whitney $P<0.01$, Figure 74e), and enhanced compulsivity compared to mice trained with standard pellets (Figure 74f).

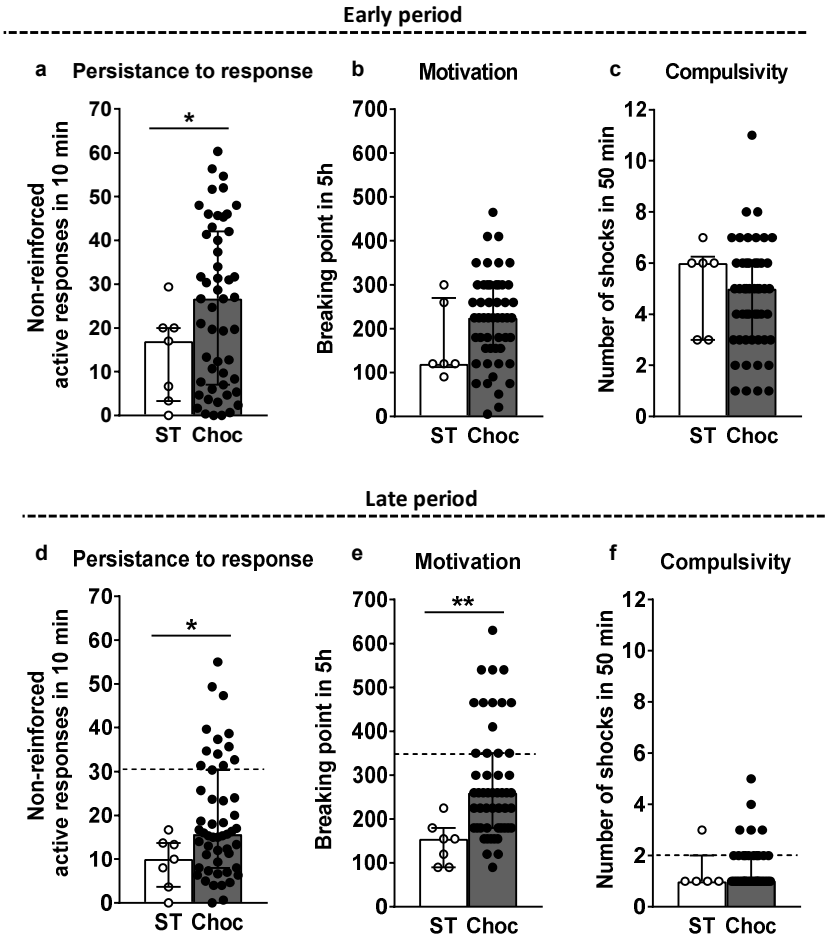

Figure 74. **Behavioral tests for the three addiction criteria in the (a-c) early period and (d-f) late period. a,d,** Persistence to response (a, t-test * *P*>0.05; d, U Mann-Whitney * *P*>0.05) **b,e,** Motivation (e, U Mann-Whitney ** *P*>0.01). **c,f,** Compulsivity. The dashed horizontal lines indicated the 75th percentile of the distribution of chocolate group, it is used as a threshold to consider a mouse positive for one criterion (n=51 mice trained with chocolate pellets, n=7 mice trained with standard pellets; individual values with the interquartile range; ST, standard)

4 additional phenotypic traits as risk factors to addiction were also evaluated to study deeper the additive phenotype: impulsivity, sensitivity to appetitive associative learning, cognitive flexibility, and

sensitivity to aversive associative learning. First, impulsivity was measured by the inability to stop an action once initiated (responding during the time-out period after each pellet delivery, 10 s). The chocolate group showed significantly higher impulsivity than standard group (t-test $P<0.01$, Figure 75).

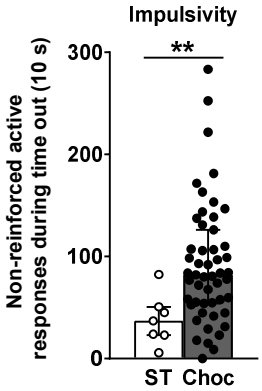

Figure 75. Impulsivity. Number of non-reinforced active responses in 50 min during three consecutive daily time out (10 s) after each pellet delivery (t-test $**P<0.01$; n=51 mice trained with chocolate pellets, n=7 mice trained with standard pellets; individual values with the interquartile range; ST, standard).

Second, appetitive associative learning was measured in the cue-induced food seeking test. It evaluates the association between the cue-light that served as a conditioned stimulus and food. In the second part of the session, the presentation of the cue-light promoted a higher food seeking in mice trained with chocolate than in mice trained with standard, although did not reach statistical difference (Figure 76a-b). Third, cognitive flexibility was evaluated in a reversal test, mice trained with chocolate pellets generally pressed more the inactive-reversed lever (previous active lever in a normal session) than mice trained with standard pellets, indicating a high cognitive flexibility impairment (Figure 77). Notably, 37% of mice from the chocolate group compared to the none of the standard group highly pressed both active and inactive levers without discrimination suggesting a compulsive seeking

for palatable pellets, although the results did not reach statistical differences.

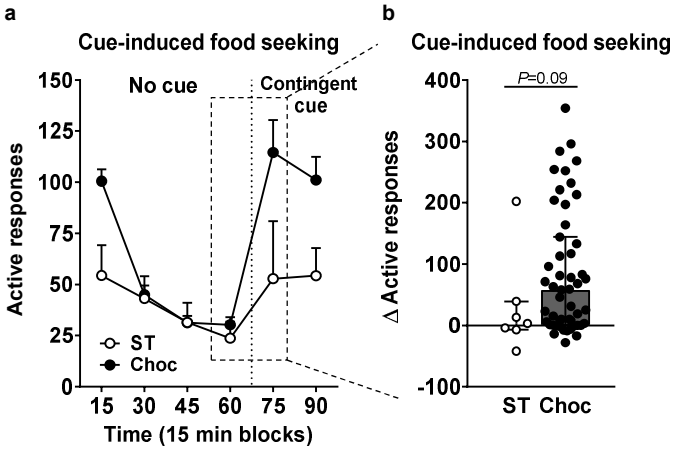

Figure 76. **Cue-induced food seeking. a,** Lever presses in the active lever and inactive lever during 60 min period during which lever-presses were not reinforced, followed by 30 min period during which active lever-presses (FR5) were associated with the cue-light without pellet delivery (mean ± SEM). **b,** Increased of active response after the presentation of the cue-light (individual values with the interquartile range; U Mann-Whitney *P*=0.09; n=51 mice trained with chocolate pellets, n=7 mice trained with standard pellets; ST, standard).

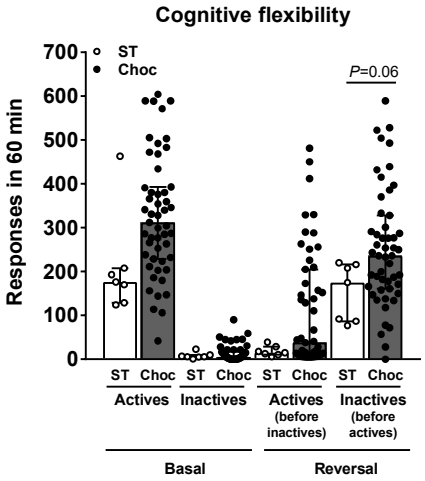

Figure 77. Cognitive flexibility measured by the reversal test. Number of responses in 60 min where active and inactive levers were reversed compared with preceding basal session (individual values with the interquartile range; U Mann Whitney *P*=0.06; n=51 mice trained with chocolate pellets, n=7 mice trained with standard pellets; ST, standard).

Finally, the aversive associative learning was tested by the ability of the shock-associated cue (the grid floor) to suppress pellets seeking the day after the shock-test. The chocolate group showed a significantly increased aversive associative learning with lower suppression of food seeking than the standard group (U Mann-Whitney *P*< 0.01, Figure 78a-b).

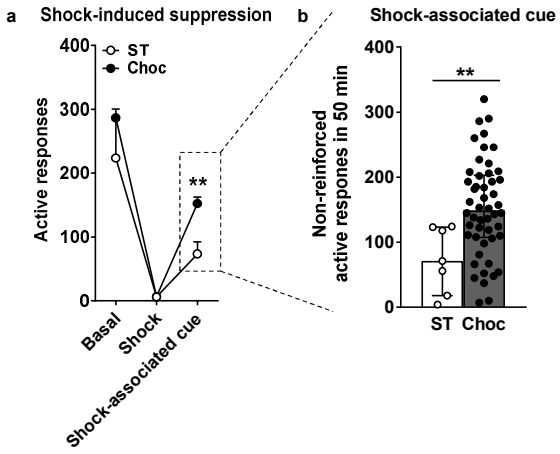

Figure 78. Shock-induced suppression. a, Active lever presses in the previous basal session before the shock-test, in the shock-test and in the following day (mean ± SEM). **b,** Number of non-reinforced active responses in 50 min in the following session after the shock-test with the same discriminative stimulus (grid floor) as shock-test in which pressing the active lever had no consequences: no shock, no pellets and no cue-light (individual values with the interquartile range; U Mann-Whitney ** *P*< 0.01; n=51 mice trained with chocolate pellets, n=7 mice trained with standard pellets; ST, standard).

Altogether, these results indicated that mice trained with chocolate-flavored pellets for a prolonged time-period showed higher addictive-behavior with compulsivity for seeking palatable food. However, the chocolate group is not totally homogeneous as it is expected in a

complex multifactorial disease like addiction. Therefore, we took an individual approach to analyze the distribution of individual values. Individual scores obtained in each criterion were used to categorized mice in addicted (covering 2-3 criteria) or non-addicted, as previously reported (Mancino *et al.*, 2015). Using this categorization, we obtained 23.5% of mice trained with chocolate pellets reaching 2-3 criteria (addicted mice) compared with the 0% of mice trained with standard pellets (Chi-square $P<0.001$, Figure 79) demonstrating that food palatability strongly promotes operant seeking behavior and loss of control over food intake.

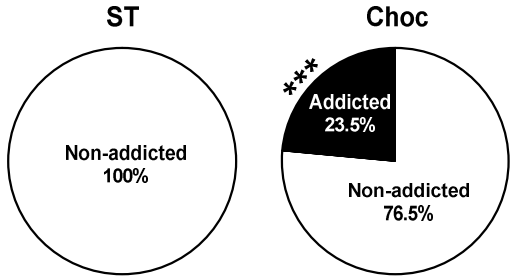

	Non-addicted		Addicted	
	0 crit	1 crit	2 crit	3 crit
ST	85.7%	14.3%	0.0%	0.0%
Choc	47.1%	29.4%	17.6%	5.9%

Figure 79. **Percentage of addicted and non-addicted mice trained with chocolate pellets and standard pellets classified on the bases of the performance at the late period** (Chi-square *** $P<0.001$, n=51 mice trained with chocolate pellets, n=7 mice trained with standard pellets; ST, standard).

Thus, this validated food addiction mouse model allows to distinguish extreme subpopulations with a vulnerable and a resilient phenotype. In this study, we were interested in order each mouse on a quantitative

gradual addiction scale. For this classification, we consider the individual score values of the three addiction criteria and the 4 phenotypic traits as factors of vulnerability to addiction of each mouse in the two extreme subpopulations. In the addicted subpopulation and in each criteria and phenotypic traits, we separated addicted mice in 4 groups depending on the percentile that they reach with their score value. A score value above the 75th percentile was punctuated with 3 points, mice between percentiles 55-75th with 2 points, between 25-75th with 1 point and beyond the 25th percentile with 0 points. On the contrary, in the non-addicted mice (0 criteria), in each of the 3 criteria and phenotypic traits, mice with a score value above the 75th percentile were punctuated with 0 points, mice between percentiles 55-75th with 1 point, between 25-75th with 2 points and beyond the 25th percentile with 3 points. Then, in both subpopulations, the scored obtained for each mouse in each criterion and phenotypic traits (1, 2, 3 score) was multiplied by 5 in the compulsivity criterion, by 4.5 in the persistence to response criterion, by 4 in the motivation criterion, by 3 in the impulsivity risk factor, by 2.5 in the cognitive flexibility, by 2 in the shock-induced suppression and by 1.5 in the cue-induced food seeking. The multiplicative value was determinate by the importance of the loss of control diagnostic criteria in the DSM-5 in the 3 addiction criteria and by the better correlation between addiction criteria and the 4 phenotypic traits considered as addiction risk factors (Figure 80a-d).

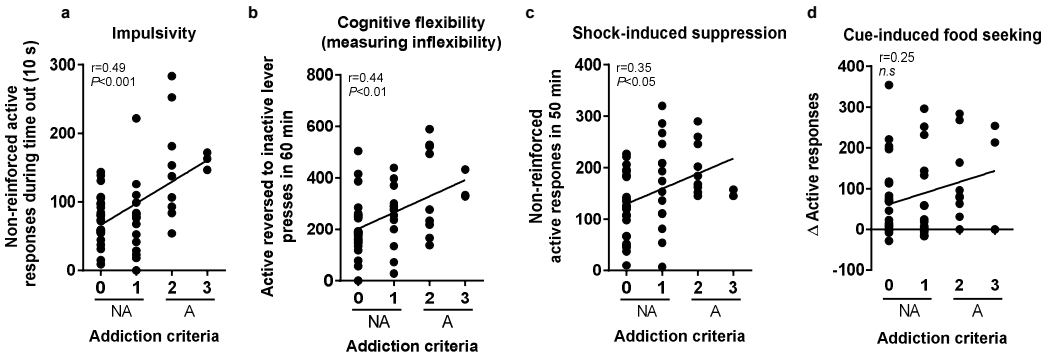

Figure 80. Correlations. Pearson correlations between individual addiction criteria and **a,** Impulsivity**,** non-reinforced active responses during time out (10 s) **b,** Cognitive flexibility impairment, active reversed to inactive lever presses in 60 min **c,** Shock-induced suppression, non-reinforced active responses in 50 min. **d,** Cue-induced food seeking, increased active responses (n=51 mice trained with chocolate pellets, NA: non-addicted, A: addicted).

Using this model, we were able to order mice in an addiction gradual scale. This was relevant for the following selection of the most addicted mice and non-addicted mice for the epigenetic studies (Figure 81).

We performed a whole miRNA and a DNA methylation analysis of mPFC and NAc of extreme addicted (n=6) and non-addicted (n=6) mice trained with chocolate pellets to characterize epigenetic marks for food addiction. No differences in the number of pellets intake between these two selected mice groups were reported assuming that the differential epigenetic changes will be due to the addictive phenotype and not to the pellets intake (Figure 82a-h).

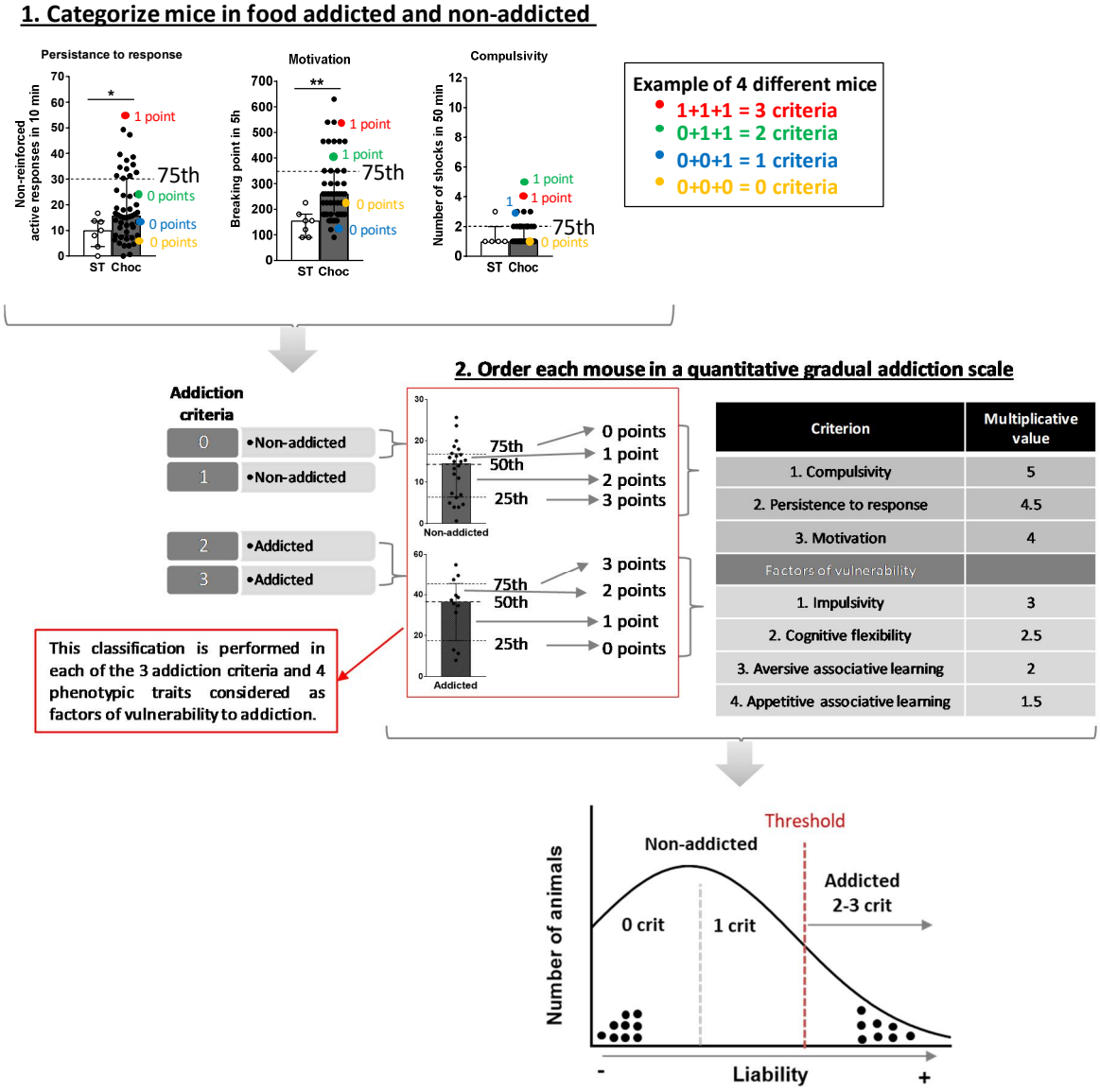

Figure 81. Model used to classify animals, first in addicted and non-addicted mice, and second on a quantitative gradual addiction scale inside the two extreme subpopulations.

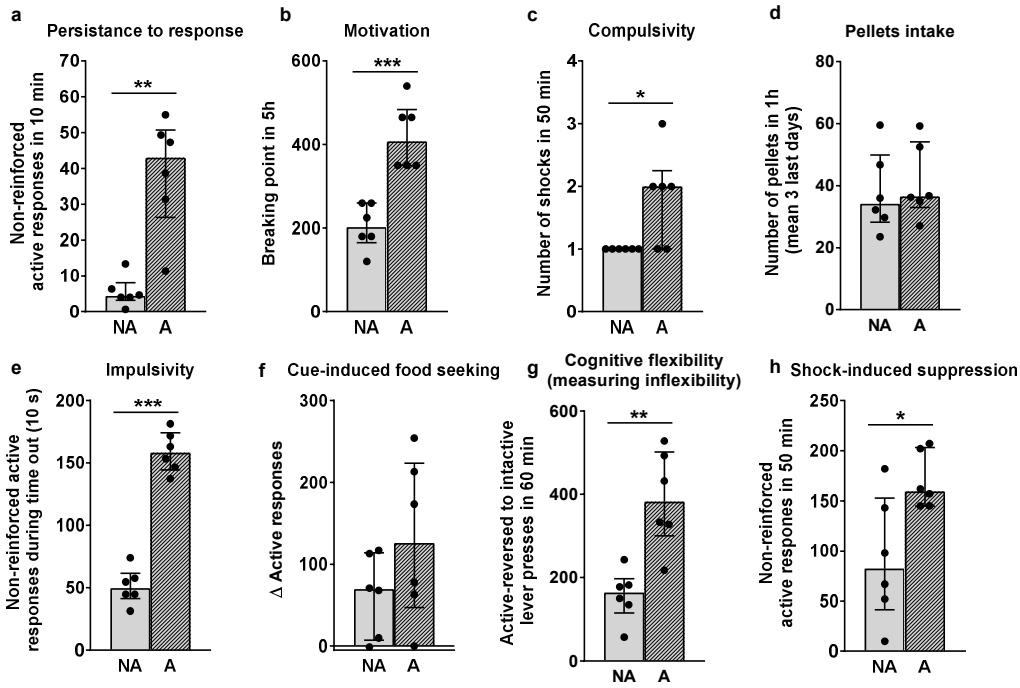

Figure 82. Behavioral tests of the three addiction criteria (a-c) and for the 4 additional factors of vulnerability to addiction (e-g) for those mice selected for the epigenetic study in addicted (A) and non-addicted (NA) mice trained with chocolate pellets. **a,** Persistence to response (U Mann-Whitney ** *P*< 0.01). **b,** Motivation (t-test *** *P*< 0.001). **c,** Compulsivity (U Mann-Whitney * *P*< 0.05). **e,** Impulsivity (t-test *** *P*< 0.01). **f,** Cue-induced food seeking. **g,** Cognitive flexibility (t-test ** *P*< 0.01). **h,** Shock-induced suppression (U Mann-Whitney * *P*< 0.05). **d,** Pellets intake in the last FR5 three sessions (n=6 addicted mice, n=6 non-addicted mice; individual values with the interquartile range).

Upon the smallRNA sequencing, the differential miRNAs found between addicted and non-addicted (discovery sample) were validated in 12 independent mice also classified as addicted and non-addicted (replica sample). Of all the miRNAs nominally differentially expressed in the discovery sample, those that have been able to replicate in the independent sample have been selected. With this strategy, 11 miRNAs

have been identified in mPFC, 9 of which were underexpressed in the addicted mice with respect to the resistant mice and 2 overexpressed (Table 5). For NAc none of the miRNA identified in the discovery sample could be replicated in the independent sample.

Table 5. Table of the validated miRNAs of the smallRNA-seq.

	Discovery			*Replica*		
miRNA	**p-value**	**FC**	**Exp**	**p-value**	**FC**	**Exp**
mmu-miR-876-5p	2,5e-04	-1,85	18,51	0,0393	-1,36	18,51
mmu-miR-211-5p	2,1e-03	-2,02	74,78	0,0381	-1,40	74,78
mmu-miR-3085-3p	7,3e-03	-1,35	232,02	1,9e-03	-1,46	232,02
mmu-miR-665-3p	8,9e-03	-1,27	337,76	4,9e-03	-1,39	337,76
mmu-miR-3072-3p	0,0174	-1,41	144,61	0,0346	-1,32	144,61
mmu-miR-124-3p	0,0265	-1,26	81006,63	0,0326	-1,16	81006,63
mmu-miR-29c-3p	0,0293	-1,33	3002,98	0,0138	-1,28	3002,98
mmu-miR-544-3p	0,0366	-1,44	77,83	0,0374	-1,32	77,83
mmu-miR-137-3p	0,0383	-1,28	9233,46	0,0315	-1,28	9233,46
mmu-miR-100-5p	0,0404	1,17	91517,51	0,0262	1,22	91517,51
mmu-miR-192-5p	0,0458	1,16	4450,81	0,0282	1,19	4450,81

Among these miRNAs, we selected 3 candidate miRNAs to perform a final functional validation with the antagomiR approach (Table 6). The aim of this approach was to downregulate the expression of these miRNA in WT mice to reproduce an addictive behavior towards palatable food in an early period of the food addiction protocol. We selected the miR-137, miR-29c and miR-665 based on the novelty of the findings and to their possible therapeutic target. miR-137 and miR-

29c levels changed after the exposure of different drugs of abuse and miR-137 has an important role in the modulation of presynaptic trafficking and neurotransmitter release proteins which has been related with neuropsychiatric traits (Siegert *et al.*, 2015; Quinn *et al.*, 2018; Su *et al.*, 2019). In turn, miR-665 has never been previously linked with addiction but it is dysregulated by microbiota changes that could be produced by an obesogenic diet (Dalmasso *et al.*, 2011; Cani *et al.*, 2016).

Table 6. **Candidate miRNAs selected for the functional validation with the antagomiR approach**.

Selected miRNA	*miRNA sequence (5'-3')*	*antagomiR sequence (5'-3')*
mmu-miR-137-3p	uuauugcuuaagaauacgcguag	Cuacgcguauucuuaagcaauaa
mmu-miR-665-3p	accaggaggcugaggucccu	agggaccucagccuccuggu
mmu-miR-29c-3p	uagcaccauuugaaaucgguua	uaaccgauuucaaauggugcua

Regarding the DNA methylation analysis, we have evaluated the nominal differentially methylated regions in the same two extreme samples of food addicted and non-addicted mice. In a first step, a targeted approach was used to study the DNA methylation profile of specific genes that were found upregulated in the mPFC of addicted mice in the transcriptomic study performed in Chapter 1. The aim was to find if the differences in the regulation of those genes between addicted and non-addicted mice could be explained by epigenetic changes, considering that we used a genetic inbreed mouse strain. The 4 genes evaluated were: *Drd2, Adora2a, Gpr88* and *Drd1* (Table 7).

Table 7. Nominal differentially methylated regions (DMR) between two extreme subpopulations of food addicted and non-addicted mice in mPFC for the genes *Drd2, Adora2a, Gpr88* and *Drd1* (mPFC: medial prefrontal cortex. The regions considered for the analysis are the genes *Drd2, Adora2a, Gpr88* and *Drd1* plus 5Kb up/downstream of them; GRCm38/mm10 assembly is used; FC: Fold Change on methylation of vulnerable to addiction mice compared to resilient to addiction mice.

Gene	Genomic position	Genomic feature	FC	p-value
Drd2	chr9:49393401-49393500	Intron 1	1,79	1,90E-02
	chr9:49393501-49393600	Intron 1	2,06	1,45E-02
	chr9:49404601-49404700	Intron 6	-2,83	4,91E-02
	chr9:49404701-49404800	Intron 6-exon 7	-4,38	3,27E-04
	chr9:49404801-49404900	exon 7	-2,04	3,86E-02
	chr9:49404901-49405000	exon 7	-2,04	3,86E-02
	chr9:49405001-49405100	exon 7 -intron 7	-2,31	2,01E-02
	chr9:49406601-49406700	intron 7	2,96	4,91E-02
	chr9:49408401-49408500	3'	-10,22	1,56E-02
Adora2a	chr10:75319001-75319100	intron 1	-4,54	1,30E-02
	chr10:75327701-75327800	intron 2	-1,91	3,58E-02
	chr10:75335101-75335200	3'	1,73	2,46E-02
	chr10:75335201-75335300	3'	1,76	1,88E-02
	chr10:75335301-75335400	3'	1,74	2,73E-02
	chr10:75336501-75336600	3'	-2,87	8,16E-03
	chr10:75336601-75336700	3'	-5,46	2,21E-02
Gpr88	chr3:116256601-116256700	5'	2,42	1,58E-02
	chr3:116257201-116257300	5'	-4,91	3,91E-02
	chr3:116257301-116257400	5'	-4,91	3,91E-02
Drd1	chr13:54053001-54053100	exon 2	-1,66	1,28E-02

Interestingly, the 4 genes contain several genomic regions hypomethylated that could be associated with a general low transcriptional repression and subsequent high protein expression. Regarding *Drd2*, the hypomethylated regions in intron 6 and exon 7 are in contiguous genomic regions enhancing the relevance of these changes. This result is in accordance with the strong upregulation of *Drd2* found in the RNA-seq in Chapter 1.

Overall, this study characterized the differential epigenetic profile, at miRNA and DNA methylation level that may be underlying the loss of inhibitory control leading to a vulnerable phenotype to develop food addiction.

Laura Domingo-Rodriguez, Sami Kumer, Angela Ramírez-López, Inigo Ruiz de Azua, Beat Lutz[#], Elena Martín-García[#], Rafael Maldonado[#].

CB_1R in CAMKIIα+ neurons is involved in the loss of control over palatable food intake in a binge eating mouse model

Under preparation.

[#] Equal seniority

Chapter 3

CB_1R in CAMKIIα^+ neurons is involved in the loss of control over palatable food intake in a binge eating mouse model

3.1. Abstract

The continued exposure and consumption of high-palatable foods could override the physiological caloric needs leading to eating disorders and obesity. The endocannabinoid system is widely involved in regulating both homeostatic and hedonic processes of food consumption. Using conditional knock-out mice of CB_1R in different neuronal subpopulations it has been identified the involvement of this endocannabinoid receptor in palatable food intake. However, it was difficult to conclude if the CB_1R expression is sufficient for this function. We used a rescue genetic strategy in CB_1R-KO mice for the selective expression of CB_1R only in Ca^{2+}/calmodulin-dependent kinase II alpha (CAMKIIα^+) neurons. In these mice, we investigated the sufficient role of the CB_1R in this glutamatergic cell-type in the compulsive-eating behavior and emotional manifestations associated with a binge eating model. We found that CAMKII-CB1-RS mice exposed to intermittent chocolate access diet displayed a phenotype mainly characterized by increased impulsivity, high motivation and enhanced compulsivity for palatable food. This phenotype substantially rescues the total CB_1R loss phenotype and suggested that CB_1R expression in CAMKIIα^+ cells is selectively mediating the loss of control over food intake.

3.2. Background

Previous studies conducted by Lutz's laboratory (not published) show that the expression of the CB_1R only in $CAMKII\alpha^+$ cells produces a rescue of the reduced food intake phenotype reported in mice lacking CB_1R in all cells (CB1-KO mice). They used a fasting/re-feeding paradigm, consisting of fasting animals for 24h and refeeding them with standard food. The food intake was measured after 1 h and 2 h of refeeding. The results showed increased food intake of CAMKII-CB1-RS than CB1-KO mice and similar to WT mice after 1 h. However, after 2 h of refeeding, CAMK-II-CB1-RS mice showed higher food intake than WT mice (Figure 83). Based on this result, we hypothesized that CAMKII-CB1-RS mice could display a phenotype characterized by impulsive- and compulsive-eating behavior rescuing the CB1-KO phenotype and suggesting an important role of the CB_1R mainly in $CAMKII\alpha^+$ cells in loss of control.

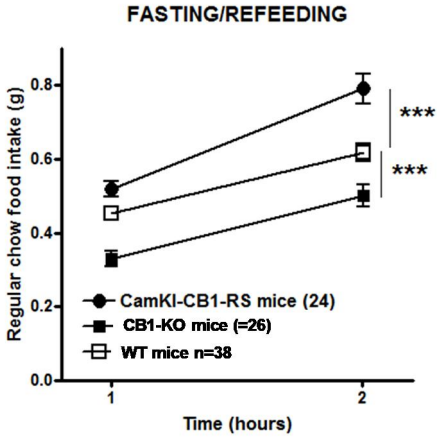

Figure 83. Fasting/refeeding paradigm. Mean of the regular chow food intake (g) in 1 h and 2 h after fasting in CAMKII-CB1-RS, CB1-KO and WT animals (***P<0.001; mean±SEM, n=24 per group).

3.2. Materials and methods

Animals

To express the CB_1R exclusively in CAMKIIα^+ cells, the recently developed rescue approach was applied (Ruehle *et al.*, 2013), whereby CB_1R function is suppressed globally in Stop-CB1 mice by a transcriptional Stop cassette flanked by two loxP sites and inserted into the 5′ UTR of the ORF-containing CB_1R exon. Crossing Stop-CB1 mice with Cre recombinase-expressing transgenic mice reactivated (i.e., rescued) CB_1R function only in Cre-expressing cells. Thus, CAMKII-CB1–RS mice were generated by mating Stop-CB1 mice with CAMKIIα iCre mice (Casanova *et al.*, 2001), whereas WT equivalent controls (CB1-RS mice) were generated by crossing Stop-CB1 mice with the general Cre-deleter mouse line EIIa-Cre (Ruehle et al., 2013). CAMKIIα iCre mice express the recombinase in the great majority of adult forebrain neurons, with the exclusion of cortical GABAergic interneurons (Casanova *et al.*, 2001). The offspring produced were genotyped for the presence of Cre and the Stop cassette. Experimental animals were mice containing the Stop cassette, phenotypically representing a CB1-null allele, $CB1^{stop/stop}$ (CB1-KO) mice; mice with CB_1 receptor rescue in CAMKII-expressing cells, $CB1^{stop/stop;camkII\text{-}cre/WT}$ (herein, CAMKII-CB1–RS) mice; and mice with CB_1 rescue in all cells (WT).

Mice were housed individually in controlled laboratory conditions (temperature at 21 ± 1°C and humidity at 55 ± 10%) and were tested during the first hours of the dark phase of a reversed light/dark cycle (lights off at 8.00 hours and on at 20.00 hours). Food and water were

available ad libitum. All experimental protocols were performed in accordance with the guidelines of the European Communities Council Directive 2010/63/EU and approved by the local ethical committee (Comitè Ètic d'Experimentació Animal-Parc de Recerca Biomèdica de Barcelona, CEEAPRBB).

Diet

Animals of each genotype with similar body weight were randomly assigned to 2 different diets at 5th week of the experiment procedure:

I) **Intermittent chocolate access diet**: mice were exposed *ad libitum* access to standard food and to chocolate-mixture hypercaloric palatable food in a free-choice manner for 2 days per week. The following 5 days of the week, mice were fed *ad libitum* with standard food. The combination of the 48h access to the free-choice and the subsequence 5 days access to standard food represents one intermittent chocolate access cycle. In each cycle, both types of foods were measured at the first 2.5h, (binge behavior), 24h and 48h (Cottone 2009, Czyzyk, Sahr, & Statnick, 2010) (Figure 84).

II) **Standard diet:** mice were exposed *ad libitum* to standard food for the 7 days of the week.

Standard food contains 3.52 kcal/g: 75% energy from carbohydrates with 8.3% of sugar, 18% from protein and 7% from fat. Chocolate-mixture hypercaloric palatable food was composed of an equitable mixed of 4 popular brand chocolate bars highly consumed by humans (MILKA®, SNICKERS®, BOUNTY® and MARS®) prepared as homogenous

food pellets containing 4.92 kcal/g: 52% energy from carbohydrates with 44.4% of sugar, 17% from protein and 24% from fat (Heyne *et al.*, 2009; Martín-García *et al.*, 2010).

Considering the 3 genotypes and the 2 different diets, we had 6 different experimental groups divided in control groups, exposed to standard diet (WT Standard, CB1-KO Standard, CAMKII-CB1-RS Standard), and binge eating groups, exposed to the intermittent chocolate access diet (WT Binge, CB1-KO Binge, CAMKII-CB1-RS Binge) (n=8-13 per group).

Experimental procedure

The entire experimental procedure was divided in two distinct parts:

I) **Basal conditions**, in which the three genotypes were exposed to standard diet during the first 4 weeks.

II) **Experimental conditions**, in which each genotype was divided in control and binge group during the following 20 weeks (5^{th}-24^{th} weeks) (Figure 84).

In basal conditions, mice were tested in a novel food exposure test in the first week for measuring impulsivity (see behavioral test section) (Lafenêtre *et al.*, 2009). Afterward, mice performed acquisition of operant training maintained by chocolate-flavored pellets during the following 3 weeks for assessing the primary reinforcing effects of chocolate-flavored pellets. Mice were trained under a FR1 schedule of reinforcement (1 h daily session) for 5 days followed by 10 days of FR5.

After FR training, mice performed a PR test (PR1) for measuring the basal motivation.

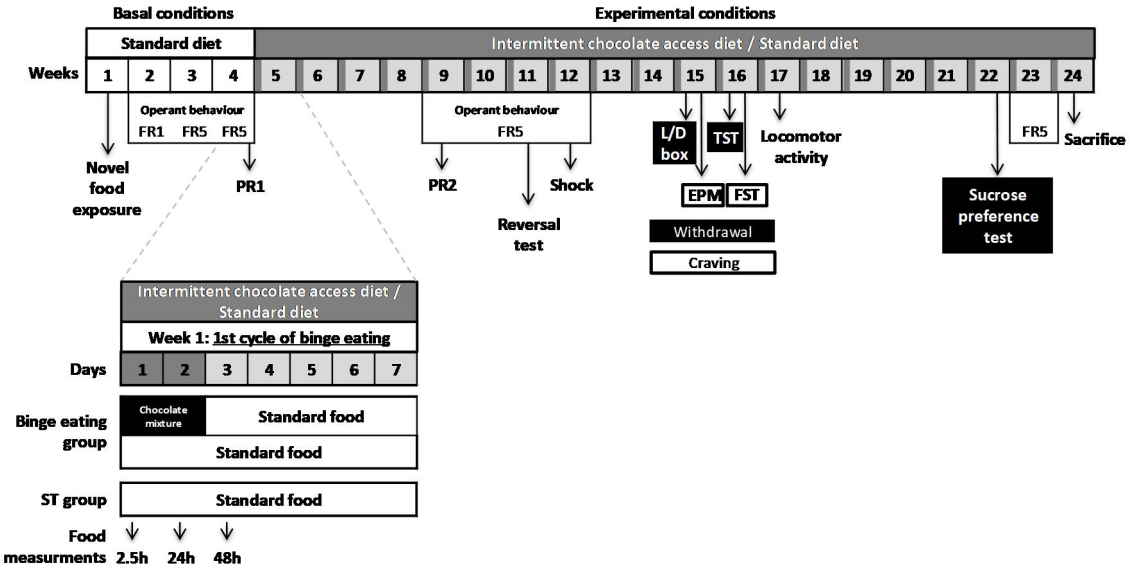

Figure 84. **Experimental procedure.** In basal conditions (all mice fed with standard diet), mice were tested in a novel food exposure test for measuring impulsivity in the first week. Next, mice performed acquisition of operant training maintained by chocolate-flavored pellets during the following 3 weeks. Specifically, mice were trained under a FR1 schedule of reinforcement (1-h daily session) for 5 days followed by 10 days of FR5. After FR training, mice performed a PR test (PR1) for measuring the basal motivation. Then, the experimental conditions period started (mice fed with intermittent chocolate access diet) and after 4 cycles of binge eating mice were under FR5 schedule of reinforcement for 4 weeks. During this second operant training, the second PR (PR2, 9th week), a reversal test and a shock test (11-12th weeks) for measuring motivation, cognitive flexibility and compulsivity respectively were completed. Then, a light dark box test (L/D box), an elevated plus maze (EPM, 15th week), a tail suspension test (TST, 16th week), a forced swimming test (FST, 16th week) and a sucrose preference test (22th week) were performed for measuring the anxiolytic- and depressive-like behavior in intermittent chocolate-mixture diet withdrawal or craving conditions. Moreover, locomotor activity (17th week) was tested.

Then, the experimental conditions period started and after 4 cycles of binge eating mice were under FR5 for 4 weeks. During this second

operant training, the second PR (PR2, 9th week), a reversal test and a shock test (11-12th weeks) were completed for measuring motivation, cognitive flexibility and compulsivity respectively. Then, a light dark box test (15th week), elevated plus maze (15th week), tail suspension test (16th week), forced swimming test (16th week) and sucrose preference test (22th week) were performed for measuring the anxiolytic- and depressive-like behavior in intermittent chocolate-mixture diet withdrawal or craving conditions. Moreover, locomotor activity (17th week) was tested. Body weight was evaluated regularly every week. The different behavioral tests are explained above.

Behavioral tests

The operant boxes, self-administration sessions, PR test, shock-test and reversal test were accurately described in the previous chapters with the difference that the operant boxes were equipped by levers instead of nose-pokes holes used in the present experiment.

Repeated exposures to a novel palatable food. This test was performed on the 1st week of the procedure to evaluate impulsivity, modified to Lafenêtre *et al.* (2009). Three hours after the onset of the light, 25 pellets of a novel palatable food (chocolate-flavored pellets of 20 mg) were placed for 15 min onto the bedding of the home cage of each animal. Consumption of the novel palatable food was measured controlling for spillage. The latencies to contact and to start eating any of the pellets were analyzed. A contact was defined as the snout of the mouse touching any of the pellets, and eating was identified as licking or biting a pellet.

Light-dark box test. This test was performed on the 15th week of the procedure in the withdrawal of binge eating diet conditions to evaluate anxiety-like behavior, as reported (Bura *et al.*, 2010; Planagumà *et al.*, 2015). The box consisted of two compartments (20 cm wide × 20 cm long × 30 cm high) connected by a 6 cm wide by 6 cm high tunnel. One compartment was painted black and maintained at 10 lux, while the other compartment was painted white, brightly illuminated (500 lux), and subdivided into three sections (distal, medial and proximal), based on the distance from the tunnel. The floor of both compartments was subdivided into squares (5x5 cm) to measure the locomotor activity. At the start of the session, mice were placed in the black compartment, head facing a corner. The latency of first entry into the white compartment and section reached in each entry, together with time spent, squares crossed, and the number of entries into both compartments were recorded and used to evaluate anxiety-like responses.

Elevated plus maze test. This test was performed on the 15th week of the procedure in craving of binge eating diet conditions to evaluate anxiety-like behavior, as reported (Llorente-Berzal *et al.*, 2013; Planagumà *et al.*, 2015). The maze consists on a plastic black cross with arms 40 cm long and 6 cm wide placed 50 cm above the floor. Two opposite arms were surrounded by walls (15 cm high, closed arms, 10 lux), while the two other arms were devoid of such walls (open arms, 200 lux). The four arms were connected by a central platform. At the start of the session, the mouse was placed at the end of a closed arm

facing the wall. During the 5 min trial, the number of entries and the time spent in each arm were recorded. Anxiety was assessed as both the time spent avoiding the open arms and the number of entries into them.

Tail suspension test. This test was performed on the 16th week of the procedure in the withdrawal of binge eating diet conditions to evaluate depressive-like behavior, as reported (Aso *et al.*, 2008; Planagumà *et al.*, 2015). Mice were suspended 50 cm above a solid surface by the use of adhesive tape applied to the tail (3/4 of the distance from the base of mouse tail). During a 6 min interval, the total time of immobility was recorded. Long periods of immobility are characteristic of a depressive-like state.

Forced swimming test. This test was performed on the 16th week of the procedure in craving of binge eating diet conditions to evaluate depressive-like behavior, as reported (Kieffer *et al.*, 2000; Planagumà *et al.*, 2015). The mouse was placed in a plastic cylinder containing warm water (27-28 °C), deep enough to prevent touching the bottom of the cylinder and forcing the mouse to swim. The trial lasted 6 min and the total time of immobility after min 2 was recorded. Time of immobility was defined as the time that the animal stopped swimming and only used minimal movements to keep the head above the water.

Sucrose preference test. This test was performed on the 22nd week of the procedure to evaluate anhedonia, as previously reported (Bura *et al.*, 2013; Planagumà *et al.*, 2015). Two bottles of water, one with 2% sucrose and the other without, were placed in the cage. Every day,

during 4 days, the position of the bottles was exchanged, and the consumption from each bottle measured. On the day of the test, the two bottles were placed again in the cage and the consumption from each recorded after a 24 h interval. The preference for sucrose was calculated as the relative amount of water with sucrose versus total liquid (water with and without sucrose) consumed by the mice.

Locomotor activity. Locomotor activity was assessed on the 17th week. Animals were assessed in locomotor activity boxes (9×20×11 cm; Imetronic, Pessac, France), equipped with 2 rows of photocell detectors, and placed in a low-luminosity environment (20–25 lux), as previously described (Berrendero *et al.*, 2005; Planagumà *et al.*, 2015). The mouse locomotor activity was recorded for 60 min as horizontal activity and vertical activity.

Statistical analysis

All statistical comparisons were performed with SPSS (IBM, version 25). Comparisons between groups were analyzed by Student t-test or U Mann-Whitney depending on the distribution defined by the Kolmogorov-Smirnov normality test. A *P* value <0.05 was used to determine statistical significance. Outliers (± 2 s.d. from the mean) were excluded. In the middle of the experiment, several mice (n=9) suffered dermatitis and were excluded from emotional manifestations tests.

3.3. Results

The rescue of the CB_1R in $CAMKII\alpha^+$ neurons is sufficient to induce a loss of control towards palatable food that is enhanced by an intermittent chocolate access diet exposure.

Excessive novelty seeking could lead to pathological forms of impulsivity (Lafenêtre *et al.*, 2009). Therefore, repeated exposures to a novel palatable food were used to evaluate the impulsive-like behavior at basal conditions. CAMKII-CB1-RS mice showed significantly less latency to approach to the novel food the first day of exposure compared to WT mice and CB1-KO mice, indicating an enhanced impulsive-like behavior (U Mann-Whitney $P< 0.01$, $P< 0.001$ Figure 85a-b). No significant differences were shown in latency to eat, the number of bites nor in the total food consumption (data not shown).

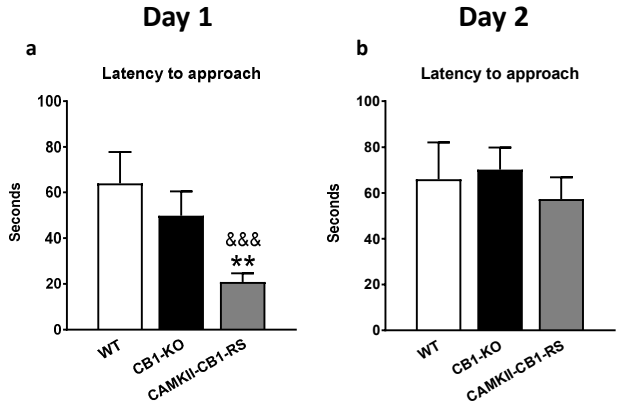

Figure 85. Repeated exposures to a novel palatable food. Latency to approach to the novel palatable food in 2 consecutive days. **a,** Day 1. **b**, Day 2 (U Mann-Whitney; ** *P*<0.01 CB1-KO vs CAMKII-CB1-RS mice; &&& p<0.001 WT vs CAMKII-CB1-RS mice; Data are expressed as mean ± SEM; 18-19 mice per group).

After the impulsivity evaluation, mice underwent an operant conditioning paradigm maintained by chocolate-flavored pellets during 15 sessions, while they received standard diet in the home cage. Firstly, mice were trained 5 sessions under FR1 followed by 10 sessions under FR5. During FR1, WT mice showed an increased number of reinforcers achieved in 1 h session compared to CB1-KO mice, as previously reported (Mancino *et al.*, 2015) (U Mann-Whitney $P< 0.05$, $P< 0.01$). This CB1-KO phenotype was totally rescued in CAMKII-CB1-RS mice, which obtained the highest number of reinforcers in each session (U Mann-Whitney $P< 0.01$, $P< 0.001$ Figure 86). Interestingly, when the effort to acquire one single pellet was increased to FR5, CAMKII-CB1-RS mice and WT mice achieved the same number of pellets and both groups were significantly above to CB1-KO group (U Mann-Whitney $P< 0.05$, $P< 0.01$) (Figure 86). After 15 sessions, each genotype started to be fed with an intermittent chocolate access diet or with standard diet as a control. After 4 weeks to diet exposure, CAMKII-CB1-RS ST and WT ST mice obtained a higher number of chocolate-flavored pellets than CB1-KO ST mice as in basal conditions. However, the CAMKII-CB1-RS mice exposed to intermittent chocolate access diet had a trend to seek more the reward than the rest of the groups (Figure 86). This effect is mainly observed in the first sessions. These results indicate that CAMKII-CB1-RS mice displayed a high sensitivity to the primary reinforcing effects of chocolate-flavored pellets that is enhanced with the chocolate exposure rescuing the CB1-KO phenotype.

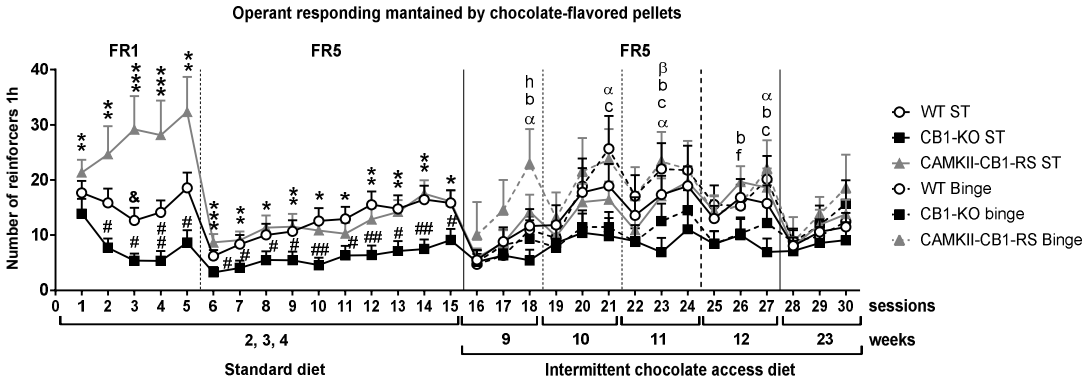

Figure 86. Operant responding maintained by chocolate-flavored pellets. Mean number of reinforces in 1 h during the acquisition training in 5 sessions of FR1 followed by 25 sessions of FR5 schedule of reinforcement. In the first 15 sessions mice were fed with standard diet and between session 16 to 30, mice were fed with an intermittent chocolate access diet (U Mann-Whitney; # p<0.05, ## p<0.01 WT vs CB1-KO; & *P*<0.05 WT vs CAMKII-CB1-RS; * *P*<0.05, ** *P*<0.01, *** *P*<0.001 CB1-KO vs CAMKII-CB1-RS; β p<0.05 WT ST vs CB1-KO ST; b p<0.05 CB1-KO ST vs CAMKII-CB1-RS ST; c p<0.05 CB1-KO ST vs WT Binge; α p<0.05 CB1-KO ST vs CAMKII-CB1-RS Binge; f p<0.05 CAMKII-CB1-RS ST vs CB1-KO Binge; h p<0.05 CB1-KO Binge vs CAMKII-CB1-RS Binge; Data are expressed as mean ± SEM; 9-15 mice per group; ST, standard).

In the operant conditioning sessions, we measured the motor impulsivity considering the time out periods, 10 s after each pellet delivery in which the active nose-poke had no consequences. CAMKII-CB1-RS mice showed a strong impulsive-like behavior with an increased number of non-reinforced active responses during the time out compared to WT and CB1-KO mice at the beginning of the operant training (FR1) (U Mann-Whitney *P*<0.01, *P*<0.001, Figure 87). This result was congruent with the reduced latency to approach for food in the novel palatable food test found at the beginning of the experiment. Then, the impulsivity was decreased in FR5 during basal conditions but emerged again in some CAMKII-CB1-RS mice when they were exposed

to intermittent chocolate access diet (U Mann-Whitney *P*<0.01, Figure 87). Thus, a rescue of the impulsive-like behavior was revealed in the CAMKII-CB1-RS mice and was enhanced with the exposition of palatable food. The expression of CB_1R only in CAMKIIα^+ neurons is sufficient to induce strong impulsivity-like behavior.

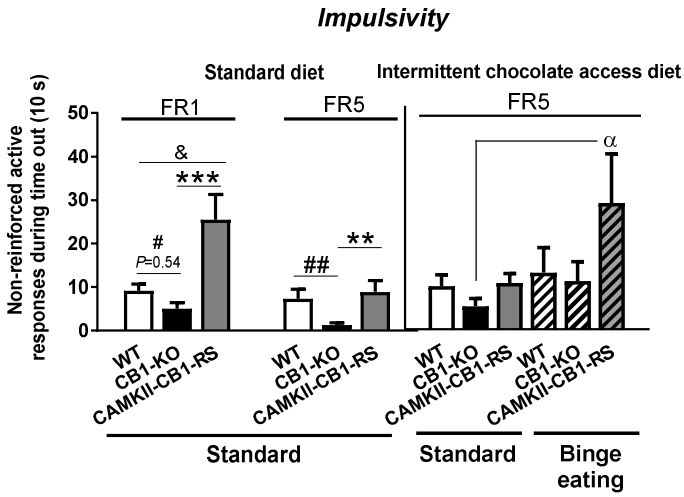

Figure 87. Impulsivity. Mean number of non-reinforced active responses during the time out period (10 s) in 1 h of FR1 and FR5 schedule of reinforcement when mice were exposed to standard diet and of FR5 when mice were exposed to intermittent chocolate access (U Mann-Whitney; ## p<0.01 WT vs CB1-KO; & *P*<0.05 WT vs CAMKII-CB1-RS; ** *P*<0.01, *** *P*<0.001 CB1-KO vs CAMKII-CB1-RS; α p<0.05 CB1-KO ST vs CAMKII-CB1-RS Binge; Data are expressed as mean ± SEM; 9-15 mice per group).

We also evaluated the motivation of mice to obtain palatable pellets using a PR test in basal conditions (PR1) and under intermittent chocolate access diet (PR2). In the first PR, CAMKII-CB1-RS mice had increased food motivation compared to CB1-KO mice (Figure 88). Notably, the breaking point reached by CAMKII-CB1-RS mice was increased in the PR2 after several cycles of binge eating with a trend to

had augmented levels of motivation for chocolate-flavored pellets than the other groups (U Mann-Whitney $P<0.05$, Figure 88).

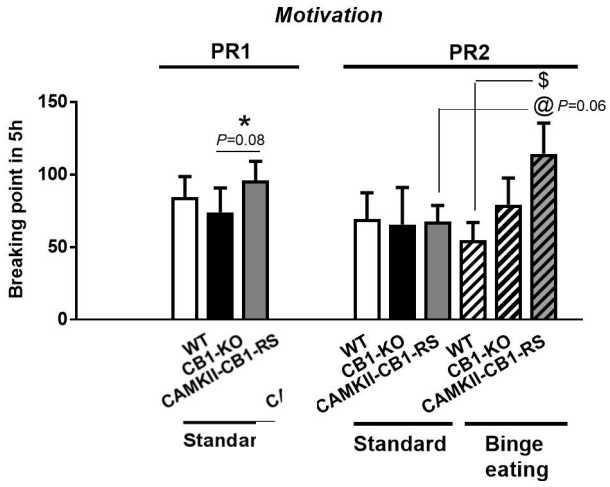

Figure 88. Motivation for chocolate-flavored pellets. Mean of breaking point in 5 h session in 2 progressive ratio tests, PR1 in basal conditions and PR2 in experimental conditions (U Mann-Whitney; * CB1-KO vs CAMKII-CB1-RS, @ CAMKII-CB1-RS ST vs CAMKII-CB1-RS Binge; $ $P<0.05$ WT Binge vs CAMKII-CB1-RS Binge; Data are expressed as mean ± SEM; 9-15 mice per group).

One week after the motivation evaluation, we tested animals in a reversal test to study cognitive flexibility. CAMKII-CB1-RS mice and WT mice showed a cognitive inflexibility trend compared to CB1-KO mice, indicated by an increased number of inactive responses (previous active responses in a normal session) when the session conditions were reversed. But, CAMKII-CB1-RS binge eating mice also showed higher number of active responses (before inactive) than other groups of mice, suggesting good cognitive flexibility. Therefore, the high number of responses in both reversed holes and the fact that 67% of CAMKII-CB1-RS binge eating mice do not discriminate between holes, suggested that conditional CAMKII mutant mice exposed to

intermittent chocolate access diet displayed a high seeking behavior for palatable pellets (Figure 89).

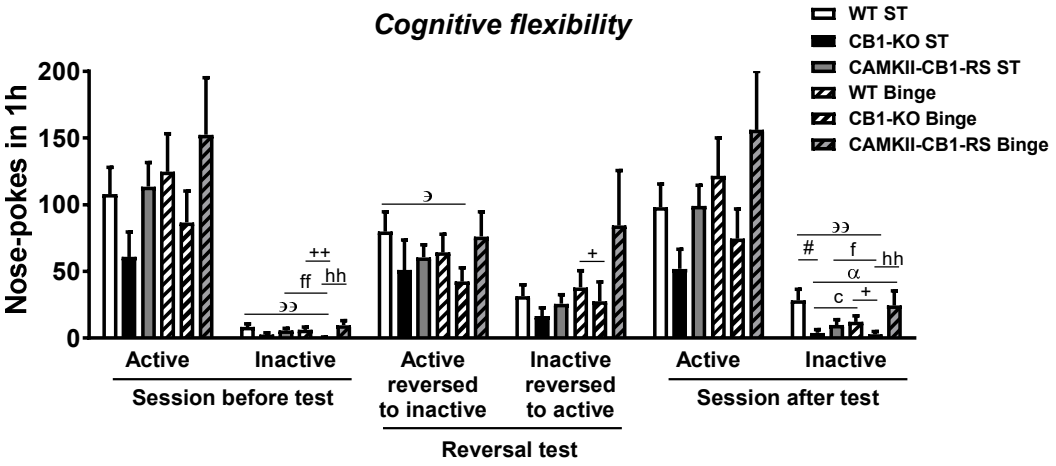

Figure 89. Cognitive flexibility measured by the reversal test. Number of responses in 1 h where active and inactive nose-poke holes were reversed compared with the preceding session and the following session (U Mann-Whitney; ə *P*<0.05, əə *P*<0.01 WT ST vs CB1-KO Binge; c *P*<0.05 CB1-KO ST vs WT Binge, α *P*<0.05 CB1-KO ST vs CAMKII-CB1-RS Binge, f *P*<0.05, ff *P*<0.01 CAMKII-CB1-RS ST vs CB1-KO Binge, + *P*<0.05 , ++ *P*<0.01 WT Binge vs CB1-KO Binge; hh *P*<0.01 CB1-KO Binge vs CAMKII-CB1-RS mice; Data are expressed as mean ± SEM; 9-15 mice per group; ST, standard).

Finally, we hypothesized that CAMKII-CB1-RS mice could show an increased compulsivity, considering that the CB_1R rescue in CAMKIIα^+ neurons was sufficient to reverse the phenotype of high impulsive-like behavior, augmented motivation and enhanced palatable food-seeking of CB1-KO mice. Therefore, compulsive behavior was evaluated in a shock-test in which the delivery of a chocolate-flavored pellet was associated with a footshock. CAMKII-CB1-RS binge mice showed a higher number of shocks than the other two groups and could not stop to seek palatable food despite harmful costs (U Mann-Whitney *P*<0.05,

Figure 90). In contrast, CB1-KO mice presented significantly less compulsive behavior in both diet conditions.

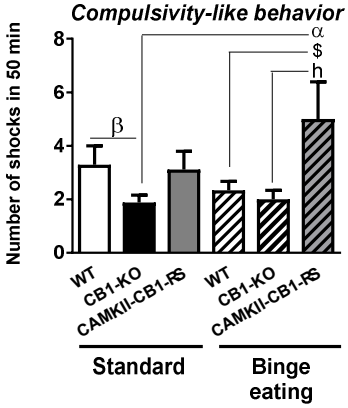

Figure 90. **Compulsivity measured by the shock test**. Number of shocks received in 50 min in the shock test in which each pellet delivery was associated with a footshock (0.25 mA; U Mann-Whitney; β *P*<0.05 WT ST vs CB1-KO ST; α *P*<0.05 CB1-KO ST vs CAMKII-CB1-RS Binge; $ *P*<0.05 WT Binge vs CAMKII-CB1-RS Binge; h *P*<0.05 CB1-KO Binge vs CAMKII-CB1-RS Binge; Data are expressed as mean ± SEM; 9-15 mice per group).

Taking into account all these findings, the CAMKII-CB1-RS mice presented a phenotype of loss of control over palatable food characterized by increased impulsivity, higher motivation, food-seeking for palatable pellets and augmented compulsivity. Thus, a rescue of the CB_1R in $CAMKII\alpha^+$ cells in an obesogenic environment is sufficient to induce a loss of control over palatable food.

The expression of CB_1R in $CAMKII\alpha^+$ neurons rescue the anxiety-like, but not the depressive-like behavior.

Emotional alterations such as anxiety and depression have been correlated with eating disorders and obesity. In addition, the endocannabinoid system has been reported to be involved in the regulation of these affective symptoms. Therefore, we evaluated the anxiety- and depressive-like behavior after 10 cycles of binge eating in withdrawal conditions, 1 day after the exposure of the chocolate, and

in craving conditions, 1 day before the exposure of chocolate (Figure 84).

In withdrawal conditions, the anxiety-like behavior was tested in a light/dark box. CB1-KO mice showed an anxiogenic phenotype spending less time in the light compartment compared to WT and CAMKII-CB1-RS mice (Figure 91a). The exposure of binge eating diet in withdrawal conditions had no effect, showing the binge groups the same phenotype as standard groups. Anxiety-like behavior was also evaluated in craving conditions (Figure 84) using the elevated plus maze. In standard groups, mutant mice lacking CB_1R in all cells had the same tendency to explore the open arms less than the two other groups (Figure 91b). CAMKII-CB1-RS mice spent the same time in open arms as WT mice suggesting that the expression of CB_1R in CAMKIIα^+ cells is sufficient to rescue the anxiety phenotype. In contrast, no differences between genotypes were found in mice exposed to intermittent chocolate-access diet in craving conditions (Figure 91b).

The characterization of depressive-like behavior was evaluated by the tail suspension test in withdrawal conditions and by the forced swimming test in craving conditions. In the tail suspension test, a depressive-like behavior in CAMKII-CB1-RS standard mice was shown not rescuing the CB1-KO standard phenotype (Figure 91c). In contrast, when mice were exposed to intermittent chocolate access diet, CAMKII-CB1-RS showed a similar lower immobility time as WT mice, only the CB1-KO mice displayed the depressive-like behavior. In the

forced swimming test, we found the same depressive-like behavior in CB1-KO and CAMKII-CB1-RS mice in both diets exposures (Figure 91d).

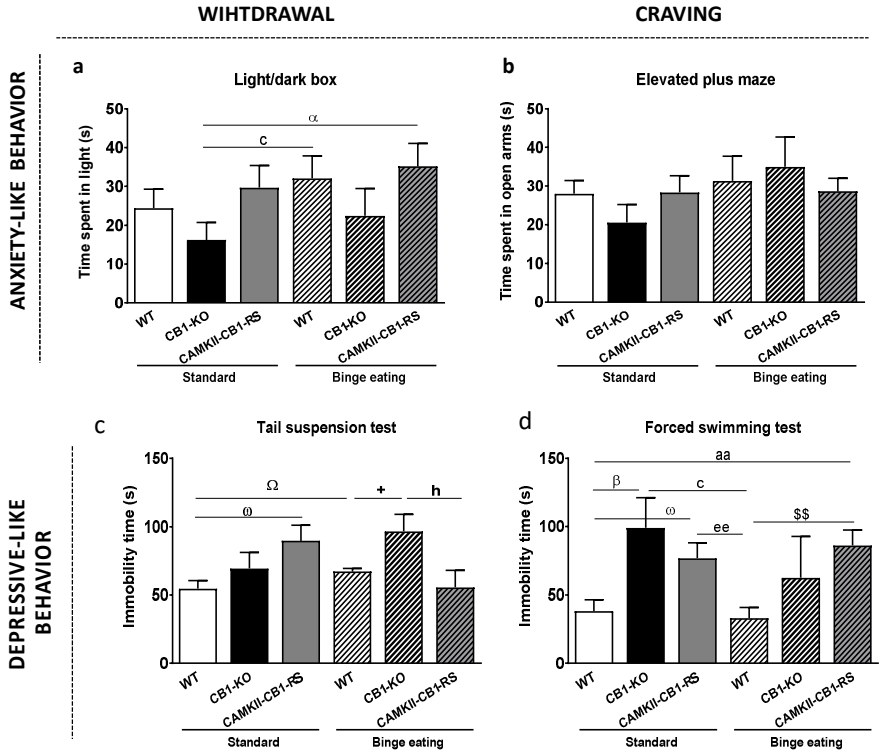

Figure 91. a-b, **Anxiety-like behavior was measured by a light/dark box test in withdrawal conditions and by an elevated plus maze in craving conditions for chocolate in a binge eating cycle. a,** Time spent in the light compartment (s) of the light/dark box. **b,** Time spent in open arms of the elevated plus maze (U Mann-Whitney c *P*<0.05 CB1-KO vs WT Binge; α *P*<0.05 CB1-KO ST vs CAMKII-CB1-RS Binge; Data are expressed as mean ± SEM; 6-13 mice per group). **c-d, Depressive-like behavior was measured by a tail suspension test in withdrawal conditions and by a forced swimming test in craving conditions for chocolate in the binge eating cycle. a,** Immobility time of the tail suspension test**. b,** Immobility time of the forced swimming test (t-test equal variances assumed; β p<0.05 WT ST vs CB1-KO ST; ω p<0.05 WT ST vs CAMKII-CB1-RS ST; ee p<0.01 CAMKII-CB1-RS ST vs WT Binge; $$ p<0.01 WT Binge vs CAMKII-CB1-RS Binge; h p<0.05 CB1-KO Binge vs CAMKII-CB1-RS Binge; T-test equal variances not assumed; aa p<0.01 WT ST vs CAMKII-CB1-RS Binge; Ω p<0.05 WT ST vs WT Binge; c p<0.05 CB1-KO ST vs WT Binge; + p<0.05 WT Binge vs CB1-KO Binge; Data are expressed as mean ± SEM; 4-13 mice per group).

Finally, to better characterize the depressive phenotype, we evaluated anhedonia. Anhedonia was measured in withdrawal conditions in a sucrose preference test based on a two-bottle choice paradigm. CB1-KO and CAMKII-CB1-RS mice fed with standard diet showed a significantly reduction of the percentage of preference for sucrose 2% compared to WT mice, which was an indicator of anhedonia and was congruent with the depressive-like behavior found (Figure 92). However, mice exposed to intermittent chocolate diet showed a reverse tendency with WT mice presenting reduced preference for sweet solution.

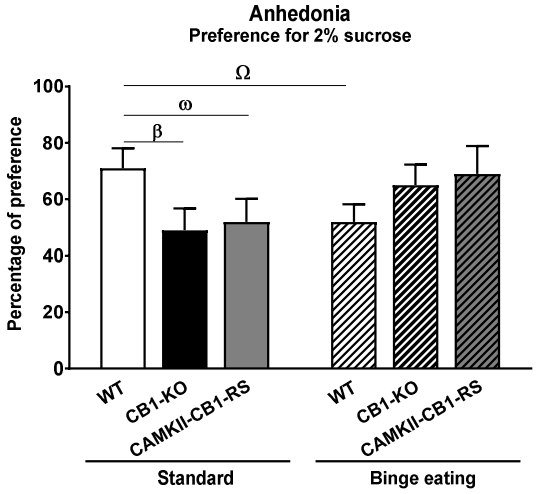

Figure 92. **Anhedonia was measured in a sucrose preference test.** Mean of 2 days of preference for 2% sucrose (U Mann-Whitney; β $p<0.05$ WT ST vs CB1-KO ST; ω $p<0.05$ WT ST vs CAMKII-CB1-RS ST; Ω $p<0.05$ WT ST vs WT Binge; Data are expressed as mean ± SEM 7-13 mice per group).

The expression of CB_1R in CAMKIIα^+ neurons is sufficient to rescue the body weight CB1-KO phenotype but not the food intake

Body weight was measured weekly as shown in Figure 93. A significantly increased body weight in CMAKII-CB1-RS mice and WT mice as compared to CB1-KO mice was found during all weeks (Repeated measures ANOVA; genotype effect, P<0.001). Thus, the selective expression of CB_1R in CAMKIIα^+ neurons is sufficient to rescue the lean CB1-KO phenotype.

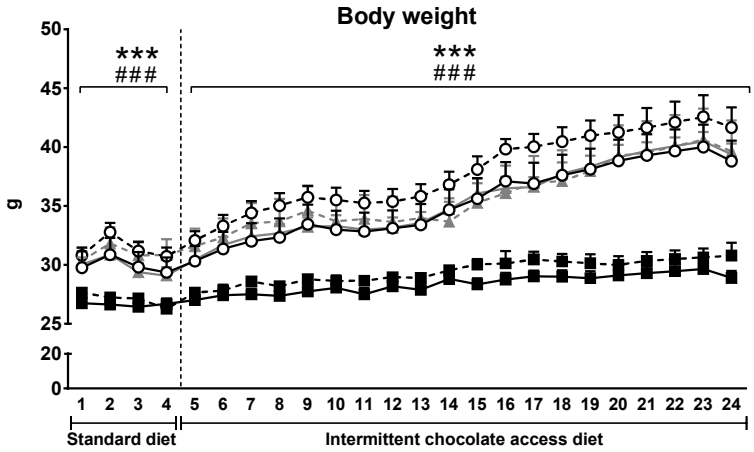

Figure 93. Body weight. Body weight was measured weekly during the whole experimental sequence in WT, CB1-KO and CAMKII-CB1-RS animals exposed to standard diet or intermittent chocolate access diet (Repeated measures ANOVA; genotype effect, *** p<0.001 CB1-KO vs CAMKII-CB1-RS, ### p<0.001 WT vs CB1-KO; Data are expressed as mean ± SEM; 8-13 mice per group).

We measured the total kcal intake at 2.5h, 24h and 48h to control food intake at the beginning of each weekly binge eating cycle. Increased caloric intake was observed in the binge eating group compared to standard animals during the entire experimental procedure (Figure 94a-c). Around 60% of kcal ingested by these mice at 2.5h were

obtained from the chocolate mixture indicating that this type of food was rewarding and produced binge behavior. At 24h and 48h, the percentage of chocolate intake was reduced to 40%. Considering that the binge behavior is measured by the intake at the first 2.5 h, CAMKII-CB1-RS and CB1-KO mice showed a similar total kcal intake, suggesting that the CB_1R expression in $CAMKII\alpha^+$ neurons is not sufficient to rescue the reduced food intake phenotype of the total CB_1R loss.

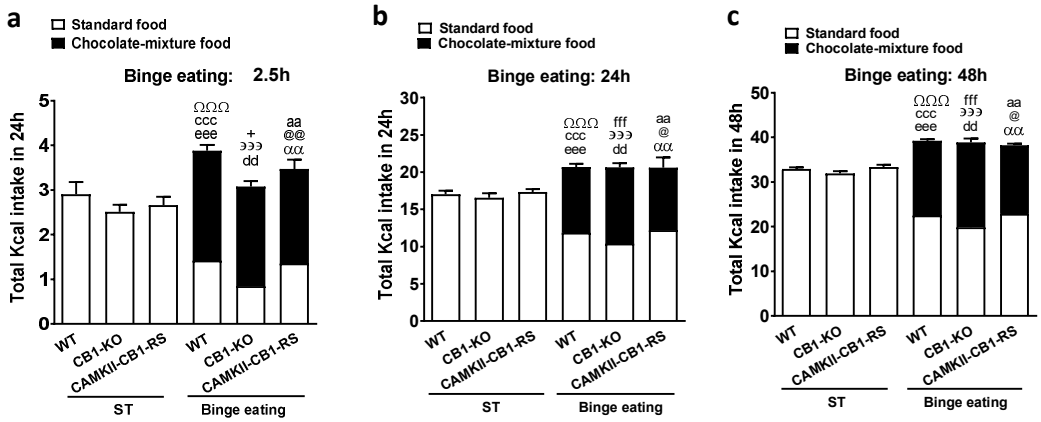

Figure 94. **Binge eating cycles. a,** Mean number of total Kcal intake in the first 2.5h of total binge eating cycles. **b**, Mean number of total Kcal intake in 24h of total binge eating cycles. **c**, Mean number of total Kcal intake in 48h of total binge eating cycles (t-test, ΩΩΩ p<0.001 WT ST vs WT Binge; ϶϶϶ p<0.001 WT ST vs WT Binge; aa p<0.01 WT ST vs CAMKII-CB1-RS Binge; ccc p<0.001 CB1-KO ST vs WT Binge; dd p<0.01 CB1-KO vs CB1-KO Binge; αα p<0.01 CB1-KO ST vs CAMKII-CB1-RS Binge; eee p<0.001 CAMKII-CB1-RS ST vs WT Binge; fff p<0.001 CAMKII-CB1-RS vs CB1-KO Binge; @ p<0.05, @@ p<0.01 CAMKII-CB1-RS ST vs CAMKII-CB1-RS Binge; + p<0.05 WT Binge vs CB1-KO Binge; Data are expressed as mean ± SEM; 8-13 mice per group).

Finally, no differences in locomotor activity (total activity, horizontal and vertical activity) were reported between genotypes discarding a possible effect of the CB_1R rescue (Figure 95).

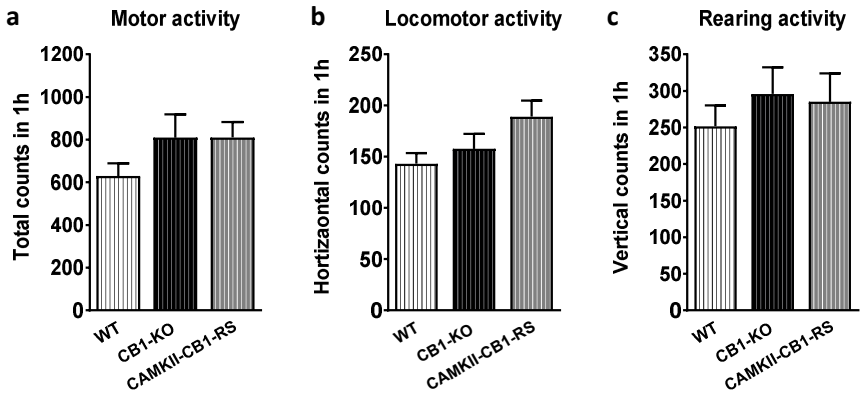

Figure 95. Locomotor activity. a, Motor activity measured by total counts in 1h. **b**, Locomotor activity measures as by horizontal counts in 1h. **c**, Rearing activity measured by vertical counts in 1h (Data are expressed as mean ± SEM; 9-15 mice per group).

Discussion

The easy access to hypercaloric and palatable foods with high addictive property in Western societies is a major contributing factor for the compulsive eating and development of food addiction and obesity. Food addiction, obesity and binge eating disorder have been closely linked (Pursey *et al.*, 2014). The concept of food addiction is still controversial and the term is not included in the DSM-5 but the construct is evolving and a validated tool for diagnosis, the Yale Food Addiction Scale (YFAS, 2.0) is widely accepted by the scientific community (Gearhardt *et al.*, 2016). This instrument is based on the criteria applied in the DSM-5 for substance use disorders, considering the increasing evidence that food addiction shares common neurobiological mechanisms with drug addiction (Lindgren *et al.*, 2018). Both, food and drug addiction are complex multifactorial chronic brain disorders that result from the interaction of multiple genes and environmental factors. Therefore, not everyone exposed to palatable food loss the control over food intake and develops food addiction suggesting an interindividual variability in the development of this addictive process. However, the precise neurobiological mechanisms underlying vulnerability or resilience to food addiction have remained elusive. By using mouse operant behavioral models combined with genetic modified mice, electrophysiological *ex-vivo* recordings, genome-wide RNA and DNA methylome sequencing, chemogenetic interference and adenoviral gene delivery, we have characterized the phenotype of resilience and vulnerability to develop compulsive intake at, genetic, epigenetic, cellular, circuit and behavioral level with special focus on the endocannabinoid and DA

systems. Understanding the neurobiological reasons leading to increased susceptibility to loss the behavioral control could be crucial to design appropriate personalized treatments for compulsive eating, which represents a transdiagnostic criterion in food addiction, binge eating disorder and obesity.

1. A specific top-down cortical pathway regulates resilience and vulnerability to develop food addiction

Three major interconnected networks are involved in the development of addiction: the limbic system, the extended amygdala and the PFC. These domains constitute three hotspots of the addiction cycle that are repetitively linked to behavioral stages that worsen over time (Koob and Volkow, 2016; Moore *et al.*, 2017). Notably, the PFC is involved in top-down regulation of cognitive flexibility, decision-making and inhibitory control and seems to play a crucial role in the transition from controlled to compulsive intake (Miller and Cohen, 2001; Chen *et al.*, 2013). This area is composed mainly by excitatory glutamatergic pyramidal neurons and inhibitory GABAergic interneurons establishing a local network that its excitability is regulated presynaptically by the CB_1R (Kano *et al.*, 2009). Considering these evidences, we predicted that the modification on the excitability of the cortical network could reproduce the resilient and the vulnerable phenotype to develop food addiction.

1.1. Investigating the modulation of cortical glutamatergic excitability by CB_1R in the resilience to develop food addiction

We first studied the phenotype of food addiction in conditional glutamatergic CB_1R mutant mice (Glu-CB1-KO) and their control littermates in an inbreed C57BL/6N background mouse strain. We used a behavioral animal model with high translational face validity to human addiction that we have recently validated (Mancino *et al.*, 2015). Thus, we mimicked the transition to addiction after repeated seeking of palatable food in an operant training during 118 sessions. We found that one quarter of a large cohort of WT mice (n=56) was classified as addicted mice, similar to the prevalence reported in humans (19.9%) using the YFAS food addiction diagnosis (Pursey *et al.*, 2014) and similar to the percentage obtained in an outbreed mouse population (Mancino *et al.*, 2015). Our findings showed that the lack of CB_1R in dorsal telencephalic glutamatergic neurons induced a strong resilience to food addiction, as revealed by the significantly reduced percentage (6.9%) of addicted mice in the mutant group. Glu-CB1-KO mice were characterized by less perseverance, reduced motivation and decreased compulsivity for highly palatable food. This resilient phenotype was not influenced by the body weight variable. Indeed, no correlation between addiction criteria and body weight was found, although mutants showed lower body weight in the late period.

Previous studies have reported that Glu-CB1-KO mice presented a phenotype with a reduction of the exploratory behavior (Häring *et al.*, 2011), increased neophobia (Lafenêtre *et al.*, 2009), high passive fear

response after conditioning, decreased food intake after fasting (Bellocchio *et al.*, 2010; Lutz *et al.*, 2015) reduced odor detection (Soria-Gómez *et al.*, 2014) and a facilitation of the associative learning (Martín-García *et al.*, 2016) (Figure 96). Indeed, cocaine self-administration studies showed a better association between the cue-light or the shock with the cocaine infusion and facilitated reversal learning in Glu-CB1-KO mice compared to WT mice (Martín-García *et al.*, 2016). The increase in cue-induced cocaine seeking was not associated with augmented motivation in PR or with compulsive seeking in shock test (Martín-García *et al.*, 2016). In agreement, Glu-CB1-KO mice showed, in our experiment with palatable food, an increased aversive associative learning tested in the shock-associated cue test. Based on these results, we hypothesized that enhanced facilitation in the associative learning could be related to an increased control of reward seeking and be considered as a protective factor to loss the behavioral control.

In the next step, we used an electrophysiological approach to evaluate the hypothesis that increased glutamatergic neuronal activity in mPFC and in their projections to the NAc plays a key role in the improved inhibitory control observed in Glu-CB1-KO mice. Our electrophysiological data revealed an increased excitatory synaptic transmission from L2/3 onto pyramidal glutamatergic neurons in L5 of the PL cortex in Glu-CB1-KO mice, as shown by the increase in mEPSCs frequency and PPF ratio. The absence of presynaptic CB_1R produces a lack of inhibition of glutamate release. These results revealed that the

deletion of CB_1R may produce an enhancement in glutamate vesicle release in a local network in the PL cortex. In agreement, previous results revealed an increased hippocampal long-term potentiation formation in animals lacking CB_1R in cortical glutamatergic neurons accompanied with increased spine density and dendritic branching, that might be resulting from the improved glutamate release (Monory *et al.*, 2015). In the following diagram, it is summarized the characterization of the Glu-CB1-KO mice phenotype (Figure 96).

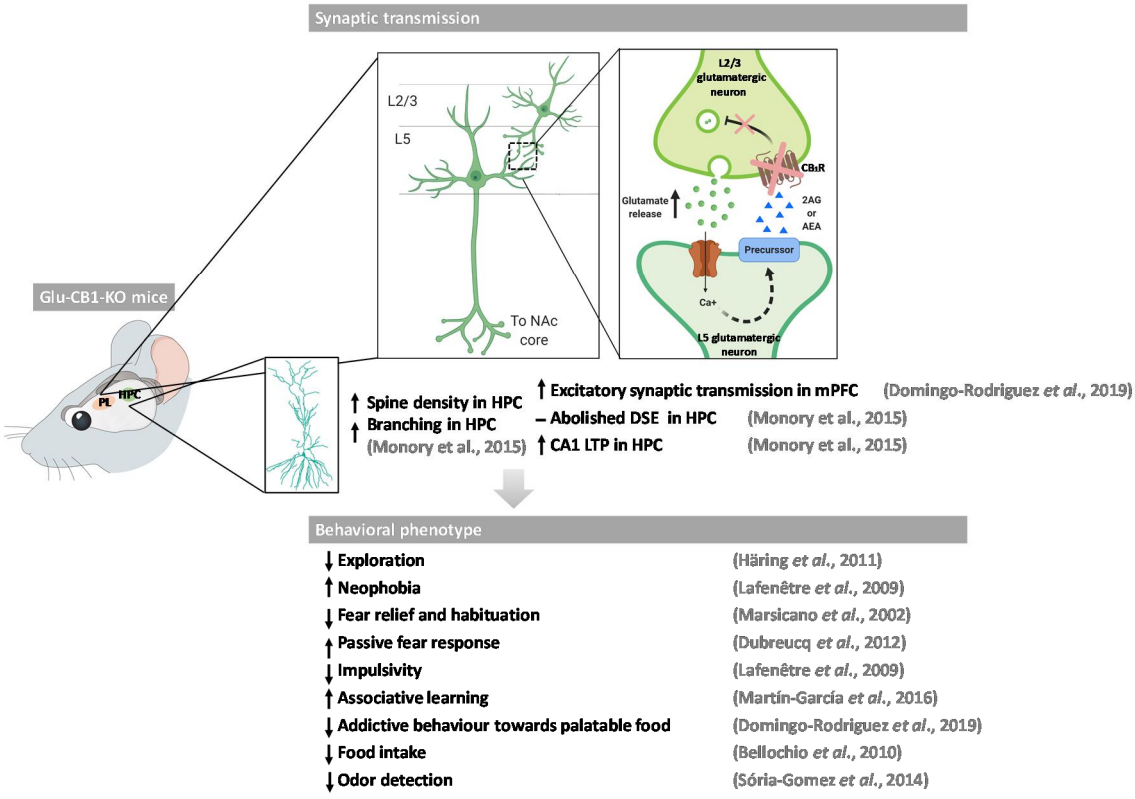

Figure 96. Characterization of conditional mutant mice lacking CB_1R in dorsal telencephalic glutamatergic neurons (Glu-CB1-KO) compared to control wild type mice. HPC, hippocampus; PFC, prefrontal cortex; LTP, long-term potentiation; DSE, depolarization-induced suppression of excitation (Adapted from Lutz *et al.*, 2015).

The blockage of CB_1R in all cells by using pharmacological or genetic tools showed a decrease in the addictive-like behavior (Mancino *et al.*, 2015) similar to the Glu-CB1-KO protective phenotype. However, the precise pathways and cell-subpopulations involved have not been characterized. In our study, we revealed that the main cells involved are the dorsal telencephalic glutamatergic neurons. Thus, the Glu-CB1-KO mice display the phenotype of the total CB1-KO, in spite of the less abundance of the CB_1R in glutamatergic than in GABAergic neurons (Steindel *et al.*, 2013; Martín-García *et al.*, 2016). This is explained by the higher connectivity of pyramidal neurons and the more effective signal transduction mechanisms of CB_1R in glutamatergic than in GABAergic cells, leading to this cell-type population a powerful control over local synaptic strength (Monory *et al.*, 2015).

1.2. Involvement of the glutamatergic PL neurons in the vulnerability and resilience to develop food addiction

Once we have found that the modulation of the cortical glutamatergic system excitability is mediating the susceptibility to develop food addiction, we studied the possible specific region within the mPFC that could play a prominent role. Previous data pointed out that the PL subregion of the mPFC is particularly involved in the addictive processes (Moorman *et al.*, 2015). Indeed, PL neurons excitability is dramatically reduced after a long cocaine self-administration exposure with the strongest effect in compulsive cocaine seeking rats (Chen *et al.*, 2013). In these rats, stimulation of the PL cortex by *in vivo* optogenetics suppressed the compulsive-behavior (Chen *et al.*, 2013).

In the same line, the repetitive transcranial magnetic stimulation applied to the human dlPFC, equivalent to the rodents PL cortex, reduced cocaine use and craving (Terraneo *et al.*, 2016). Therefore, we chose this subregion of the mPFC and we decreased the glutamatergic activity of the PL region by using a Cre-dependent chemogenetic approach in Nex-Cre mice. CNO-induced silencing of glutamatergic neurons in hM4Di-injected mice increased the percentage of addicted animals, showing high values in motivation and compulsivity for palatable food. These results revealed a crucial role of the PL region in the development of food addiction and are in agreement with the previous data indicating that PL activation mimics addictive behavior.

In contrast, other reports suggested that the PL is more involved in promoting addictive behavior rather than suppressing it. Thus, pharmacological inactivation of PL blocked cue-induced reinstatement of cocaine (McFarland and Kalivas, 2001) and photoinhibition of PL attenuated cocaine-induced reinstatement (Stefanik *et al.*, 2013). These apparently opposite functions of the PL area could be explained by the reward-related paradigm used. We are using a self-administration model combined with a punishment (footshock associated with reward), whereas the other studies used a reinstatement model (environmental cue associated with reward). Both paradigms rely on the association between environmental factors and reward. Therefore, it could be suggested that the PL mediates response conflict and is recruited in either reinforcing or aversive associative learning, playing a key role in both reinstatement or

punishment models (Jasinska *et al.*, 2015; Smith and Laiks, 2018). Based on these results, the phenotype of better associative learning suggested in Glu-CB1-KO mice is congruent with the increased excitability of the PL area, indicating that these mice have an enhanced association between the cue and the punishment with the reward, conferring an augmented inhibitory control. Taking into account the crucial role given to the amygdala in the addiction framework in forming associative fear- and reward-related memories (Russo and Nestler, 2013), we could speculate that in Glu-CB1-KO mice the activity of this area could also be altered. Additional research is needed to study the involvement of the amygdala in the development of food addiction.

1.3. Involvement of the selective PL-NAc core pathway in the loss of control over food intake

Our study has revealed the involvement of the glutamatergic system in the PL area in the development of compulsive eating. However, it remains still unknown which is the specific downstream target of PL projections involved in food addiction. Pyramidal glutamatergic neurons of the PL cortex project to different brain areas, such as the hippocampus, VTA, amygdala and NAc among others, conferring to the mPFC a complex connectivity role as a central hub of communications (Moorman *et al.*, 2015). Considering that the PL area preferentially projects to the core part of the NAc (Riga *et al.*, 2014; Cui *et al.*, 2018), we specifically targeted the PL-NAc core pathway using a dual viral vector approach. For this purpose, we injected an AAV expressing a

Cre-dependent inhibitory DREADD in PL and a retrograde AAV-variant expressing *Cre* recombinase into the NAc core to specifically inhibit this network. Using this dual viral vector approach in combination with a chronic delivery of CNO ligand, we found that the silencing the PL-NAc core projections enhanced specifically the compulsive eating behavior and animals could not stop palatable food self-administration despite negative consequences. The other addiction criteria, persistence to response and motivation, were not modified with this pathway modulation. These criteria represent different endophenotypes from compulsivity and consequently, the neuronal pathways recruited could be different. In the persistence to response, mice have difficulty to stop food seeking, although pressing the active lever is not reinforced. Thus, the reward is not present and this behavior could indicate a persistent desire or unsuccessful efforts to cut down due to an habit formation or disruption of extinction learning. This process involves hippocampal and dorsal striatal pathways (Schmitzer-Torbert *et al.*, 2015). In turn, motivation is more related to reward processing and involves VTA and NAc pathways (Volkow *et al.*, 2017).

The successful silencing of PL-NAc core cortical pyramidal neurons using our dual vector approach was demonstrated by patch-clamp experiments, showing a decreased firing rate and membrane resistance in neurons expressing hM4Di receptors exclusively in the presence of CNO. This result confirms that driving compulsive food seeking was underlined by a reduced PL-NAc core activity. A recent study using resting-state functional connectivity identified a different

close network, the PL-ventral striatal circuit, that its connectivity became negative following a prolonged self-administration of methamphetamine (Hu *et al.*, 2019). This circuit was defined as the "Stop circuit" and was reported to be dysregulated in the compulsive behavior. In turn, a "Go circuit" formed by the orbitofrontal cortex-dorsal striatal projections is strengthened in the perseverance of reinforcement despite punishment (Pascoli *et al.*, 2015, 2018) (Figure 97).

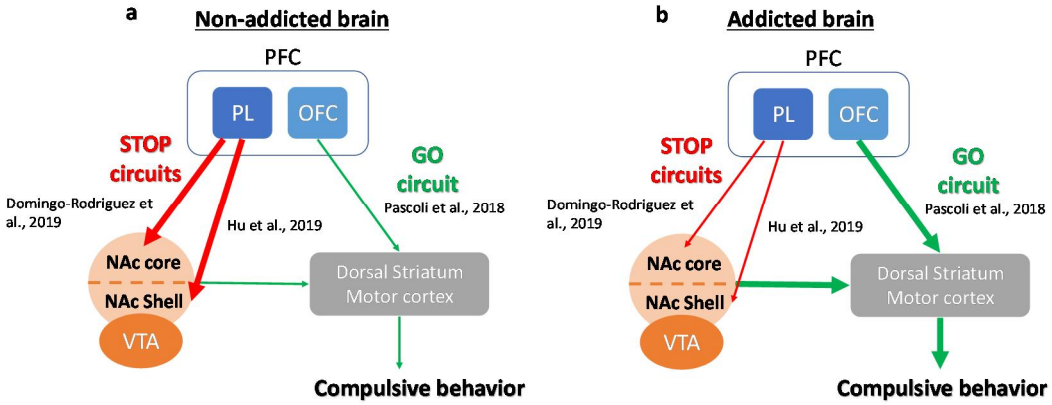

Figure 97. A simplified model proposing an imbalance of two neuronal circuits, the Go and the Stop circuits underlying addiction. a, Non-addicted brain. When these circuits result in proper inhibitory control and decision making**. b, Addicted brain**. During addiction, the enhanced expectation value of the substance in the reward overcomes the control circuit. This favors a positive-feedback loop initiated by the consumption of the drug. PFC, prefrontal cortex; PL, prelimbic; OFC, orbitofrontal cortex; NAc, nucleus accumbens; VTA, ventral tegmental area (Modified N. D. Volkow et al., 2011).

This is in agreement with the hypothesis that with chronic drug exposure more and more dorsal loops are recruited for habit formation. The possible involvement of the orbitofrontal-dorsal striatum pathway in the food addiction model has never been

investigated. Nevertheless, increased orbitofrontal activity has been reported in response to food palatable cues and following high-calorie beverage consumption in obese/overweight subjects (Yokum *et al.*, 2011; Tomasi *et al.*, 2015; Feldstein Ewing *et al.*, 2017). Thus, the orbitofrontal cortex is involved in attributing salience value to food, helping to assess its expected pleasantness and palatability as a function of its context (Volkow *et al.*, 2013). Together, these results suggest that compulsive palatable food intake could be the result of an imbalance between the Stop and the Go circuits. Identifying the individual strength of both networks may be helpful for restoring the physiological balance between them. Thus, individualized noninvasive brain stimulation therapies could be potentially useful to strengthen or weaken the stop and go circuits, respectively. To date, studies using high-frequency repetitive transcranial magnetic stimulation of the dlPFC reported reduced cocaine and food cravings in cocaine abusers and obese subjects (Terraneo *et al.*, 2016; Ferrulli *et al.*, 2019). The efficacy of this technique might be explained by the induction of long-term neuroplastic changes modifying the cortical excitability of the area stimulated and consequently the projections to subcortical areas (Diana *et al.*, 2017).

1.4. Analyzing the transcriptomic changes underlying the susceptibility to compulsive palatable food intake

After prolonged highly palatable food exposure, Glu-CB1-KO mice showed an enhanced inhibitory control to palatable food operant seeking that strongly reduced the transition from controlled to

compulsive seeking. However, a small percentage (6.9%) of mutant mice became addicted. Therefore, the lack of a single gene was not enough to totally block the transition to addiction, as expected for a multifactorial disease. This evidence highlights the complex and multifactorial nature of food addiction and prompted us to study the transcriptomic changes underlying the resilient and vulnerable phenotype to develop food addiction. The comparison of the transcriptomic profiles in the mPFC between addicted and non-addicted mice revealed an upregulation of four prominent genes in addicted mice independently of the genotype: *Drd2, Adora2A, Gpr88* and *Drd1.* All these genes encode G-protein-coupled receptors and are notoriously involved in the excitability modulation of neurobiological pathways recruited in addiction (Le Merrer *et al.*, 2012). D_2R and the adenosine A_{2A} receptor ($A_{2A}R$), encoded by *Drd2* and *Adora2A* respectively, are colocalized in the mPFC glutamatergic terminals. They synergistically interact inhibiting the cortical synaptic transmission (Real *et al.*, 2018) contrary to the well stablished postsynaptic antagonistic interaction between these two receptors in the GABAergic MSNs of the striatum (Ferre *et al.*, 2008). This result is in accordance with our hypothesis of decreased excitability of glutamatergic synaptic transmission in the mPFC of addicted mice. Regarding *GPR88*, inactivation of this gene enhanced the excitability of both D1 and D2 MSNs in the striatum (Quintana *et al.*, 2012). Thus, we could speculate that the upregulation of GPR88 in the mPFC could contribute to inhibit the glutamatergic transmission. With respect to *Drd1* gene, D_1R in the striatum conforms the direct pathway (GO) which promotes the

approach to addictive behavior opposite to the D_2R stimulating the indirect pathway (NO GO) (Salgado and Kaplitt, 2015) (Figure 98). In contrast, in the mPFC, D_1R stimulation decreases the release of glutamate onto L5 pyramidal cells (Gao *et al.*, 2001) similar to D_2R does (Real *et al.*, 2018). Moreover, the activation of D_1R reduced GABA release onto cortical FS interneurons that are inhibiting the pyramidal cells (Towers and Hestrin, 2008) Thus, the increased of D_1R in the addicted mPFC could contribute to the decreased excitability of the glutamatergic projecting NAc neurons.

In this thesis, we have focused on the *Drd2* gene because it is the most differentially expressed gene in addicted mice, and to our knowledge, this is the first study revealing an increased expression of the gene encoding for D_2R in the mPFC in the context of addiction. In contrast, the levels of D_2R in the striatum has been classically implicated in this disorder (Volkow *et al.*, 1993). Thus, neuroimaging studies reported a downregulation of D_2R in the striatum, which correlated with a hypofunction of the PFC in cocaine abusers (Volkow *et al.*, 1993, Wang *et al.*, 2001). In agreement, a specific *Drd2* polymorphism (rs1800497) was associated with the "Reward deficiency syndrome", consisting in a hypodopaminergic state due to the compromised D_2Rs (Blum *et al.*, 1996). The decreased of D_2R activity in the striatum promotes susceptibility to compulsive behaviors trying to compensate for the insufficient DA activity (Wang *et al.*, 2001). However, the specific role of the D_2R in the mPFC in compulsive intake remains unknown.

In the mPFC, D_2R is mainly localized presynaptically in the terminals of L2/3 glutamatergic cortical layers producing an inhibitory effect on the L5 glutamatergic neurons (Real *et al.*, 2018) (Figure 98). Previous studies have also demonstrated that the excitatory neurotransmission from deep cortical layers to limbic structures, specifically the PL-NAc core projections, is regulated by presynaptic D_2R in the NAc (Cui *et al.*, 2018). These specific glutamatergic projections from the PL area directly innervate the D2-MSNs in the NAc that are integrated into the indirect pathway (Cui *et al.*, 2018). The activation of D_2R diminishes the presynaptic release of glutamate from PL to NAc D2-MSNs (Cui *et al.*, 2018) (Figure 98). Therefore, the modulation by DA of the deep layer circuits through D_1R and D_2R in the mPFC is extremely complex and the final output may result from summed actions or different receptors in glutamatergic cells and interneurons (Tritsch and Sabatini, 2012).

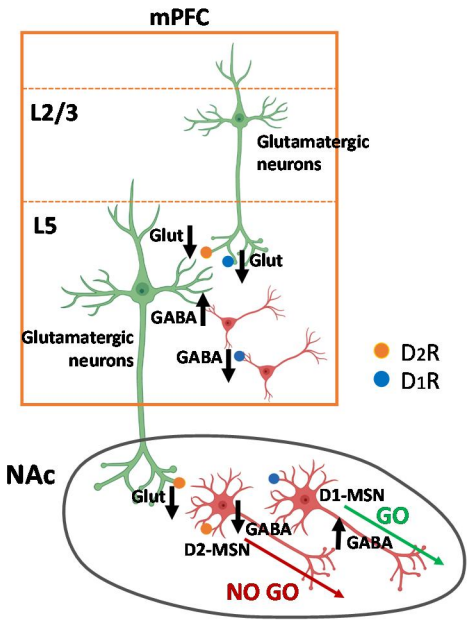

Figure 98. Simplified diagram of the principal localization of D_1R and D_2R and their function in the medial prefrontal cortex (mPFC) and nucleus accumbens (NAc).

1.5. Role of D_2R in the vulnerability and resilience to develop food addiction

According to these findings and to our previous transcriptomic and chemogenetic results, we predicted that the upregulation of *Drd2* gene in PL-NAc core pathway could have a critical role in promoting the vulnerability to develop food addiction by decreasing the excitability of this pathway. Our *in situ* hybridization experiments demonstrated endogenous *Drd2* mRNA expression in the PL of naïve WT mice, although at very low levels close to the limit of detection. Therefore, we assume that addicted mice may have a significant increase in endogenous *Drd2* mRNA levels based on gene expression results. We aimed at mimicking the upregulation of *Drd2* gene expression found in the mPFC of addicted mice by overexpressing D_2R selectively in the PL-NAc core projections. Our results revealed that mice overexpressing D_2R in this pathway showed enhanced compulsive eating behavior despite the aversive consequences. Additionally, *in vitro* electrophysiological recordings in L5 PL pyramidal neurons projecting to NAc core with a D_2R overexpression revealed a decreased firing rate and membrane resistance after the application of the D_2R selective agonist quinpirole or dopamine. This result confirmed that the overexpression of D_2R reduced the excitability of this specific cortico-subcortical pathway.

Therefore, our results provide a new mechanism of the loss of inhibitory control for food seeking behavior involving the D_2R in PL cortical projections to NAc core. In particular, the upregulation of D_2R

diminished the excitability of the pyramidal neurons in the PL projecting to NAc core. This upregulation is supposed to occur in both postsynaptic dendrites in the PL area and in the presynaptic glutamatergic terminals in the NAc core. It was previously reported that the inhibition of the D2-MSNs in the NAc core enhanced motivation for cocaine in a self-administration paradigm, but not for standard food (Bock *et al.*, 2013). Other studies, showed that the upregulation of D_2R in D2-MSNs enhances the willingness to work for food by weakening the canonical indirect pathway projections to the ventral pallidum (Gallo *et al.*, 2018). Considering these results, we predict that reduced glutamatergic transmission in the NAc core coming from PL will decrease the activation of D2-MSN indirect pathway, thereby suppressing the avoidance behavior (NO GO response) and promoting the loss of control towards palatable food consumption, characterizing the vulnerable phenotype (Figure 99). In turn, the resilient phenotype showed in our mutants may be underpinned by the increased excitability of the glutamatergic transmission in the PL and in the NAc core due to the lack of the CB_1R. We postulate that increased activation of PL-NAc projections stimulates the GABAergic D2-MSNs indirect pathway, thereby facilitating the avoidance behavior (NO GO response) (Figure 100).

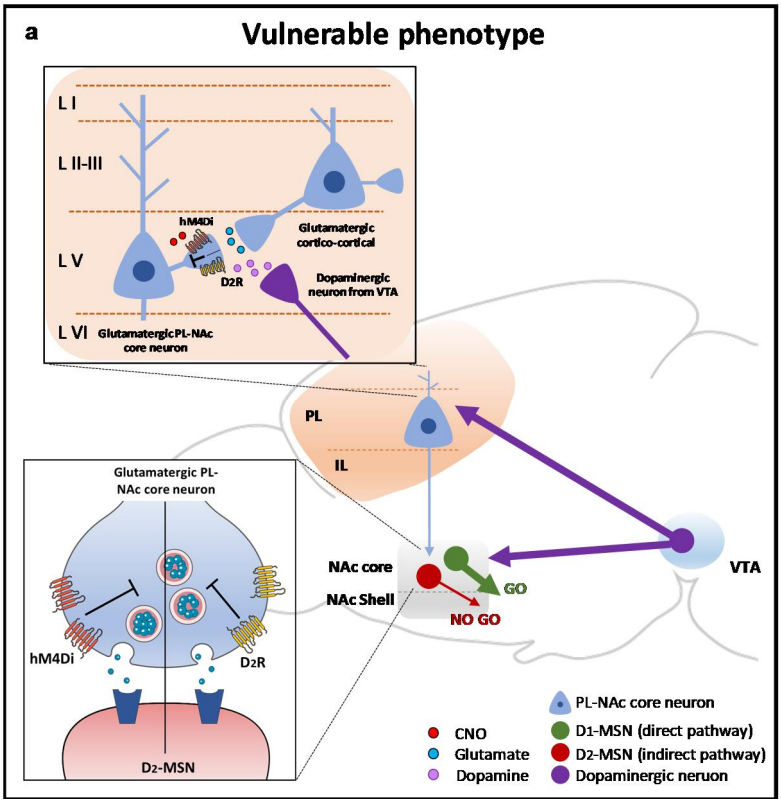

Figure 99. Schematic summary of the PL mPFC-NAc core pathway regulation of vulnerability to develop food addiction. Overexpression of hM4Di receptors or D_2R in PL neurons projecting to NAc core and the subsequent activation of these receptors by CNO and dopamine, respectively, produced a decreased excitatory transmission of this network, thereby reducing the activation of D2-MSN indirect pathway in NAc core. The decreased activity of the indirect pathway suppressed the avoidance behavior (NO GO response) facilitating the D1-MSN direct pathway activity promoting the approach behavior (GO response). PL, prelimbic; IL, infralimbic; NAc, nucleus accumbens; VTA, ventral tegmental area; D1-MSN, dopamine D1 medium spiny neuron; D2-MSN, dopamine D2 medium spiny neuron; D_2R, dopamine D2 receptor; hM4Di, human muscarinic 4 designer inhibitory Gi receptor.

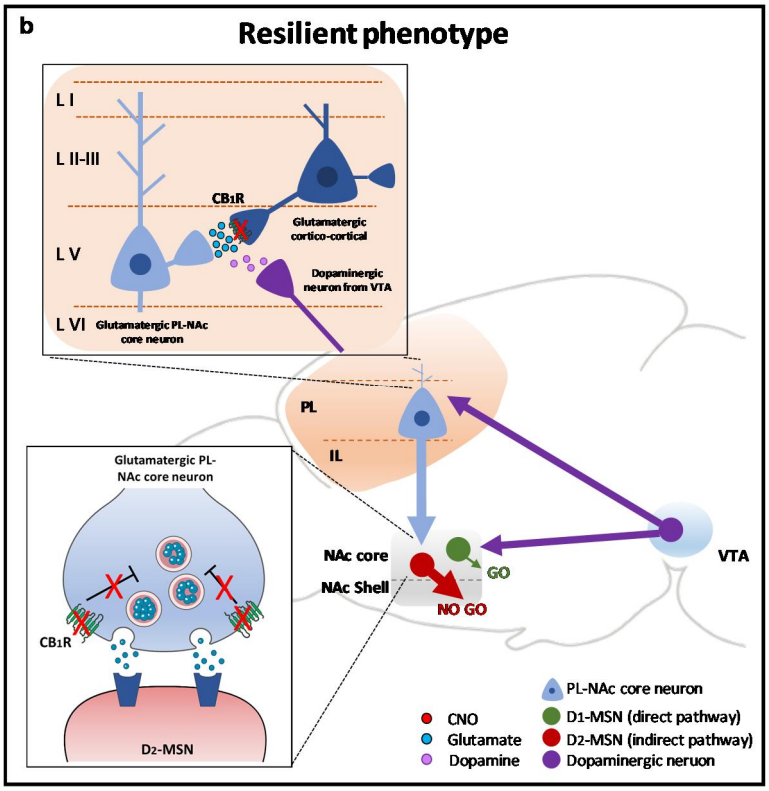

Figure 100. Schematic summary of the PL mPFC-NAc core pathway regulation of resilience to develop food addiction. Deletion of the CB_1R in dorsal telencephalic glutamatergic neurons increased glutamate release in local cortical networks increasing excitatory glutamatergic transmission in L5 prelimbic neurons projecting to NAc core. Subsequently, the increased glutamatergic transmission from cortical pyramidal neurons stimulated D2-MSN indirect pathway in NAc core facilitating the avoidance behavior (NO GO response). PL, prelimbic; IL, infralimbic; NAc, nucleus accumbens; VTA, ventral tegmental area; D1-MSN, dopamine D1 medium spiny neuron; D2-MSN, dopamine D2 medium spiny neuron; D_2R, CB_1R, cannabinoid receptor type-1.

In summary, we elucidated the crucial role of the glutamatergic PL-NAc core pathway modulated by CB_1R and D_2R as a critical mechanism for the loss of inhibitory control for palatable food seeking and consumption. The increase in the activity of this pathway plays a key role in resilience to develop food addiction.

2. Differential epigenetic profile of vulnerable and resilient phenotypes to develop food addiction

The purpose of the following study was to investigate the neurobiological mechanisms underlying why some individuals are vulnerable to the molecular changes induced by palatable food while others remain resistant. Such as in the previous study, we used inbreed mice on a C57BL/6 J background to control the genetic variable. Thus, we questioned why genetically homogeneous mice with a constant environment presented different susceptibilities to addition. This question appeals to the "stochastic individuality" term, which is defined by behavioral variance despite identical genotypes exposed to similar environments (Honegger and de Bivort, 2018). A plausible answer to this question is the epigenetic changes caused by small differences in the environment (Nestler and Lüscher, 2019). This is supported by human studies performed in monozygotic twins. Indeed, the examination of differences in DNA methylation and histone acetylation of a large cohort of monozygotic twins revealed remarkable differences in their overall content and genomic distribution of 5-methylcytosine DNA and histone acetylation affecting the whole gene-expression (Fraga *et al.*, 2005). These epigenetic differences have been prompted to explain the different susceptibility to develop psychiatric diseases, such as schizophrenia and bipolar disorder (Dempster *et al.*, 2011). Preclinical studies have investigated the epigenetic alterations induced by drugs of abuse (Nestler, 2014). However, the epigenetic signatures produced by prolonged palatable food intake or the

epigenetic changes that could confer a different vulnerability to develop food addiction have never been investigated.

In this thesis, we evaluated the epigenetic signatures of food addiction resilient and vulnerable phenotype. For this purpose, we studied the DNA methylation and the miRNAs profiling at the genome-wide level of the mPFC and NAc in extreme addicted and non-addicted mice to palatable food. Animals were exposed to chocolate-flavored pellets and standard pellets as a control, in the food addiction mouse model. Similar to our first study, 23.5% of WT mice from the chocolate group displayed an addictive-like behavior with enhanced persistence to response, increased motivation and augmented compulsivity, compared to 0% of the standard group. Afterward, we ordered the addicted and the non-addicted animals to define the susceptibility to develop food addiction by using the individual scores achieved in the 3 addiction criteria and considering 4 additional phenotypic traits as factors of vulnerability to addiction (Figure 101). Not all the 4 phenotypic traits risk factors had similar relevance, and we quantified their strength depending on its correlation with the 3 addictive behavior. The phenotypic trait that had the best correlation with the addictive criteria was the impulsivity trait. This was consistent with the strongest evidence for an association between the impulsivity personality trait and addiction (Koob and Volkow, 2010). In agreement, it was demonstrated that the transition to compulsive drug intake can be predicted by measures of impulsivity (Belin *et al.*, 2008). Similarly to drugs, a previous study in rats demonstrated that the impulsivity trait

confers an increased propensity to develop food addiction-like behaviors with uncontrollable overeating of palatable food (Velázquez-Sánchez *et al.*, 2014). The cognitive flexibility trait was the second phenotypic trait that correlates with addiction, with higher values of inflexibility shown in addicted mice. Cognitive flexibility measures the ability to change responding to a previously rewarded stimulus (Stalnaker *et al.*, 2009). Addiction involves a disruption in this cognitive ability associated with a hypofunction of the prefrontal and orbitofrontal cortical areas. Drug addicted mice have been reported to show difficulties in changing drug-seeking triggered by stimuli associated with drug reward (Goldstein and Volkow, 2011; Kakoschke *et al.*, 2018). The remain two phenotypic traits evaluated were related to associative learning. Aversive associative learning (association between the cue and the punishment) was impaired in addicted mice and significantly correlated with addiction criteria. However, the appetitive associative learning (association between the cue and the reward) was not significantly correlated. This cue-reactivity trait is often triggered by cues in the environment that have been previously associated with drug-taking experience. Individuals for whom the cue reaches incentive salience are the ones most likely to exhibit relapse (Saunders and Robinson, 2010). The lack of significant results could be explained by the fact that different addiction-related traits are associated with different phases of addiction (Morrow and Flagel, 2016) and in our case we are not evaluating relapse. In contrast, we observed in our first experiment that Glu-CB1-KO mice with a resilient phenotype displayed a facilitated appetitive associative learning. This

apparent discrepancy could be explained because the association between an environmental stimulus and a reward is a normal learning process. However, chronic exposure to the addictive substance in vulnerable individuals leads to long-lasting changes in the circuits underlying learning and memory processes. Consequently, aberrant learning emerged in the addicted subjects under these conditions, attributing incentive salience to the conditioned stimulus. Cues are already sufficient to stimulate craving for the drug (Torregrossa *et al.*, 2011).

Considering these addiction criteria and these addicted-related factors, animals were ordered in a quantitative gradual addiction scale (Figure 101).

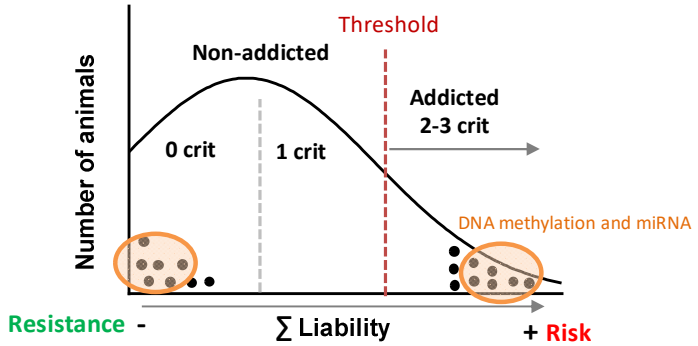

Phenotypic traits as protective factors
1. Low impulsivity
2. High cognitive flexibility
3. High aversive associative learning
4. Low salience cue-reactivity (aberrant learning)

Phenotypic traits as risk factors
1. High impulsivity
2. Cognitive inflexibility
3. Low aversive associative learning
4. High salienced cue-reactivity (aberrant leaning)

Figure 101. Classification of the addicted and non-addicted animals on a quantitative gradual addiction scale. The most extreme mice were selected to perform the analysis of the differential DNA methylation and the miRNA changes.

2.1. Investigating the DNA methylation changes of targeted upregulated addiction genes

We used methyl-binding protein immunoprecipitation followed by high throughput sequencing (MBD-seq) to study the DNA methylation in the mPFC of ordered extreme food addicted compared to non-addicted mice. In a first step, we used a targeted approach to analyze the epigenetic changes produced in the 4 candidate genes (*Drd2, Adora2a*, *Gpr88* and *Drd1*), in which we found a pronounced gene upregulation in addicted mice in the previous transcriptomic study. The evaluation of the whole DNA methylome changes will be performed In future studie.

The direct correlation between DNA methylation with transcriptional adaptations is really complex. Although methylation in promoter regions and intron 1 are mostly associated with transcriptional repression (Anastasiadi *et al.*, 2018), methylation in intragenic regions is associated with enhanced gene expression (Kato and Iwamoto, 2014). The deceased methylation found in *Adora2a* and *Gpr88* in 5' and intron 1 genomic regions is aligned with the increased expression obtained in the RNA-seq. No significant results were obtained with respect to *Drd1*. However, there was a decreased DNA methylation in intron 6 and exon 7 in contiguous genomic regions of *Drd2* gene. These regions are involved in the alternative splicing of *Drd2* resulting in long (D2L) or short (D2S) isoforms (Usiello *et al.*, 2000). It has been described that a specific polymorphism in intron 6 altered the D2S/D2L splicing, reducing the formation of D2S relative to D2L, which was associated

with higher susceptibility to cocaine abuse (Moyer *et al.*, 2011). Therefore, we could speculate that the increased expression of *Drd2* found in food addicted mice could be underlied by an imbalance of the alternative splicing in favor of the D2L isoform produced by an intron 6 genomic region hypomethylation. The enhancement of the postsynaptic D2L isoform could reduce the excitability of the cortical-subcortical pathways producing a vulnerable phenotype to develop food addiction. In agreement, we reproduced in our previous study this vulnerable phenotype by overexpressing the D2L in the PL-NAc core pathway.

Overall, our DNA methylome results are in accordance with our transcriptomic observations in addicted mice, suggesting that the epigenetic changes could explain the individual susceptibility to loss the behavioral control over food intake in a similar genetic mouse population with a controlled environment.

2.2. miRNA profile of vulnerable versus resilient mice to develop food addiction

In parallel to the DNA methylation study, we investigated the epigenetic miRNA changes using a non-targeted approach that evaluates the whole miRNA epigenetic signatures in the genome. We showed that a history of palatable food self-administration with a loss of behavioral control changes the expression profile of 11 miRNAs in the mPFC of vulnerable mice compared to the resistant ones. Addicted mice showed a marked reduction in the levels of miR-876, miR-211, miR-3085, miR-665, miR-3072, miR-124, miR-29c, miR-544, miR-137 in

the mPFC compared to non-addicted mice. Moreover, 2 miRNAs were upregulated in mPFC of addicted mice, miR-100 and miR-192. In contrast, no changes were observed in these mice in the NAc.

Interestingly, some of these miRNAs have been previously associated with drug addiction. Thus, it has been described that miR-124 is downregulated in the NAc of mice chronically exposed to cocaine (Chandrasekar and Dreyer, 2009) and is associated with cocaine dependence in a case-control study (Cabana-Domínguez *et al.*, 2018). Additionally, miR-124 is involved in the cocaine-mediated microglial activation through regulating microglial toll-like receptors and downstream transcriptional factors (Periyasamy *et al.*, 2018).

miR-137 is an important regulator of presynaptic plasticity due to the gene expression modulation of proteins involved in presynaptic vesicle trafficking and neurotransmitter releases, such as synaptotagmin-1, N-ethylmaleimide-sensitive fusion protein and complexin-1 (Siegert *et al.*, 2015). Cocaine self-administration decreased miR-137 in the NAc core and in the dorsomedial striatum (Quinn *et al.*, 2018). Moreover, several evidences support the involvement of miR-137 and its targeted genes network in neuropsychiatric traits, including schizophrenia risk (Sakamoto and Crowley, 2018), a condition that is highly comorbid with addiction and eating disorders (Buckley *et al.*, 2009; Kouidrat *et al.*, 2014).

miR-29c belongs to the miR-29 family highly expressed in the human and rodent nervous system. Reduced expression of miR-29c has been

reported in the NAc of mice following a model of methamphetamine- and cocaine-induced locomotor sensitization (Su *et al.*, 2019).

Together, all these results have in common a marked reduction in levels of miR-124, miR-137 and miR-29c in the NAc in the same line as our findings in the mPFC. These data are consistent with previous evidence indicating a strong modulation of both brain areas in the addictive process (Koob and Volkow, 2016) and with our observation involving PFC-NAc pathway in the loss of control over palatable food intake.

On the other hand, miR-192 and miR-665 have never been previously related to addiction, although miR-192 has been associated with obesity. This miRNA is increased in the exosomal miRNA profile in obese subjects, and treatment of lean mice with exosomes isolated from obese mice induces glucose intolerance and insulin resistance (Castaño *et al.*, 2018). In turn, miR-665 and one of its targeted genes, Abcc3, were dysregulated in microbiota colonization demonstrating that microbiota modulates host miRNA expression, which could regulate host gene expression (Dalmasso *et al.*, 2011). Interestingly, the gut microbiota is altered during diet-induced obesity (Cani *et al.*, 2016). Thus, the exposure to palatable food in vulnerable mice could modify the gut microbiota leading to changes in this miRNA.

Overall, our findings indicate the involvement of specific miRNAs in food addiction. However, the underlying targeted protein-coding genes and pathways through which miRNAs produced addiction-associated synaptic and circuit plasticity are still unknown. In a near future, we will start with the functional validation of three candidate miRNAs (miR-

137, miR-29c and miR-665) with the antagomiR approach to evaluate if their downregulation produces a vulnerable phenotype in a short period of time. In parallel, deep bioinformatics analysis combining miRNA, DNA methylation and transcriptomic data will be performed to find cross-talks and correlations between them and to identify the gene networks engaged. In addition, we still do not know whether both miRNA and DNA methylation changes are developed in the transition to addiction and/or are preexistent to this condition. Considering that DNA methylation is the more stable posttranscriptional modification (Bogdanović and Lister, 2017), epigenetic changes at this level could be produced at early stages of the development by specific environmental factors (Peña *et al.*, 2014). Thus, DNA methylation changes could be a predisposing factor to addiction. In contrast, an earlier study suggested that levels of addiction-related miRNAs are altered during each stage of the addiction process in vulnerable animals (Quinn *et al.*, 2018). Thus, miRNAs changes could be produced in the transition to addiction and our results could be a static picture just showing the changes at the end of the addiction cycle when a dramatical loss of the inhibitory control occurs.

Recent studies showed that epigenetic marks are differentially produced depending on the type of cells. Indeed, differentially DNA methylation in D1-MSN and D2-MSN of the NAc results in different susceptibility to social defeat stress (Hamilton *et al.*, 2018). Moreover, epigenetic modifications and the subsequent gene expression alteration occurred in glutamatergic neurons as opposed to GABAergic

cells of the orbitofrontal area in heroin abusers (Kozlenkov *et al.*, 2017). Therefore, these observations could explain our negative results in the NAc and suggest that future studies evaluating the epigenetic signature in food addicted mice have to consider the cell-type specificity (De Sa Nogueira *et al.*, 2018).

The current pharmacological treatments available for addiction and eating disorders act on a specific protein, such as opioid receptors, serotonin or DA reuptake. However, the recent advances in the genomic and epigenetic fields point out that targeting a set of genes involved in the pathology would provide a better therapeutic outcome. Thus, our results provide encouraging findings indicating DNA methyltransferases, chromatin remodeling proteins and miRNA inhibitors or upregulators as interesting therapeutic targets in food addiction. On the other, miRNAs are possible useful biomarkers since a significant number of them, called circulating miRNAs, have been observed in the bloodstream (Chen *et al.*, 2008). In this sense, a large study conducted in smokers versus non-smokers highlighted the increased circulating miR-124 in smoker subjects (Banerjee *et al.*, 2015). miR-124 is a neuron-specific miRNA, indicating that its presence as a circulating miRNA reflects a detected miRNA in bloodstream secreted from neurons (Smith and Kenny, 2018). More studies in this framework are needed to consider circulating miRNAs as possible biomarkers in addiction and specifically in food addiction.

3. CB_1R in CAMKIIα+ neurons is involved in the loss of control over palatable food intake in a binge eating mouse model

The endocannabinoid system is a key player in homeostatic and hedonic regulation of food intake through the CB_1R, and dysregulation of this system has been related to eating disorders and obesity. The cellular mechanisms promoted by CB1R activation have been widely investigated, but the differential effects produced by the CB1R activation in specific cell-types such as GABAergic or glutamatergic neurons have been only partially addressed. The majority of the studies have used a "loss of function" approach in which mutant mice lack the CB1R in a specific cell population. This strategy helped in characterizing the involvement of the endocannabinoid receptor in many phenotypic functions (Monory et al., 2006; Bellocchio et al., 2010; Martín-García et al., 2016). However, a limitation of this approach is that it is difficult to conclude if the CB1R expression is sufficient for the function studied. Thus, the "rescue" strategy, in which the CB1R is deleted from all the cells and only is expressed in a specific cell population, could be a valuable tool to stablish somehow causal relationships between the CB1R expression and a specific phenotype (Ruehle et al., 2013).

In this third study, a conditional rescue mouse line selectively expressing the CB_1R in CAMKIIα^+ neurons was generated. In these mutant mice, the expression of CB_1R was restricted mainly to glutamatergic cortical neurons (Casanova et al., 2001). Therefore, we aimed to evaluate the role of the CB_1R in CAMKIIα^+ neurons in the loss of inhibitory control and the emotional manifestations associated with

binge eating disorder. For this purpose, we used an operant conditioning model combined with behavioral tests to measure anxiety and depression in CAMKII-CB1-RS, CB1-KO and WT mice exposed to a binge eating diet.

We found that CAMKII-CB1-RS mice displayed a phenotype of high impulsivity- and compulsivity-like behavior with increased primary reinforcing effects of chocolate-flavored pellets compared to CB1-KO mice. Indeed, this phenotype was accompanied by an augmented motivation for palatable pellets. In accordance, the opposite genetic mutant mice, Glu-CB1-KO, expressing CB_1R in all cells except in glutamatergic cortical neurons, displayed the opposite phenotype. We reported in our first study that Glu-CB1-KO mice showed a reduced motivation, impulsivity and compulsivity for palatable food using a food addiction mouse model. A previous publication confirmed the non-impulsivity trait of these mice using a novelty palatable food seeking test (Lafenêtre *et al.*, 2009). Therefore, these results suggest that CB_1R in glutamatergic cortical neurons is sufficient to induce a loss of control over palatable food intake. Considering the increased glutamatergic presynaptic drive found in Glu-CB1-KO mice (see electrophysiological results in experiment 1), we could speculate that the cortical excitability is reestablished in CAMKII-CB1-RS mice similarly to WT mice or could be slightly decreased due to a high CB_1R activity only in glutamatergic cells. A reduction of the cortical excitability in a CB_1R-dependent manner may explain the addictive-like phenotype

shown by CAMKII-CB1-RS mice similar to our first findings with the chemogenetic inhibition of PL excitatory neurons.

Additionally, the exposure to a binge eating diet during several weeks produced a robust effect in CAMKII-CB1-RS mice, increasing the seeking for palatable food despite the growing effort to achieve it or despite negative consequences compared to CAMKII-CB1-RS mice exposed to the standard diet.

The next step was to evaluate the affective manifestations associated to binge eating diet exposure in the different genotypes. No significant interaction between the genetic and the diet variables was found providing a difficult interpretation of the results obtained in the anxiety- and depressive-like behaviors. However, the effect of the genetic variable was significant in some cases and we found interesting results using the rescue of the phenotype strategy. The CB1-KO mice showed an increased anxiety-like behavior, as it was previously reported (Lutz *et al.*, 2015). This anxiogenic phenotype was substantially rescued in CAMKII-CB1-RS mice showing similar levels of anxiety as WT mice. In accordance, previous studies using similar Glu-CB1-RS modified genetic mice expressing CB_1R only in glutamatergic neurons also showed similar anxiety-like behavior to WT mice and differentially to CB1-KO mice (Ruehle *et al.*, 2013). Additionally, the expression of the CB_1R in glutamatergic neurons has been reported to play a key role in the anxiolytic effects produced by low doses of cannabinoids (Rey *et al.*, 2012). Thus, the modulation of the glutamatergic CB_1R in the mPFC seems critical for anxiety-like

behaviors. Several areas are involved in the control of anxiety behavior, but the amygdala seems to play a prominent role (Babaev *et al.*, 2018). Hyperexcitability of the amygdala in response to negative stimuli has been observed in patients with several types of anxiety disorders (Tovote *et al.*, 2015). The basolateral part of the amygdala receives excitatory projections from the mPFC, processes the information and sends it via glutamatergic inputs to the lateral subdivision of the central amygdala (Babaev *et al.*, 2018).

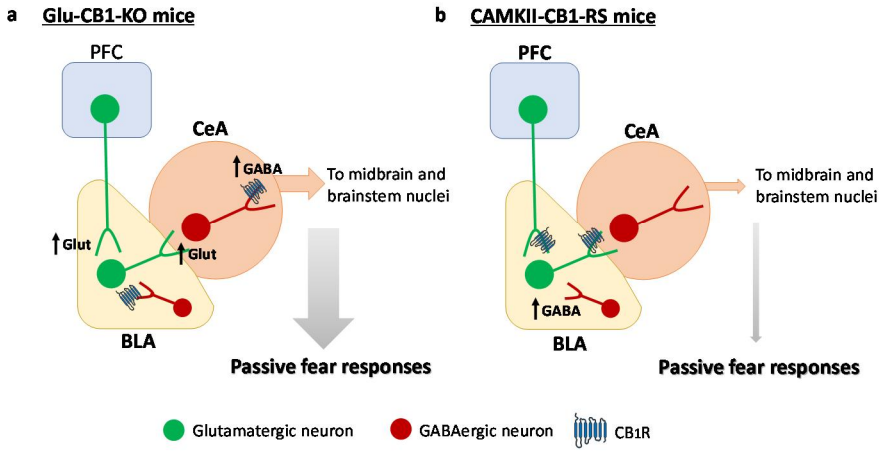

Figure 102. Diagram of the excitatory and inhibitory synaptic transmission in the amygdala modulated by the CB_1R in **a,** Glu-CB1-KO mice and in **b,** CMAKII-CB1-RS mice. PFC, prefrontal cortex; BLA, basolateral amygdala; CeA, central amygdala; glut, glutamate (Modified from Busquets-Garcia *et al.*, 2015).

In mice lacking CB_1R in glutamatergic neurons (Glu-CB1-KO mice), all the glutamate projections are overactivated leading to a hyperactivation of the central amygdala that increases passive fear responses (Busquets-Garcia *et al.*, 2015) (Figure 102a). In contrast, we could speculate that the hyperexcitability of the glutamatergic neurons is not produced in CAMKII-CB1-RS mice, reducing the activation of the

central amygdala and decreasing the fear and anxiety responses (Figure 102b).

We also measured the depressive-like behavior in all genotypes. The CB1-KO mice showed higher immobility time than WT mice and similar to the CAMKII-CB1-RS mice. Thus, the expression of the CB_1R in $CAMKII\alpha^+$ cells not rescued the depressive-like behavior produced by the total deletion of the CB_1R. This result was supported by the clear anhedonic phenotype shown in both CAMKII-CB1-RS and CB1-KO compared to WT mice. Similar results showing an enhanced despair behavior were obtained in CB1-KO mice (Aso *et al.*, 2008). Human brain neuroimaging studies have demonstrated the involvement of several brain regions in depressive-like behavior such as the PFC, hippocampus, striatum, amygdala and thalamus (Drevets, 2001). Moreover, optogenetics manipulations highlighted the complexity of the connectivity among them and the different roles of each neuronal subpopulation (Muir and Bagot, 2019). Thus, the failure in the rescue of the depressive-like behavior is in accordance with these results indicating that this complex behavior is not mainly mediated by glutamatergic transmission.

Together, our data indicate that CB_1R expression in $CAMKII\alpha^+$ neurons provides a substantial rescue of the anxiogenic, but not the depressive effects produced by the global CB_1R loss. Thus, the neuronal circuits involving processes mediated by CB_1R are vastly complex, and future experiments expanding the neuronal subtypes where CB_1R function is rescued are needed.

Our model to induce binge-like eating behavior mimicks important features of the binge eating disorder human pathology in the absence of caloric restriction. Mice consume more food in a brief period of time than controls (standard) under the same conditions, and this behavior was repeated over all binge eating cycles. Moreover, the palatable diet used was similar in the composition of foods that are frequently consumed during binge episodes in humans (Brownley *et al.*, 2016). However, our model has a limitation since no clear differences were shown in anxiety- and depressive-like behavior between binge eating and control groups, independently of the genotype, in agreement with previous studies (Czyzyk *et al.*, 2010). Therefore, this model does not reflect the often association of binge eating disorder and theses emotional components (Rosenbaum and White, 2015). Thus, we are modeling the aberrant overeating behavior and the loss of control but not the affective manifestations of the binge eating disorder in humans. One possible explanation could be that anxiety- and depressive-like behaviors could be developed after more prolonged exposure to the binge eating diet.

To sum up, this study reveals that the CB_1R in CAMKIIα^+ neurons plays a key role in the loss of behavioral control characterized by enhanced impulsivity, motivation and compulsivity for palatable food in a binge eating mouse model. The expression of CB_1R in CAMKIIα^+ neurons rescues the anxiogenic phenotype of the total conditional CB1-KO mice. Our experiments provide additional information about the role of CB_1R in neuronal circuits underlying loss of control over food intake.

4. Concluding remarks

The current thesis has identified new mechanistic explaining the loss of control over food intake. These findings could open new therapeutic research possibilities for food addiction and other psychiatric disorders with alterations in compulsive behavior, such as obsessive-compulsive disorder (van den Heuvel *et al.*, 2016). Our findings highlight the endocannabinoid system through CB_1R and the DA system through D_2R as significant modulators of the top-down cortico-striatal pathways mediating the resilience and the vulnerability to compulsive palatable eating. Due to the multifactorial etiology of addiction, several factors at the epigenetic, cellular and molecular levels contributed together to this susceptibility. Nevertheless, it remains unknown whether these differential changes between food addicted- and non-addicted-like mice were preexisting traits or were developed during the addiction process. Additionally, the fact that the whole experiments do not include female mice constitutes a limitation of this thesis not ruling out gender differences in these findings.

To conclude, this thesis provides new neurobiological evidences supporting the acceptance of the food addiction construct, which could help to identify novel strategies to address this pathology.

Conclusions

The present thesis allows to draw the following conclusions:

1. The lack of CB_1R in dorsal telencephalic glutamatergic neurons induces a strong resilience phenotype to develop food addiction characterized by less perseverance, reduced motivation and decreased compulsivity for highly palatable food.

2. The increased inhibitory control shown in Glu-CB1-KO mice is mediated by an enhanced excitatory synaptic transmission of pyramidal glutamatergic neurons in PL cortex.

3. Chemogenetic inhibition of glutamatergic PL neurons promotes motivation and compulsivity for palatable food indicating a key role of this area in the development of food addiction.

4. The selective silencing of PL-NAc core pathway leads to a food addictive-like phenotype with loss of inhibitory control and compulsive food seeking.

5. Transcriptomic analysis reveals an increase of *Drd2* gene in the mPFC of addicted compared to non-addicted mice that could underlie food addiction susceptibility.

6. Overexpression of *Drd2* gene in the specific PL-NAc core network promotes compulsive eating behavior providing a new mechanism of the loss of inhibitory control.

7. Epigenetic studies analyzing the DNA methylation in food addicted mice reveal hypomethylated contiguous genomic regions in *Drd2* gene in accordance with our previous transcriptomic results.

8. The prolonged exposure to palatable food leading to addictive-like behavior involved changes in the miRNA profile. Eleven miRNAs in the mPFC of vulnerable mice were differentially expressed compared to the resistant ones.

9. The expression of the CB_1R exclusively in $CAMKII\alpha^+$ neurons is sufficient to promote a loss of control over food intake with increased impulsivity- and compulsivity-like behaviors in a binge eating mouse model. This genetic modification is accompanied by a substantial rescue of the anxiogenic, but not the depressive phenotype associated with the global CB_1R loss.

10. Our results provide neurobiological evidences supporting the acceptance of the food addiction construct, which could open new therapeutic possibilities for this pathology and for other psychiatric disorders with alterations in compulsive behavior.

References

Abdalla, M. M. I. (2017) Central and peripheral control of food intake, *Endocrine Regulations*, 51(1), pp. 52–70.

Agulhon, C. *et al.* (2013) Modulation of the autonomic nervous system and behaviour by acute glial cell G_q protein-coupled receptor activation *in vivo*, *The Journal of Physiology*, 591(22), pp. 5599–5609.

Alexander, G. M. *et al.* (2009) Remote Control of Neuronal Activity in Transgenic Mice Expressing Evolved G Protein-Coupled Receptors, *Neuron*, 63(1), pp. 27–39.

Alger, B. E. and Kim, J. (2011) Supply and demand for endocannabinoids, *Trends in Neurosciences*, 34(6), pp. 304–315.

Alonso, P. *et al.* (2015) Deep Brain Stimulation for Obsessive-Compulsive Disorder: A Meta-Analysis of Treatment Outcome and Predictors of Response, *PLOS ONE*. Edited by V. Sgambato-Faure, 10(7), p. e0133591.

Alvarez-Curto, E. *et al.* (2011) Developing Chemical Genetic Approaches to Explore G Protein-Coupled Receptor Function: Validation of the Use of a Receptor Activated Solely by Synthetic Ligand (RASSL), *Molecular Pharmacology*, 80(6), pp. 1033–1046.

American Psychiatric Association (1994) *Diagnostic and Statistical Manual of Mental Disorders, 4th Edition, Text Revision (DSM-IV-TR)*. Edited by 2000 American Psychiatric Association. Washington, DC. USA.

American Psychiatric Association (2013) *Diagnostic and Statistical Manual of Mental Disorders, 5th Edition (DSM-5)*. Washington, DC. USA.

Anastasiadi, D., Esteve-Codina, A. and Piferrer, F. (2018) Consistent inverse correlation between DNA methylation of the first intron and gene expression across tissues and species, *Epigenetics & Chromatin*. BioMed Central, 11(1), p. 37.

Anders, S. and Huber, W. (2010) Differential expression analysis for sequence count data, *Genome Biology*. BioMed Central, 11(10), p. R106.

Anders, S., Pyl, P. T. and Huber, W. (2015) HTSeq--a Python framework to work with high-throughput sequencing data., *Bioinformatics (Oxford, England)*. Oxford University Press, 31(2), pp. 166–9.

Armbruster, B. N. *et al.* (2007) Evolving the lock to fit the key to create a family of G protein-coupled receptors potently activated by an inert ligand., *Proceedings of the National Academy of Sciences of the United States of America*, 104(12), pp. 5163–8.

Aso, E. *et al.* (2008) BDNF impairment in the hippocampus is related to enhanced despair behavior in CB_1 knockout mice, *Journal of Neurochemistry*. Blackwell Publishing Ltd, 105(2), pp. 565–572.

Aston-Jones, G. and Deisseroth, K. (2013) Recent advances in optogenetics and pharmacogenetics, *Brain Research*. Elsevier, 1511, pp. 1–5.

Atwood, B. K. and Mackie, K. (2010) CB2: a cannabinoid receptor with an identity crisis, *British Journal of Pharmacology*, 160(3), pp. 467–479.

Avena, N. M. and Bocarsly, M. E. (2012) Dysregulation of brain reward systems in eating disorders: neurochemical information from animal models of binge eating, bulimia nervosa, and anorexia nervosa., *Neuropharmacology*. NIH Public Access, 63(1), pp. 87–96.

Babaev, O., Piletti Chatain, C. and Krueger-Burg, D. (2018) Inhibition in the amygdala anxiety circuitry, *Experimental & Molecular Medicine*. Nature Publishing Group, 50(4), p. 18.

Babbs, R. K. *et al.* (2013) Decreased caudate response to milkshake is associated with higher body mass index and greater impulsivity, *Physiology & Behavior*, 121, pp. 103–111.

Baik, J.-H. (2013) Dopamine signaling in food addiction: role of dopamine D2 receptors., *BMB reports*. Korean Society for Biochemistry and Molecular Biology, 46(11), pp. 519–26.

Ball, K. T., Combs, T. A. and Beyer, D. N. (2011) Opposing roles for dopamine D1- and D2-like receptors in discrete cue-induced reinstatement of food seeking, *Behavioural Brain Research*, 222(2), pp. 390–393.

Banerjee, A., Waters, D., Camacho, O. M. and Minet, E. (2015) Quantification of plasma microRNAs in a group of healthy smokers, ex-smokers and non-smokers and correlation to biomarkers of tobacco exposure., *Biomarkers : biochemical indicators of exposure, response, and susceptibility to chemicals*. Taylor & Francis, 20(2), pp. 123–31.

Basar, K. *et al.* (2010) Nucleus accumbens and impulsivity, *Progress in Neurobiology*, 92(4), pp. 533–557.

Beaulieu, J.-M. and Gainetdinov, R. R. (2011) The Physiology, Signaling, and Pharmacology of Dopamine Receptors, *Pharmacological Reviews*, 63(1), pp. 182–217.

Belin, D. *et al.* (2008) High impulsivity predicts the switch to compulsive cocaine-taking., *Science (New York, N.Y.)*, 320(5881), pp. 1352–5.

Belin, D. and Deroche-Gamonet, V. (2012) Responses to novelty and vulnerability to cocaine addiction: contribution of a multi-symptomatic animal model., *Cold Spring Harbor perspectives in medicine*. Cold Spring Harbor Laboratory Press, 2(11).

Bello, N. T., Lucas, L. R. and Hajnal, A. (2002) Repeated sucrose access influences dopamine D2 receptor density in the striatum., *Neuroreport*, 13(12), pp. 1575–8.

Bellocchio, L. *et al.* (2010) Bimodal control of stimulated food intake by the endocannabinoid system., *Nature neuroscience*. Nature Publishing Group, 13(3), pp. 281–3.

Bentivoglio, M. and Morelli, M. (2005) The organization and circuits of mesencephalic dopaminergic neurons and the distribution of dopamine receptors in the brain, in S.B. Dunnett, M. Bentivoglio, A. Bjorklund, T. H. (ed.) *In Dopamine*, pp. 1–107.

Berrendero, F. *et al.* (2005) Nicotine-induced antinociception, rewarding effects, and physical dependence are decreased in mice lacking the preproenkephalin gene., *The Journal of neuroscience : the official journal of the Society for Neuroscience*, 25(5), pp. 1103–12.

Bersoux, S., Byun, T. H., Chaliki, S. S. and Poole, K. G. (2017) Pharmacotherapy for obesity: What you need to know, *Cleveland Clinic Journal of Medicine*, 84(12), pp. 951–958.

Blum, K. *et al.* (1996) Increased prevalence of the Taq I A1 allele of the dopamine receptor gene (DRD2) in obesity with comorbid substance use disorder: a preliminary report., *Pharmacogenetics*, 6(4), pp. 297–305.

Blum, K. *et al.* (2000) Reward deficiency syndrome: a biogenetic model for the diagnosis and treatment of impulsive, addictive, and compulsive behaviors., *Journal of psychoactive drugs*, 32 Suppl, pp. i–iv, 1–112.

Bock, R. *et al.* (2013) Strengthening the accumbal indirect pathway promotes resilience to compulsive cocaine use, *Nature Neuroscience*. Nature Publishing Group, 16(5), pp. 632–638.

Bogdanović, O. and Lister, R. (2017) DNA methylation and the preservation of cell identity, *Current Opinion in Genetics & Development*. Elsevier Current Trends, 46, pp. 9–14.

Bonaventura, J. *et al.* (2018) Chemogenetic ligands for translational neurotheranostics, *bioRxiv*, p. 487637.

Bray, G. A. (2004) Medical Consequences of Obesity, *The Journal of Clinical Endocrinology & Metabolism*. Narnia, 89(6), pp. 2583–2589.

Bromberg-Martin, E. S., Matsumoto, M. and Hikosaka, O. (2010) Dopamine in Motivational Control: Rewarding, Aversive, and Alerting, *Neuron*. Cell Press, 68(5), pp. 815–834.

Brownley, K. A. *et al.* (2016) Binge-Eating Disorder in Adults: A Systematic Review and Meta-analysis., *Annals of internal medicine*. NIH Public Access, 165(6), pp. 409–20.

Bruinsma, K. and Taren, D. L. (1999) Chocolate: food or drug?, *Journal of the American Dietetic Association*, 99(10), pp. 1249–1256.

Buckley, P. F., Miller, B. J., Lehrer, D. S. and Castle, D. J. (2009) Psychiatric Comorbidities and Schizophrenia, *Schizophrenia Bulletin*, 35(2), pp. 383–402.

Bura, A. S. *et al.* (2013) Operant self-administration of a sigma ligand improves nociceptive and emotional manifestations of neuropathic pain, *European Journal of Pain*, 17(6), pp. 832–843.

Bura, S. A., Burokas, A., Martín-García, E. and Maldonado, R. (2010) Effects of chronic nicotine on food intake and anxiety-like behaviour in CB(1) knockout mice., *European neuropsychopharmacology : the journal of the European College of Neuropsychopharmacology*. Elsevier B.V. and ECNP, 20(6), pp. 369–78.

Burgos-Robles, A., Vidal-Gonzalez, I. and Quirk, G. J. (2009) Sustained conditioned responses in prelimbic prefrontal neurons are correlated with fear expression and extinction failure., *The Journal of neuroscience : the official journal of the Society for Neuroscience*. NIH Public Access, 29(26), pp. 8474–82.

Burns, H. D. *et al.* (2007) [18F]MK-9470, a positron emission tomography (PET) tracer for in vivo human PET brain imaging of the cannabinoid-1 receptor, *Proceedings of the National Academy of Sciences*, 104(23), pp. 9800–9805.

Burrows, T. *et al.* (2017) Food Addiction, Binge Eating Disorder, and Obesity: Is There a Relationship?, *Behavioral Sciences*. Multidisciplinary Digital Publishing Institute, 7(4), p. 54.

Busquets-Garcia, A. *et al.* (2015) Dissecting the cannabinergic control of behavior: The where matters, *BioEssays*, 37(11), pp. 1215–1225.

Busquets-Garcia, A., Bains, J. and Marsicano, G. (2018) CB1 Receptor Signaling in the Brain: Extracting Specificity from Ubiquity., *Neuropsychopharmacology : official publication of the American College of Neuropsychopharmacology*. Nature Publishing Group, 43(1), pp. 4–20.

Busquets Garcia, A., Soria-Gomez, E., Bellocchio, L. and Marsicano, G. (2016) Cannabinoid receptor type-1: breaking the dogmas, *F1000Research*, 5, p. 990.

Cabana-Domínguez, J., Arenas, C., Cormand, B. and Fernàndez-Castillo, N. (2018) MiR-9, miR-153 and miR-124 are down-regulated by acute exposure to cocaine in a dopaminergic cell model and may contribute to cocaine dependence., *Translational psychiatry*. Nature Publishing Group, 8(1), p. 173.

Calabresi, P. *et al.* (2014) Direct and indirect pathways of basal ganglia: a critical reappraisal, *Nature Neuroscience*. Nature Publishing Group, 17(8), pp. 1022–1030.

Calu, D. J. *et al.* (2013) Optogenetic inhibition of dorsal medial prefrontal cortex attenuates stress-induced reinstatement of palatable food seeking in female rats., *The Journal of neuroscience : the official journal of the Society for Neuroscience*. NIH Public Access, 33(1), pp. 214–26.

Cani, P. D. *et al.* (2016) Endocannabinoids--at the crossroads between the gut microbiota and host metabolism., *Nature reviews. Endocrinology*, 12(3), pp. 133–43.

Carlezon, W. A. and Thomas, M. J. (2009) Biological substrates of reward and aversion: A nucleus accumbens activity hypothesis, *Neuropharmacology*. Pergamon, 56, pp. 122–132.

Caron, A. and Richard, D. (2017) Neuronal systems and circuits involved in the control of food intake and adaptive thermogenesis, *Annals of the New York Academy of Sciences*.

John Wiley & Sons, Ltd (10.1111), 1391(1), pp. 35–53.

Carr, D. B. *et al.* (2000) Projections from the rat prefrontal cortex to the ventral tegmental area: target specificity in the synaptic associations with mesoaccumbens and mesocortical neurons., *The Journal of neuroscience : the official journal of the Society for Neuroscience*. Society for Neuroscience, 20(10), pp. 3864–73.

Casanova, E. *et al.* (2001) A CamKIIalpha iCre BAC allows brain-specific gene inactivation., *Genesis (New York, N.Y. : 2000)*, 31(1), pp. 37–42.

Cassin, S. E. *et al.* (2019) Ethical, stigma, and policy implications of food addiction: A scoping review, *Nutrients*, 11(4), pp. 1–18.

Castañeda, T. R. *et al.* (2010) Ghrelin in the regulation of body weight and metabolism, *Frontiers in Neuroendocrinology*, 31(1), pp. 44–60.

Castaño, C., Kalko, S., Novials, A. and Párrizas, M. (2018) Obesity-associated exosomal miRNAs modulate glucose and lipid metabolism in mice., *Proceedings of the National Academy of Sciences of the United States of America*. National Academy of Sciences, 115(48), pp. 12158–12163.

Castelnuovo, G. *et al.* (2017) Cognitive behavioral therapy to aid weight loss in obese patients: current perspectives., *Psychology research and behavior management*. Dove Press, 10, pp. 165–173.

Castillo, P. E., Younts, T. J., Chávez, A. E. and Hashimotodani, Y. (2012) Endocannabinoid signaling and synaptic function., *Neuron*, 76(1), pp. 70–81.

Chandrasekar, V. and Dreyer, J.-L. (2009) microRNAs miR-124, let-7d and miR-181a regulate Cocaine-induced Plasticity, *Molecular and Cellular Neuroscience*, 42(4), pp. 350–362.

Chen, B. T. *et al.* (2013) Rescuing cocaine-induced prefrontal cortex hypoactivity prevents compulsive cocaine seeking., *Nature*. Nature Publishing Group, 496(7445), pp. 359–362.

Chen, X. *et al.* (2008) Characterization of microRNAs in serum: a novel class of biomarkers for diagnosis of cancer and other diseases, *Cell Research*, 18(10), pp. 997–1006.

Chen, X. *et al.* (2015) The First Structure–Activity Relationship Studies for Designer Receptors Exclusively Activated by Designer Drugs, *ACS Chemical Neuroscience*. American Chemical Society, 6(3), pp. 476–484.

Di Chiara, G. and Imperato, A. (1988) Drugs abused by humans preferentially increase synaptic dopamine concentrations in the mesolimbic system of freely moving rats., *Proceedings of the National Academy of Sciences of the United States of America*. National Academy of Sciences, 85(14), pp. 5274–8.

Di Chiara, G. (2002) Nucleus accumbens shell and core dopamine: differential role in

behavior and addiction, *Behavioural Brain Research*. Elsevier, 137(1–2), pp. 75–114.

Childers, S. R. and Deadwyler, S. A. (1996) Role of cyclic AMP in the actions of cannabinoid receptors., *Biochemical pharmacology*, 52(6), pp. 819–27.

Chiu, C. Q., Puente, N., Grandes, P. and Castillo, P. E. (2010) Dopaminergic modulation of endocannabinoid-mediated plasticity at GABAergic synapses in the prefrontal cortex., *The Journal of neuroscience : the official journal of the Society for Neuroscience*. Society for Neuroscience, 30(21), pp. 7236–48.

Christensen, R. *et al.* (2007) Efficacy and safety of the weight-loss drug rimonabant: a meta-analysis of randomised trials, *The Lancet*. Elsevier, 370(9600), pp. 1706–1713.

Clark, M. A., Douglas, M. and Choi, J. (2018) *Eukaryotic Epigenetic Gene Regulation | OpenStax Biology 2e*.

Cleary, D. R., Ozpinar, A., Raslan, A. M. and Ko, A. L. (2015) Deep brain stimulation for psychiatric disorders: where we are now, *Neurosurgical Focus*, 38(6), p. E2.

Colantuoni, C. *et al.* (2001) Excessive sugar intake alters binding to dopamine and mu-opioid receptors in the brain, *Neuroreport*, 12(16), pp. 3549–3552.

Compton, W. M., Dawson, D. A., Goldstein, R. B. and Grant, B. F. (2013) Crosswalk between DSM-IV dependence and DSM-5 substance use disorders for opioids, cannabis, cocaine and alcohol., *Drug and alcohol dependence*. NIH Public Access, 132(1–2), pp. 387–90.

Conceição, E. M. *et al.* (2014) What is 'grazing'? Reviewing its definition, frequency, clinical characteristics, and impact on bariatric surgery outcomes, and proposing a standardized definition, *Surgery for Obesity and Related Diseases*. Elsevier, 10(5), pp. 973–982.

Considine, R. V. *et al.* (1996) Serum Immunoreactive-Leptin Concentrations in Normal-Weight and Obese Humans, *New England Journal of Medicine*, 334(5), pp. 292–295.

Cooper, S., Robison, A. J. and Mazei-Robison, M. S. (2017) Reward Circuitry in Addiction, *Neurotherapeutics*.

Corbit, L. H. (2016) Effects of obesogenic diets on learning and habitual responding, *Current Opinion in Behavioral Sciences*. Elsevier, 9, pp. 84–90.

Cornelis, M. C. *et al.* (2016) A genome-wide investigation of food addiction, *Obesity*. John Wiley & Sons, Ltd, 24(6), pp. 1336–1341.

Cottone, P. *et al.* (2009) CRF system recruitment mediates dark side of compulsive eating., *Proceedings of the National Academy of Sciences of the United States of America*. National Academy of Sciences, 106(47), pp. 20016–20.

Creed, M., Pascoli, V. J. and Lüscher, C. (2015) Refining deep brain stimulation to emulate optogenetic treatment of synaptic pathology, *Science*, 347(6222), pp. 659–664.

Crunelle, C. L. *et al.* (2012) Substrates of neuropsychological functioning in stimulant dependence: a review of functional neuroimaging research., *Brain and behavior*. Wiley-Blackwell, 2(4), pp. 499–523.

Cui, Q. *et al.* (2018) Dopamine receptors mediate strategy abandoning via modulation of a specific prelimbic cortex–nucleus accumbens pathway in mice, *Proceedings of the National Academy of Sciences*, 115(21), pp. E4890–E4899.

Czyzyk, T. A., Sahr, A. E. and Statnick, M. A. (2010) A Model of Binge-Like Eating Behavior in Mice That Does Not Require Food Deprivation or Stress, *Obesity*. Blackwell Publishing Ltd, 18(9), pp. 1710–1717.

D'Addario, C. *et al.* (2014) Endocannabinoid signaling and food addiction., *Neuroscience and biobehavioral reviews*. Elsevier Ltd, 47, pp. 203–24.

Dalmasso, G. *et al.* (2011) Microbiota modulate host gene expression via microRNAs., *PloS one*. Public Library of Science, 6(4), p. e19293.

Davis, A. A., Edge, P. J. and Gold, M. S. (2014) New Directions in the Pharmacological Treatment of Food Addiction, Overeating, and Obesity, *Behavioral Addictions*. Academic Press, pp. 185–213.

Davis, C. *et al.* (2011) Evidence that 'food addiction' is a valid phenotype of obesity, *Appetite*, 57(3), pp. 711–717.

Davis, C. *et al.* (2013) 'Food addiction' and its association with a dopaminergic multilocus genetic profile, *Physiology & Behavior*, 118, pp. 63–69.

Davis, C. (2013) From Passive Overeating to 'Food Addiction': A Spectrum of Compulsion and Severity, *ISRN Obesity*. Hindawi Limited, 2013.

Davis, C. (2015) The epidemiology and genetics of binge eating disorder (BED), *CNS Spectrums*, 20(6), pp. 522–529.

Davis, C. (2016) A commentary on the associations among 'food addiction', binge eating disorder, and obesity: Overlapping conditions with idiosyncratic clinical features, *Appetite*.

Dembrow, N. and Johnston, D. (2014) Subcircuit-specific neuromodulation in the prefrontal cortex, *Frontiers in Neural Circuits*, 8(June), pp. 1–9.

Dempster, E. L. *et al.* (2011) Disease-associated epigenetic changes in monozygotic twins discordant for schizophrenia and bipolar disorder., *Human molecular genetics*, 20(24), pp. 4786–96.

Deroche-Gamonet, V., Belin, D. and Piazza, P. V. (2004) Evidence for addiction-like behavior in the rat., *Science (New York, N.Y.)*, 305(5686), pp. 1014–7.

De Deurwaerdère, P., Lagière, M., Bosc, M. and Navailles, S. (2013) Multiple controls

exerted by 5-HT2C receptors upon basal ganglia function: from physiology to pathophysiology, *Experimental Brain Research*, 230(4), pp. 477–511.

Diana, M. *et al.* (2017) Rehabilitating the addicted brain with transcranial magnetic stimulation, *Nature Reviews Neuroscience*. Nature Publishing Group, 18(11), pp. 685–693.

DiFeliceantonio, A. G. and Small, D. M. (2019) Dopamine and diet-induced obesity, *Nature Neuroscience*. Nature Publishing Group, 22(1), pp. 1–2.

Dodd, G. T. and Tiganis, T. (2017) Insulin action in the brain: Roles in energy and glucose homeostasis, *Journal of Neuroendocrinology*, 29(10), p. e12513.

Domingos, A. I. *et al.* (2011) Leptin regulates the reward value of nutrient, *Nature Neuroscience*, 14(12), pp. 1562–1568.

Doris, J. M., Millar, S. A., Idris, I. and O'Sullivan, S. E. (2019) Genetic polymorphisms of the endocannabinoid system in obesity and diabetes, *Diabetes, Obesity and Metabolism*. John Wiley & Sons, Ltd (10.1111), 21(2), pp. 382–387.

Douglas, R. J. and Martin, K. A. C. (2004) Neuronal Circuits of the Neocortex, *Annual Review of Neuroscience*, 27(1), pp. 419–451.

Doura, M. B. and Unterwald, E. M. (2016) MicroRNAs Modulate Interactions between Stress and Risk for Cocaine Addiction, *Frontiers in Cellular Neuroscience*, 10, p. 125.

Drevets, W. C. (2001) Neuroimaging and neuropathological studies of depression: implications for the cognitive-emotional features of mood disorders, *Current Opinion in Neurobiology*. Elsevier Current Trends, 11(2), pp. 240–249.

Dreyer, J. K., Herrik, K. F., Berg, R. W. and Hounsgaard, J. D. (2010) Influence of Phasic and Tonic Dopamine Release on Receptor Activation, *Journal of Neuroscience*, 30(42), pp. 14273–14283.

Druga, R. (2009) Neocortical inhibitory system., *Folia biologica*, 55(6), pp. 201–17.

Ducci, F. and Goldman, D. (2012) The Genetic Basis of Addictive Disorders, *The Psychiatric clinics of North America*. NIH Public Access, 35(2), p. 495.

Everitt, B. J. and Robbins, T. W. (2005) Neural systems of reinforcement for drug addiction: from actions to habits to compulsion, *Nature Neuroscience*, 8(11), pp. 1481–1489.

Everitt, B. J. *et al.* (2008) Neural mechanisms underlying the vulnerability to develop compulsive drug-seeking habits and addiction, *Philosophical Transactions of the Royal Society B: Biological Sciences*, 363(1507), pp. 3125–3135.

Feldman, J. and Eysenck, S. (1986) Addictive personality traits in bulimic patients, *Personality and Individual Differences*. Pergamon, 7(6), pp. 923–926.

Feldstein Ewing, S. W. *et al.* (2017) Overweight adolescents' brain response to sweetened beverages mirrors addiction pathways., *Brain imaging and behavior*. NIH Public Access, 11(4), pp. 925–935.

Fernandez-Aranda, F., Karwautz, A. and Treasure, J. (2018) Food addiction: A transdiagnostic construct of increasing interest, *European Eating Disorders Review*.

Ferre, S. *et al.* (2008) An Update on Adenosine A2A-Dopamine D2 Receptor Interactions: Implications for the Function of G Protein-Coupled Receptors, *Current Pharmaceutical Design*, 14(15), pp. 1468–1474.

Ferrulli, A., Macrì, C., Massarini, S. and Luzi, L. (2019) Effects of deep transcranial magnetic stimulation on satiety and body weight control in obesity: Results of a randomized controlled study, *Brain Stimulation*. Elsevier, 12(2), pp. 486–487.

Finlayson, G. (2017) Food addiction and obesity: Unnecessary medicalization of hedonic overeating, *Nature Reviews Endocrinology*. Nature Publishing Group, 13(8), pp. 493–498.

Fletcher, P. C. and Kenny, P. J. (2018) Food addiction: a valid concept?, *Neuropsychopharmacology*. Nature Publishing Group, 43(13), pp. 2506–2513.

Flint, A. J. *et al.* (2014) Food-addiction scale measurement in 2 cohorts of middle-aged and older women., *The American journal of clinical nutrition*. American Society for Nutrition, 99(3), pp. 578–86.

Flores, Á., Maldonado, R. and Berrendero, F. (2013) Cannabinoid-hypocretin cross-talk in the central nervous system: what we know so far, *Frontiers in Neuroscience*. Frontiers, 7, p. 256.

Fraga, M. F. *et al.* (2005) Epigenetic differences arise during the lifetime of monozygotic twins., *Proceedings of the National Academy of Sciences of the United States of America*. National Academy of Sciences, 102(30), pp. 10604–9.

Friedman, J. M. (2004) Modern science versus the stigma of obesity, *Nature Medicine*, 10(6), pp. 563–569.

Gallo, E. F. *et al.* (2018) Accumbens dopamine D2 receptors increase motivation by decreasing inhibitory transmission to the ventral pallidum, *Nature Communications*. Nature Publishing Group, 9(1), p. 1086.

Gao, W. J., Krimer, L. S. and Goldman-Rakic, P. S. (2001) Presynaptic regulation of recurrent excitation by D1 receptors in prefrontal circuits., *Proceedings of the National Academy of Sciences of the United States of America*. National Academy of Sciences, 98(1), pp. 295–300.

Gearhardt, A. N., Corbin, W. R. and Brownell, K. D. (2009) Preliminary validation of the Yale Food Addiction Scale., *Appetite*, 52(2), pp. 430–6.

Gearhardt, A. N. *et al.* (2012) An examination of the food addiction construct in obese patients with binge eating disorder., *The International journal of eating disorders*. NIH Public Access, 45(5), pp. 657–63.

Gearhardt, A. N., Boswell, R. G. and White, M. a (2014) The association of 'food addiction' with disordered eating and body mass index., *Eating behaviors*. Elsevier Ltd, 15(3), pp. 427–33.

Gearhardt, A. N., Corbin, W. R. and Brownell, K. D. (2016) Development of the Yale Food Addiction Scale Version 2.0., *Psychology of Addictive Behaviors*, 30(1), pp. 113–121.

Gebert, L. F. R. and MacRae, I. J. (2019) Regulation of microRNA function in animals, *Nature Reviews Molecular Cell Biology*. Nature Publishing Group, 20(1), pp. 21–37.

Gérard, N. *et al.* (2011) Brain Type 1 Cannabinoid Receptor Availability in Patients with Anorexia and Bulimia Nervosa, *Biological Psychiatry*. Elsevier, 70(8), pp. 777–784.

Gerfen, C. R. and Surmeier, D. J. (2011) Modulation of Striatal Projection Systems by Dopamine, *Annual Review of Neuroscience*. Annual Reviews, 34(1), pp. 441–466.

Goebbels, S. *et al.* (2006) Genetic targeting of principal neurons in neocortex and hippocampus of NEX-Cre mice, *genesis*, 44(12), pp. 611–621.

Goldstein, R. Z. and Volkow, N. D. (2011) Dysfunction of the prefrontal cortex in addiction: neuroimaging findings and clinical implications., *Nature reviews. Neuroscience*. NIH Public Access, 12(11), pp. 652–69.

Gomez, J. L. *et al.* (2017) Chemogenetics revealed: DREADD occupancy and activation via converted clozapine, *Science*, 357(6350), pp. 503–507.

González-Muniesa, P. *et al.* (2017) Obesity, *Nature Reviews Disease Primers*, 3(1), p. 17034.

Gordon, E. *et al.* (2018) What Is the Evidence for 'Food Addiction?' A Systematic Review, *Nutrients*. Multidisciplinary Digital Publishing Institute, 10(4), p. 477.

Granero, R. *et al.* (2018) Corrigendum: Validation of the Spanish Version of the Yale Food Addiction Scale 2.0 (YFAS 2.0) and Clinical Correlates in a Sample of Eating Disorder, Gambling Disorder and Healthy Control Participants, *Frontiers in Psychiatry*. Frontiers, 9, p. 321.

Greeno, C. G. and Wing, R. R. (1994) Stress-induced eating., *Psychological bulletin*, 115(3), pp. 444–64.

Greenway, F. L. *et al.* (2010) Effect of naltrexone plus bupropion on weight loss in overweight and obese adults (COR-I): a multicentre, randomised, double-blind, placebo-controlled, phase 3 trial., *Lancet (London, England)*. Elsevier, 376(9741), pp. 595–605.

Grilo, C. M., White, M. A. and Masheb, R. M. (2009) DSM-IV psychiatric disorder

comorbidity and its correlates in binge eating disorder, *International Journal of Eating Disorders*, 42(3), pp. 228–234.

Guettier, J.-M. *et al.* (2009) A chemical-genetic approach to study G protein regulation of beta cell function in vivo., *Proceedings of the National Academy of Sciences of the United States of America*, 106(45), pp. 19197–202.

Gutiérrez-Martos, M. *et al.* (2017) Cafeteria diet induces neuroplastic modifications in the nucleus accumbens mediated by microglia activation, *Addiction Biology*.

Haliloglu, B. and Bereket, A. (2015) Hypothalamic obesity in children: pathophysiology to clinical management, *Journal of Pediatric Endocrinology and Metabolism*, 28(5–6), pp. 503–13.

Hamani, C. *et al.* (2017) Subthalamic Nucleus Deep Brain Stimulation: Basic Concepts and Novel Perspectives, *eneuro*. Society for Neuroscience, 4(5), p. ENEURO.0140-17.2017.

Hamer, D. (2002) Rethinking Behavior Genetics, *Science*, 298(5591), pp. 71–72.

Hamilton, P. J. *et al.* (2018) Cell-Type-Specific Epigenetic Editing at the Fosb Gene Controls Susceptibility to Social Defeat Stress, *Neuropsychopharmacology*. Nature Publishing Group, 43(2), pp. 272–284.

Hammond, D. C. (2011) What is Neurofeedback: An Update, *Journal of Neurotherapy*, 15(4), pp. 305–336.

Harat, M. *et al.* (2016) Nucleus accumbens stimulation in pathological obesity, *Neurologia i Neurochirurgia Polska*, 50(3), pp. 207–210.

Häring, M., Kaiser, N., Monory, K. and Lutz, B. (2011) Circuit specific functions of cannabinoid CB1 receptor in the balance of investigatory drive and exploration., *PloS one*. Edited by H. A. Burgess, 6(11), p. e26617.

Hebebrand, J. *et al.* (2014) 'Eating addiction', rather than 'food addiction', better captures addictive-like eating behavior, *Neuroscience & Biobehavioral Reviews*. Pergamon, 47, pp. 295–306.

Heber, D. and Carpenter, C. L. (2011) Addictive genes and the relationship to obesity and inflammation., *Molecular neurobiology*. Springer, 44(2), pp. 160–5.

Heidbreder, C. A. and Groenewegen, H. J. (2003) The medial prefrontal cortex in the rat: evidence for a dorso-ventral distinction based upon functional and anatomical characteristics, *Neuroscience & Biobehavioral Reviews*, 27(6), pp. 555–579.

Hermann, H., Marsicano, G. and Lutz, B. (2002) Coexpression of the cannabinoid receptor type 1 with dopamine and serotonin receptors in distinct neuronal subpopulations of the adult mouse forebrain, *Neuroscience*. Pergamon, 109(3), pp. 451–460.

Hetherington, M. M. and MacDiarmid, J. I. (1993) "Chocolate addiction": a preliminary study of its description and its relationship to problem eating., *Appetite*, 21(3), pp. 233–46.

van den Heuvel, O. A. *et al.* (2016) Brain circuitry of compulsivity, *European Neuropsychopharmacology*. Elsevier, 26(5), pp. 810–827.

Heyne, A. *et al.* (2009) An animal model of compulsive food-taking behaviour, *Addiction Biology*. Blackwell Publishing Ltd, 14(4), pp. 373–383.

Hilker, I. *et al.* (2016) Food Addiction in Bulimia Nervosa: Clinical Correlates and Association with Response to a Brief Psychoeducational Intervention, *European Eating Disorders Review*. John Wiley & Sons, Ltd, 24(6), pp. 482–488.

Hollander, J. A. *et al.* (2010) Striatal microRNA controls cocaine intake through CREB signalling, *Nature*, 466(7303), pp. 197–202.

Honegger, K. and de Bivort, B. (2018) Stochasticity, individuality and behavior, *Current Biology*. Cell Press, 28(1), pp. R8–R12.

Honey, C. R. *et al.* (2017) Deep Brain Stimulation Target Selection for Parkinson's Disease, *Canadian Journal of Neurological Sciences / Journal Canadien des Sciences Neurologiques*, 44(1), pp. 3–8.

Hopkins, M. *et al. The Regulation of Food Intake in Humans*, *Endotext*. MDText.com, Inc.

Hu, Y. *et al.* (2019) Compulsive drug use is associated with imbalance of orbitofrontal- and prelimbic-striatal circuits in punishment-resistant individuals, *Proceedings of the National Academy of Sciences*, p. 201819978.

Hua Li, J. *et al.* (2013) A Novel Experimental Strategy to Assess the Metabolic Effects of Selective Activation of a Gq-Coupled Receptor in Hepatocytes In Vivo, *Endocrinology*, 154(10), pp. 3539–3551.

Hübel, C., Marzi, S. J., Breen, G. and Bulik, C. M. (2019) Epigenetics in eating disorders: a systematic review., *Molecular psychiatry*. Europe PMC Funders, 24(6), pp. 901–915.

Ifland, J. *et al.* (2015) Clearing the Confusion around Processed Food Addiction, *Journal of the American College of Nutrition*, 34(3), pp. 240–243.

Ivezaj, V., White, M. A. and Grilo, C. M. (2016) Examining binge-eating disorder and food addiction in adults with overweight and obesity., *Obesity (Silver Spring, Md.)*. NIH Public Access, 24(10), pp. 2064–9.

Jaber, M., Robinson, S. W., Missale, C. and Caron, M. G. (1996) Dopamine receptors and brain function., *Neuropharmacology*, 35(11), pp. 1503–19.

Jackman, S. L. and Regehr, W. G. (2017) The Mechanisms and Functions of Synaptic

Facilitation, *Neuron*, 94, pp. 447–464.

Jacob, J. J. and Isaac, R. (2012) Behavioral therapy for management of obesity., *Indian journal of endocrinology and metabolism*. Wolters Kluwer -- Medknow Publications, 16(1), pp. 28–32.

Jaenisch, R. and Bird, A. (2003) Epigenetic regulation of gene expression: how the genome integrates intrinsic and environmental signals, *Nature Genetics*, 33(S3), pp. 245–254.

Jasinska, A. J., Chen, B. T., Bonci, A. and Stein, E. A. (2015) Dorsal medial prefrontal cortex (MPFC) circuitry in rodent models of cocaine use: Implications for drug addiction therapies, *Addiction Biology*, 20(2), pp. 215–226.

Johnson, P. M. and Kenny, P. J. (2010) Dopamine D2 receptors in addiction-like reward dysfunction and compulsive eating in obese rats, *Nature Neuroscience*, 13(5), pp. 635–641.

Kakoschke, N., Aarts, E. and Verdejo-García, A. (2018) The Cognitive Drivers of Compulsive Eating Behavior., *Frontiers in behavioral neuroscience*. Frontiers Media SA, 12, p. 338.

Kalivas, P. W. and O'Brien, C. (2008) Drug Addiction as a Pathology of Staged Neuroplasticity, *Neuropsychopharmacology*. Nature Publishing Group, 33(1), pp. 166–180.

Kano, M., Ohno-shosaku, T., Hashimotodani, Y. and Uchigashima, M. (2009) Endocannabinoid-Mediated Control of Synaptic Transmission, pp. 309–380.

Kato, T. and Iwamoto, K. (2014) Comprehensive DNA methylation and hydroxymethylation analysis in the human brain and its implication in mental disorders, *Neuropharmacology*. Pergamon, 80, pp. 133–139.

Kessler, R. C. *et al.* (2013) The Prevalence and Correlates of Binge Eating Disorder in the World Health Organization World Mental Health Surveys, *Biological Psychiatry*, 73(9), pp. 904–914.

Khan, Z. U. *et al.* (1998) Prominence of the dopamine D2 short isoform in dopaminergic pathways, *Proceedings of the National Academy of Sciences*, 95(13), pp. 7731–7736.

Kieffer, B. L. *et al.* (2000) Mice deficient for δ- and μ-opioid receptors exhibit opposing alterations of emotional responses, *Nature Genetics*. Nature Publishing Group, 25(2), pp. 195–200.

Klawonn, A. M. and Malenka, R. C. (2019) Nucleus Accumbens Modulation in Reward and Aversion, *Cold Spring Harbor Symposia on Quantitative Biology*, p. 037457.

Klok, M. D., Jakobsdottir, S. and Drent, M. L. (2007) The role of leptin and ghrelin in the regulation of food intake and body weight in humans: a review, *Obesity Reviews*, 8(1), pp. 21–34.

Koob, G. F. and Le Moal, M. (2008) Addiction and the Brain Antireward System, *Annu. Rev.*

Psychol, 59, pp. 29–53.

Koob, G. F. and Volkow, N. D. (2010) Neurocircuitry of addiction., *Neuropsychopharmacology : official publication of the American College of Neuropsychopharmacology*, 35(1), pp. 217–38.

Koob, G. F. (2013) The Dark Side of Addiction: Dysregulated Neuroadaptation of Emotional Neurocircuits, *Biological Research on Addiction*, 00(00), pp. 179–186.

Koob, G. F. and Volkow, N. D. (2016) Neurobiology of addiction: a neurocircuitry analysis, *The Lancet Psychiatry*. Elsevier Ltd, 3(8), pp. 760–773.

Kornstein, S. G., Kunovac, J. L., Herman, B. K. and Culpepper, L. (2016) Recognizing Binge-Eating Disorder in the Clinical Setting: A Review of the Literature., *The primary care companion for CNS disorders*. Physicians Postgraduate Press, Inc., 18(3).

Korrekturen, D. (2014) Part II Animal Models in Specific Disease Areas of Drug Discovery.

Kouidrat, Y., Amad, A., Lalau, J.-D. and Loas, G. (2014) Eating disorders in schizophrenia: implications for research and management., *Schizophrenia research and treatment*. Hindawi Limited, 2014, p. 791573.

Kozlenkov, A. *et al.* (2017) DNA Methylation Profiling of Human Prefrontal Cortex Neurons in Heroin Users Shows Significant Difference between Genomic Contexts of Hyper- and Hypomethylation and a Younger Epigenetic Age, *Genes*. Multidisciplinary Digital Publishing Institute, 8(6), p. 152.

Krashes, M. J. *et al.* (2011) Rapid, reversible activation of AgRP neurons drives feeding behavior in mice, *Journal of Clinical Investigation*, 121(4), pp. 1424–1428.

Krashes, M. J., Shah, B. P., Koda, S. and Lowell, B. B. (2013) Rapid versus delayed stimulation of feeding by the endogenously released AgRP neuron mediators GABA, NPY, and AgRP., *Cell metabolism*, 18(4), pp. 588–95.

Krützfeldt, J. *et al.* (2005) Silencing of microRNAs in vivo with 'antagomirs', *Nature*. Nature Publishing Group, 438(7068), pp. 685–689.

Kuhlman, S. J. and Huang, Z. J. (2008) High-resolution labeling and functional manipulation of specific neuron types in mouse brain by Cre-activated viral gene expression., *PloS one*. Edited by R. O. L. Wong, 3(4), p. e2005.

Kupchik, Y. M. *et al.* (2015) Coding the direct/indirect pathways by D1 and D2 receptors is not valid for accumbens projections, *Nature Neuroscience*. Nature Publishing Group, 18(9), pp. 1230–1232.

Kupchik, Y. M. and Kalivas, P. W. (2017) The Direct and Indirect Pathways of the Nucleus Accumbens are not What You Think, *Neuropsychopharmacology*. Nature Publishing Group, 42(1), pp. 369–370.

Kure Liu, C. *et al.* (2019) Brain Imaging of Taste Perception in Obesity: a Review, *Current Nutrition Reports*. Springer US, 8(2), pp. 108–119.

Lafenêtre, P., Chaouloff, F. and Marsicano, G. (2009) Bidirectional regulation of novelty-induced behavioral inhibition by the endocannabinoid system, *Neuropharmacology*, 57, pp. 715–721.

Lammel, S. *et al.* (2012) Input-specific control of reward and aversion in the ventral tegmental area, *Nature*. Nature Publishing Group, 491(7423), pp. 212–217.

LaPlant, Q. *et al.* (2010) Dnmt3a regulates emotional behavior and spine plasticity in the nucleus accumbens, *Nature Neuroscience*, 13(9), pp. 1137–1143.

Laporte, S. A., Miller, W. E., Kim, K.-M. and Caron, M. G. (2002) β-Arrestin/AP-2 Interaction in G Protein-coupled Receptor Internalization, *Journal of Biological Chemistry*, 277(11), pp. 9247–9254.

Lau, B. K., Cota, D., Cristino, L. and Borgland, S. L. (2017) Endocannabinoid modulation of homeostatic and non-homeostatic feeding circuits, *Neuropharmacology*. Pergamon, 124, pp. 38–51.

Lee, A. T., Vogt, D., Rubenstein, J. L. and Sohal, V. S. (2014) A Class of GABAergic Neurons in the Prefrontal Cortex Sends Long-Range Projections to the Nucleus Accumbens and Elicits Acute Avoidance Behavior, *Journal of Neuroscience*, 34(35), pp. 11519–11525.

Lee, Anthony T. *et al.* (2014) Pyramidal Neurons in Prefrontal Cortex Receive Subtype-Specific Forms of Excitation and Inhibition, *Neuron*, 81(1), pp. 61–68.

Lee, D. J., Elias, G. J. B. and Lozano, A. M. (2018) Neuromodulation for the treatment of eating disorders and obesity., *Therapeutic advances in psychopharmacology*. SAGE Publications, 8(2), pp. 73–92.

Lee, M. W. and Fujioka, K. (2009) Naltrexone for the treatment of obesity: review and update, *Expert Opinion on Pharmacotherapy*. Taylor & Francis, 10(11), pp. 1841–1845.

Lerma-Cabrera, J. M., Carvajal, F. and Lopez-Legarrea, P. (2016) Food addiction as a new piece of the obesity framework., *Nutrition journal*. BioMed Central, 15, p. 5.

Limpens, J. H. W. *et al.* (2015) Pharmacological inactivation of the prelimbic cortex emulates compulsive reward seeking in rats, *Brain Research*. Elsevier, 1628, pp. 210–218.

Linardon, J., Wade, T. D., de la Piedad Garcia, X. and Brennan, L. (2017) The efficacy of cognitive-behavioral therapy for eating disorders: A systematic review and meta-analysis., *Journal of Consulting and Clinical Psychology*, 85(11), pp. 1080–1094.

Lindgren, E. *et al.* (2018) Food addiction: A common neurobiological mechanism with drug abuse., *Frontiers in bioscience (Landmark edition)*, 23, pp. 811–836.

Llorente-Berzal, A. *et al.* (2013) Sex-Dependent Psychoneuroendocrine Effects of THC and MDMA in an Animal Model of Adolescent Drug Consumption, *PLoS ONE*. Edited by Y. Abreu-Villaça. Public Library of Science, 8(11), p. e78386.

Lüscher, C. and Slesinger, P. A. (2010) Emerging roles for G protein-gated inwardly rectifying potassium (GIRK) channels in health and disease., *Nature reviews. Neuroscience*. NIH Public Access, 11(5), pp. 301–15.

Lustig, R. H., Schmidt, L. A. and Brindis, C. D. (2012) The toxic truth about sugar, *Nature*, 482(7383), pp. 27–29.

Lutz, B., Marsicano, G., Maldonado, R. and Hillard, C. J. (2015) The endocannabinoid system in guarding against fear, anxiety and stress., *Nature reviews. Neuroscience*. NIH Public Access, 16(12), pp. 705–18.

Madura, J. A., Dibaise, J. K. and DiBaise, J. K. (2012) Quick fix or long-term cure? Pros and cons of bariatric surgery., *F1000 medicine reports*. Faculty of 1000 Ltd, 4, p. 19.

Mancino, S. *et al.* (2015) Epigenetic and Proteomic Expression Changes Promoted by Eating Addictive-Like Behavior., *Neuropsychopharmacology : official publication of the American College of Neuropsychopharmacology*. American College of Neuropsychopharmacology, 40(12), pp. 2788–800.

Mannella, F., Gurney, K. and Baldassarre, G. (2013) The nucleus accumbens as a nexus between values and goals in goal-directed behavior: a review and a new hypothesis., *Frontiers in behavioral neuroscience*. Frontiers Media SA, 7, p. 135.

Marcus, M. D. and Wildes, J. E. (2012) Obesity in DSM-5, *Psychiatric Annals*, 42(11), pp. 431–435.

Margolis, E. B. *et al.* (2012) Identification of Rat Ventral Tegmental Area GABAergic Neurons, *PLoS ONE*. Edited by L. Groc. Public Library of Science, 7(7), p. e42365.

Marhe, R. *et al.* (2013) Individual differences in anterior cingulate activation associated with attentional bias predict cocaine use after treatment., *Neuropsychopharmacology : official publication of the American College of Neuropsychopharmacology*. Nature Publishing Group, 38(6), pp. 1085–93.

Marinelli, S. *et al.* (2009) Self-modulation of neocortical pyramidal neurons by endocannabinoids, *Nature Neuroscience*, 12(12), pp. 1488–1490.

Markus, C. R., Rogers, P. J., Brouns, F. and Schepers, R. (2017) Eating dependence and weight gain; no human evidence for a 'sugar-addiction' model of overweight, *Appetite*. Elsevier Ltd, 114, pp. 64–72.

Marsicano, G. *et al.* (2002) The endogenous cannabinoid system controls extinction of aversive memories., *Nature*, 418(6897), pp. 530–4.

Martín-García, E. *et al.* (2010) Central and peripheral consequences of the chronic blockade of CB $_1$ cannabinoid receptor with rimonabant or taranabant, *Journal of Neurochemistry*. Blackwell Publishing Ltd, 112(5), pp. 1338–13351.

Martín-García, E. *et al.* (2011) New operant model of reinstatement of food-seeking behavior in mice., *Psychopharmacology*, 215(1), pp. 49–70.

Martín-García, E. *et al.* (2014) Frequency of cocaine self-administration influences drug seeking in the rat: optogenetic evidence for a role of the prelimbic cortex., *Neuropsychopharmacology : official publication of the American College of Neuropsychopharmacology*. Nature Publishing Group, 39(10), pp. 2317–30.

Martín-García, E. *et al.* (2016) Differential Control of Cocaine Self-Administration by GABAergic and Glutamatergic CB1 Cannabinoid Receptors., *Neuropsychopharmacology : official publication of the American College of Neuropsychopharmacology*, pp. 1–14.

Di Marzo, V. *et al.* (2001) Leptin-regulated endocannabinoids are involved in maintaining food intake, *Nature*. Nature Publishing Group, 410(6830), pp. 822–825.

Di Marzo, V. and Matias, I. (2005) Endocannabinoid control of food intake and energy balance., *Nature neuroscience*, 8(5), pp. 585–9.

Di Marzo, V. and De Petrocellis, L. (2010) Endocannabinoids as regulators of transient receptor potential (TRP) channels: A further opportunity to develop new endocannabinoid-based therapeutic drugs., *Current medicinal chemistry*, 17(14), pp. 1430–49.

Maze, I. *et al.* (2010) Essential Role of the Histone Methyltransferase G9a in Cocaine-Induced Plasticity, *Science*. American Association for the Advancement of Science, 327(5962), pp. 213–216.

Maze, I. *et al.* (2014) G9a influences neuronal subtype specification in striatum, *Nature Neuroscience*. Nature Publishing Group, 17(4), pp. 533–539.

McFarland, K. and Kalivas, P. W. (2001) The circuitry mediating cocaine-induced reinstatement of drug-seeking behavior., *The Journal of neuroscience : the official journal of the Society for Neuroscience*, 21(21), pp. 8655–63.

McHugh, R. K., Hearon, B. A. and Otto, M. W. (2010) Cognitive behavioral therapy for substance use disorders., *The Psychiatric clinics of North America*. NIH Public Access, 33(3), pp. 511–25.

Melis, M. *et al.* (2004) Endocannabinoids mediate presynaptic inhibition of glutamatergic transmission in rat ventral tegmental area dopamine neurons through activation of CB1 receptors., *The Journal of neuroscience : the official journal of the Society for Neuroscience*, 24(1), pp. 53–62.

Le Merrer, J. *et al.* (2012) Protracted abstinence from distinct drugs of abuse shows regulation of a common gene network, *Addiction Biology*, 17(1), pp. 1–12.

Meule, A. *et al.* (2014) Correlates of food addiction in obese individuals seeking bariatric surgery, *Clinical Obesity*. John Wiley & Sons, Ltd (10.1111), 4(4), p. n/a-n/a.

Meule, A. (2015) Focus: Addiction: Back by Popular Demand: A Narrative Review on the History of Food Addiction Research, *The Yale Journal of Biology and Medicine*. Yale Journal of Biology and Medicine, 88(3), p. 295.

Meule, A. (2019) A Critical Examination of the Practical Implications Derived from the Food Addiction Concept, *Current Obesity Reports*. Current Obesity Reports, 8(1), pp. 11–17.

Milano, W. *et al.* (2013) The pharmacological options in the treatment of eating disorders., *ISRN pharmacology*. Hindawi Limited, 2013, p. 352865.

Miller, E. K. and Cohen, J. D. (2001) An integrate theory of PFC function, *Annual Review of Neuroscience*, 24, pp. 167–202.

Mishra, A., Anand, M. and Umesh, S. (2017) Neurobiology of eating disorders - an overview, *Asian Journal of Psychiatry*. Elsevier Science B.V., 25, pp. 91–100.

Molle, R. D. *et al.* (2017) Gene and environment interaction: Is the differential susceptibility hypothesis relevant for obesity?, *Neuroscience and Biobehavioral Reviews*, 73, pp. 326–339.

Monory, K. *et al.* (2006) The endocannabinoid system controls key epileptogenic circuits in the hippocampus., *Neuron*, 51(4), pp. 455–66.

Monory, K. *et al.* (2015) Cannabinoid CB1 receptor calibrates excitatory synaptic balance in the mouse hippocampus., *The Journal of neuroscience : the official journal of the Society for Neuroscience*. Society for Neuroscience, 35(9), pp. 3842–50.

Monteleone, P. *et al.* (2005) Blood Levels of the Endocannabinoid Anandamide are Increased in Anorexia Nervosa and in Binge-Eating Disorder, but not in Bulimia Nervosa, *Neuropsychopharmacology*. Nature Publishing Group, 30(6), pp. 1216–1221.

Monteleone, P. *et al.* (2009) Association of *CNR1* and *FAAH* endocannabinoid gene polymorphisms with anorexia nervosa and bulimia nervosa: evidence for synergistic effects, *Genes, Brain and Behavior*. John Wiley & Sons, Ltd (10.1111), 8(7), pp. 728–732.

Monteleone, P. and Maj, M. (2013) Dysfunctions of leptin, ghrelin, BDNF and endocannabinoids in eating disorders: Beyond the homeostatic control of food intake, *Psychoneuroendocrinology*. Pergamon, 38(3), pp. 312–330.

Moore, C. F., Sabino, V., Koob, G. F. and Cottone, P. (2017) Pathological Overeating: Emerging Evidence for a Compulsivity Construct, *Neuropsychopharmacology*. Nature Publishing Group, 42(7), pp. 1375–1389.

Moore, C. F. *et al.* (2018) Neuropharmacology of compulsive eating, *Philosophical Transactions of the Royal Society B: Biological Sciences*, 373(20170024).

Moorman, D. E., James, M. H., McGlinchey, E. M. and Aston-Jones, G. (2015) Differential roles of medial prefrontal subregions in the regulation of drug seeking, *Brain Research*. Elsevier, 1628, pp. 130–146.

Morales, P., Reggio, P. H. and Jagerovic, N. (2017a) An Overview on Medicinal Chemistry of Synthetic and Natural Derivatives of Cannabidiol., *Frontiers in pharmacology*. Frontiers Media SA, 8, p. 422.

Morales, P., Hurst, D. P. and Reggio, P. H. (2017b) Molecular Targets of the Phytocannabinoids: A Complex Picture, in *Progress in the chemistry of organic natural products*, pp. 103–131.

Morrow, J. D. and Flagel, S. B. (2016) *Neuroscience of resilience and vulnerability for addiction medicine: From genes to behavior*. 1st edn, *Progress in Brain Research*. 1st edn. Elsevier B.V.

Moyer, R. A. *et al.* (2011) Intronic polymorphisms affecting alternative splicing of human dopamine D2 receptor are associated with cocaine abuse., *Neuropsychopharmacology : official publication of the American College of Neuropsychopharmacology*. Nature Publishing Group, 36(4), pp. 753–62.

Muir, J. and Bagot, R. C. (2019) Optogenetics: Illuminating the Neural Circuits of Depression, *Neurobiology of Depression*. Academic Press, pp. 147–157.

Nestler, E. J. and Hyman, S. E. (2010) Animal models of neuropsychiatric disorders., *Nature neuroscience*. NIH Public Access, 13(10), pp. 1161–9.

Nestler, E. J. (2014) Epigenetic mechanisms of drug addiction., *Neuropharmacology*. NIH Public Access, 76 Pt B(0 0), pp. 259–68.

Nestler, E. J. and Lüscher, C. (2019) The Molecular Basis of Drug Addiction: Linking Epigenetic to Synaptic and Circuit Mechanisms, *Neuron*, 102(1), pp. 48–59.

Neville, M. J., Johnstone, E. C. and Walton, R. T. (2004) Identification and characterization of ANKK1: A novel kinase gene closely linked to DRD2 on chromosome band 11q23.1, *Human Mutation*, 23(6), pp. 540–545.

Nieh, E. H. *et al.* (2015) Decoding neural circuits that control compulsive sucrose seeking., *Cell*. Elsevier, 160(3), pp. 528–41.

Nikolova, Y. S., Ferrell, R. E., Manuck, S. B. and Hariri, A. R. (2011) Multilocus Genetic Profile for Dopamine Signaling Predicts Ventral Striatum Reactivity, *Neuropsychopharmacology*. Nature Publishing Group, 36(9), pp. 1940–1947.

Novelle, M., Diéguez, C., Novelle, M. G. and Diéguez, C. (2018) Food Addiction and Binge Eating: Lessons Learned from Animal Models, *Nutrients*. Multidisciplinary Digital Publishing Institute, 10(1), p. 71.

O'Brien, J., Hayder, H., Zayed, Y. and Peng, C. (2018) Overview of MicroRNA Biogenesis, Mechanisms of Actions, and Circulation., *Frontiers in endocrinology*. Frontiers Media SA, 9, p. 402.

O'Sullivan, S. E. (2009) Cannabinoids go nuclear: evidence for activation of peroxisome proliferator-activated receptors, *British Journal of Pharmacology*, 152(5), pp. 576–582.

Onaivi, E. S., Ishiguro, H., Gu, S. and Liu, Q.-R. (2012) CNS effects of CB2 cannabinoid receptors: beyond neuro-immuno-cannabinoid activity., *Journal of psychopharmacology (Oxford, England)*. NIH Public Access, 26(1), pp. 92–103.

Onaolapo, A. Y. and Onaolapo, O. J. (2018) Food additives, food and the concept of 'food addiction': Is stimulation of the brain reward circuit by food sufficient to trigger addiction?, *Pathophysiology*. Elsevier, 25(4), pp. 263–276.

Padwal, R. S. and Majumdar, S. R. (2007) Drug treatments for obesity: orlistat, sibutramine, and rimonabant, *The Lancet*, 369(9555), pp. 71–77.

Parsons, L. H. and Hurd, Y. L. (2015) Endocannabinoid signalling in reward and addiction.

Parylak, S. L., Koob, G. F. and Zorrilla, E. P. (2011) The dark side of food addiction, *Physiology & Behavior*. Elsevier, 104(1), pp. 149–156.

Pascoli, V., Terrier, J., Hiver, A. and Lüscher, C. (2015) Sufficiency of Mesolimbic Dopamine Neuron Stimulation for the Progression to Addiction, *Neuron*. Cell Press, 88(5), pp. 1054–1066.

Pascoli, V. *et al.* (2018) Stochastic synaptic plasticity underlying compulsion in a model of addiction, *Nature*. Springer US, 564(7736), pp. 366–371.

Paxinos, G. and Franklin, K. B. J. (2001) *The Mouse Brain in Stereotaxic Coordinates*. 2nd Editio. Academic Press, San Diego.

Pelchat, M. L. *et al.* (2004) Images of desire: food-craving activation during fMRI., *NeuroImage*, 23(4), pp. 1486–93.

Pelloux, Y., Murray, J. E. and Everitt, B. J. (2013) Differential roles of the prefrontal cortical subregions and basolateral amygdala in compulsive cocaine seeking and relapse after voluntary abstinence in rats., *The European journal of neuroscience*. Wiley-Blackwell, 38(7), pp. 3018–26.

Peña, C. J., Bagot, R. C., Labonté, B. and Nestler, E. J. (2014) Epigenetic Signaling in Psychiatric Disorders, *Journal of Molecular Biology*, 426(20), pp. 3389–3412.

Pepino, M. Y., Stein, R. I., Eagon, J. C. and Klein, S. (2014) Bariatric surgery-induced weight loss causes remission of food addiction in extreme obesity, *Obesity*. John Wiley & Sons, Ltd, 22(8), pp. 1792–1798.

Periyasamy, P. *et al.* (2018) Cocaine-Mediated Downregulation of miR-124 Activates Microglia by Targeting KLF4 and TLR4 Signaling., *Molecular neurobiology*. NIH Public Access, 55(4), pp. 3196–3210.

Pertwee, R. G. *et al.* (2010) International Union of Basic and Clinical Pharmacology. LXXIX. Cannabinoid Receptors and Their Ligands: Beyond CB1 and CB2, *Pharmacological Reviews*, 62(4), pp. 588–631.

Peters, J., LaLumiere, R. T. and Kalivas, P. W. (2008a) Infralimbic Prefrontal Cortex is Responsible for Inhibiting Cocaine Seeking in Extinguished Rats, *The Journal of neuroscience : the official journal of the Society for Neuroscience*. NIH Public Access, 28(23), p. 6046.

Peters, J., Vallone, J., Laurendi, K. and Kalivas, P. W. (2008b) Opposing roles for the ventral prefrontal cortex and the basolateral amygdala on the spontaneous recovery of cocaine-seeking in rats, *Psychopharmacology*. Springer-Verlag, 197(2), pp. 319–326.

Peterson, R. E. *et al.* (2012) Binge Eating Disorder Mediates Links between Symptoms of Depression, Anxiety, and Caloric Intake in Overweight and Obese Women., *Journal of obesity*. Hindawi Limited, 2012, p. 407103.

Phillips, P. C. (2008) Epistasis--the essential role of gene interactions in the structure and evolution of genetic systems., *Nature reviews. Genetics*. NIH Public Access, 9(11), pp. 855–67.

Piazza, P. V. and Deroche-Gamonet, V. (2013) A multistep general theory of transition to addiction., *Psychopharmacology*, 229(3), pp. 387–413.

Pierce, K. L., Premont, R. T. and Lefkowitz, R. J. (2002) Seven-transmembrane receptors, *Nature Reviews Molecular Cell Biology*, 3(9), pp. 639–650.

Pistillo, F., Clementi, F., Zoli, M. and Gotti, C. (2015) Nicotinic, glutamatergic and dopaminergic synaptic transmission and plasticity in the mesocorticolimbic system: Focus on nicotine effects, *Progress in Neurobiology*. Elsevier Ltd, 124, pp. 1–27.

Planagumà, J. *et al.* (2015) Human N-methyl D-aspartate receptor antibodies alter memory and behaviour in mice, *Brain*, 138(1), pp. 94–109.

Pursey, K. *et al.* (2014) The Prevalence of Food Addiction as Assessed by the Yale Food Addiction Scale: A Systematic Review, *Nutrients*. Multidisciplinary Digital Publishing Institute, 6(10), pp. 4552–4590.

Pursey, K. M., Davis, C. and Burrows, T. L. (2017) Nutritional Aspects of Food Addiction, *Current Addiction Reports*. Springer International Publishing, 4(2), pp. 142–150.

Quinn, R. K. *et al.* (2018) Temporally specific miRNA expression patterns in the dorsal and ventral striatum of addiction-prone rats, *Addiction Biology*, 23(2), pp. 631–642.

Quintana, A. *et al.* (2012) Lack of GPR88 enhances medium spiny neuron activity and alters motor- and cue-dependent behaviors, *Nature Neuroscience*, 15(11), pp. 1547–1555.

Randolph, T. G. (1956) The descriptive features of food addiction; addictive eating and drinking., *Quarterly journal of studies on alcohol*, 17(2), pp. 198–224.

Reich, R., Cloninger, C. R. and Guze, S. B. (1975) The multifactorial model of disease transmission: I. Description of the model and its use in psychiatry., *The British journal of psychiatry : the journal of mental science*, 127, pp. 1–10.

Rey, A. A., Purrio, M., Viveros, M.-P. and Lutz, B. (2012) Biphasic effects of cannabinoids in anxiety responses: CB1 and GABA(B) receptors in the balance of GABAergic and glutamatergic neurotransmission., *Neuropsychopharmacology : official publication of the American College of Neuropsychopharmacology*, 37(12), pp. 2624–34.

Riga, D. *et al.* (2014) Optogenetic dissection of medial prefrontal cortex circuitry, *Frontiers in Systems Neuroscience*, 8(December), pp. 1–19.

Rinaldi-Carmona, M. *et al.* (1994) SR141716A, a potent and selective antagonist of the brain cannabinoid receptor, *FEBS Letters*. John Wiley & Sons, Ltd, 350(2–3), pp. 240–244.

Robinson, S. M. and Adinoff, B. (2016) The Classification of Substance Use Disorders: Historical, Contextual, and Conceptual Considerations., *Behavioral sciences (Basel, Switzerland)*. Multidisciplinary Digital Publishing Institute (MDPI), 6(3).

Rogers, P. J. (2017) Food and drug addictions: Similarities and differences, *Pharmacology Biochemistry and Behavior*. Elsevier Inc., 153, pp. 182–190.

Romer, A. L. *et al.* (2019) Dopamine genetic risk is related to food addiction and body mass through reduced reward-related ventral striatum activity, *Appetite*. Elsevier Ltd, 133, pp. 24–31.

Rosenbaum, D. L. and White, K. S. (2015) The relation of anxiety, depression, and stress to binge eating behavior, *Journal of Health Psychology*, 20(6), pp. 887–898.

Rossi, M. A. and Stuber, G. D. (2018) Overlapping Brain Circuits for Homeostatic and Hedonic Feeding., *Cell metabolism*. Elsevier, 27(1), pp. 42–56.

Rossi, M. A. *et al.* (2019) Obesity remodels activity and transcriptional state of a lateral hypothalamic brake on feeding., *Science (New York, N.Y.)*. American Association for the Advancement of Science, 364(6447), pp. 1271–1274.

Rössner, S. *et al.* (2000) Weight Loss, Weight Maintenance, and Improved Cardiovascular Risk Factors after 2 Years Treatment with Orlistat for Obesity, *Obesity Research*, 8(1), pp. 49–61.

Roth, B. L. (2016) DREADDs for Neuroscientists, *Neuron*. Elsevier Ltd, 89(4), pp. 683–694.

Ruehle, S. *et al.* (2013) Cannabinoid CB1 receptor in dorsal telencephalic glutamatergic neurons: distinctive sufficiency for hippocampus-dependent and amygdala-dependent synaptic and behavioral functions, *The Journal of neuroscience : the official journal of the Society for Neuroscience*, 33 (25), pp. 10264–77.

Russell-Mayhew, S., von Ranson, K. M. and Masson, P. C. (2010) How does overeaters anonymous help its members? A qualitative analysis., *European eating disorders review : the journal of the Eating Disorders Association*, 18(1), pp. 33–42.

Russo, S. J. and Nestler, E. J. (2013) The brain reward circuitry in mood disorders, *Nature Reviews Neuroscience*, 14(9), pp. 609–625.

De Sa Nogueira, D., Merienne, K. and Befort, K. (2018) Neuroepigenetics and addictive behaviors: Where do we stand?, *Neuroscience & Biobehavioral Reviews*. Pergamon.

Sakamoto, K. and Crowley, J. J. (2018) A comprehensive review of the genetic and biological evidence supports a role for MicroRNA-137 in the etiology of schizophrenia., *American journal of medical genetics. Part B, Neuropsychiatric genetics : the official publication of the International Society of Psychiatric Genetics*. NIH Public Access, 177(2), pp. 242–256.

Salgado, S. and Kaplitt, M. G. (2015) The nucleus accumbens: A comprehensive review, *Stereotactic and Functional Neurosurgery*, 93(2), pp. 75–93.

Sanchis-Segura, C. and Spanagel, R. (2006) Behavioural assessment of drug reinforcement and addictive features in rodents: an overview, *Addiction Biology*, 11(1), pp. 2–38.

Sandoval, D., Cota, D. and Seeley, R. J. (2008) The Integrative Role of CNS Fuel-Sensing Mechanisms in Energy Balance and Glucose Regulation, *Annual Review of Physiology*, 70(1), pp. 513–535.

Sangha, S. *et al.* (2014) Alterations in reward, fear and safety cue discrimination after inactivation of the rat prelimbic and infralimbic cortices., *Neuropsychopharmacology : official publication of the American College of Neuropsychopharmacology*. Nature Publishing Group, 39(10), pp. 2405–13.

Santana, N., Mengod, G. and Artigas, F. (2009) Quantitative analysis of the expression of dopamine D1 and D2 receptors in pyramidal and GABAergic neurons of the rat prefrontal cortex, *Cerebral Cortex*, 19(4), pp. 849–860.

Santana, N. and Artigas, F. (2017) Laminar and Cellular Distribution of Monoamine Receptors in Rat Medial Prefrontal Cortex, *Frontiers in Neuroanatomy*, 11(September), pp. 1–13.

Saunders, B. T. and Robinson, T. E. (2010) A Cocaine Cue Acts as an Incentive Stimulus in Some but not Others: Implications for Addiction, *Biological Psychiatry*, 67(8), pp. 730–736.

Schaumberg, K. *et al.* (2017) The Science Behind the Academy for Eating Disorders' Nine Truths About Eating Disorders, *European Eating Disorders Review*, 25(6), pp. 432–450.

Schlicker, E. and Kathmann, M. (2001) Modulation of transmitter release via presynaptic cannabinoid receptors., *Trends in pharmacological sciences*, 22(11), pp. 565–72.

Schmidt, J., Kärgel, C. and Opwis, M. (2017) Neurofeedback in Substance Use and Overeating: Current Applications and Future Directions, *Current Addiction Reports*. Springer International Publishing, 4(2), pp. 116–131.

Schmitzer-Torbert, N. *et al.* (2015) Post-training cocaine administration facilitates habit learning and requires the infralimbic cortex and dorsolateral striatum., *Neurobiology of learning and memory*, 118, pp. 105–12.

Schratt, G. (2009) microRNAs at the synapse, *Nature Reviews Neuroscience*, 10(12), pp. 842–849.

Schulte, E. M., Avena, N. M. and Gearhardt, A. N. (2015) Which Foods May Be Addictive? The Roles of Processing, Fat Content, and Glycemic Load.

Schulte, E. M., Potenza, M. N. and Gearhardt, A. N. (2017) A commentary on the 'eating addiction' versus 'food addiction' perspectives on addictive-like food consumption, *Appetite*. Academic Press, 115, pp. 9–15.

Schulte, E. M. and Gearhardt, A. N. (2017) Development of the Modified Yale Food Addiction Scale Version 2.0, *European Eating Disorders Review*, 25(4), pp. 302–308.

Schulte, E. M. and Gearhardt, A. N. (2018) Associations of Food Addiction in a Sample Recruited to Be Nationally Representative of the United States, *European Eating Disorders Review*. John Wiley & Sons, Ltd, 26(2), pp. 112–119.

Sellayah, D., Cagampang, F. R. and Cox, R. D. (2014) On the evolutionary origins of obesity: a new hypothesis., *Endocrinology*, 155(5), pp. 1573–88.

Sesack, S. R., Aoki, C. and Pickel, V. M. (1994) Ultrastructural localization of D2 receptor-like immunoreactivity in midbrain dopamine neurons and their striatal targets., *The Journal of neuroscience : the official journal of the Society for Neuroscience*, 14(1), pp. 88–106.

Sesack, S. R. and Grace, A. A. (2010) Cortico-Basal Ganglia Reward Network: Microcircuitry, *Neuropsychopharmacology*. Nature Publishing Group, 35(1), pp. 27–47.

Van Sickle, M. D. *et al.* (2005) Identification and Functional Characterization of Brainstem Cannabinoid CB2 Receptors, *Science*, 310(5746), pp. 329–332.

Siegert, S. *et al.* (2015) The schizophrenia risk gene product miR-137 alters presynaptic plasticity, *Nature Neuroscience*, 18(7), pp. 1008–1016.

De Silva, P. and Eysenck, S. (1987) Personality and addictiveness in anorexic and bulimic patients, *Personality and Individual Differences*. Pergamon, 8(5), pp. 749–751.

Skibicka, K. P. *et al.* (2011) Ghrelin directly targets the ventral tegmental area to increase

food motivation, *Neuroscience*, 180, pp. 129–137.

Smink, F. R. E., van Hoeken, D. and Hoek, H. W. (2012) Epidemiology of Eating Disorders: Incidence, Prevalence and Mortality Rates, *Current Psychiatry Reports*. Current Science Inc., 14(4), pp. 406–414.

Smith, A. C. W. and Kenny, P. J. (2018) MicroRNAs regulate synaptic plasticity underlying drug addiction, *Genes, Brain and Behavior*, 17(3), pp. 1–11.

Smith, D. G. and Robbins, T. W. (2013) The Neurobiological Underpinnings of Obesity and Binge Eating: A Rationale for Adopting the Food Addiction Model, *Biological Psychiatry*, 73(9), pp. 804–810.

Smith, R. J. and Laiks, L. S. (2018) Behavioral and neural mechanisms underlying habitual and compulsive drug seeking, *Progress in Neuro-Psychopharmacology and Biological Psychiatry*. Elsevier, 87(May 2017), pp. 11–21.

Solinas, M., Justinova, Z., Goldberg, S. R. and Tanda, G. (2006) Anandamide administration alone and after inhibition of fatty acid amide hydrolase (FAAH) increases dopamine levels in the nucleus accumbens shell in rats, *Journal of Neurochemistry*. John Wiley & Sons, Ltd (10.1111), 98(2), pp. 408–419.

Solinas, M. *et al.* (2018) Dopamine and addiction: what have we learned from 40 years of research, *Journal of Neural Transmission*. Springer Vienna, pp. 1–36.

Soria-Gómez, E. *et al.* (2009) Pharmacological enhancement of the endocannabinoid system in the nucleus accumbens shell stimulates food intake and increases c-Fos expression in the hypothalamus, *British Journal of Pharmacology*. John Wiley & Sons, Ltd (10.1111), 151(7), pp. 1109–1116.

Soria-Gómez, E. *et al.* (2014) The endocannabinoid system controls food intake via olfactory processes, *Nature Neuroscience*. Nature Publishing Group, 17(3), pp. 407–415.

Stahl, S. M. (2013) Impulsivity, compulsivity, and addiction, *Stahl's Essential Psychopharmacology*, pp. 537–575.

Stalnaker, T. A., Takahashi, Y., Roesch, M. R. and Schoenbaum, G. (2009) Neural Substrates of Cognitive Inflexibility after Chronic Cocaine Exposure, *Neuropharmacology*, pp. 63–72.

Stamatakis, A. M. *et al.* (2013) A Unique Population of Ventral Tegmental Area Neurons Inhibits the Lateral Habenula to Promote Reward, *Neuron*. Cell Press, 80(4), pp. 1039–1053.

Stefanik, M. T. *et al.* (2013) Optogenetic inhibition of cocaine seeking in rats., *Addiction biology*. Wiley-Blackwell, 18(1), pp. 50–3.

Steindel, F. *et al.* (2013) Neuron-type specific cannabinoid-mediated G protein signalling in mouse hippocampus, *Journal of Neurochemistry*, 124(6), pp. 795–807.

Stella, N. (2009) Endocannabinoid signaling in microglial cells, *Neuropharmacology*, 56, pp. 244–253.

Steward, T. *et al.* (2018) Food addiction and impaired executive functions in women with obesity, *European Eating Disorders Review*. John Wiley & Sons, Ltd, 26(6), pp. 574–584.

Stuber, G. D., Britt, J. P. and Bonci, A. (2012) Optogenetic modulation of neural circuits that underlie reward seeking, *Biological Psychiatry*. Elsevier Inc., 71(12), pp. 1061–1067.

Su, H. *et al.* (2019) Regulation of microRNA-29c in the nucleus accumbens modulates methamphetamine -induced locomotor sensitization in mice, *Neuropharmacology*. Pergamon, 148, pp. 160–168.

Terraneo, A. *et al.* (2016) Transcranial magnetic stimulation of dorsolateral prefrontal cortex reduces cocaine use: A pilot study, *European Neuropsychopharmacology*. Elsevier, 26(1), pp. 37–44.

Tervo, D. G. R. *et al.* (2016) A Designer AAV Variant Permits Efficient Retrograde Access to Projection Neurons., *Neuron*. NIH Public Access, 92(2), pp. 372–382.

Tomasi, D. and Volkow, N. D. (2013) Striatocortical pathway dysfunction in addiction and obesity: differences and similarities., *Critical reviews in biochemistry and molecular biology*, 48(1), pp. 1–19.

Tomasi, D. *et al.* (2015) Overlapping patterns of brain activation to food and cocaine cues in cocaine abusers, *Human Brain Mapping*, 36(1), pp. 120–136.

Torregrossa, M. M., Corlett, P. R. and Taylor, J. R. (2011) Aberrant learning and memory in addiction., *Neurobiology of learning and memory*. NIH Public Access, 96(4), pp. 609–23.

Tovote, P., Fadok, J. P. and Lüthi, A. (2015) Neuronal circuits for fear and anxiety, *Nature Reviews Neuroscience*, 16(6), pp. 317–331.

Towers, S. K. and Hestrin, S. (2008) D1-like dopamine receptor activation modulates GABAergic inhibition but not electrical coupling between neocortical fast-spiking interneurons., *The Journal of neuroscience : the official journal of the Society for Neuroscience*. Society for Neuroscience, 28(10), pp. 2633–41.

Trapnell, C. *et al.* (2010) Transcript assembly and quantification by RNA-Seq reveals unannotated transcripts and isoform switching during cell differentiation., *Nature biotechnology*. NIH Public Access, 28(5), pp. 511–5.

Trigo, J. M. *et al.* (2010) The endogenous opioid system: A common substrate in drug addiction, *Drug and Alcohol Dependence*. Elsevier, 108(3), pp. 183–194.

Tritsch, N. X. and Sabatini, B. L. (2012) Dopaminergic Modulation of Synaptic Transmission in Cortex and Striatum, *Neuron*. Elsevier Inc., 76(1), pp. 33–50.

Tritsch, N. X., Ding, J. B. and Sabatini, B. L. (2012) Dopaminergic neurons inhibit striatal output through non-canonical release of GABA, *Nature*. Nature Publishing Group, 490(7419), pp. 262–266.

Tsou, K. *et al.* (1998) Immunohistochemical distribution of cannabinoid CB1 receptors in the rat central nervous system, *Neuroscience*. Pergamon, 83(2), pp. 393–411.

Urban, D. J. and Roth, B. L. (2015) DREADDs (Designer Receptors Exclusively Activated by Designer Drugs): Chemogenetic Tools with Therapeutic Utility, *Annual Review of Pharmacology and Toxicology*, 55(1), pp. 399–417.

Usiello, A. *et al.* (2000) Distinct functions of the two isoforms of dopamine D2 receptors., *Nature*, 408(6809), pp. 199–203.

Velázquez-Sánchez, C. *et al.* (2014) High Trait Impulsivity Predicts Food Addiction-Like Behavior in the Rat, *Neuropsychopharmacology*, 39(10), pp. 2463–2472.

Velázquez-Sánchez, C. *et al.* (2015) Seeking behavior, place conditioning, and resistance to conditioned suppression of feeding in rats intermittently exposed to palatable food., *Behavioral neuroscience*, 129(2), pp. 219–24.

Vlasov, K., Van Dort, C. J. and Solt, K. (2018) Optogenetics and Chemogenetics, in *Methods in enzymology*, pp. 181–196.

Volkow, N. D. *et al.* (1993) Decreased dopamine D2 receptor availability is associated with reduced frontal metabolism in cocaine abusers, *Synapse*. John Wiley & Sons, Ltd, 14(2), pp. 169–177.

Volkow, N. D. and O'Brien, C. P. (2007) Issues for DSM-V: should obesity be included as a brain disorder?, *The American journal of psychiatry*, 164(5), pp. 708–10.

Volkow, Nora D. *et al.* (2008) Low dopamine striatal D2 receptors are associated with prefrontal metabolism in obese subjects: Possible contributing factors, *NeuroImage*. Academic Press, 42(4), pp. 1537–1543.

Volkow, N. D, Wang, G.-J., Fowler, J. S. and Telang, F. (2008) Overlapping neuronal circuits in addiction and obesity: evidence of systems pathology, *Philosophical Transactions of the Royal Society B: Biological Sciences*, 363(1507), pp. 3191–3200.

Volkow, N. D. *et al.* (2011) Food and Drug Reward: Overlapping Circuits in Human Obesity and Addiction, in, pp. 1–24.

Volkow, Nora D, Wang, G.-J. and Baler, R. D. (2011) Reward, dopamine and the control of food intake: implications for obesity., *Trends in cognitive sciences*, 15(1), pp. 37–46.

Volkow, N. D. and Muenke, M. (2012) The genetics of addiction., *Human genetics*. NIH Public Access, 131(6), pp. 773–7.

Volkow, N. D., Wang, G.-J., Tomasi, D. and Baler, R. D. (2013) Obesity and addiction: neurobiological overlaps, *Obesity Reviews*. John Wiley & Sons, Ltd (10.1111), 14(1), pp. 2–18.

Volkow, N. D. and Baler, R. D. (2015) NOW vs LATER brain circuits: implications for obesity and addiction., *Trends in neurosciences*.

Volkow, N. D., Koob, G. F. and McLellan, A. T. (2016) Neurobiologic Advances from the Brain Disease Model of Addiction, *New England Journal of Medicine*, 374(4), pp. 363–371.

Volkow, N. D., Wise, R. A. and Baler, R. (2017) The dopamine motive system: Implications for drug and food addiction, *Nature Reviews Neuroscience*, 18(12), pp. 741–752.

Volkow, N. D. and Boyle, M. (2018) Neuroscience of addiction: Relevance to prevention and treatment, *American Journal of Psychiatry*, 175(8), pp. 729–740.

Volkow, N. D., Michaelides, M. and Baler, R. (2019) The Neuroscience of Drug Reward and Addiction, *Physiological Reviews*, 99(4), pp. 2115–2140.

Wang, G.-J. *et al.* (2014) Effect of combined naltrexone and bupropion therapy on the brain's reactivity to food cues, *International Journal of Obesity*. Nature Publishing Group, 38(5), pp. 682–688.

Wang, G. J. *et al.* (2001) Brain dopamine and obesity., *Lancet (London, England)*. Elsevier, 357(9253), pp. 354–7.

Weiner, B. and White, W. (2007) The *Journal of Inebriety* (1876-1914): history, topical analysis, and photographic images, *Addiction*, 102(1), pp. 15–23.

Wells, A. S., Read, N. W., Laugharne, J. D. and Ahluwalia, N. S. (1998) Alterations in mood after changing to a low-fat diet., *The British journal of nutrition*, 79(1), pp. 23–30.

Westwater, M. L., Fletcher, P. C. and Ziauddeen, H. (2016) Sugar addiction: the state of the science., *European journal of nutrition*. Springer, 55(Suppl 2), pp. 55–69.

Wexler, B. E. *et al.* (2001) Functional Magnetic Resonance Imaging of Cocaine Craving, *American Journal of Psychiatry*, 158(1), pp. 86–95.

WHO (2017).

Williams, L. M. (2012) Hypothalamic dysfunction in obesity, *Proceedings of the Nutrition Society*, 71(4), pp. 521–533.

Wise, R. A. (2009) Roles for nigrostriatal--not just mesocorticolimbic--dopamine in reward and addiction., *Trends in neurosciences*. Elsevier, 32(10), pp. 517–24.

Wonderlich, S. A. *et al.* (2009) The validity and clinical utility of binge eating disorder, *International Journal of Eating Disorders*. Edited by B. T. Walsh. John Wiley & Sons, Ltd,

42(8), pp. 687–705.

Wynne, K., Stanley, S., McGowan, B. and Bloom, S. (2005) Appetite control, *Journal of Endocrinology*, 184(2), pp. 291–318.

Yamaguchi, T. *et al.* (2011) Mesocorticolimbic Glutamatergic Pathway, *Journal of Neuroscience*. Society for Neuroscience, 31(23), pp. 8476–8490.

Yanfang Xia, Joseph R. Driscoll, Linda Wilbrecht, Elyssa B. Margolis, Howard L. Fields, and G. O. H. (2011) Nucleus Accumbens Medium Spiny Neurons Target Non-Dopaminergic Neurons in the Ventral Tegmental Area, *The Journal of Neuroscience*, pp. 31(21):7811–7816.

Yang, H. *et al.* (2018) Nucleus Accumbens Subnuclei Regulate Motivated Behavior via Direct Inhibition and Disinhibition of VTA Dopamine Subpopulations, *Neuron*. Cell Press, 97(2), pp. 434-449.e4.

Yilmaz, Z., Hardaway, J. A. and Bulik, C. M. (2015) Genetics and Epigenetics of Eating Disorders., *Advances in genomics and genetics*. NIH Public Access, 5, pp. 131–150.

Yokum, S., Ng, J. and Stice, E. (2011) Attentional Bias to Food Images Associated With Elevated Weight and Future Weight Gain: An fMRI Study, *Obesity*, 19(9), pp. 1775–1783.

Zigman, J. M., Bouret, S. G. and Andrews, Z. B. (2016) Obesity Impairs the Action of the Neuroendocrine Ghrelin System, *Trends in Endocrinology & Metabolism*, 27(1), pp. 54–63.

Zimmermann, T. *et al.* (2018) Neural stem cell lineage-specific cannabinoid type-1 receptor regulates neurogenesis and plasticity in the adult mouse hippocampus, *Cerebral Cortex*. Narnia, 28(12), pp. 4454–4471.

Zou, S. and Kumar, U. (2018) Cannabinoid receptors and the endocannabinoid system: Signaling and function in the central nervous system, *International Journal of Molecular Sciences*, 19(3).